TUDelft

Delft University of Technology

Committee I.1 Environment

Babanin, Alexander; Bernardino, M.; von Bock und Polach, F.; Campos, R.; Ding, J.; van Essen, S.M.; Gaggero, T.; Haroutunian, M. ; Katsardi, V.; More Authors

Important note
To cite this publication, please use the final published version (if applicable).
Please check the document version above.

COMMITTEE I.1
ENVIRONMENT

COMMITTEE MANDATE

Concern for descriptions of the ocean environment, especially with respect to wave, current and wind, in deep and shallow waters, and ice, as a basis for the determination of environmental loads for structural design. Attention shall be given to statistical description of these and other related phenomena relevant to the safe design and operation of ships and offshore structures. The committee is encouraged to cooperate with the corresponding ITTC committee.

AUTHORS/COMMITTEE MEMBERS

Chairman: Alexander Babanin
            Mariana Bernardino
            Franz von Bock und Polach
            Ricardo Campos,
            Jun Ding
            Sanne van Essen
            Tomaso Gaggero
            Maryam Haroutunian
            Vanessa Katsardi
            Alexander Nilva
            Arttu Polojarvi
            Erik Vanem
            Jungyong Wang
            Huidong Zhang
            Tingyao Zhu

KEYWORDS

Environment, metocean conditions, wind-generated waves, surface winds, ocean currents, sea ice, wave-coupled phenomena, deep water, shallow water, climate, extreme conditions, wave-ice interaction

CONTENTS

1.   INTRODUCTION AND METOCEAN FORCING

Environment Committee of ISSC, by its Mandate, deals with the Metocean environments. "In offshore and coastal engineering, metocean refers to the syllabic abbreviation of meteorology and (physical) oceanography" (Wikipedia). Metocean research covers dynamics of the ocean-interface environments: the air-sea surface, atmospheric boundary layer, upper ocean, the sea bed within the wavelength proximity (~100 m for wind-generated waves), and coastal areas. Metocean disciplines broadly comprise maritime engineering, marine meteorology, wave forecast, operational oceanography, oceanic climate, sediment transport, coastal morphology, and specialised technological disciplines for in-situ and remote sensing observations. Metocean applications incorporate offshore, coastal and Arctic engineering; navigation, shipping and naval architecture; marine search and rescue; environmental instrumentation, among others. Often, both for design and operational purposes the ISSC community is interested in Metocean Extremes which include extreme conditions (such as extreme tropical or extra-tropical cyclones), extreme events (such as rogue waves) and extreme environments (such as Marginal Ice Zone, MIZ). Certain Metocean conditions appear extreme, depending on applications (e.g. swell seas are benign for recreational sailing, but can be dangerous for dredging operations and are extreme for vessels transporting liquids).

This report builds on the work of the previous Technical Committees in charge of Environment.

The goal continues to be to review scientific and technological developments in the Metocean field from the last report, and to provide context of the developments, in order to give a balanced, accurate and up to date picture about the natural environment as well as data and models which can be used to accurately simulate it. The content of this report also reflects the interests and subject areas of the Committee membership, in accordance with the ISSC I.1 mandate. The Committee has continued cooperation with the Environment Committee of ITTC and with ISSC Committee V.6 Ocean Space Utilization.

The Committee consisted of members from academia, research organizations, research laboratories and classification societies. The Committee formally met as a group in person two times before the COVID onset: in Glasgow, Scotland on the 9th of June 2019, before the 38th International Conference on Ocean, Offshore and Arctic Engineering (OMAE 2019) and in Melbourne, Australia on the 10th of November 2019, following the 15th International Workshop on Wave Hindcasting and Forecasting. It's also held a number of regular teleconferences: two before the face-to-face meetings and seven after, once international travel was stopped by the pandemic.

Additionally, Committee members met on an ad-hoc basis during their international travels in 2019. With the wide range of subject areas that this report must cover, and the limited space, this Committee report does not purport to be exhaustive; however, the Committee believes that the reader will be presented a fair and balanced view of the subjects covered, and we recommend this report for the consideration of the ISSC 2022 Congress.

The report consists of 11 Sections: two of which include the Introduction and Conclusions, and nine are the main content. The opening Section 1 outlines and defines Metocean Forcings which can affect the offshore design and operations and are the subject of this Review Chapter. The review of publications starts from progress in Analytical Theory in 2018-2021, Section 2. It covers the basic framework of experimental, numerical, remote sensing and all the other methods and approaches in Metocean science and engineering. Numerical Modelling (Section 3) is one of the most rapidly developing research and application environments over the past two decades, it allows us to extend the theory when analytical solutions are not possible, and to complement (or even replace) some of the experimental approaches of the past. Computer

simulations will always need verification, validation and calibration of their outcomes through experiments and observations, particularly in engineering applications and offshore Metocean science. Therefore, Section 4 (Measurements and Observations) is the largest in the Chapter. Section 5 is effectively a modern extension of the measurement section – it is dedicated to Remote Sensing. Over the last four decades, the remote sensing has both become a powerful instrumental tool for field observations and remains an active area of engineering research in its own right as we see through growing developments of new capabilities in this space.

While the first five chapters are broadly dedicated to direct outcomes of Metocean research, the rest of the chapters focus more on analysis and indirect outputs. With mounting amounts of collected data: numerical, experimental, remote sensing, - Section 6 discusses advances in Data Analysis, and Section 7 in Statistics, its Theory and Analysis. Section 8, on Wave-Coupled Phenomena, reflects one of the most rapidly developing areas in Metocean science, particularly important in our era of numerical modelling. It accommodates various topics of interactions between small-scale phenomena (waves) and large-scale processes in the air-sea environments: wave breaking, wave-current and wave-ice interactions, wave influences in the Atmospheric Boundary Layer (ABL) and in the upper ocean, and complex wave-coupled modelling in the full combined air-sea-ice-wave system. Most essential for offshore engineering, is modelling and understanding of Extreme Events and Conditions, which are the subject of Section 9. Last, but not the least, Section 10 discusses Wind-Wave Climate which is connected to the global climate change. This connection is threaded throughout other sections of the chapter and is of utmost significance in offshore Metocean design and planning.

2.   ANALYTICAL THEORY

This chapter focuses on three main areas with regards to recent advances in analytical theories; these include advances in deepwater theories, advances in shallow water theories and advances in modelling of oceans waves in interaction with other phenomena. These are presented next, respectively.

2.1   *Advances in non-linear wave theories*

2.1.1   *The merits of non-linear wave theories*

Nonlinear partial differential equations (PDEs) are known to be useful tools in various real life, including shallow water, modelling.

One recent study which can be implemented to solve various nonlinear space-time fractional differential equations was carried out by Ali & Nuruddeen (2017) who used two methods including the Kudryashov method (exponential function) and the modified extended "tanh" expansion method (trigonometric and hyperbolic functions) with the Riccati differential equation, to analytically investigate and create various solutions for the Benney-Luke Equation (BLE), a conformal space-time fractional equation). The BLE featured in the study includes fractional derivatives in both the spatial and the temporal variables. Various solutions including the singular periodic wave's shapes, kink-type solution shapes were constructed in this study and singular soliton solution shapes obtained for the problem. Using graphical illustrations, the authors found that the applied methods are capable of producing exact solutions which were found in previous studies.

In another study, Osborne (2018) applied Multiperiodic Fourier Series (MFS) as solutions for integrable nonlinear ocean wave equations in one or two dimensions with two equations, both the Korteweg-de Vries (KdV) and nonlinear Schodinger equations are illustrated. The author highlights that "multiperiodic Fourier series have the advantage that the coherent structures of soliton physics are encoded in the formulation so that solitons, breathers, vortices, etc. are contained in the temporal evolution of the nonlinear power spectrum and phases".

The focus of Osborne (2018) is on constructing analytical results for a nonlinear wave equation. The method is used to compute both the physical properties of the nonlinear wave equations (for example, Stokes waves) and results for nonlinear stochastic properties including the correlation and coherence functions as well as the power spectra. As the Baker-Mumford theorem has been applied to construct the multiperiodic functions, the author suggests that the singularities can be included to approximately solve equations with "blow-ups", using MFS. Noting the assumption of one- or two-dimensional wave equations used in this study, another study is discussed in section 2.3 which highlights the fact that this assumption, applied to most current wave models, significantly alters the wave process, especially when interacting with other phenomena.

An interesting phenomenon when studying ocean waves is the interaction between long and short waves. Pan et al. (2018) investigated the effects of the divergent terms (i.e. the product of short wave modal wavenumber and long wave amplitude being >>1) which appear in high-order expansions analysis of such interactions, using mode decomposition. The aim of the study was to observe how the divergent terms influence the convergence of the expansion. In this study, products are not calculated in the physical domain; instead, model convolution is used for all operations in the spectral domain. Moreover, only after the analytical cancellations as discussed above, the results are stored. Although this approach introduces extra computational complexity because of the modal convolution and generalising it is complicated, it may in principle keep the dimension-reduction property and side-step the numerical ill-conditioning. The application of the Dirichlet-Neumann operator and mathematical induction, support (in theory) that the results are obtainable in a general case.

On the interaction of long waves, Kurt et al. (2019) have used both the sub-equation and residual power series methods to obtain new exact and approximate solutions of the generalised Hirota-Satsuma coupled KdV system of equations model. This has been carried out by first finding an approximate solution as a series of travelling wave (which are progressive waves that almost keep shape while traveling in a specific direction) solutions. Subsequently, these results are handled by taking the fractional derivatives in the conformable sense. Finally, the exact solutions are checked through substitution into the corresponding system using a symbolic computational software package. The study concludes that both the methods were applied easily and effectively, and the results point to their reliability; therefore, they can be applied to determine the dynamics of various fractional PDEs.

2.1.2 *Wave theories and deep water*

With regards to recent advances in deep water wave modelling approaches, in 2017, Dyachenko et al. (2017) proposed and analysed a new compact form of the Hamiltonian equation to model gravity-based ocean waves at the surface of deep water. The method, which gives a spatial wave equation, is most suitable for modelling artificial waves created in a controlled laboratory environment (i.e. with the use of wavemakers). The proposed method can be applied to define pre-breaking waves. In addition, similar to the Korteweg-de Vries equation which is generalised to the Kadomtsev-Petviashvili equation, these wave models can be generalised to almost 2D waves. The authors highlight the simplicity of the method as one of its advantages.

In another study, Demiray & Bulut (2017) investigated the below Generalised Gardner Equation (GGE) to find new exact solutions:

$$u_t + (p + qu^n + ru^{2n})u_x + u_{xxx} = 0, n \geq 0 . \tag{2.1}$$

To do so the Extended Trial Equation Method (ETEM) was used to find the exact solutions of GGE (e.g. soliton, rational, Jacobi elliptic and hyperbolic function). These solutions highlight

various aspects of the solutions to the Nonlinear Evaluation Equations (NLEEs). Subsequently, real and imaginary values of some of those exact solutions have been drawn in 2D and 3D graphics for some parameters. The research illustrates that ETEM can be applied as a powerful mathematical tool to obtain various analytical solutions of GGE and can be extended to other NLEEs in theory of solitons' domain.

Looking more specifically into deep ocean rogue waves, Dematteis et al. (2018) investigated the appearance of rogue waves and propose a method to identify ocean states that could occur before a rogue wave. To do so, the Modified NonLinear Schrodinger (MNLS) equation is applied in 1D. The assumption is that the random initial conditions are normally distributed, and a spectrum approximating a unidirectional sea state has been used. The available information from the spectrum combined with the MNLS dynamics allows the ocean surface elevation to be reliably estimated and predicted.

Dematteis et al. (2018) conclude that rogue waves occur when unlikely pockets of wave configurations introduce large disturbances in the surface height. It is interesting that sea states that precursor rogue waves and these pockets include wave patterns which are of regular height, but very specific in shape which can be identified explicitly. Identifying these specific wave patterns could lead to the early detection of rogue waves. Combining Monte Carlo sampling with large deviations theory simplifies the calculations of potential rogue wave precursors to an optimisation problem which is solvable efficiently.

2.2 Investigating shallow water equations

A preliminary study was conducted by Henry & Thomas (2017) to predict the regular and 2D surface waves following the recovery of pressure at the sea bed. They included in their model, the presence of a steady current which may comprise an arbitrary velocity distribution. This is as a result of their literature review which highlighted that previously existing methods which use pressure recovery in the presence of current mainly assume currents to be either constant or with constant vorticity; in those cases the wavefield becomes irrotational.

Using the Moderate Current Approximation (MCA), Henry & Thomas (2017) describe the sea bed pressure relationship with surface elevation in shallow waters and discuss the effect of the pressure function on the seabed on the free-surface profile elevation. They present a general pressure-stream function relation for regular waves interacting with an arbitrary profiled current and identify the importance of a change in velocity. Their results point to a good approximation for various current profiles, however they acknowledge that the accuracy of their model is dependent on the velocity of the current that is inputted. They conclude that their method could be applied to both near shore and offshore environments.

Francius & Kharif (2017) extended the Rienecker & Fenton (1981)'s method and applied it to numerically model and investigate the normal-mode perturbations of a 2D finite-amplitude gravity wave propagating on a linear shear current. The assumption is that the current is of constant vorticity. Their approach allows the waves to be modelled accurately with or without critical layers and pressure anomalies. Using this linear stability analysis, which was carried out both in deep and shallow waters, and extends the scope and results of previous simulations, it is possible to extend a weakly nonlinear (Schrödinger equation) analytical result (from past literature) to higher values of the wave steepness and fully nonlinear waves.

The results of Francius & Kharif (2017) research also led to the discovery of new instability bands (in addition to modulation instabilities). These instabilities correspond to quartet and quintet instabilities, not sideband disturbances. It was observed that the growth rate of the quartet instabilities will increase with a rise in the shear in opposite shear currents. This

is the opposite effect for most unstable sideband instabilities whose growth rate would reduce with increased shear.

2.3   *Waves interacting with other phenomena*

Although the interaction of waves with other phenomena (current, ice, etc.) does not changes the non-linearity, it certainly adds extra turbulence and complexity to the system which needs to be included in the model. Next recent advances in such models are reviewed.

2.3.1   *Wave- ice interaction*

With the significant effect of climate change on the melting of polar ice, increase in the Fluid-Ice-Structure Interaction (FISI) scenarios is inevitable. This, combined with the opening of Arctic routes, calls for more attention to the topic of FISI.

Huang et al. (2019) investigated the ocean wave interaction with large sheet of ice which due to their size proportions (can be several kilometres) would have a dominant hydroelastic response as opposed to a rigid body motion. The interaction was modelled using a combination of methods: CFD to simulate the hydroelastic interaction between ocean wave and ice, Navier-Stokes equations simulating the fluid domain and the St. Venant Kirchhoff solid model to include a simulation of ice deformation. These were complimented with a fluid-structure coupling scheme. Their approach, when compared to experimental results was shown to be able to capture previously left out phenomena such as predicting "overwash".

Kellner et al. (2019) used machine learning to predict ice behaviour. Ice material models often limit the accuracy of ice related simulations. The reasons for this are manifold, e.g. complex ice properties. One issue is linking experimental data to ice material modelling, where the aim is to identify patterns in the data that can be used by the models. Commonly given transition strain rates for freshwater and saltwater ice are 10^{-4} s^{-1} and 10^{-3} s^{-1}, respectively, at -10°C. One of the major challenges is the definition of ductile to brittle failure transition. A comprehensive (publicly available) database has been setup with experimental data gathered from literature. The database is analysed with correlation analysis, principal component analysis and Decision Trees (DT).

Results illustrate that the transition strain rate for freshwater ice given by the DT is one magnitude higher than the literature values ($10^{3.05}$). A possible reason for this deviation is that the DT strain rate is based on a dataset which lumps together the results of different experimental setups and conditions. Another unexpected result is that the DT transition strain rates for saltwater and freshwater ice are almost identical. However, for the saltwater ice DT, the transition strain rate only applies to temperatures lower than -9.95° C. Hence it cannot be seen as a general transition strain rate in a strict sense. As such, a direct comparison to literature values or the freshwater transition strain rate is less meaningful.

2.3.2   *Wave-current interaction*

Wave-current interaction is a complex phenomenon and as discussed by Babanin et al. (2017), probably least developed of all wave-other-phenomena interactions when it comes to mathematical modelling accuracy. Babanin et al. (2017)'s review of various approaches in modelling this interaction stresses that most currently applied theories and mathematical models used to model the three-dimensional oceans, are two-dimensional; although maybe more straight forward, this is understandably not an accurate representation of the waves and significantly alters the wave processes. When developing wave models, especially when considering any interaction with currents, both linear and nonlinear effects of currents on waves must be included for an accurate representation.

One main concern is the "non-existence" of nonlinear effects in the aforementioned models. So, although linear effects are assumed to be included, although not usually verified, the nonlinear effects including, interactions with currents with horizontal or vertical velocity gradients and energy and momentum exchanges between wave and the current and so on are either left out intentionally or are simply "unknown". Moreover, through Stokes drift and more importantly radiation stress caused by the loss of momentum in breaking waves, ocean waves can significantly affect the currents on the water surface. These affects, again, are predominantly non-existent in current ocean circulation models. Babanin et al. (2017) argue that due to their significant effect on currents behaviour, wave models must be reintroduced through coupling with circulation models, but they advise caution. This is directed mainly towards currently available wave forecast models which produce "approximate" rather than "accurate" fluxes for input and dissipation. This approximation is enough to predict, reasonably well, the resulting wave growth and height, however, and especially in finite depths, where wave breaking is significant, it is crucial to take into account the effects of waves on currents which are known and accounted for in coastal circulation.

Babanin et al. (2017) add that in addition to the above, the inclusion of the interaction between turbulence and wave-current is becoming more popular; although comparatively small in energy magnitude, they point that this interaction may be important in terms of additional and missing feedback in the atmospheric boundary layer, where waves and currents are generated by airflow. They conclude that all these complex dynamics, some not totally understood and modelled, point to a research field worthy of further investigation to benefit engineers and scientists in various disciplines.

3.   NUMERICAL MODELLING

3.1   Waves

3.1.1   Phase resolving models

Phase-resolving modelling of sea waves can be based on different techniques, such as analytical models, models based on (non-linear) potential flow, or computational fluid dynamics (CFD). Recent analytical work include Alberello et al. (2016) and Johannessen (2020), who developed analytical methods to derive the second-order kinematics underneath measured wave elevations. These methods can be applied to measurements in a wave basin or in the field, but it cannot deal with breaking waves. Non-linear potential flow wave modelling can yield good results as long as waves do not break, and viscosity plays a small role. Recent work on non-linear potential flow codes includes Ducrozet et al. (2020), who used a higher-order spectral method for backwards wave propagation towards a wave generator, and Bitner-Gregersen & Gramstad (2019), who used a higher-order spectral method to compare linear, second-order and third-order spatial and temporal wave statistics. Codes based on this approach are increasingly used in combination with fully non-linear CFD, for instance to initialize the wave domain or to perform wave propagation up to a certain critical wave crest for wave-structure interaction (see e.g. Li et al. (2021c)).

There have been significant advances in fully non-linear CFD modelling of non-linear waves during recent years. These advances have been mostly related to particle-based Smoothed Particle Hydrodynamics (SPH) and grid-based Eulerian Navier-Stokes (NS) methods. Many CFD studies have focused on the detailed modelling of steep or breaking wave events, for application for instance in wave impact studies on maritime structures. Examples include Ge et al. (2018) for slamming loads on a sailing ship with NS method OpenFOAM, Bandringa & Helder (2018) for breaking wave impacts on a floating platform with NS method ComFLOW,

Bandringa et al. (2020) for green water loads on a sailing ship with ComFLOW, and Kawamura et al. (2016) for green water impacts on a sailing ship with SPH.

Validation of individual steep and breaking wave modelling in CFD can be done by comparing the wave elevation and kinematics to particle image velocimetry (PIV) measurements. This type of validation was performed by Düz et al. (2017, 2020) for Navier-Stokes volume-of-fluid CFD method ComFLOW (stand-alone or coupled with non-hydrostatic potential flow tool SWASH), and by Alberello & Iafrati (2019) for a coupling of higher-order spectral method HOSM with a Navier-Stokes solver. These papers show good wave elevation and kinematics results for steep waves and breakers that do not include an air pocket, even with single-phase volume-of-fluid methods. However, the vertical water particle velocities at the tip of the wave crest were lower in the numerical simulations than the experiments in all three publications. Tomaselli & Christensen (2017) overturning breaking wave results with a two-phase CFD solver that can account for air entrainments. They showed that including the air bubble resulted in a significantly different impact loading on a cylinder.

The aforementioned studies focus on very short time traces and the modelling of a single extreme wave crest. Lande & Johannessen (2018) presented a comparison between two different CFD codes (ComFLOW and open-source BASILISK) for the propagation of steep and breaking short-crested waves, which is associated with larger three-dimensional domains. Generally, the results show that propagation of these highly nonlinear irregular waves are quite reproducible. An overview of wave reproduction techniques in CFD, both based on events and for longer time traces, is provided by van Essen et al. (2020). Three-hour wave-only simulations with CFD are also used in Bunnik & de Ridder (2018) to derive loads on wind turbines. Baquet et al. (2017) and Baquet et al. (2019) directly include the structure models in the CFD domain for long durations, with good results. The quality of the CFD modelling results still depends on the choices made in the wave input, grid and time step settings. Rapuc et al. (2018) presented guidelines on wave modelling with grid-based CFD methods and Pákozdi et al. (2016) provided a procedure for the reproduction of extreme wave events from a basin in CFD.

While the CFD-based techniques have advanced in modelling detailed wave and loading events, they still remain computationally expensive. Non-linear potential flow methods are faster, but cannot be reliably applied to modelling of wave breaking and stability. Therefore, coupling tools with different levels of fidelity seems a promising approach for long-term wave impact assessment. Coupling can be performed either directly or in incremental steps during design. The latter idea is the background of the wave screening approaches in Bunnik et al. (2018), Bunnik et al. (2019), Stansberg (2020) and van Essen et al. (2021), which use a quick (weakly non-)linear tool to identify critical events. Before a low-fidelity linear or non-linear potential flow wave method is used to identify wave events, they have to be translated to inflow conditions for a CFD calculation or an experiment. This procedure is not straightforward. For stationary structures at zero speed, Johannessen & Lande (2018) propose a solution where linear wave events are substituted with a similar fully non-linear event from a database. Also Pákozdi et al. (2019) describe a new fully non-linear potential flow tool, which works within a framework that can also be applied to perform two-phase Navier-Stokes CFD calculations, allowing more efficient modelling on various fidelity levels. Bouscasse et al. (2020) present guidelines for the coupling of wave and CFD solvers.

3.1.2   Spectral models

The scientific community has developed a series of phase-averaged spectral models called Third Generation wave models such as WAM (WAve Model: WAMDI Group, 1988), WAVEWATCH III (WW3: Tolman (2009); Tolman et al. (2002)) and SWAN model

(Simulating Waves Nearshore: Booij et al. (1999) and Ris et al. (1999)) which are being widely applied for global as well as regional ocean state forecasts up to the nearshore zone. An overall review of the present situation and challenges in wind waves modelling is presented in Cavaleri et al. (2018), in particular of the inner and coastal seas. The theories of many physical processes are still unclear. For the nearshore processes, Beyramzade & Siadatmousavi (2017) implemented two viscoelastic models in SWAN and assess their performances for field applications. A new parameterization to improve the performance of SWAN in simulating significant wave heights (SWH) in coastal waters was introduced in Lin & Sheng (2017). To investigate wave damping due to porous seabeds in nearshore areas, the wave dissipation coefficient for submerged porous media was incorporated into the WWM model Hsu et al. (2018). Yevnin & Toledo (2018) derived an analytical source term for the bottom reflection of oblique incident waves in the spectral wave models, proved to be in excellent agreement with the mild-slope equation for different slopes, wave periods and attack angles. To parameterize the dissipative effects of small, unresolved coastal features in computational mesh, Mentaschi et al. (2018) developed an open-source library for the estimation of the transparency coefficients, which has been implemented in WW3. Notably, in WW3, the well recalibrated and verified observation-based source terms were updated to ST6 for parameterizations of wind input, wave breaking, and swell dissipation terms Liu et al. (2019d).

Generally, the present day third-generation wave models are capable of predicting the waves reasonably well, but their accuracies can be improved with specific local seas. Umesh et al. (2017) made a series inter-comparison of regional wave hindcast in the northwest coastal domain of India. They concluded that the JONSWAP model could not describe the high-frequency tail (Umesh & Swain (2018); Umesh et al. (2018)). The model coupling methodology was used in nearshore wave transformation for the NACCS using STWAVE and provided overall good nearshore wave estimates (Bryant & Jensen (2017)). Liu et al. (2017) intercompared the performance of WW3 and University of Miami Wave Model (UMWM) under hurricane condition, and concluded that UMWM shows less accuracy than WW3 in specification of bulk wave parameters. A coastal wave forecast system based on SWAN for the East Coast of Korea waters was developed and validated in Caires et al. (2018). Campos et al. (2018b) investigated three types of surface-wind product calibration and their impact to nine wave hindcasts constructed using WW3 in the South Atlantic Ocean. Chen et al. (2018a) provided a framework for coupling Finite-Volume Community Ocean Model (FVCOM) and the SWAN using Model Coupling Toolkit. Dora & Kumar (2018) revealed that the NCEP/CFSR wind is comparatively reasonable in simulation of nearshore waves using the SWAN model nested by WW3 at an island sheltered coast Karwar. A high-resolution SWAN wind wave hindcast model was implemented and calibrated for the Sea of Marmara in Kutupoğlu et al. (2018). Chen et al. (2018b) emphasized the importance of spatial resolutions in wave simulations in the open ocean using WW3 and SWAN. Mahmoudof et al. (2018) mentioned the importance of breaker index in SWAN during wind wave modelling in very shallow water at the Southern Coast of the Caspian Sea. Perrie et al. (2018) made a comparison between different wave model systems, they suggested that the performance of WW3-ST4m was the overall best. For the West Mediterranean basin, SWAN was implemented and evaluated with high spatial resolution and accuracy in the northern and southern parts in Amarouche et al. (2019). Typhoon waves in the shallow waters around the Zhoushan Islands were simulated using WW3 in Sheng et al. (2019).

Wave models are widely used in the wave hindcast studies, for the purpose of long-term study of wave climate and wave energy distribution. Lavidas & Venugopal (2018) made an overall review of the spectral models' status in the process of wave power assessments at the European coastline regions and the Black Sea. In the context of wave climate study, a thirty-seven year

wave hindcast (1979-2015) in Chesapeake Bay was generated by SWAN and applied to extreme value analysis for specific return periods (Niroomandi et al. (2018)). Li et al. (2018d) presented a long-term trend of SWH in China's coastal seas based on both satellite measurements and numerical hindcasts by WW3. The possible local changes in the wave climate for the coastal waters off eastern Canada were analysed based on simulations of the waves from a WW3 in Wang et al. (2018e). Long-Term characterization of sea conditions in the East China Sea was presented using SWH and wind speed hindcast in Zheng et al. (2018). A global high-resolution ocean wave model was improved by assimilating the satellite altimeter SWH in Yu et al. (2018b). For the assessment of wave power in specific seas, SWAN was applied to reflect the spatial distribution of the wave power in the Iberian coastal environment in Rusu (2018). An assessment of wave power resource for Portugal continental coast was presented, using thirty three years (1979-2012) of wave hindcast based on SWAN nested WW3 system in Silva et al. (2018).

3.2   Ice

Numerical modelling of sea ice often has problems where ice failure has a major role. This is one major factor making the modelling challenging. Scientific questions related to sea ice span across scales and, roughly, modelling is currently performed fairly independently on geophysical scale and on engineering scale. The geophysical scale modelling, often related to sea ice dynamics, is performed on scales $10^4…10^6$ m. Common work on this scale focuses on understanding the ice growth, melting, and motion of ice on the scale of polar ice pack, studies using coupled climate system models, and research on the effects of climate change on sea ice. The engineering scale simulations, usually performed on ice-structure interaction, are performed either on the scales of $10^0…10^2$ m or $10^{-2}…10^0$ m. First is the scale for modelling ice-structure interaction processes and latter for material modelling or modelling of individual ice-structure contacts, respectively.

3.2.1   Geophysical scale

Geophysical scale models often use continuum models and central questions appear to have been related to the rheological models with an ability to describe fine scale ice features and sub-grid scale phenomena. This goal is important for, not only increasing the predictive power of large-scale sea ice dynamics models, but allowing the use of large-scale models for operational forecasting or with predicting ice behaviour close to coastal areas (Holt et al. (2017)). From the aspect of sea ice dynamics, ice deformation events are highly localized spatially and temporally, and techniques for catching these events with high enough resolution are needed (Rampal et al. (2019)). Central parameter for large-scale models is the strength of ice; compressive strength in this scale is commonly related to ice ridging. Roberts et al. (2019) describe a model, which describes the ridge microporosity and energetics of ridging in a form that can be used in earth system models.

Further, Weiss & Dansereau (2017), Hutter et al. (2018) and Dansereau et al. (2021) present, describe and at least partly validate rheological models with increased capabilities to describe strong discontinuities in the ice cover. The need for even higher resolution in modelling sea ice appears to have been widely recognized by the ice dynamics community in Blockley et al. (2020); Hunke et al. (2020) limits for the applicability of the currently used continuum models has been recently questioned. Discrete element method (DEM) is considered as one technique to be used for such work as it allows modelling of individual ice features, such as ice floes, and their interaction. Some large-scale models relying on DEM already exist with more developments in the near future.

3.2.2   Engineering scale

In engineering scale ice mechanics, DEM is readily a commonly used simulation technique and is been used in a variety of applications as described by a recent review by Tuhkuri & Polojärvi (2018). In addition to traditional DEM, modelling by using event based dynamics, have also recently emerged as an alternative in van den Berg et al. (2018). Recent work on numerical simulations on intact ice has focused on mechanics of ice loading processes. Ranta et al. (2018a) and Ranta & Polojärvi (2019) studied the mechanisms that limit ice loads on inclined structures and were able to derive simplified buckling and local crushing models, respectively, which predicted the maximum load values with fair accuracy. Bridges et al. (2019) used DEM together with laboratory scale experiments to study how ice properties affected ice loading process and ice encroachment, the tendency of ice advancing on top of a structure, on shallow water offshore structures. Lemström et al. (2020) focused on DEM modelling of a similar ice loading scenario.

Some of the recent studies have also focused on assessing the scatter in the ice load, that is, the aim has been to gain insight on the sensitivity of the ice loading process (Ranta et al. (2018b), van den Berg et al. (2020)). A common way to perform this type of studies is to vary the boundary or initial conditions, and ice feature configurations and repeat loading processes. Simulations are an ideal platform to use in such studies, since they allow full control on ice parameters and a large number of repeated numerical experiments.

Often ice engineering problems, such as ship-ice and ice-slender structure interaction, require three-dimensional modelling of the failure process of intact ice sheets. Doing this in sound physically based simulations is not straightforward, but effective techniques are starting to be developed Lilja et al. (2019a, 2019b, 2021). There are also linear elastic fracture mechanics-based approaches for modelling ice failure. Such approaches can increase the efficiency of the simulation ice failure and have been successfully used by van den Berg at al. (2019), even if the applicability of using linear elastic fracture mechanics in connection with ice has been questioned by some authors. Hasegawa et al. (2019) introduced a fairly simple three-dimensional model for deformable and failing ice floes, but the approach presented would allow modelling larger ice sheets as well.

Instead of modelling intact ice, there have been several recent efforts on studying ice resistance on ships when a ship travels through an ice floe field or an ice ridge. Models with capability to describe interaction of individual ice features are well suited for such studies. Van den Berg et al. (2019) and Yang et al. (2021a) studied the effect of floe geometry on the total ice resistance of a ship. The two studies yielded similar results, as it was found that the ice resistance decreased when the floes became more round. Model by van den Berg et al. (2019) was two dimensional, but allowed floes to fail. Yang et al. (2021a) suggest that three-dimensional modelling is needed, since the rafting of the floes has a role in the process. Polojärvi et al. (2021) also studied ship passage through a floe field by using three-dimensional DEM (Fig. 1), but instead of ice resistance, focused on ice loads and compared the results to full-scale measurements. Further, approaches for studying the same problem when accounting for hydrodynamics as well, has been described by Mucha (2019), Yang et al. (2020) and Huang et al. (2020). Gong et al. (2019a, 2019b) investigated ice rubble resistance on a ship and found that the ridge resistance is proportional to length of an ice ridge, that is, the extent of the ice ridge into the direction of ship motion. This finding could affect the techniques used for route planning in ice. Work that includes all features – three-dimensional simulations accounting for ice failure and hydrodynamics in lengthy loading process – does not exist yet.

Recent work in modelling ice using finite element method (FEM) has been focusing on engineering scale ice simulations on material modelling and failure. O'Connor et al. (2020)

introduced a numerical implementation of a micromechanics based viscoelastic material model for saline ice. Such models are of importance in studies, where the energy dissipation due to ice deformation is needed to be accounted for. Such studies could include accurate models for wave-ice interaction or even larger scale ice models making notions on pre-failure behaviour ice. Kolari (2017) introduced a wing-crack based damage model to study the failure of quasi-brittle materials, and further Kolari (2019) showed, that it can be successfully applied to modelling the failure of ice samples under bi-axial compressive stress. Integrating detailed material and failure models to ice-structure interaction simulations could increase their accuracy and reliability, yet the computational efficiency may become a restricting factor for such developments. One step towards increased efficiency is the approach by Gribanov et al. (2018a, 2018b), where ice failure is modelled using cohesive elements and parallel computing based on graphics processing units.
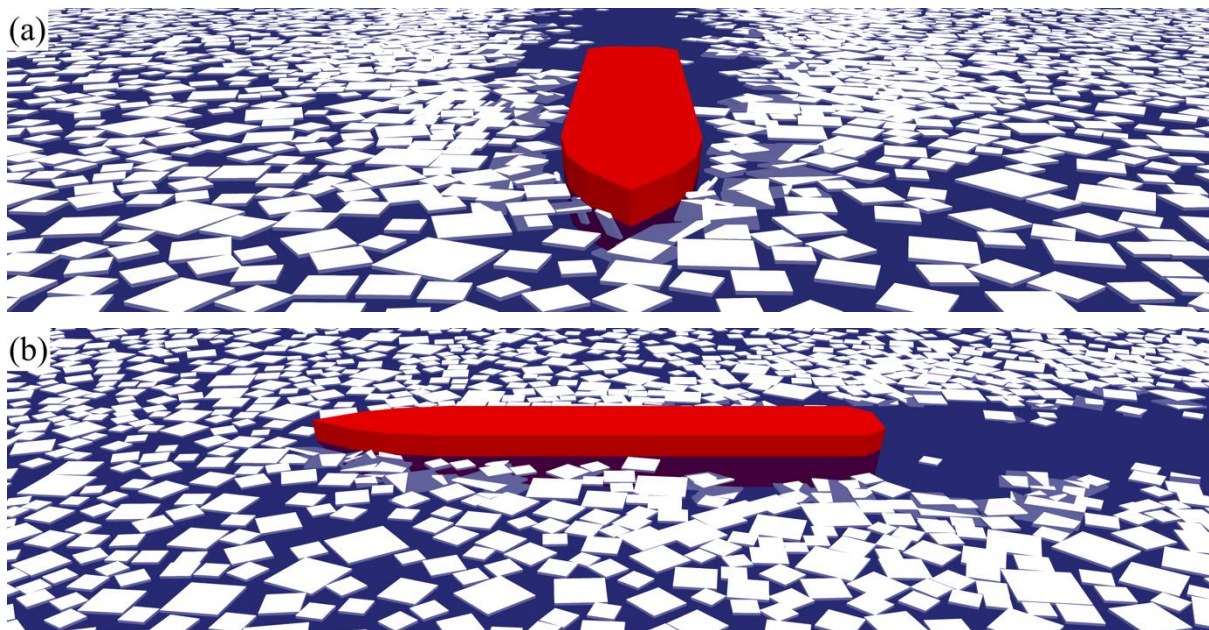
Figure 3.1: Three-dimensional discrete element simulation snapshots from (a) the front and (b) the side of a ship advancing through an idealized ice floe field (Polojärvi et al. (2021)).

4.   MEASUREMENTS AND OBSERVATIONS

4.1   Waves

4.1.1   Laboratory measurements

Instrumentation and approach

Measurement and calibration of wave elevation in wave basins is important for a correct representation of specified wave conditions. Tukker et al. (2019) investigated the accuracy of resistance-type wave measurement probes, and concluded that such instruments are not fully linear. Corrections to conventional linear calibration are proposed in order to obtain the correct wave elevations, and some possible improvements to the probes are suggested. More general, Collins et al. (2018) presented qualitative metrics to evaluate the quality of wave fields in basins, and Huang & Zhang (2018) presented acceptance criteria for experimental wave crest distributions. Iterative wave calibration procedures are common practice for position-controlled wave generators. Reich et al. (2018) present an assessment of a similar procedure for force-controlled wave generators. The metric proposed by Perlin & Bustamante (2016) can be used to compare the similarity of two wave records, both in phase and amplitude.

Some new approaches in laboratory scale observation techniques have also been developed. Most of these are based on image processing. An innovative image-processing method developed to track the free surface elevation by submerged air bubbles is presented by Vargas et al. (2020). Douglas et al. (2020) showed that wave run-up characteristics can also be measured from image-processing results. Van Meerkerk et al. (2020) used an "scanning stereo-PLIF" measurement system consisting of a stereo-camera set-up to measure time-dependent two-dimensional free-surface elevations over a domain length of 100 mm. This was successful down to amplitudes of 0.2 mm. Watanabe et al. (2019) reconstructed 3D wave fields using a stereo-camera system, and successfully used these results to validate a non-linear method to derive the wave field in a larger domain. Bakker et al. (2021) discusses a particle image velocimetry (PIV) system based on pulsed LED light for measurement of the kinematics in wave impacts, as less complicated alternative to conventional laser-based PIV. Han et al. (2018b) evaluated the uncertainty of PIV measurements in the wake of a ship. The results of this study in a semi steady flow will be different than for PIV measurements in waves, but the principles of the uncertainty assessment can be used as reference. Finally, Jacobi (2020) presents a method to derive amongst other things pressure fields from velocity data measured with PIV.

The development of numerical methods such as CFD increases the quality requirements for laboratory measurements. The knowledge about the kinematics underneath waves for instance becomes more and more important, as numerical methods show their importance for wave impacts on marine structures. Johannessen (2020) developed an analytical method to derive the 2nd order kinematics underneath measured wave elevations. Such a method can be applied to measurements in a wave basin or in the field, but it cannot deal with breaking waves. Detailed PIV measurements of steep and breaking wave crests were presented by Alberello & Iafrati (2019), Düz et al. (2017, 2020); some examples are shown in the Figure 4.1. These publications also show comparisons with the wave kinematics in CFD, which shows that it can provide quite good results. Shallow-water kinematics of waves moving over a bar were measured using high-resolution optical instrumentation by van der A et al. (2017).
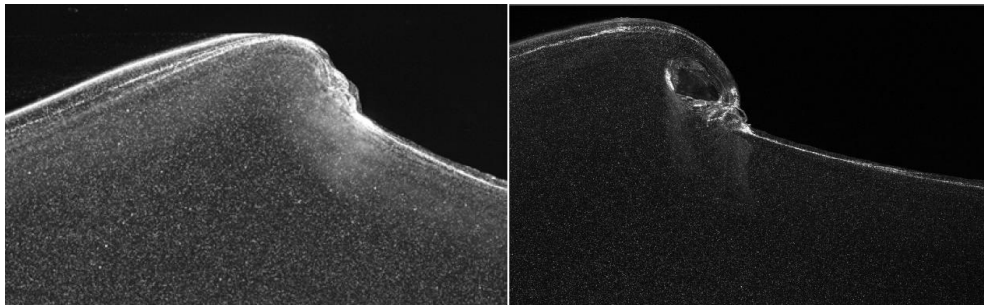
Figure 4.1: PIV images of a spilling (left) and plunging (right) breaking wave
(Düz et al. (2020); Copyright © 2020 ASME).

When generating waves in basin, it is important to be aware of the basin limitations, and possible unwanted wave effects. Van Essen et al. (2020) presents an overview of what is important when experimental wave modelling is reproduced numerically or vice versa. This requires consideration of non-linear wave effects and (unwanted) basin effects. Reflections and basin sloshing modes on shallow water (Pákozdi et al. (2019)) have to be considered when model test results are used in design. It was shown by (van Essen & Lafeber (2017)) that small 3D residual currents with strengths around 1-2 cm/s may occur in seakeeping or ocean basins under the influence of repeated wave generation (Figure 4.2). These decay very slowly, and they can influence sensitive measurements such as added resistance of ships in waves or current loads on structures. These small currents and details of wave breaking may reduce the

repeatability of wave fields in basins; an evaluation of the resulting variability of the wave field is presented by van Essen (2019). Wave generators always introduce unwanted spurious waves, due to the difference between their shape and real-world wave kinematics profiles. Such effects are usually minimized at the wave generator using classical 2nd order wave theory developed in the 1960s. Khait & Shemer (2019) present an improvement of this wave generator correction theory based on fully non-linear wave models instead of 2nd order theory. All of these basin effects have to be considered when a deterministic wave event needs to be generated at a target location in a basin. This requires non-linear backward translation of the event to the wave generator, in order to determine the required wave generation motions. Many methods apply an iterative procedure to do this: for example Niu et al. (2020) presents an iterative method to generate a deterministic extreme wave event in a basin, based on 2nd order wave generation theory. Ducrozet et al. (2020) describes a non-iterative 'time reversal' method to do this, which they validated for steep and highly non-linear wave events.

Another important issue to be aware of during wave experiments is scale effects. A detailed study of all aspects to consider in sloshing waves in an LNG tank was presented by Bogaert (2018). This included a study of the surface instabilities, air inclusions and shape of the incoming waves. This is important for the scaling of wave impacts on LNG tank walls, but also for that of undisturbed waves. Van Essen et al. (2020) also discusses scale effects in steep and nearly breaking wave crests in a model basin, focusing on the incoming waves of the tests presented in Scharnke (2019). This study showed that scale effects and the effect of air pressure in steep and breaking waves are small, as long as there are no air inclusions or surface instabilities. Babanin & Palenque (2021) announced the start of a field measurement campaign on the effects of air pressure and fetch on wind-wave interaction models, at high-altitude Lake Titikaka. The outcomes of this study may also be relevant to understand scale effects in air pressure above propagating waves in laboratory testing.
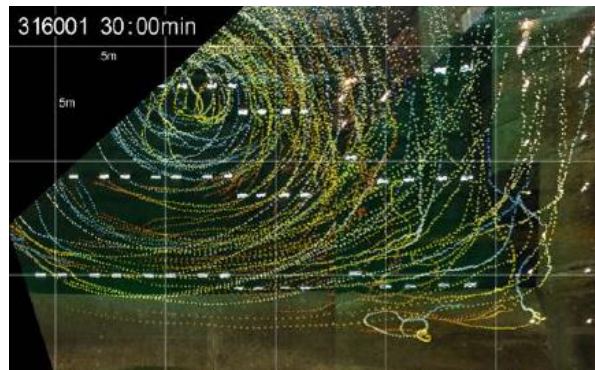
Figure 4.2: Visualised current patterns at the edge of a seakeeping basin after oblique wave generation ((van Essen & Lafeber (2017); Copyright © 2017 ASME).

Wave flumes

A new wavemaker was proposed to reduce the reflection effects of waves in hydraulic wave flumes (Mahjouri et al. (2020)). Various physical model tests are reported being carried out in wave flumes including the wave overtopping discharge quantification experiments (Williams et al. (2019)), particle tracking velocimetry experiments (Calvert et al. (2019)), Stokes' wave theory validation experiments (Windt et al. (2021)) and the wave breaking kinematics experiments (Craciunescu & Christou (2020), Liang et al. (2020), Xu et al. (2020b)).

Wave tanks

A wave tank is a laboratory setup for observing the behaviour of surface waves from large beach morphology investigations to complex harbour and breakwater models. In recent years,

many research works have been conducted in wave tanks. Wang et al. (2019c) explored seabed instability and the law for pore pressure response under wave actions under the scale basin of the Yellow River Delta. Xu et al. (2019) experimentally investigate the generating results of space-time focusing waves based on different wave spectra, they found that the focusing time strongly relates to the energy of the highest-frequency wave component of the wave spectrum. The generation of tsunami waves are investigated in Lima et al. (2019). The propagation of waves under different reef fringed coasts is investigated in Yao et al. (2019, 2020).

McAllister et al. (2019) studied the generation of rogue waves such as the Draupner wave in laboratory conditions. They concluded that waves with a very large steepness and height can occur in crossing seas with angles between 60 and 120 degrees. The result at 120 deg is shown in Figure 4.3. These results are supported by Dong et al. (2019), who showed that non-linear energy transfer during wave-wave interactions is very sensitive to the crossing angle of two interacting wave groups and that the severity of wave breaking increases with increasing crossing angle.
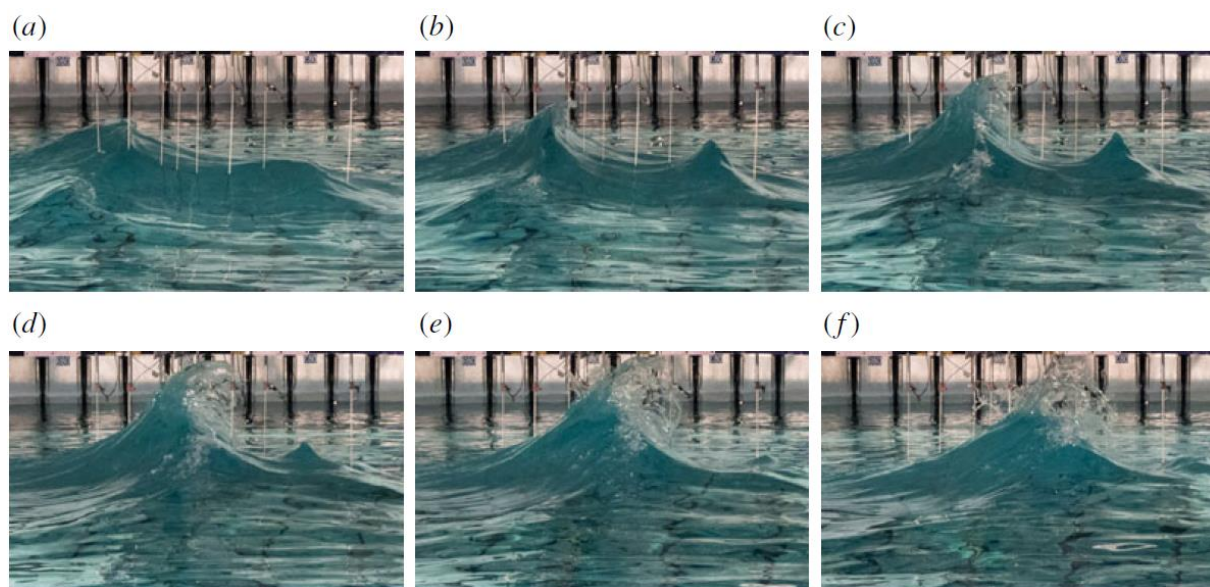
Figure 4.3: Images of the free surface taken at intervals of 100 ms in the wave basin (0.6 s at field scale), showing the most successful reconstruction of the Draupner wave for a crossing angle of 120 deg. Breaking is observed in front of an upward projected jet, which does not limit wave crest height under these crossing-sea conditions. McAllister et al. (2019); Open Access Article under Creative Commons Attribution licence; © 2018 Cambridge University Press.

Plans for some new wave basins were developed within the mandate period. The "atmosphere" or "multi-phase wave lab", a wave basin inside an autoclave, was built in the Netherlands (Novaković et al. (2020)). It can be used to model sloshing wave impacts, where pressure, temperature, current and gas composition can be varied. In Belgium, a shallow-water towing tank and a "coastal and ocean basin" are under construction (Geerts et al. (2018), Troch et al. (2018)). The latter basin will have the ability to generate waves in combination with currents and wind in different directions in shallow and intermediate water depths. ITTC (2017) also lists a new seakeeping and manoeuvring basin in India and a new towing tank with wave generation facilities in China.

Wind-wave flumes

Air-sea momentum transfer was investigated in a 15-m-long wind-wave tank by Curcic & Haus (2020); they found an overestimate of 10-m wind speed and an underestimate of the drag coefficient in surface flux parameterization in operational weather prediction model.

Wave-ice tanks

Water wave attenuation by grease ice is a key mechanism for the polar regions, as waves in ice influence many phenomena such as ice drift, ice breaking and ice formation. Ocean wave forecasts in the ice-covered seas also require reliable modelling of ice effect on wave propagation.

Experiments in wave-ice tanks are a profound means to investigate experimentally wave ice interaction. Aalto University and the Hamburg Ship Model Basin (HSVA) are two ice testing facilities for model test experiments with a wave maker. Additionally, smaller wave-ice flumes exist such as at the University of Melbourne (SIWWI).

In scaled experiments using artificial model ice, the model ice that was designed for ship-ice interaction, might cause scale effects due to the relatively low stiffness (von Bock und Polach et al. (2019)). This stiffness does not scale correctly. In order to overcome this problem von Bock und Polach et al. (2020) proposed a new method by increasing the strength of the ice, which also increases the stiffness while at the same time the thickness is reduced to scale the critical bending moment and stiffness correctly, while accepting a reduced thickness.

Dimensional data and curve fittings face challenges when applying them to scenarios with altered conditions (Yu et al. (2019). On such basis Yu et al. (2019) introduced three dimensionless numbers reflecting the relative significance of effects due to ice inertia, effective elasticity and viscosity. Those can be used to identify the dynamic similarity between different scales.

Parra et al. (2020) conducted experiments at SIWWI with identical waves in level ice, ice floes and grease ice. The comparison showed that ice floes attenuated waves the least and level ice the most. The experiments have not been at scale and scaling methods are not yet established. An alternative to experiments with aqueous ice is presented in Sree et al. (2020) using a viscoelastic material, a blended mixture of white oil and Polydimethylsiloxane (PDMS). The experiments and the variation of material properties underlined the significance of the modelling of the viscoelasticity of ice for the wave attenuation. Experiments at Aalto Ice Tank with a wave spectrum of (Passerotti et al. (2020)) showed a frequency dependent wave attenuation in the form of f^3 which agrees with full-scale observations (Meylan et al. (2018)). A different set of experiments conducted at HSVA indicated the increase damping for shorter waves in ice (Hartmann et al., (2020)).

In a small-scale wave tank experiment, PIV combined with an array of ultrasonic probes were used to measure wave elevation by Cheng et al. (2019), Rabault et al. (2019). These publications examine a single-period wave propagating through an array of ice floes using both physical measurement and a theoretical approach. Laboratory observations of wave energy attenuation in fragmented sea ice cover composed of interacting, colliding floes are quantified by Herman et al. (2019). Dependence of the attenuation and dispersion of surface waves in a variety of ice covers in wave frequency and ice conditions are also investigated and demonstrated by Yiew et al. (2019).

Wave-current and towing tanks

It is important to investigate the effects of current on wind waves, called the Doppler shift, at both normal and extremely high wind speeds. Takagaki et al. (2020) used three different types

of wind-wave tanks along with a fan and pump to demonstrate the effect of the Doppler shift of wind waves and currents in laboratories. They found that at normal wind speeds, the significant waves are accelerated by the surface current. A weakly nonlinear model is more suitable for small-amplitude waves and strongly nonlinear and even breaking waves, which are typical for extreme wind conditions (over 30m/s) (Takagaki et al. (2020)).

In 4.1.1.3 some experiments to study the occurrence of rogue waves in wave basins were described. Toffoli et al. (2019) experimentally and numerically studied another rogue wave theory: that rogue waves can be generated in waves in opposing current. It was shown in two different basins that weakly non-linear waves can thus rapidly change to strongly non-linear waves, increasing the probability of rogue waves. Liao et al. (2018) also studied rogue wave occurrence in waves opposing a current. They showed that the breathers (strongly non-linear wave solutions focused on space and oscillating in time) can also evolve in opposing currents.

4.1.2   Field observations

Buoys and platforms

The majority of existing in-situ wave measurements are done using moored buoys. Buoys can be spherical, discus, spar, or boat-shaped hull. The most popular and widely used method measures buoy motion and converts the buoy motion into wave motion based on the hydrodynamic characteristics of the buoy. As shown in Figure 4.4, changes are being made to the super-structure configuration of NDBC buoys with the advent of the smaller hulls, improved battery packs, less power required and new compact sensor packages (Ardhuin et al. (2019b)). Recently, a low-cost, real-time, solar-powered wave measurement buoy named Spotter was developed. Overall, Spotter-derived bulk statistical parameters were within 10% of respective quantities derived from a Datawell buoy (Raghukumar et al. (2019)).
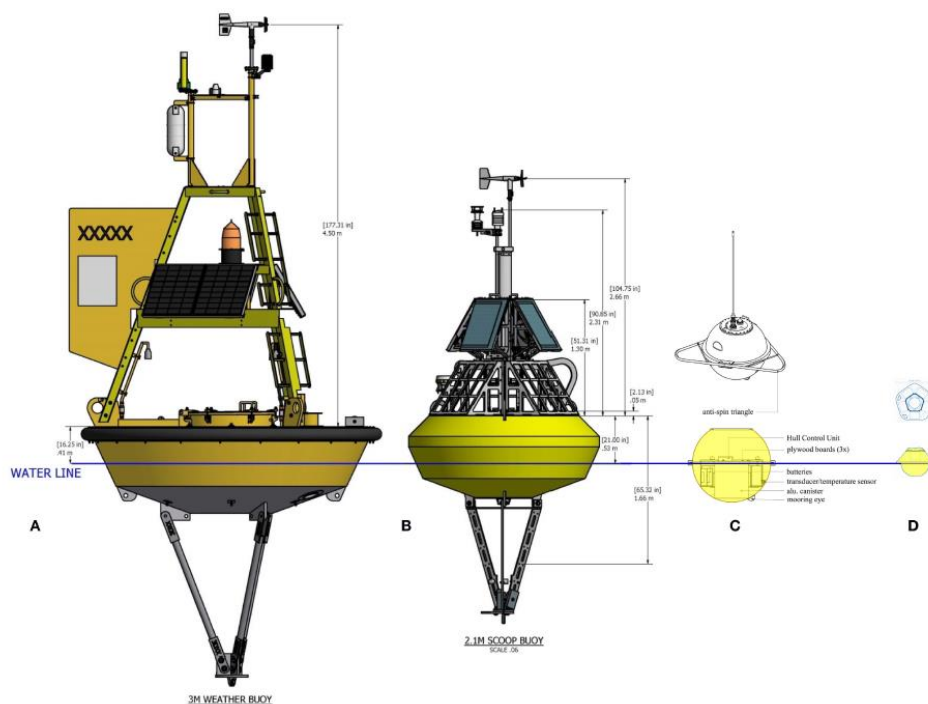
Figure 4.4: Schematics of existing and planned super-structures of NDBC moored buoys measuring waves (credit Eric Gay, NDBC; Ardhuin et al. (2019b). (A) is the standard design of 3-m discus buoys. (B) is the new SCOOP design with a 2.1 m diameter that is replacing many buoys. (C) is the schematic for the Mark 4 Datawell waverider with a 0.9 m hull diameter and (D) is the schematic of a Spotter buoy made by Spoondrift. Used with permission from Frontiers in Marine Science.

The Lagrangian motions of wave buoys applied to measure waves in the field may affect their measurements. This was evaluated using model experiments with a Lagrangian and Eulerian measurement next to each other in McAllister & van den Bremer (2019, 2020), see Figure 4.5. Based on these measurements, it was concluded that the motion of a wave-following buoy should not significantly affect the measured wave crest statistics or spectral parameters, and that discrepancies observed for in-situ buoy data are most likely a result of filtering. This was confirmed by van Essen et al. (2018), who showed that filters applied in a typical Datawell buoy roughly remove the frequency content below 1s and above 20s period. Thomson et al. (2015) compared the measurements of a clean buoy and one with biofouling side by side, concluding that only the high-frequency response of the buoy was affected by the fouling. Average parameters such as significant wave height, peak period and direction were not affected.
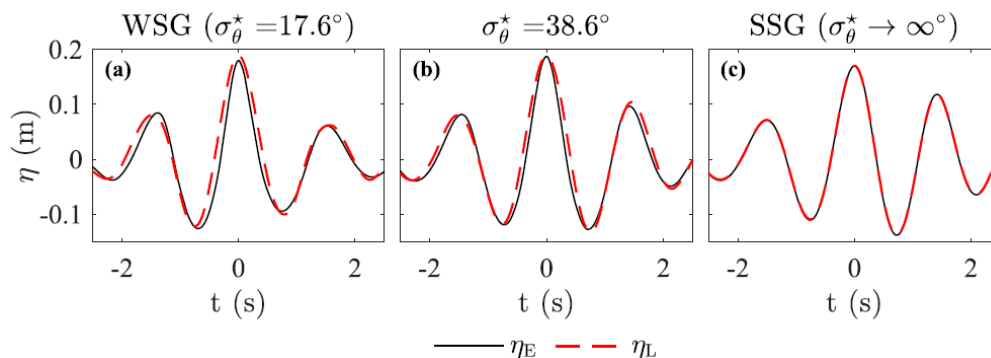
Figure 4.5: Comparison of total measured Eulerian (black lines) and Lagrangian (red dashed lines) free surface elevation for three different wave groups in McAllister & van den Bremer (2019). © American Meteorological Society. Used with permission.

Waves measured using a directional wave buoy at a location with 15 m water depth in the near-shore waters of the Gulf of Mannar during a 1-year period were reported in Amrutha & Kumar (2017). The annual average value (0.84 m) of the SWH in this area was comparable to that along the coastal waters of the Indian subcontinent. A dense network of buoys along the Brazilian coast, equipped with several meteorological and oceanographic sensors were reported in Pereira et al. (2017). In Collins et al. (2018), two deep-sea moorings were deployed 780 km off the coast of southern Taiwan for 4-5 months. Directional wave spectra, wind speed and direction, and momentum fluxes were recorded on two Extreme Air-Sea Interaction buoys during the close passage of several tropical cyclones . Dally (2018) conducted a cross-shelf wave transformation experiment off the Atlantic coast of north Florida for 53 days using two ADCPs. The data was used to test the ability of the SWAN (Gen2) nearshore wave transformation model. In Barbariol et al. (2019) a wave buoy was deployed in the Southern Ocean (south of New Zealand) for 170 days. This moored buoy transmitted spectral and time domain observations, including measurements during a storm with a particularly large individual wave of 19.4 m crest-to-trough height. After the 170 days, the buoy broke free of its mooring and started drifting, still transmitting the essential data.

Some local platform observations of winds, surface currents, and ocean waves are also reported, e.g. at the Southern Ocean (Babanin et al. (2019), Derkani et al. (2021), Young (2019)), the Northwestern Mediterranean Sea (Lorente et al. (2021)), the northeastern coast of the Persian Gulf (Heidarzadeh et al. (2019)), the Black Sea (Yurovsky et al. (2019)), a coastal station 4 km offshore L'Estartit in the Mediterranean Sea (Salat et al. (2019)), in Lake Erie (Valipour et al. (2019) and in a lagoon of the South China Sea focusing on typhoon characteristics (Cai et al. (2020)).

Under the requirement of reducing instrument costs, other in-situ observing techniques including the High-Frequency radar system (Saviano et al. (2019)), the Stereographic analysis of digital images system (Molfetta et al. (2020)), and the anti-typhoon riser system ((Jin et al. (2021)) are also used to estimate the parameters of sea states.

Rogue waves are hard to predict. Most studies therefore use laboratory modelling or simulations to study them (see e.g. 4.1.1.3). Häfner et al. (2021b) use a different approach: they applied machine learning methods to the large Free Ocean Wave Dataset (FOWD, (Häfner et al. (2021a)) in order to detect rogue waves. This database includes data from 158 buoys along the US coast and other areas, among which 1.5 billion individual wave crests, of which around 100,000 are considered rogue by the 2Hs definition. Based on this study, it was concluded that traditionally applied indicators for rogue wave occurrence (e.g. surface elevation kurtosis, steepness and Benjamin-Feir index) are weak predictors for real-world rogue waves. Instead, crest-trough correlation seems the dominating parameter in all studied conditions, water depths and locations. For rogue crests it was concluded that skewness, steepness and Ursell number are the strongest predictors, in line with second-order theory.

Drifters and ARGO fleet

Today, various system and devices are involved in monitoring global oceans to provide in-situ data in real-time or near real-time atmospheric, physical, and ocean measurements. The systems include, but not limited to, various buoys, drifters, gliders, sailing drones, aerial drones, and ocean observing satellites. While permanent buoy deployments can be a substantial challenge, drifting buoys, wave gliders and other moving platforms can prove feasible and valuable solution in this challenge for a combined international effort. The present state of global observations of surface winds, currents, and wave is reviewed in Rosa et al. (2021), Villas Bôas et al. (2019).

The most famous program is the Global Climate Observing System (GOOS), which consists of six main programs: Argo, the Data Buoy Cooperation Group, OceanSITES, the Global Ocean Ship-based Hydrographic Investigation Program, the Global Sea Level Observing System, and the Ship Observation Team (Davidson et al. (2019)). Wave gliders are a novel approach in keeping the unmanned observation platforms in the ocean with the help of wave-power. Lagrangian drifting floats are employed extensively for the measurement of ocean's currents especially near the surface. The Global Drifter Program (GDP) that was initiated by GOOS is covering the ocean with the help of 1250 drifter buoys, which were accomplished in September 2005 (Iqbal et al. (2019)). In Figure 4.6, the status in March 2018 of the elements of the GOOS, as tracked by the Joint Technical Commission on Marine Meteorology, is presented. The dots representing platform locations are sized to be visible, but the actual coverage of the ocean remains sparse.
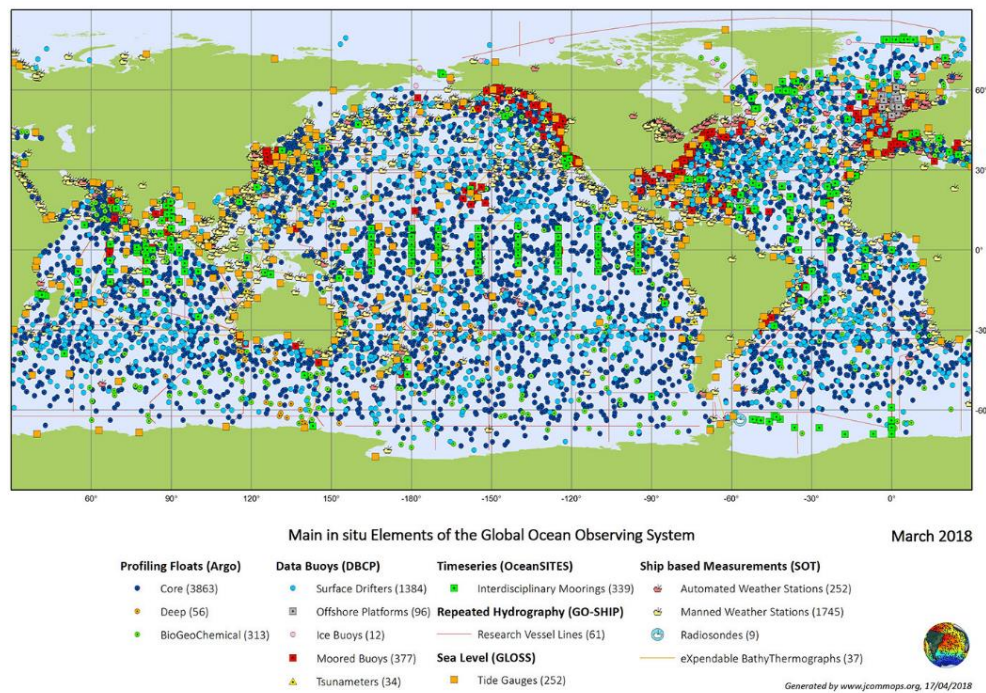
Figure 4.6: Main in site observation elements of the Global Ocean Observation System (Weller et al. (2019). Used with permission from Frontiers in Marine Science.

The drifter's global array is critical in fulfilling the desire for a thorough data set of real-time observations on global scale. In addition, these drifters are involved in the recording of both winds and the ocean's surface salinities The major contribution of the Argo's program is considered to be the observation of the seasonal to decadal climate variability in the ocean.

Gliders

The data from assimilating gliders is commonly used in short-term field observation experiment observations. In Northern South China Sea, glider observations are used to improve real-time marine forecasting skills (Peng et al. (2019)).

Measurements from sailing ships

Wave measurements from sailing ships can either be performed using ship radar (see 5.1), or using "ship as a wave buoy" (SAWB) techniques. In SAWB, the measured onboard ship motions, accelerations or stresses are used to derive the prevailing (directional) wave conditions. Of course this has some limitations connected to the ship response functions; for wave periods at which the ship does not or hardly move the wave elevation cannot be derived. This is similar to the limitations of wave buoys (see 4.1.2.1), but the latter are designed specifically to minimize issues in common wave periods. Ships are generally not, and the measurement quality for wave period ranges will depend on the ship dimensions and shape. An overview of available SAWB techniques is provided by Nielsen (2017), which also includes a discussion of such limitations. Another limitation is that ships generally avoid very bad weather, so the performance in extreme wave conditions requires additional validation.

SAWB measurements are usually done using the global ship motions derived from acceleration sensors. Nielsen & Dietz (2020) showed that it is possible to derive good directional wave spectra (compared to hindcast data) based on motion measurements at a containership, but that this estimate is sensitive for measurement errors in the advance speed of the vessel. Nielsen et al. (2019) shows how the estimated wave spectrum can be improved using a network of multiple sailing ships in the same area, attributing weights to the wave spectra obtained from

the motions of each of them. Chen et al. (2020b) used measured hull bending stresses instead of accelerations to derive the directional wave spectrum around two containerships and compared that to hindcast data and wave radar measurements. This approach was successful in the estimation of wave height and relative direction, but not of wave period. This is not surprising, as response functions of global ship bending moments are high for a relatively narrow range of periods. Mas-Soler et al. (2018) derived the wave spectrum around a model-scale semi-submersible based on its motions, with a focus on more extreme wave conditions. This worked well for the experimental conditions, using a method to estimate viscous damping in the ship motions. The aforementioned studies used first principles response functions to derive the wave spectrum. When the prevailing wave conditions around a ship are known (e.g. from a nearby buoy or platform, from hindcast data or from model experiments), data driven techniques can also be used to connect ship motions to wave conditions. This was done using regression methods by Thompson et al. (2019), who successfully derived wave heights from ship motions. The machine learning methods used by Düz et al. (2021); Mak & Düz (2019a, 2019b) successfully derived relative wave directions from the motions. Scholcz & Mak (2020) used deep learning to estimate the full directional wave spectrum. This was successful for the peak wave directions, but less for the peak wave period and height. SAWB techniques are also discussed in II.2 Dynamic Response.

After post-processing, ship navigation radar measurements (see Chapter 6.1) can also be used in combination with wave propagation and ship motion theory to predict ship motions in real time, for instance the next few minutes (Alford et al. (2015), Connell et al. (2015), Naaijen (2018); Naaijen et al. (2018)). This can be used in operation to identify a quiet period for lifting or the need to reduce speed. Complicated steps in this procedure are the derivation of wave height from the radar images and correct (non-linear) directional wave propagation from the edges of the radar image to the ship. The method from Watanabe et al. (2019), see also 4.1.1.1, can in theory also be used to reconstruct the wave field based on ship radar measurements instead of stereo camera images of the wave field.

Wave statistics based on hindcast databases along ship tracks

The current standard wave scatter diagrams in e.g. IACS (2001) were based on visual observations of several decades ago. Great progress has been made in wave modelling and global numerical hindcast wave datasets since then. Studies to investigate the possibility to improve the IACS wave standard based on global hindcast wave datasets have been carried out, e.g. by (Austefjord (2019), de Hauteclocque et al. (2020), Sasmal et al. (2019)). In these studies, several global hindcast wave datasets such as ERA5/ECMWF, IOWAGA/IFREMER regarding the North Atlantic Area were validated against measurements. Hindcast data were also compared with buoy and altimeter data in Ribal & Young (2019) and a comparison of hindcast databases and buoy measurements for the Southern North Sea was presented by van Essen & Peters (2017). These studies confirm that overall, global hindcast wave datasets give quite consistent results and agree fairly well with local measurements (although in specific coastal areas there may be significant differences). Application of these datasets to derive the wave scatter diagram for the wave standard of ship design seems possible today. On the other hand, local hindcast wave statistics and those actually encountered by sailing merchant ships are likely to be different. Considering that the wave statistics actually encountered are more important for design and operation of ships from a safety point of view, some studies on the wave statistics encountered by merchant ships in their voyages have been conducted recently in Austefjord (2019), Miratsu et al. (2019, 2020), Oka et al. (2018), Oka et al. (2019a), Oka et al. (2019b). In these studies, the wave statistics encountered by ships navigating at the North Atlantic Area were firstly estimated by different hindcast wave datasets, through matching the Automatic Identification System (AIS) tracks of merchant ships in different time periods. It

was confirmed that the actually encountered significant wave heights are several meters smaller than those purely based on the hindcast data. However, the available number of years of AIS data is very limited, so there is a challenge to combine the AIS and hindcast wave datasets in a 25-year long time period (which is considered as the design lifetime for various types of merchant ships).

Regarding this challenge, Sasmal et al. (2021b) proposes a statistical model representing storm avoidance by merchant ships and apply it to a newly computed 25-year wave hindcast "TodaiWW3-NK" (Sasmal et al. (2021a)) in the North Atlantic Ocean. The statistical model links the storm intensity based on the wave hindcast data with the distance of the ship from the storm center which is derived from the 2 years and 11 months of ship position records based on AIS. By the proposed statistical model, the 25-year wave statistics encountered by merchant ships in the North Atlantic Ocean is derived. The consequence analysis (quantitative evaluation) based on both the 25-year wave statistics (wave scatter diagram) encountered by merchant ships mentioned above and the 25-year wave statistics in natural is conducted by Miratsu et al. (2021) regarding different ship motions and wave loads. It is confirmed that there is a difference which is around 0.85 between the 25 year long-term prediction values of the ship motions and wave loads evaluated by the 25-year wave statistics (wave scatter diagram) encountered by merchant ships and those evaluated by the 25-year wave statistics in natural. Furthermore, it is indicted in Sasmal et al. (2021b) that this storm avoidance model can be further improved to consider local environmental conditions, as the ship may change its route depending on the locally determined wave height, wave period, relative wave direction, wind speed, and so forth.

4.2   Winds

Ocean surface wind measurements are an important component of the global observing system and are routinely assimilated in numerical weather prediction models. Long-term, continuous in-situ observations of wind speed are distributed in various locations around the world, e.g. over the North Atlantic (Lux et al. (2018)), Dome C, East Antarctica (Genthon et al. (2021)), the south of Sri Lanka (Luo et al. (2018)), Hong Kong (Shu et al. (2020)), Shenzhen (Luo et al. (2020)). Most observations are based on Airborne wind lidar and aerial vehicles (Shimura et al. (2018)). The main usage of in-situ data is to investigate the wind power potential and wind loads of wind turbines, or to provides validation of the satellite observations (Borderies et al. (2019), Li et al. (2018b), Mukhtar et al. (2020), Tian et al. (2019), Yan et al. (2020)).

Over the open ocean, satellite retrievals play a crucial role since they are able to provide near global coverage in a relatively short space of time. Full wind vector information (i.e. speed and direction) can be inferred from "active" microwave radar instruments known as scatterometers. Various satellite missions have been developed for the observing purpose. A new generation of L-band sensors, such as ESA's Soil Moisture Ocean Salinity mission, have the capability to provide information on the ocean-surface wind speed under high wind and rain conditions (Cotton et al. (2018)). The BuFeng-1A/B twin satellites were part of the first Chinese global navigation satellite system reflectometry (GNSS-R) satellite mission (Jing et al., 2019).

Satellite-derived wind speed for open oceans to mesoscale model-simulated wind speed for coastal waters can be used to verify the Weather Research and Forecast (WRF) modelled wind speed (Takeyama et al. (2020), Xu et al. (2020a)). Satellite-derived data products are widely used to evaluate the wind energy resources (Guo et al. (2021a), Shu & Jesson (2021), Uchida (2018)).

Wind loads can be very important for offshore structures during typhoons. For this reason, Xie et al. (2019) analysed the relationships between the wind gust factor, mean wind speed and

turbulence intensity based on long-term wind observations at a platform in the South China Sea.

4.3   *Currents*

Ocean currents are often considered to consist of the following components: (i) the geostrophic currents; (ii) tidal currents; (iii) wind-driven Ekman currents; (iv) wave-induced Stokes drift; and (v) small scale features (e.g. eddies, fronts and filaments).

In-situ measurements of ocean current velocity are very limited and sparse. Though the traditional ship-based hydrographical surveys may have a good spatial and temporal resolution, they are usually only available in very limited regions and periods. There are only two ways to provide real-time in-situ velocity measurements of ocean current globally. The first approach is to inverse the near-surface ocean current in the upper 15 m or so through the trajectories of the surface drifters. There are about 1,500 drifting buoys deployed worldwide, implying the effective resolution of global ocean surface current observations is roughly 400–500 km on average. The resolution barely meets the research needs for large-scale processes. The second approach is to derive the ocean geostrophic velocity in the upper 2000 m from the temperature and salinity profiles obtained by Array for Real-time Geostrophic Oceanography floats (Argo floats). Currently, there are about 4,000 Argo floats deployed worldwide with an effective resolution of 200-300 km (see 4.1.2), and obviously, the spatial resolution is insufficient to capture small-scale ocean dynamics. In-situ observations have the disadvantage that they only cover a fraction of the ocean surface, and are normally not used directly for trajectory calculations.

A more effective way to directly observe ocean surface current is through satellite remote sensing technology (see also Chapter 5). Sea Surface Height (SSH) measured by satellite radar altimeters can be used to derive the surface geostrophic current, while Doppler shift of central frequency measured by synthetic aperture radar (SAR) can be used to retrieve the surface current speed. It is known that ocean fronts, vortices and filaments at scales below 10 km are important, but measurements of ocean surface dynamics at these scales are rare. The increasing capabilities of numerical methods require validation at smaller scales too. This led to the SEASTAR initiative, which is a satellite mission concept that will address this observational gap with synoptic two-dimensional imaging of total ocean surface current vectors and wind vectors at 1 km resolution (Gommenginger et al. (2019)). Directional wave spectra will also be derived. However, there are many challenges regarding the remote sensing observations. Due to the constraints of the satellite altimetry, the measured SSH can only be used to derive balanced motions, usually the geostrophic component of the realistic ocean surface current. For satellite upgrade programs, only geostrophic current and tidal velocity can be derived from the altimetry measured SSH (Qiu et al. (2020)). On the other hand, the SSH-derived geostrophic current is not accurate to describe the equatorial currents, due to the invalidity of geostrophic approximation in the equatorial region. Using surface drifters is a possible way to remedy the current observations in equatorial regions. In addition, other ageostrophic components, including the Ekman current and the tidal current, cannot be effectively obtained by the present observational methods (Ardhuin et al. (2019a)). Present observational methods are unable to achieve coastal and island/reef current measurements from SSH on a global scale, because the coastal dynamic processes are complicated and generally geostrophic-unbalanced (Gommenginger et al. (2019)). Acoustic tomography systems can be used to fill in the blanks (Chen et al. (2021)). The deficiency of satellite altimetry in the coastal region is also a problem. Although some satellites or remote sensings, such as SAR (Yang et al. (2021b)) and shore-based high-frequency radar (Aoki & Kataoka (2018)), can obtain scalar current in the coastal waters, they are too sparse or limited, and facing a high level of financial and human resource

investment to have global real-time coverage (Capodici et al. (2019)). Finally, current satellite altimetry is unable to describe ocean water motions in non-equilibrium states, such as submesoscale processes. High-resolution satellite imagery has shown that mesoscale processes are accompanied by very strong submesoscale processes that have a very fast-changing structure at a time scale of days. Such dynamic processes dominate over 50% of the heat flux (Su et al. (2018)) in the upper ocean and 20–50% of the primary production, but cannot be directly observed by current satellite remote sensing.

4.4   Ice

4.4.1   Laboratory measurements

Gharamti et al. (2021b) performed fracture experiments on rectangular edge notched, warm, fresh water ice specimens, largest of which had side length of 36 m. The specimen dimension covered a size range of 1:39, largest for ice tested under laboratory conditions. Complex size and rate effects were observed: There was a size effect at low rates but no size effect at high rates, and a rate effect for the larger test sizes but only weak or no rate effect for the smallest test size. Another study focusing on ice failure, this time under compressive loading due to ice-to-ice contact, was performed by Prasanna (2020). The study demonstrated that the ice specimens can go through shear-like failure in ice-structure interaction process, and gives means for more accurate discrete element modelling of ice.

Cyclic loading experiments on ice have been performed for tens of years, yet there has been also a considerable amount of recent work on the topic, likely due to wave-ice interaction having gained an increasing amount of interest during recent years. Laboratory-scale experiments by Wei et al. (2020a) showed that ice specimens (average specimen temperature -2.5°C) floating in water dissipate more energy during compressive cyclic loading than dry specimens tested in the same ambient temperature (specimen temperature -10°C). The study did not answer why the change occurred in detail, but highlighted the need to account for the test conditions. Iliescu et al. (2017), Murdza et al. (2020), Murdza et al. (2021a), Murdza et al. (2021b) used cyclic loading tests to study fatigue behaviour of both saline and freshwater ice. The experiments were performed on laboratory grown and natural ice specimens. Surprisingly, the authors found that their ice specimens strengthened as a result of cyclic loading. During the above-mentioned campaign Gharamti et al. (2021a) applied cyclic loading on their ice specimens. The ice response was overall elastic-viscoplastic and no significant viscoelasticity or major recovery was detected. Latter features are often reported in literature on ice. See also section 5.1.1.5 on combined wave-ice laboratory measurements.

4.4.2   Field observations

A vast number of new observations on Arctic ice pack was collected during the largest multidisciplinary Arctic expedition to date, the MOSAiC (Multidisciplinary drifting Observatory for the Study of Arctic Climate) in winter 2019-2020 (Krumpen et al. (2020)). The goal was to gain insight to quantify relevant processes impacting the sea ice mass and energy budget. The expedition had participation from several groups globally with results and analysis currently going on and published during upcoming years (Linow & Dierking (2017), Oikkonen et al. (2017), Suominen et al. (2017a, 2017b), Hutter et al. (2018), Hutter et al. (2019), Wang et al. (2021d).

5.   REMOTE SENSING

In this Chapter, the state of the art review of remote sensing technology in ocean environment monitoring is provided. There are several ways to monitor the ocean environment and this document provides the recent technology using radars and Synthetic Aperture Radars (SARs) from ship, onshore, aircraft, and satellite. Ocean remote sensing with SAR was reviewed in

various applications including oceanic surface and wave characteristics, sea surface wind, and bathymetry and so on (Yang et al. (2018)). Raizer (2019) provided an in-depth review of the fundamentals of ocean optics with various technologies including optical, satellite, data analysis and fusion with multi sensor concepts.

5.1   Ship radars

Shipborne high frequency surface wave radar (SHFSWR) has been widely applied to monitor ocean environments such as wave, current and wind for many years. Although it has high maneuverability, the challenges to use the shipborne radar are motion-induced oscillation/peaks and complicated ship motion on radar Doppler spectra. To overcome these problems, several studies have been proposed. Gangeskar (2018) developed an image process algorithm and hardware to provide ocean surface current measurement from a fixed site or moving site such as ships using X-Band Radar. The image processing data were validated against in situ data from a fixed platform in the North Sea and from a moving ship in the Barents Sea. Both measurements showed encouraging results and future work was discussed. Xie et al. (2017) and Xie et al. (2018) used the mathematical model of the wind direction based on first order cross section for SHFWR and a method for unambiguous wind direction with a single antenna. The results were compared with experimental results of the real data collected in Taiwan Strait and showed the good agreement. Zhao et al. (2020a) studied ocean surface wind direction field estimation using compact shipborne HF radar with single angle of view. A direction-finding algorithm incorporating the Doppler shifts were used and compared with the experimental results.

Yao et al. (2018) studied first-order shipborne SHFWR cross section with oscillation motion model based on the ship seakeeping theory for single frequency waves. Simulation results show that the horizontal oscillation motion can induce more peaks in the Doppler spectrum and suggested a motion compensation method to suppress the effect of the platform motion. Gill et al. (2018) provided a method for motion compensation for HFSWR on a floating platform. Four different deconvolution methods for the radar cross-section data were discussed and an iterative Tikhonov regularisation deconvolution technique was suggested. A yaw compensation algorithm for anchored floating HF radar and the vessel's vertical motion for significant wave height estimation using linear wave theory were studied by Yi et al. (2021b) and Xie et al. (2019) respectively.

Zhao et al. (2019) used a sea clutter suppression method using Cross-Loop/Monopoly (CLM) array combined with a multiple signal classification (MUSIC) algorithm to retrieve the target DOA (direction-of-arrival) for shipborne HF radar. The results compared with experimental data showed the improved suppression performance. McCann & Bell (2018) proposed a simple calibration method for accurate geographic registration of ship-borne radar imagery.

5.2   Coastal radars

There are several research works regarding improvement of the ocean current, wind and wave field measurements using coastal HF radars. Wyatt (2018) provided an insight of HF radar capabilities to measure wave, currents and tidal power. Wyatt et al. (2018) used two WERA HF radars to measure surface velocity and compared with field measurements. The study examined several different quality-control procedures and filters to improve data quality. The evaluation of the surface current measurements were performed by many researchers. Lu et al. (2018) developed a new algorithm of dispersion relation model extraction for current retrieval using X band radar and it provided better accuracy and stability than those from the traditional algorithm. Dzvonkovskaya et al. (2018) used a shored based HF radar system to measure tsunami-induced surface current velocity in real time while tsunami waves are crossing the

shelf edge and moving in shallow water. Wei et al. (2020b) used two OSMAR071 HF radars and four moored ADCPs to evaluate the surface currents in the Taiwan Strait under different sea states and showed best performance at sea state 4. Best practices for HF radars operation and maintenance were discussed by Mantovani et al. (2020). Ermoshkin et al. (2019) used coherent X-band and Ka-band panoramic digital radars to measure surface current and wind waves. They proposed a method using Doppler velocities and estimation of the fluctuation sensitivity.

Li et al. (2018c) explained a hybrid sky-surface wave radar system which was first introduced in 2007 to extract the ocean surface current. The advantage of this system is to monitor large-area sea states. The challenge is an ionospheric model which can be changed. The system can use multi receivers of the distributed radar systems (shore-based or shipborne) which can improve the results. Zhang et al. (2021b) proposed a method to suppress nonhomogeneous sea clutter in high frequency hybrid sky-surface wave radar to improve the measurement accuracy.

Many examples of wave field monitoring (including significant wave heights) and their evaluation were studied. Qiu et al. (2017) proposed a new modulation transfer function to improve both range and azimuth dependency for coastal wave fields and validated with in-situ buoy data in terms of retrieval accuracies of peak and mean wave periods. Tian et al. (2018) used a compact HF radar with a small antenna for wave height field measurement based on the first order Doppler spectra. The results estimated were compared with the buoy measurements and provided the validity of the method. Dicopoulos et al. (2018) used the data from CODAR SeaSonde and improved the wave measurements including wave height. Navarro et al. (2019) proposed a shadowing mitigation method based on filtering and interpolation to estimate the sea state parameters including significant wave height with high accuracy in shallow waters using X-band coastal marine radar. Chen et al. (2019c) studied the difference between shore-based coherent microwave radar and HF radar. Both radars are effective for near shore wave height monitoring in near real time with comparison of measured data from the wave buoy. Some differences between those radar in terms of the principle of wave measurements and coverage/spatial resolution of them were discussed.

Dao et al. (2019) evaluated HF radar for ocean surface wave fields under winter monsoon. Two different radar systems (LERA and CODAR) were used. They provided a comparison of the wave height evolution and discussed the uncertainties under the winter monsoon conditions. Zeng et al. (2019) studied the wave-current interaction for better wave prediction. They provided detailed analysis and application of wave-current interaction by using the effect of current on HF radar first order spectral power. Silva et al. (2020) proposed a nonlinear method for the extraction of the directional ocean wave spectrum from bistatic HFSWR based on bistatic cross-section formulation. Zinchenko et al. (2021) presented sea surface reconstruction from X-band marine radar images using a phase-resolved method for wave elevation map and its spectral component. The comparison between the reconstructed and true wave elevation/wave spectra showed good improvement/agreement, respectively. Wu et al. (2018) studied ocean environmental parameters including wind speeds and wave parameters using ERA-Interim reanalysis data in China Offshore Seas in different sea conditions. Zhao et al. (2020b) used a compact multi-frequency HF radar using a circular array (MHF-C) to estimate wind direction.

5.3   *Airborne radars*

Jansen et al. (I2018) introduced the development of X-band airborne multichannel SAR (MSAR) to monitor ocean environment. They proposed a new efficient channel-balancing algorithm to provide a consistent performance in various ocean conditions. Huang et al. (2018b) developed a multi rotor UAV-RTK GNSS (Unmanned aerial vehicle – real time

kinematic Global Navigation Satellite System) with a robotic lidar and AHRS (altitude and heading reference system) to measure wave and tide in coastal areas. They provided comparable results from in-situ measurements. Sutherland et al. (2018) study airborne lidar to measure the surface wave field in the marginal ice zone (MIZ) in the Beaufort Sea in Oct 2015. The results were compared with buoy data and showed good agreement.

Nadai (2019) showed the application of airborne synthetic aperture radar (SAR) to analyse the dependence of ocean wind direction on ocean surface backscattering. The normalized radar cross section (NRCS) of ocean surface backscattering from SAR depends on the wind speed and direction relative to the radar. The proposed airborne SAR assessed the wind direction/speed dependence of the NRCS. The wind direction showed a good agreement with airborne scatterometers but showed the large dependence on a NRCS model. Zhao et al. (2021) provided sea spike suppression method for airborne X-band SAR data since the sea spikes can cause significant interference to high-resolution SAR images. The method is based on an optimum polarization ratio in the SAR images and the detailed process was explained. Sun et al. (2021) evaluated airborne IRA (Interferometric Radar Altimeter) using wave-induced sea surface elevation (SSE) and its spectrum. A mean filtering algorithm was used to suppress the random phase noise. The results showed the dependency of the size of the filter window on sea-state conditions. Sletten et al. (2021) proposed to measure ocean surface current using an ultrahigh frequency synthetic aperture radar (UHF SAR) using aircraft. For the analysis, a wave dispersion method was used and compared with standard ATI-SAR processing. Both methods proved capable in measuring the surface velocity front, but the change in velocity, as measured by the two methods, showed significant difference.

5.4   Satellite observations

Remote sensing using satellites would be the most effective way to monitor the ocean environment in terms of the coverage and high resolution. Many researches have been trying to improve wave field monitoring. Jiang et al. (2018) re-analysed/corrected altimeter sensor interim geophysical dataset records (SIGDR) from China's first ocean dynamic environment satellite Haiyang-2A to improve significant wave heights measurements. Ren et al. (2019) used spaceborne SAR and RAR (Real Aperture Radar) as the joint retrieval method to provide directional ocean wave spectra. SAR works on medium incident angles (20°-50°) but RAR measures at low incident angles (0° to 10°). Each Radar also has its own limitation of retrieval and this study proposed a joint method to derive the full wave spectra at small scale. Various data sources were also used to validate the method and most of the retrieved parameters showed comparable results. Hauser et al. (2021) provided a new space borne system namely the China France Oceanography Satellite (CFOSAT) for measuring ocean surface parameters and the paper provides the ocean wave assessment by comparing in-situ observation. The Surface Waves Investigation and Monitoring (SWIM) Ku-band Radar was on-board to measure the spectral properties of surface ocean waves. The paper shows that SWIM can provide the spectral properties in the wavelength range from 70 to 500m and other information such as wave parameters which are complementary to other observations. Wan et al. (2020) studies were based on 2 RADARSAT-2 SAR SLC (Single Look Complex) data and the cross-spectrum method, the distributions of significant wave heights and mean wave periods of ocean waves were inverted and the distributions of the wave power density were calculated. The results were compared with buoys and wave models in nearshore water and showed the effectiveness of the SAR. Wang et al. (2019d) used Gaofen-3's quad-polarized wave model SAR images with cross spectral technique to evaluate the ocean wave spectra. The results were compared with buoy data to prove the feasibility and suggested operational implementation. Wang et al. (2018d) showed the capability of compact polarized SAR (RadarSat-2) to retrieve ocean wave field parameters. Ortiz & Lorenzzetti (2018) developed a new method to assess deep water

multimodal wave systems using polarimetric SAR image. Dinardo et al. (2021) used a new waveform by Doppler beam integration in the range direction of so called Range Integrated Power (RIP), to develop a new retracker (SAMOSA2) from the Sentinel-3 SAR. The study validated the performance improvement in terms of altimetric parameters such as sea surface height and significant wave heights in the North East Atlantic.

To improve the data accuracy, a machine learning technique has been widely used for the analysis. Collins et al. (2019) studied the effect of polarization and incident angle on the significant wave height from SAR data (RADARSAT2) using neural network methods. Quach et al. (2020) used a dataset over 750,000 collocations from the Sentinel-1 SAR and radar altimetry and trained a DNN regression model to predict significant wave heights. The deep learning method reduced the error by half. Tapoglou et al. (2021) applied a machine learning technique for satellite-based sea state prediction using 240 Sentinel-1 satellite images. They used the Artificial Neural Network (ANN) combined with a Monte Carlo simulation to simulate the significant wave height. It provided not only comparable performance but also high resolution spatial distribution of significant wave heights. For internal solitary wave monitoring, Kozlov & Zubkova (2019) used the high resolution spaceborne SAR (Envisat) to observe internal solitary waves in the Arctic Ocean. Zhang et al. (2020) used the spaceborne compact polarimetric (CP) SAR to classify ocean internal solitary waves (ISWs). They used 140 fully polarized satellite images and proved that some CP features contain enough information to find and identify ISWs.

Several wind speed/direction measurement studies, using satellite images, were also performed. Abdalla et al. (2018) evaluated the significant wave height and wind speed from CryoSat-2 SAR. A detailed method was addressed and results were compared with ECMWF Integrated Forecasting System (IFS) output as well as in-situ and Jason-2 observations. Young & Donelan (2018) used 30 years of altimeter and radiometer measurements of wind speed and wave height from a satellite database and provided detailed descriptions of global wind and wave climate to compare with each other and ERA–I model reanalysis data. Wang et al. (2018c) examined wind retrieval using NRCS from Gaofen-3 (China's first C-band full polarization synthetic aperture radar imaging satellite). Li et al. (2021d) measured the ocean surface current field (velocity and direction) using the same radar and showed the good agreement with ocean model data. Fan et al. (2018) used C-band dual-polarization RADARSAT-2 and Sentinel-1A SAR image to retrieve wind direction of a tropical Cyclone. This study provided the difference in VV and VH polarization and compared the results with various other sources. It suggested that VH-polarization showed better precision of the wind speed retrieval. Migliaccio et al. (2019) used a Sentinel-1 SAR data to study speckle dependence on ocean surface wind field. Hutchings & Long (2019) used a RapidScat which is a dual pencil-beam Ku-band scatterometer on the ISS. They produced RapidScat wind estimates on an ultrahigh resolution and showed the improvements. Ozbahceci (2020) studied extreme value statistics of wind speed and wave height based on combined radar altimeter data from different satellite missions. Nilsen et al. (2019) proposed a novel approach to Bayesian ocean wind retrieval from the SAR data. Gao et al. (2020) showed the possibility to retrieve Tropical Cyclone (TC) ocean surface wind speed from Sentinel-1 Satellites SAR images. Some limitations/improvements including prior input of wind direction and saturation of NRCS were discussed. Yi et al. (2021a) studied ocean diurnal wind variation measured by remote sensing satellites including CYGNSS and compared with ECMWF EFA5 data, which showed a consistent results. Pascual et al. (2021) studied the sensitivity of Cyclone GNSS data to wind direction using the kurtosis of the delayed-Doppler map (DDM) samples and guided potential wind direction estimation from CYGNSS data in the future. Guo et al. (2021b) proposed a new method to retrieve wind speed from GNSS-R by using delay-Doppler map (DDM) observables

based on particle swarm optimization (PSO). Zhou et al. (2021) used Sentinel-1 SAR images to retrieve sea surface wind speed from textures and tested for hurricane conditions and its room mean-square differences was 1.28 m/s.

Ice monitoring and tracking research using satellites has been performed. Komarov & Buehner (2018) developed adaptive probability thresholding in automated detection of ice and open water from RADARSAT-2 dual polarization HH-HV image. A set of verification tests showed a decrease in the fraction of misclassified ice and open water sample from 0.35% to 0.09%, while the fraction of correctly classified ice and water samples decreased 72.2% to 65.4%. Ding et al. (2020) studied the phase differences from the polarimetric SAR measurements from RADARSAT-2 satellite, which could provide the phase information for ice segmentation from the open water. Their work was validated with in-situ ice observation for new frazil ice in the marginal ice zone. They also proposed the operational implementation of automatic unsupervised methods for sea ice detection and classification in the marginal ice zone. Sun & Li (2021) provided an effective denoising algorithm for Sentinel-1 extra wide mode HV polarized images to monitor sea ice in MIZ. Barbat et al. (2021) developed an iceberg tracking method using machine learning techniques and provided a case study with Weddell Sea region's Advanced SAR (ASAR) data. Xue et al. (2021) introduced the first C-Band SAR small satellite (HISEA-1) for ocean remote sensing. It has a spatial resolution of 1 m/ a width of 100 km and it can detect sea ice, ocean wind/wave and rises. The paper showed the potential applications due to the low cost/high resolution but it was still in the commissioning stage, which required more calibration.

6. DATA ANALYSIS

This chapter is dedicated to the analysis of environmental data in more detail, following a deeper statistical investigation to extract information from large multi-dimensional datasets. As a fast-growing field, many interesting studies have been published recently and the amount of tools nowadays is impressive. The chapter starts with a fundamental step that is often overlooked, related to quality control – extremely important to ensure reliable results at any type of analysis and modelling. The next part describes the assessments of wind and wave data from satellites, reanalysis, and forecast models, quantifying errors and uncertainties of environmental data. The final and largest part describes the machine learning and big data developments, with numerous studies in the last few years.

6.1 Quality Control of observations

The main quality control methods and guidelines for meteorological and oceanographic data processing are provided by the World Meteorological Organization (WMO), the National Data Buoy Center (NDBC) and Integrated Ocean Observing System (IOOS). The handbooks and manuals, WMO (2018), NDBC (2009) and IOOS (2019) provide the procedures and control checks to be followed, which is further complemented by specific studies described as follows.

In Lucio-Eceiza et al. (2018a) a quality control (QC) process has been developed and implemented on an observational database of surface wind speed and direction in north-eastern North America. The database combines the observations of three different institutions spanning from 1953 to 2010. The QC is focused on data management issues: data transcription and collection; differences in measurement units and recording times; detection of sequences of duplicated data; unification of calm and true north criteria for wind direction; and detection of physically unrealistic data measurements. The QC presented in the paper is structured in six phases: 1) compilation (duplication of data or data not in chronological order); 2) duplication errors; 3) physical consistency in the ranges of recorded values; 4) temporal consistency, regarding abnormally high/low variability in the time series; 5) detection of long-term biases;

and 6) removal of isolated records. The first three phases are analysed in PART I of the paper while Phase from 4 to 6 in PART II (see paragraph below). Phase 1 had the higher impact on data while phase 2 and 3 had a lower impact. Around 0.1% of wind speed and wind direction records have been identified as erroneous and deleted.

Lucio-Eceiza et al. (2018b) is the second part of the previous described article. The paper focuses on the detection of measurement errors and deals with low-variability errors, like the occurrence of unrealistically long calms, and high-variability problems, like rapid changes in wind speed; some types of biases in wind speed and wind direction are also considered. The most pervasive error type in terms of affected sites and erased data corresponds to unrealistic low wind speeds (89% of sites affected with 0.35% records removed). The amount of detected and corrected/removed records in Part II (9%) is approximately two orders of magnitude higher than that of Part I.

Cosoli et al. (2018) describes a quality-control procedure and its impact on data collected by the High-Frequency Ocean Radar (HFR) network in Australia with the commercial phased-array (WERA) HFR type. The proposed iterative procedure was specially designed to remove anomalous observations associated with strong signal-to-noise ratio (SNR) peaks caused by the 50 Hz sources. The procedure iteratively fits a polynomial along the radial beam (1-D case) or a surface (2-D case) to the SNR associated with the radial velocity. Observations that exceed a detection threshold were then identified and flagged. The paper suggests that a fine-tuning of the thresholds is beneficial to improving the overall quality of the HFR data set. Tests performed across several mooring locations also suggested that a single threshold for SNR value may not be adequate for the entire domain and that this threshold may vary over time as a result of varying environmental factors, external noise, interference sources, or other problems. Another quality control applied to radar data is Lipa et al. (2019) who describe a method for radial velocity maps derived from radar echo voltage cross spectra measured by broad-beam high frequency radars, showing examples of its application to broad-beam radars operating at four sites.

Cerlini et al. (2020) analysed hourly temperature time series from 2010 to 2017 in Italy applying basic and extended quality control procedures following World Meteorological Organization (WMO) standards. The spatio-temporal method used to reconstruct the data was a linear interpolation for 1hr gaps and the empirical orthogonal function (EOF) algorithm for gaps $\geq$ 2 hr. The introduction of a complete and homogeneous data set of hourly reanalysis ERA5/ECMWF allowed for the reconstruction of the longest gaps with statistical and physical consistency.

6.2 *Error metrics and assessments*

The limitations and errors of environmental databases must be known before using it in any ocean engineering application. A valuable description of error metrics and statistical tools for the assessments can be found in Mentaschi et al. (2013), Willmott & Matsuura (2005), and Jolliff et al. (2009). Recently, the reanalysis that has received the most attention is the ECMWF ERA5 global reanalysis (Hersbach et al. (2020)), with many papers evaluating the product. ERA5 is based on the Integrated Forecasting System (IFS) Cy41r2 which was operational in 2016 and benefits from a decade of developments in model physics, core dynamics and data assimilation. The ERA5 high-resolution atmospheric and oceanic global data from 1950 onwards, is publicly available and has overperformed its predecessors.

Parsons et al. (2018) shows that wind fields of ERA5 compare well against altimeter and buoy data. When examining individual events, authors found deficiencies, in particular with extreme tropical and extra-tropical cyclones. Studying the application to wind power modelling,

Olauson (2018) showed that ERA5 performs better than a previous reanalysis MERRA-2 in all analysed aspects; correlations are higher, mean absolute and root mean square errors are in average around 20% lower and distributions are more similar to those for measurements. Jourdier (2020) confirmed the high skills of ERA5 wind products but they draw attention to the occasional underestimated winds in some locations. In the Southern Antarctic Peninsula, Tetzner et al. (2019) performed a validation of ERA5 compared to in-situ observations from 13 automatic weather stations (AWS), reporting a significant improvement of ERA5 over ERA-Interim in terms of temperature and surface winds. The authors argued that the slight underestimation in the wind speed can be attributed to interplay of topographic factors and the effect of local wind regimes. In terms of wind gusts, Minola et al. (2020) compared ERA5 with hourly near-surface wind speed and gust observations across Sweden for 2013–2017. They concluded that ERA5 shows closer agreement than the previous ERA-Interim reanalysis with regard to both mean wind speed and gust measurements, although significant discrepancies are still found for inland and mountainous regions.

Regarding cyclonic events, Bian et al. (2021) describes that ERA5 reanalysis can resolve stronger tropical cyclone winds, which leads to more valid outer size samples, especially for the radii of 12 and 15 m/s winds, and for the cases with outer sizes of <300 km - being the distribution characteristics of the outer size in the ERA5 reanalysis closer to the observation. Gramcianinov et al. (2020) analysed and compared ERA5 and NCEP/CFSR data from 1979 to 2019 with 1-hourly outputs, regarding their ability to reproduce storm tracks and the main characteristics of cyclones at middle and high latitudes in the Atlantic Ocean. Their results show that ERA5 has 3.7% more cyclones than CFSR, which can be related to the finer resolution; however, CFSR presents stronger cyclonic winds than ERA5.

A few studies addressed the quality of wave products of ERA5. Bruno et al. (2020) analysed the performance of ERA5 in a swell dominated region in the Western Arabian Sea. The authors concluded that ERA5 wave model overestimates the swell wave heights, whereas the wind waves' height prediction is highly influenced by the wave developing conditions. Shi et al. (2021) evaluated the accuracy of ERA5 wave reanalysis in China using six buoys. They reported that the difference between the significant wave height of ERA 5 and the buoys varies from -0.35 m to 0.30 m for the three shallow water locations, and for the three deep locations, the variation ranges from -0.09 m to 0.09 m – with ERA5 containing positive biases which suggests an overall overestimation for all locations. However, during the tropical cyclone period, Shi et al. (2021) found a large underestimation (32%) of the maximum significant wave height in the ERA5 dataset, concluding that ERA5 data cannot be directly used for design applications without site-specific validation. In order to overcome these limitations in the ERA5 wave products, Law-Chune et al. (2021) developed a new global reanalysis, WAVERYS, including assimilation of altimeter wave data and directional wave spectra provided by Sentinel-1, adding also wave-current interactions by using the ocean reanalysis GLORYS. The results indicate that scatter index of SWH from the WAVERYS is improved by about 9% with respect to the ERA5 wave dataset, having additional good accuracy of swell propagation thanks to the assimilation of directional wave spectra.

In summary, various uncertainties exist in hindcasts due to the inabilities of numerical models to resolve all the complicated atmosphere-sea interactions, and the lack of certain ground truth observations. Abdolali et al. (2021) conducted a comprehensive analysis of an atmospheric model performance in hindcast mode (Hurricane Weather and Research Forecasting model HWRF) and its 40 ensembles during severe events, evaluating the model accuracy and uncertainty for hurricane track parameters, and wind speed collected along satellite altimeter tracks and at stationary source point observations. The study on Hurricane Irma reveals that wind and wave observations during this extreme event are within ensemble spreads, while both

atmospheric and wave models have wide spreads over areas with landmass, maximum uncertainty in the atmospheric model is at hurricane eye in contrast to the wave model.

Moving from reanalysis to forecast assessments, Campos et al. (2018c) performed a validation of surface winds and waves from the NCEP ensemble forecast system by using 29 Metocean buoys. They found the largest errors in NCEP/GWES, beyond forecast day 3, are associated with winds above 14 m/s and waves above 5 m. Extreme percentiles after the day-8 forecast reach 30% of underestimation for both 10-m wind and significant wave height. The comparison of probabilistic and deterministic wave forecasts shows an improvement of predictability on the scatter component of the errors, where the error for surface winds drops from 5 m/s in the deterministic runs, associated with extreme events at longer forecast ranges, to values around 3 m/s using the ensemble prediction. As a result, GWES waves are better predicted, with a reduction in error from 2 m to less than 1.5 m for significant wave height. These results are confirmed by another assessment of the NCEP ensemble forecasts of Campos et al. (2020b) using altimeter data covering the whole globe. They concluded that it is essential to use ensemble forecast products to obtain reliable wind and wave forecasts beyond 7 days of forecast range at mid- and high latitudes.

Recent assessments of satellite data can be found in Ribal & Young (2019) and Ribal & Young (2020), regarding altimeter and scatterometer data respectively. Ribal & Young (2019) shows the wind and wave evaluation of 13 altimeters, namely GEOSAT, ERS-1, TOPEX, ERS-2, GFO, JASON-1, ENVISAT, JASON-2, CRYOSAT-2, HY-2A, SARAL, JASON-3 and SENTINEL-3A, against National Oceanographic Data Center (NODC) buoy data. Great value is added through the Quantile-Quantile comparisons between altimeter and buoy data as well as between altimeters. Ribal & Young (2020) evaluated the wind speed from seven different scatterometers, namely ERS-1, ERS-2, QuikSCAT, MetOp-A, OceanSat-2, MetOp-B, and Rapid Scatterometer (RapidScat) also against National Data Buoy Center (NDBC). Besides the assessments, both studies applied quality-control and performed a calibration of the satellite data, which resulted in a high-quality database, well organized and publicly available.

6.3   *Data mining and Machine Learning applied to ocean modelling*

Data mining methods and neural network models have become very popular due to their relatively low computational cost, and great ability to improve environmental analyses and forecasts by using large datasets of observations. Moreover, these tools are useful to pre- and post-process traditional numerical models, as well as extracting information from multiple data sources.

In Mahmoodi & Ghassemi (2018), three typical outlier detection algorithms: Box-plot (BP), Local Distance-based Outlier Factor (LDOF), and Local Outlier Factor (LOF) methods are used to detect outliers in significant wave height (Hs) records. The historical wave data are taken from National Data Buoy Center (NDBC). Each method presented different results that are highly dependent on the parameters used. It has been concluded that the LOF and Box plot were of low and high sensitivity in outlier detection in studied data sets. The voting method was used to obtain better outlier identification that achieved higher performances than the other methods in outlier detection.

In Portilla-Yandún et al. (2019) two different methods are used to mine large wave spectra databases: Spectral Partitions Statistics (SPS) and Self-Organizing Maps (SOM). The aim of the paper is to improve the characterization of the directional wave climate at a site, providing a more complete and consistent description than that obtained from traditional statistical methods based on integral spectral parameters (e.g., Hs, Tm, θm). The methods are applied to a 37-year long (1979–2015) model dataset of directional wave spectra at a study site in the

western Mediterranean Sea. The statistics given by SPS and SOM methods are consistent with the statistics based on integral parameters but more informative as they operate in the frequency-direction domain. In the long-term statistics SOS and SOM identify more complex wave systems than the standard integral parameters helping in quantifying cross-sea conditions. The SOM as the advantage of providing the spectral shape but SOM is not indicated to represent extremes.

Wei (2018) studied different data mining models namely k-nearest neighbors (kNN), linear regressions (LR), model trees (M5), multilayer perceptron (MLP) neural network, and support vector regression (SVR) algorithms to setup a forecasting model for the wave height at shore during typhoons. The data used for testing and training were data in typhoons occurred during 2002-2011 and 2012-2013 recorded by the Londong buoy off the northeast coast of Taiwan. For the purpose of forecasting the conclusions of the paper are that MLP and SVR result are the optimal ones compared with other models when averaging the RMSE measures of the four model cases. In addition, regarding wave heights classification M5 provide the superior outcomes at small wavelet level compared with other models, MLP has the optimum outcomes at the large wavelet and small/moderate wave levels compared with other models, and SVR provides the optimal outcomes at the long wave and high/very high wave levels of all models.

In Wang et al. (2019b) a method combining wavelet neural network (WNN), classifying threshold and two detecting strategies was presented for detecting anomalies in ocean fixed-point observing time series. Two types of marine observing time series from a buoy, deployed at the National Ocean Test Site of China, were selected to evaluate the method: surface salinity (SS) and surface current speed (SCP). WNN were used to simulate the non-anomalous behaviours based on the normal variations in ocean observing series, and two detecting strategies (i.e. observation strategy and prediction strategy) were designed to find new unknown anomalies. The classifying threshold was determined by the estimated distribution of historical residuals. The WNN developed in the paper can work in an unsupervised setting and it has been found that it is more tolerant to noise and more sensitive to anomalies with temporal dependencies than traditional methods.

The topic of abnormal data mining in ocean Argo buoy monitoring data was studied by Jiang et al. (2019). Dense regions were established in K-MEDOIDS clustering algorithm with the help of density accessibility of density clustering. Based on dynamic layer number, a new calculation method of domain radius and density was proposed, and the initial clustering center was selected with both, considering density and similarity. At the same time, an anomaly detection algorithm was proposed, which the criterion to judge marine anomaly data is based on the result of clustering combined with point sets in dense regions. The paper states that the new improved algorithm avoids the disadvantages of sensitive initial clustering center and high update iteration times of central point.

The existence of multiple numerical wave forecasts leads to the question of which one should be used in practical ocean engineering applications, which was investigated by Campos et al. (2021) through decision algorithms. They developed random forest (RF) post-processing models to identify the best wave forecast between two National Centers for Environmental Protection (NCEP) products (deterministic and ensemble). The supervised learning classifier was trained using National Data Buoy Center (NDBC) buoy data and the RF model accuracies were analysed as a function of the forecast time. A careful feature selection was performed by evaluating the impact of the wind and wave variables (inputs) on the RF accuracy. The results showed that the RF models were able to select the best forecast at certain forecast ranges using input information of significant wave height, wave direction and period, and ensemble spread.

The challenges and limitations of such RF predictions for longer forecast ranges are discussed in order to support future studies in this area.

The stacked auto-encoder is a neural network approach in machine learning for feature extraction. It attempts to model high-level abstractions and to reduce data dimensions by using multiple processing layers. Therefore, combining the concept of a dynamic data-driven system with a stacked auto-encoder neural network will help to obtain the dynamic data correlation or relationship between the prediction results and actual data in a dynamic environment. The study presented by Lin et al. (2018) applied the concept of a dynamic data-driven system to obtain the correlations between the prediction goals and number of different combination results. Association analysis, sequence analysis, and stacked auto-encoder neural network were successfully employed to design a dynamic data-driven system based on deep learning. Additionally a rich discussion and recommendation on environmental data selection for the training of machine learning models that predicts wind patterns is provided by Goulart & Camargo (2021).

Ellenson et al. (2020) used a machine learning algorithm, the bagged regression tree, to detect error patterns within 24-h forecasts of significant wave height time series. The input to the machine learning algorithm were bulk parameter outputs of the numerical wave model WAVEWATCHIII and wind information from the Global Forecast System (GFS/NCEP) at buoy locations along the California-Oregon border in the United States. The outputs of the algorithm are predictions of hourly deviations between numerical model output and buoy observations of significant wave height. When these deviations were applied as corrections to the forecasts, the performance was improved, confirming that the error pattern was successfully detected by the machine learning algorithm. As a descriptive tool, the algorithm delineated regions of similar error within the context of model phase space (Hs and Tm). For Hs greater than the 95th percentile value (5.4 m), the algorithm detected differences in model phase space associated with mean error patterns.

The next papers describe studies that proposed long short-term memory (LSTM) networks for the quick prediction of significant wave heights. Fan et al. (2020) emphasised that LSTM leads to higher accuracy than conventional neural networks. They developed LSTM models for 1-h and 6-h predictions at ten stations using the wind speed of the past 4 h and the wave height and wind direction of the past 1 h as input parameters. The LSTM prediction results were obtained and compared against results from a back propagation neural network, extreme learning machine, support vector machine, residual network, and random forest algorithm. Their results showed the powerful ability of LSTM to perform short and long-term predictions. The simulating waves nearshore-LSTM (SWAN-LSTM) model was proposed by them to make a single-point prediction, and it outperformed the standard SWAN model with an improvement in accuracy of over 65%. Similarly, Alqushaibi et al. (2021) proposed an enhanced weight-optimized neural network based on Sine Cosine Algorithm (SCA) to accurately predict wave height. Three neural network models named Long Short-Term Memory (LSTM), Vanilla Recurrent Neural Network (VRNN), and Gated Recurrent Network (GRU) were developed and improved – validated against metocean datasets. The original LSTM, VRNN, and GRU are implemented and used as benchmarking models. The results show that the optimized models outperform the original three benchmarking models in terms of MSE, RMSE and MAE.

Hu et al. (2021) applied novel ML methods based on XGBoost and a Long Short-Term Memory (LSTM) recurrent neural network to predict wave height and period at Lake Erie. They trained and validated the ML models with buoy data sets from 1994 to 2015, and then used the trained models to predict significant wave height (Hs) and peak period (Tp) for 2016 and 2017. The XGBoost model yielded the best overall performance, with Mean Absolute Percentage Error

(MAPE) values of 15.6%–22.9% in Hs and 8.3%–13.4% in Tp. The LSTM model yielded MAPE values of 23.4%–30.8% in Hs and 9.1%–13.6% in Tp. An unstructured grid of WW3 model applied to Lake Erie resulted in MAPE values of 15.3%–21.0% in Hs and 12.5%–19.3% in Tp; however, WW3 underestimated both parameters during strong wind events, with relative biases of -11.76% to -14.15% in Hs and -15.59% to -19.68% in Tp. The XGBoost and LSTM models improve on these predictions with relative biases of -2.56% to -10.61% in Hs and -8.08% to -10.13% in Tp. Besides the improved performance, the ML models run significantly faster than the numerical wave model WW3, which reinforces the promising operational applications of machine learning algorithms.

Zhang et al. (2021c) investigated the possibility of using machine learning to correct numerical forecasts of wave height series by incorporating predictions into a long short-term memory model (LSTM). The LSTM takes a combined wave height representation, which is formed from a current wave height measurement and a subsequent Simulating Waves Nearshore (SWAN) numerical prediction, as the input and generates the corrected numerical prediction as the output. The correction is achieved by two modules in cascade, i.e., the LSTM module and the Gaussian approximation module. The LSTM module characterizes the correlation between measurement and numerical prediction. The Gaussian approximation module models the conditional probabilistic distribution of the wave height given the learned LSTM. Experimental results confirmed that LSTM effectively improves the accuracy of wave height prediction from SWAN, for the prediction time varying from 3 to 72 h.

The machine learning approaches are being widely used for the prediction of wave heights, as described above. However, these approaches involve batch learning algorithms that are not well-equipped to address the demands of a continuously changing data stream. In Kumar et al. (2017) they conduct a study to predict the daily wave heights in different geographical regions using sequential learning algorithms, namely the Minimal Resource Allocation Network (MRAN) and the Growing and Pruning Radial Basis Function (GAP-RBF) network. They compare the performance of MRAN and GAP-RBF with Support Vector Regression (SVR) and Extreme Learning Machine (ELM). The performance study results show that the MRAN and GAP-RBF outperform the SVR and ELM with minimal network resources, in the daily wave height prediction. Neural networks can approximate any complex nonlinear process without a priori knowledge of the underlying physics and sequential learning algorithms do not need re-training and are capable of learning as data arrives, concluding that Minimal Resource Allocation Network (MRAN) can predict the significant wave heights more accurately than the other networks.

In Oh & Suh (2018), a hybrid model is developed by combining the empirical orthogonal function analysis and wavelet analysis with the neural network (abbreviated as EOFWNN model). The past wave height data at multiple locations and the past and future meteorological data in the surrounding area including the wave stations, are used as input data. The model then forecasts the wave heights at the locations for various lead times. The developed model is employed to forecast the wave heights at eight wave observation stations in the coastal waters around the East/Japan Sea. The EOFWNN model is proven to be a promising tool for forecasting wave heights at multiple locations, where the past wave height data and the past and future meteorological data in the surrounding area are available.

A data-driven warning model based on an artificial neural network (ANN) is proposed in Doong et al. (2018) to predict the possibility of Costal Freak Waves occurrence. Seven parameters (significant wave height, peak period, wind speed, wave groupiness factor, Benjamin Feir Index (BFI), kurtosis, and wind-wave direction misalignment) collected prior to the occurrence of the CFW are used to develop the model. The buoy data associated with 40

known CFW events are used for model training, and the data associated with 23 events are used for validation. The accuracy rate (ACR) exceeds 90% and the recall rate (RCR) exceeds 87%, demonstrating the accuracy of the proposed model. This warning model has been implemented in operational runs since 2016.

Law et al. (2020) presents a framework on the use of data-driven models based on Artificial Neural Network (ANN) in predicting the spatial–temporal evolution of wave fields in real-time from a given wave field record upstream. A short-term deterministic or phase-resolved wave prediction in real-time has been demonstrated using both linear wave theory (LWT) and Artificial Neural Network (ANN) model. Time domain forecast of free surface elevation and individual waves. They choose a wave environment south of Albany, Western Australia, which is known to be swell-dominated, and simulate many realisations of long-crested random waves using Higher Order Spectral Method (HOSM) for each sea-state sampled from the scatter diagrams of that particular location.

In Berbić et al. (2017), real-time prediction of significant wave heights for the following 0.5-5.5 h is provided, using information from 3 or more time points. In the first stage, predictions are made by varying the quantity of significant wave heights from previous time points and various ways of using data are discussed. Afterwards, in the best model, according to the criteria of practicality and accuracy, the influence of wind is taken into account. Predictions are made using two machine learning methods — artificial neural networks (ANN) and support vector machine (SVM). The models were built using the built-in functions of software Weka, developed by Waikato University, New Zealand.

Artificial neural networks (ANNs) applied to nonlinear wave ensemble averaging are developed and studied for Gulf of Mexico simulations in Campos et al. (2019a), as a follow-up study started in Campos (2017) using machine learning models applied to single points. Campos et al. (2019) proposed an approach that expands the conservative arithmetic ensemble mean (EM) from the NCEP Global Wave Ensemble Forecast System (GWES) to a nonlinear mapping that better captures the differences among the ensemble members and reduces the systematic and scatter errors of the forecasts. The ANNs have the 20 members of the GWES as input, and outputs were trained using observations from six buoys. The variables selected for the study were the 10-m wind speed (U10), Hs, and Tp for the year of 2016. ANNs were built with one hidden layer using a hyperbolic tangent basis function. Several architectures with 12 different combinations of neurons, eight different filtering windows (time domain), and 100 seeds for the random initialization were studied and constructed for specific forecast days from 0 to 10. The results show that a small number of neurons are sufficient to reduce the bias, while 35–50 neurons produce the greatest reduction in both the scatter and systematic errors. The main advantage of the methodology using ANNs is not on short-range forecasts but at longer forecast ranges beyond 4 days. The nonlinear ensemble averaging using ANNs was able to improve the correlation coefficient on forecast day 10 from 0.39 to 0.61 for U10, from 0.50 to 0.76 for Hs, and from 0.38 to 0.63 for Tp, representing a gain of five forecast days when compared to the EM currently implemented.

Next, a nonlinear ensemble averaging in global scale was developed by Campos et al. (2020a) using neural networks applied to one year (2017) of Global Ocean Wave Ensemble forecast System (GWES) data provided by NCEP. Post-processing algorithms were developed based on multilayer perceptron neural networks (NN) trained with altimeter data to improve the global forecast skill, from nowcast to forecast ranges up to 10 days, including significant wave height (Hs) and wind speed (U10). The NN models were constructed using six variables sourced from 21 ensemble members, plus latitude, sin/cos of longitude, sin/cos of time, forecast lead time, and GWES cycle. The sensitivity NN tests considered 26 different numbers of

neurons, 10 seeds for initial conditions, and 3 equally-divided datasets; for a total of 780 NN experiments. Assessments using 2,507,099 paired satellite/GWES fields showed that a simple NN model with few neurons was able to reduce the systematic errors for short-range forecasts, while a NN with more neurons is required to minimize the scatter error at longer forecast ranges. The bias of the widely used EM of GWES that varies from -10% to 10% for Hs compared to altimeters can be reduced to values within 5%. The RMSE of day-10 forecasts from the NN simulations indicated a gain of two days in predictability when compared to the EM, at global scale, using a reasonably simple post-processing model with low computational cost.

The intense increase in offshore operational activities warrants periodical and accurate prediction of the wave characteristics. Usually, complex numerical models that require high computational power are used in this prediction. To overcome these challenges of these numerical models, Kumar et al. (2018b) proposed the use of an ensemble of Extreme Learning Machine (Ens-ELM) to predict the daily wave height. They exploit the randomness of initialization in ELM to obtain better generalization performance by constructing an Ensemble of ELM, with the parameters of each ELM initialized in distinct regions of the input space. For each sample in the data set, the output of the ELM with the least mean square for each sample in the data set is reported as its output. The authors study the performance of the Ens-ELM to predict the daily wave height in 10 stations of varying terrains from Gulf of Mexico, Brazil and Korean region. The Ens-ELM network is trained using the past wave data and the measured atmospheric conditions obtained in these stations between Jan 1, 2011 and Dec 31, 2014 and is tested with data in these stations between Jan 1, 2015 and Aug 30, 2015. In this study, the performance of Ens-ELM is evaluated in comparison with ELM, Online Sequential ELM (OS-ELM), and Support Vector Regression (SVR). The study shows that the Ens-ELM out performs ELM, OS-ELM and SVR in the daily wave height prediction.

In James et al. (2018) a machine learning framework is developed to estimate ocean-wave conditions. By supervised training of machine learning models on many thousands of iterations of a physics-based wave model, accurate representations of significant wave heights and period can be used to predict ocean conditions. A model of Monterey Bay was used as the example test site; it was forced by measured wave conditions, ocean-current nowcasts, and reported winds. These input data along with model outputs of spatially variable wave heights and characteristic period were aggregated into supervised learning training and test data sets, which were supplied to machine learning models. James et al. (2018) showed that these machine learning models replicated wave heights from the physics-based model with a root-mean-squared error of 9 cm and correctly identify over 90% of the characteristic periods for the test-data sets. Impressively, transforming model inputs to outputs through matrix operations requires only a fraction (< 1/1000th) of the computation time compared to forecasting with the physics-based model.

In addition to the wave modelling studies described above, Kumar et al. (2019) developed a model output statistics (MOS) guidance model by using the neural network technique for a bias-corrected rainfall forecast. The model was developed over the Indian window (0-40°N and 60-100°E) by using the observed and global forecast system (GFS) T-1534 model output (up to 5 days) at a 0.125°×0.125° regular grid during the summer monsoon (June–September) 2016. The skill of the developed MOS model forecast against the observed 0.125°×0.125° grid rainfall data is obtained for the summer monsoon (June–September) 2017. The skill of the MOS model rainfall forecast is found to show good improvement over the T-1534 model's direct forecast over the Indian window. In general, the T-1534 model's direct forecast shows high skill, but the forecast obtained by using the MOS model shows better skill than the direct

model's forecast, although a major improvement is seen for the Day 1 forecast at the national level.

Making deductions and expectations about climate has been a challenge all through mankind's history. Challenges with exact meteorological directions assist to foresee and handle problems well in time. Different strategies have been investigated using various machine learning techniques in reported forecasting systems. Current research investigates climate as a major challenge for machine information mining and deduction. Accordingly, in Saba et al. (2017) a hybrid neural model (MLP and RBF) was developed to enhance the accuracy of weather forecasting. The proposed hybrid model ensures precise forecasting due to the specialty of climate anticipating frameworks. The study concentrates on the data representing Saudi Arabia weather forecasting. The main input features employed to train individual and hybrid neural networks included average dew point, minimum temperature, maximum temperature, mean temperature, average relative moistness, precipitation, normal wind speed, high wind speed and average cloudiness. The output layer was composed of two neurons to represent rainy and dry weathers; and trial and error approach was adopted to select an appropriate number of inputs to the hybrid neural network. Saba et al. (2017) demonstrated that MLP forecasting results are better than RBF, however, the proposed simplified hybrid neural model comes out with better forecasting accuracy as compared to both individual networks. Additionally, results are better than reported in the state of art, using a simple neural structure that reduces training time and complexity.

Cui & Fearn (2018) investigated the use of convolutional neural networks (CNN) for near infrared (NIR) calibration. They proposed a unified CNN structure that can be used for general multivariate regression purpose. The comparison between the CNN method and the partial least squares regression (PLSR) method was done on three different NIR datasets of spectra and lab reference values. Datasets are from different sources and contain 6998, 1000 and 415 training and 618, 597 and 108 validation samples, respectively. Their results indicated that compared to the PLSR models, the CNN models are more accurate and less noisy. The convolutional layer in the CNN model can automatically find the suitable spectral preprocessing filter on the dataset, which significantly saves efforts in training the model.

6.4   *Big data and machine learning applied to wind modelling*

Numerous methods have been proposed to improve wind-speed forecasting in recent decades. These methods can be categorized into three types: physical approaches, statistical approaches and artificial-intelligence models. Statistical methods usually involve the auto-regressive integrated moving-average model (ARIMA), quantile-regression model (QR), and Kalman-filter model and achieve more accurate short-term wind-speed predictions than physical models (not long-term). However, the fluctuating and intermittent characteristics of wind-speed sequences require more complicated functions to capture the non-linear relationships rather than assuming a linear correlation structure.

Precise and reliable wind-speed prediction is vital for wind-farm operational planning. However, wind speed series usually have complex features, such as non-linearity and volatility, which makes the wind energy forecasting highly difficult. Aimed at this challenge, Qu et al. (2019) proposes a forecasting architecture based on a new hybrid decomposition technique (HDT) and an improved flower-pollination algorithm (FPA)-back propagation (BP) neural network prediction algorithm. The proposed HDT combines the complete ensemble empirical mode decomposition adaptive noise (CEEMDAN) and the empirical wavelet transform (EWT), which is unique, since the EWT is specifically employed to further decompose the high frequency intrinsic mode functions (IMFs) generated by CEEMDAN to reduce prediction complexity. And then an improved BPNN with the flower-pollination algorithm is applied to

forecast all of the decomposed IMFs and modes. To investigate the forecasting ability of the proposed model, the wind speed data collected from two different wind farms in Shandong, China were used for multi-step ahead forecasting. The experimental results show that the proposed model performs remarkably better than all of the other considered models in one-step to five-step wind speed forecasting, which indicates that the proposed model is highly suitable for non-stationary multi-step wind speed forecasting.

In Ma et al. (2019) they compared different AI algorithms for wind speed forecast, including: back-propagation neural network (BPNN), support vector machine (SVM), bagging, AdaBoost, random forest (RF), long short-term memory (LSTM), seasonal autoregressive integrated moving average (SARIMA), SVM with ensemble empirical mode decomposition (EEMD-SVM), and NCL-NN with wavelet denoising (WAT-NCL) models. They proposed a hybrid model that uses the wavelet analysis technique (WAT) for denoising, a negative correlation learning neural network (NCL-NN) ensemble, and an ensemble structure optimized using particle-swarm optimization (PSO). The approach was called WAT-NCL-PSO. The wavelet analysis technique (WAT) has become an effective tool for signal denoising in data preprocessing in many areas, because the topicality of wavelet analysis is good in terms of time series and frequency. Another valuable similar contribution can be found in Qu et al. (2017).

Multi-layer perceptron neural networks (MLP-NN) are widely utilized in forecasting applications but optimal training of these networks is still a challenge. A comprehensive assessment of MLP training approaches comprising of three stages was performed in Samet et al. (2019). First, the prediction performance was evaluated using twelve training algorithms. Next, optimization algorithms are utilized to enhance the best obtained network parameters obtained from the first step and the performance of eight optimization algorithms is evaluated. Finally, a novel modification is used to improve the performance of the optimization algorithms. Wavelet transformation is used to extract the features which will be fed to the MLP-NN as input data. The impact of utilizing Wavelet Transformation (WT) is studied, which is applied to case study time series in order to smooth out the intermittent nature of wind speed data and study the effect of WT on prediction precision. The twelve classic training algorithms: Basic Gradient Descent (BGD), Gradient Descent with Momentum (GDM), Fletcher-Reeves Conjugate Gradient (FRCG), Polak-Ribie're Conjugate Gradient (PRCG), Powell-Beale Conjugate Gradient (PBCG), Scaled Conjugate Gradient (SCG), Adaptive Learning Rate (ALR), Resilient Backpropagation Algorithm (Rprop), Broyden-Fletcher-Goldfarb-Shanno (BFGS), One Step Secant (OSS), Levenberg-Marquardt (LM), Bayesian Regularization (BR). Then the MLP-NN is further optimized around 10% of the most accurate results obtained in the previous step: Differential Evolution (DE), Genetic Algorithm (GA), Firefly Algorithm (FA), Particle Swarm Optimization (PSO), Imperial Competition Algorithm (ICA), Artificial Bee Colony (ABC), Bat Algorithm (BA), Cuckoo Optimization Algorithm (COA).

In Begam & Deepa (2019), an optimized nonlinear neural network architectural model integrated with a modified firefly algorithm and particle swarm optimization is proposed to perform multistep wind-speed forecasting for specific target sites. Factors that influence wind speed include temperature, atmospheric pressure, humidity, moisture in the air, rainfall and so on. Neural network models are used in forecasting applications due to their stability, adaptability, ability to handle large quantities of data, nonlinearity and generalizability. Their reason for developing an optimized nonlinear neural network model is that individual models each have their own advantages and limitations, leading to lower accuracy in forecasting and sometimes to instability. The developed novel nonlinear neural network model proposed by Begam & Deepa (2019) is based on a new, modified version of the firefly and particle swarm optimization algorithms. The new optimization algorithm was hybridized to obtain optimal weight and bias values for individual neural networks. They concluded that the developed

model for wind-speed time series data for the considered target sites shows better performance than the other models considered for comparison.

A hybrid method of short-term wind speed forecast was proposed in Yu et al. (2018a) by the wavelet packet decomposition, density-based spatial clustering of applications with noise, and the Elman neural network (WPD-DBSCAN-ENN). First, the WPD was applied to decompose a raw wind speed series into several subseries. The gradient boosted regression trees (GBRT) algorithm was then applied to determine the structure of the ENNs for each sub-wind series. The training dataset was then clustered by the DBSCAN to select the representative data for the ENNs. A key parameter in the DBSCAN was chosen through a new method. The wind speed forecast was simulated by the ENNs leading to successful results showed by Yu et al. 2018. They finally argued that autoregressive integrated moving average model (ARIMA) is a popular statistical method but it cannot handle nonlinear problems.

To improve the wind speed prediction accuracy, Wavelet Transform (WT) is widely employed to disaggregate an original wind speed series into several sub series before forecasting. Nevertheless, the highest frequency sub series usually has a great disturbance on the final prediction. Yu et al. (2017a) applied a Singular Spectrum Analysis (SSA) to make further processing on the highest frequency sub series, instead of making no modification on or getting rid of it, and therefore increase the forecast accuracy. So a hybrid decomposition technology called Improved WT (IWT) was proposed by the authors. Meanwhile, a new hybrid model IWT-ENN combined with IWT and Elman Neural Network (ENN) was also designed. The procedure of IWT was systematically investigated. Their experimental results show that: (1) the performance of the hybrid model IWT-ENN has a great improvement compared to that of others including the persistence method, ENN, Auto-Regressive (AR) model, Back Propagation Neural Network (BPNN) and Empirical Mode decomposition (EMD)-ENN; (2) compared to the two general strategies where the highest frequency sub series is without retreatment or eliminated, the new proposed hybrid model IWT-ENN has the best prediction performance.

Since the wind speed signal is stochastic and intermittent, it is difficult to achieve their satisfactory prediction. In Liu et al. (2018), a novel hybrid deep-learning wind speed prediction model, which combines the empirical wavelet transformation and two kinds of recurrent neural network, is proposed. In the new model, the empirical wavelet transformation is adopted to decompose the raw wind speed data into several sub-layers. The long short-term memory neural network, a deep learning algorithm based method, is utilized to predict the low-frequency wind speed sub-layers. The Elman neural network, a mainstream recurrent neural network, is built to predict the high-frequency sub-layers. In the executed forecasting experiments, eleven different forecasting models are included to validate the real prediction performance of the proposed model. The experimental results indicate that the proposed model has satisfactory performance in the high-precision wind speed prediction. Wang & Wu (2016) also argue that the decomposition algorithms can effectively improve the prediction performance of the built models through decomposing the intermittent raw wind time series into several more stationary sub-layers. Among the decomposition algorithms, the WD (Wavelet Decomposition), the WPD (Wavelet Packet Decomposition), the EMD (Empirical Mode Decomposition), the EEMD (Ensemble Empirical Mode Decomposition) and the FEEMD (Fast Ensemble Empirical Mode Decomposition) are widely recognized and used in the wind speed prediction.

In Xiao et al. (2017), a novel combination wind speed prediction model is proposed based on the EWT, LSTM network and Elman neural network. The model is composed of three steps as: (a) the EWT is adopted to decompose the raw wind speed data into several sub-layers; (b)

the LSTM network is employed to predict the low-frequency sub-layer, while the Elman neural network is employed to predict the high-frequency sub-layers; (c) the prediction results of each sub-layer are summarized to obtain the final results for the original wind speed data. According to Hu et al. (2017), the EWT can effectively identify and extract a finite number of intrinsic modes of a wind speed time series. The major steps of the EWT algorithm can be described as: (a) extending the signal; (b) executing the Fourier transform; (c) extracting the boundaries; (d) building the filter bank; (e) extracting the sub-bands.

The majority of previous studies tended to emphasize the structural improvement of individual forecasting models without considering the validity of data preprocessing. This can result in poor forecasting accuracy due to their failure to fully capture the effective information of the wind speed data. A new approach is proposed by Wang et al. (2019a), which successfully combines a data preprocessing technique with a linear combination method. Further, a new neural network framework is employed to determine the required combination weights to ensure improved prediction performance, thereby overcoming the drawback of the low accuracy of individual prediction models. Based on the above statement, this paper presents a novel combination prediction model that synthesizes the data preprocessing technique, dynamic weight generation framework, and several forecasting algorithms, namely support vector machine (SVM), extreme learning machine (ELM), bat algorithm-back propagation (BA-BP), and Elman ANN (EANN). In more detail, according to the decomposition and integration framework, the raw wind speed sequences are first decomposed into several components by the VMD algorithm; then, these sequences are reconstructed into a new time series, thereby ensuring that the original sequences no longer contain a high-frequency noise signal. Next, the processed wind speed data is used as input to each model for forecasting. Then, a dynamic weight combination approach, called the in-sample training-validation pair-based neural network weighting (IPN) (Wang et al. (2018a)) is employed to yield the relative optimal combination weights. Following this, the individual model weights are predicted using an RBF neural network; and finally a linear weighted approach is adopted to obtain the prediction results.

In order to enhance the accuracy of short-term wind speed prediction, a hybrid model based on VMD-WT and PCA-BP-RBF neural network is proposed in Zhang et al. (2019b). In data pre-processing period, the non-stationary wind speed sequence is decomposed into a number of relatively stationary intrinsic mode functions (IMF) by variational mode decomposition (VMD); then WT algorithm is used to perform secondary denoising on each IMF. At the same time, several factors affecting wind speed are introduced, from which the input features that participated in the prediction are selected by PCA-BP method. Next, the RBF neural network is utilized to predict each IMF. Finally, all IMF prediction results are aggregated to obtain the final wind speed value. Combining the data of Spanish and Chinese wind farms, the experiment results show that: (1) compared with EMD, VMD-WT can better solve the problems of modal aliasing and endpoint effect, which can make the periodic characteristics of each IMF more obvious, then promote the forecasting performance; (2) using PCA-BP method to filter the model input data, the redundant and irrelevant information is eliminated, the complexity of the model is reduced, and the predictive performance of RBF model is improved; (3) compared with other traditional models, the hybrid model proposed by Zhang et al. (2019b) has greatly improved the accuracy in short-term wind speed forecasting.

Many existing studies consider the spatio-temporal correlation of wind speed but ignore the influence of meteorological factors on wind speed with changes in time and space. Therefore, to obtain a reliable and accurate forecasting result, a novel multifactor spatio-temporal correlation model for wind speed forecasting is proposed in (Chen et al., 2019b) by combining a convolutional neural network and a long short-term memory neural network. The

convolutional neural network is used to extract the spatial feature relationship between the meteorological factors at various sites. The long short-term memory neural network is used to extract the temporal feature relationship between the historical time points. Meanwhile, a new data reconstruction method based on a three-dimensional matrix is developed to represent the proposed multifactor spatio-temporal correlation model.

In Zhao et al. (2020a) a novel data-driven method to perform short-term combination forecasts of average wind speed and wind turbulent standard deviation is presented. Actual data from China wind farm is utilized to execute the case experiments. According to atmospheric boundary layer theory and correlation analysis of the two prediction targets, their time-delay items are combined as the model input features. One-dimensional convolutional neural network is innovatively applied for this work to excavate the timing coupled information in data. Inspired by Pauta criterion, adaptive parameter named as "turbulent standard deviation multiplicator" is defined, which is the specific value of predicted average wind speed error and wind turbulent standard deviation. It is decided as the medium to extend the study to probabilistic framework. Based on its quantile analysis, the statistical significance of the parameter is verified and the prediction results can be integrated to achieve 4 h ahead probabilistic wind speed forecasts.

In Li et al. (2019a) an innovative framework for multi-step wind speed prediction using Wind Speed and Turbulence Intensity-based Recursive Neural Network is developed. In this study, real-time turbulence intensity is measured from wind speed, and multi-resolution features of wind speed and turbulence intensity are deployed as input for the prediction model. Ensemble recursive neural network is designed to execute prediction on multiple prediction intervals ranging from 10 min to 12 h with two different integrating strategies. Experimental results indicate that: (1) The proposed model dramatically outperforms conventional machine learning models on multi-step wind speed prediction; (2) The reliable wind speed prediction requires that the maximum time-resolution of turbulence intensity should be longer than prediction interval; (3) Turbulence intensity features involved prediction will achieves higher accuracy than the approaches that apply signal processing on raw wind speed, especially on middle long-term prediction. Therefore, this innovative scheme for multi-step wind speed prediction can be of immense utility to apply data-driven methods for accurate long-term wind speed prediction. According to Li et al. (2019a), wind speed prediction mainly comprises two categories: data-driven model based prediction and physical model based prediction. With aspect to physical model based prediction, Weather Research and Forecasting (WRF) and Numerical Weather Prediction (NWP) are the most popular technics tackling middle term and long-term wind speed prediction in large scale of area and spatial resolution.

Based on a review over the last 5 years' publications, ANN, deep learning methods and hybrid models are most frequently used in wind speed prediction. In order to alleviate the level of uncertainty in raw wind speed series, signal processing methods such as empirical mode decomposition/ensemble empirical mode decomposition (EMD/EEMD), variational mode decomposition (VMD), and wavelet analysis thrived. These new approaches decompose original time series into subseries of different patterns of frequencies which then can be analysed separately.

In Wang et al. (2017a) a novel deep learning based ensemble approach is proposed for probabilistic wind power forecasting. In this approach, an advanced point forecasting method is originally proposed based on wavelet transform and convolutional neural network. Wavelet transform is used to decompose the raw wind power data into different frequencies. The nonlinear features in each frequency that are used to improve the forecast accuracy are later effectively learned by the convolutional neural network. The uncertainties in wind power data,

i.e., the model misspecification and data noise, are separately identified thereafter. Consequently, the probabilistic distribution of wind power data can be statistically formulated. The proposed ensemble approach has been extensively assessed using real wind farm data from China, and the results demonstrate that the uncertainties in wind power data can be better learned using the proposed approach and that a competitive performance is obtained.

Overlooked in the literature is the influence of atmospheric turbulence and stability measurements in improving model predictions. It has been well-established through observations and physical models that these effects can have considerable influence on wind farm power production; yet consideration of these effects in statistical models is almost entirely absent from the literature. In Optis & Perr-Sauer (2019), the impact of atmospheric turbulence and stability inputs on statistical model predictions of wind farm power output in analysed. Hourly observations from a wind farm in the Pacific Northwest United States located in very complex terrain are used. Five common learning algorithms and nine atmospheric variables are considered, representing some measure of turbulence or stability. They found a considerable improvement in hourly power predictions when some measure of turbulence or stability is included in the model. In particular, turbulent kinetic energy was found to be the most important variable apart from wind speed and more important than wind direction, pressure, and temperature. By contrast, the choice of learning algorithm is shown to be relatively less important in improving predictions. Based on this work, Optis & Perr-Sauer (2019) recommend that turbulence and stability variables become standard inputs into statistical models of wind farm power production. The authors argue that, as statistical models require historical training data, such models also have the advantage of continuous improvement as more historical training data becomes available. It is therefore surprising that statistical models used for wind power forecasting, as reviewed in the literature, rarely consider turbulence or stability measures as inputs. Rather, models always make use of wind speeds, often wind directions, and sometimes temperature, air pressure, and humidity. The key question for the authors is whether adding turbulence or stability features can improve model predictions, and if so, how the magnitude of those improvements compares to model performance across the different learning algorithms.

7. STATISTICS, THEORY AND ANALYSIS

Probabilistic modelling and statistical analysis of environmental conditions is important. It will give a necessary input to structural reliability assessments and risk analysis of ships and other marine structures and provides a means to identify design conditions the structures are expected to withstand. In this section of the report, recent developments in statistical modelling of relevant met-ocean variables describing the environment at sea will be reviewed and presented. This includes a review of statistical modelling applied to such data, for example wave parameters, but also some theoretical and methodological developments from other fields of applications will be reviewed. This section of the report is divided into different sup-sections addressing various aspects of statistical modelling of the environment, such as long-term and short-term statistics, extreme value analysis, non-stationary analysis and covariate effects, multivariate analysis and joint distributions, machine learning applications and spatial statistics. This distinction into sub-topics may be somewhat arbitrary, and some papers address several of these topics, e.g. non-stationary, multivariate extreme value statistics for spatial data, but it is believed to be useful to still keep separate subsections for the main aspects.

7.1 Long-term and short-term statistics

Information about the statistics of relevant metocean variables is of great importance for the design of ships and other marine structures. Typically, the ocean environment can be described by long-term statistics of relevant sea state variables, for example significant wave height (H_S),

or by short-term statistics of wave parameters conditional on the sea state, for example individual wave heights within a stationary sea state. A common assumption is then that the ocean environment can be described as a piecewise stationary process, with stationary sea states of duration a few hours. Then, if the interest is in the long-term distribution of some wave parameter, say individual wave height, this can be found by combining the long-term distribution of the sea state, say $\mathbf{X}$, and the short-term distribution of the wave parameters of interest, say $\mathbf{Y}$ and integrating over all sea states

$$f_{\mathbf{Y}}(\mathbf{y}) = \int f_{Y|X}(\mathbf{y}|\mathbf{x}) \, f_{\mathbf{X}}(\mathbf{x}) dx. \tag{7.1}$$

Often, the long-term distribution of sea state variables may be discretized in the form of a scatter diagram, in which case the integral above translates to a sum. However, this implicitly neglects the serial correlation at various scales, and how to combine short-term distributions of individual waves with long-term distributions of sea states remains an active area of research.

In this section, various developments in modelling either the long-term distribution of sea state variables, short-term distribution of wave parameters or the combination of these to form long-term distribution of wave parameters will be reviewed. It should be noted that some statistical models have been well established in the industry to describe sea state and individual wave variables, e.g. a Weibull (often in its translated 3-parameter form) for significant wave height or a Rayleigh distribution (linear waves), Tayfun distribution or Forristall distribution (non-linear waves) for individual wave heights. Particular attention is given to developments related to shallow and intermediate water wave statistics, since this has historically not been given as much attention and it may be questionable how well standard statistical models describe such data. Note that the sea state variables and the wave variables may be multivariate, but multivariate modelling will be covered in subsection 7.4.

The translated 3-parameter Weibull distribution is often assumed to model significant wave height. However, a recent study suggests that another 3-parameter Weibull distribution, the exponentiated Weibull distribution with an additional shape parameter may fit the data better, especially if fitted by weighted least squares methods that emphasize the data in the tail of the distribution more in the model fitting Haselsteiner & Thoben (2020). Several candidate models for the probabilistic description of significant wave height are examined in Soukissian (2021), and compared to a model not previously applied to ocean data, i.e., the extended generalized inverse Gaussian distribution. According to the reported results, the proposed new distribution outperforms the other model candidates included in the study, for several, but not all datasets that were applied.

Typically, a statistical distribution is fitted to measurement data, but due to the often-limited availability of long-term in-situ measurements, statistical models are often fitted to wind-wave hindcast data. However, an approach to integrate model data and measured data in statistical modelling of significant wave height is proposed in Dentale et al. (2018), where model data are used as indicators and buoy data from nearby locations are used for bias correction and uncertainty evaluation.

It is acknowledged that some wave conditions are more hazardous to marine structures than others, for example waves with high steepness and waves from crossing sea states or unexpectedly severe wave conditions due to rapid development of the conditions. Hence, long-term statistics of potentially hazardous sea states are addressed in Teich et al. (2018), limited to crossing sea states, unusually steep waves and rapidly developing sea states, as opposed to modelling all sea states. Specifically, an enhancement factor defined to describe rapidly developing seas, wave steepness and directional spreading are analysed. The distributions of these variables are reported in terms of box-plots and scatter diagrams for selected locations

and seasons, but there is no parametric modelling of the distributions. The statistics associated with steep waves and steep sea states are also addressed in Myrhaug (2018), where spectral wave steepness is modelled as a lognormal distribution conditioned on significant wave height.

A rather different approach for modelling wave heights is proposed in Wang et al. (2017b), based on fractals and fractal theory. The methodology is extended in Liu et al. (2019b). They find that records of significant wave height exhibit weak fractality and suggest that their proposed method can be used to estimate design wave conditions for long return periods.

Long-term distributions of individual wave or crest heights require combining the short-term distribution of wave or crest heights in a sea state with the long-term distribution of sea states. Three different ways of estimating long-term distributions of individual wave and crest heights are discussed in Mackay & Johanning (2018c), assuming independent individual waves, independent highest wave height in a sea state and independent highest wave height in a storm, respectively. They found that methods that ignore the serial correlation of sea states tend to be biased and that storm-based approaches are more accurate. A generalized equivalent storm model for the long-term statistics of individual wave heights and crests is proposed in Mackay & Johanning (2018b). Methods to estimate the probability of extreme individual wave heights are also proposed in Mackay & Johanning (2018a) based on peaks-over-threshold analysis on random maxima in different sea states and based on the distribution of significant wave heights and wave model runs are also presented in Bulgakov et al. (2018).

A novel approach to combine the long-term statistics of sea states and the short term conditional distributions of extreme structural response is proposed in Gramstad et al. (2020). It applies a sequential sampling technique and a Gaussian process emulator for the response in order to achieve long-term extreme structural response assessment, accounting for both long-term and short-term variability.

The statistical properties of individual wave heights and crests with a particular focus on rogue waves are investigated in Gramstad et al. (2018a). The occurrence of rogue waves in measured data is compared to that predicted from statistical distributions such as Rayleigh, Forristall and Tayfun (for crests), and it was concluded that wave and crest heights generally follow the Forristall distributions relatively well. The exception is data from buoy measurements, which are known to underestimate wave crests. The physical constraints for exceeding probabilities of deep water rogue waves were studied in Mendes et al. (2021). Statistics of rogue waves in crossing sea states were also investigated in Gramstad et al. (2018b) and it is shown that the maximum crest elevation in such situations depends on the crossing angle, with an effect that is opposite to the nonlinear effects. Extreme waves in crossing sea states are also discussed in Brennan et al. (2018). The study in Støle-Hentschel et al. (2019) suggest that the extreme wave statistics in a mixed sea, composed of a wind-sea component and a following swell could appear to be milder than the extreme wave statistics of the wind sea alone. However, analysis of the two sea states separately reveals that the extreme wave statistics of wind sea can be nearly unaffected by the presence of a following swell. Statistics of extreme waves in single and mixed sea states were also studied in Wang et al. (2021c), and the shape and height of extreme wind waves are analysed in Alvise et al. (2017), based on space-time extremes.

The short-term distribution of individual wave periods in combined seas is investigated in Huang & Dong (2019), where parametric mixture distributions are suggested. The mixture models are compared with theoretical and parametric models for a number of different types of mixed sea states, including in-situ measured data and simulated data exhibiting two-peaked spectra. The paper suggests that the mixture distribution models yield improved modelling of the individual wave periods in combined seas.

The statistics of trough depths are perhaps less studied compared to wave crests. However, Wang (2018a) proposes to model individual trough depths in a sea state by way of a transformed Rayleigh distribution. They show that this gives a better fit to the data than the standard Rayleigh distribution that does not account for nonlinear effects. Wave trough exceedance probabilities in nonlinear seas are also studied in Wang (2018b) based on asymptotic expansions of the up-crossing rates and a transformation relating the non-Gaussian sea surface process with a Gaussian process.

Rogue waves have received much attention lately, and a statistical theory for rogue waves, based on large deviation theory is proposed in Dematteis et al. (2019). It allows for estimation of the far tail of the probability density function for the surface elevation and hence to estimate extreme event probabilities. Moreover, the method describes the precursors of rogue waves enabling early detection and prediction of the likelihood of extreme events within a given time window (Dematteis et al. (2018)).

7.1.1   Shallow water statistics

There has recently been much interest in the statistics of shallow water waves, and it is an open question to what extent statistical models used to describe deep ocean waves apply to waves in shallower waters. A recent study based on deep waters measurements presented in Kvingedal et al. (2018) suggests that the Forristall distributions for individual wave and crest heights generally fits the deep-water data well, but that it is less accurate in steeper sea states corresponding to high wind speeds. It is suggested that more research should be carried out at more shallow water depths. Results from a new laboratory study, based on data generated in different experimental facilities, are reported in Karmpadakis et al. (2019), where possible departures from commonly applied statistical distributions for crest heights due to different sea state steepness and water depths are investigated. They found that nonlinear effects beyond second order are important in intermediate water depths. However, the dissipative effects of wave breaking which increases with increased steepness reduces the nonlinear effects and the relative importance of wave breaking increases as the water depth reduces. Notwithstanding, they report that nonlinear amplifications of the crest height are largest in the shallower effective water depth. They conclude that systematic departures from the commonly applied Forristall model are evident and that an important challenge for future work is to derive a simple crest height distribution that incorporates such nonlinear effects.

Statistical analysis of data from large scale experiments of unidirectional waves propagating over a variable bottom profile presented in Zhang et al. (2019a) indicates that whereas the Rayleigh distribution performs well for individual waves in deep waters, it underpredicts the probability of large waves in shallower waters. A number of statistical distributions were fitted to the shallow water data, and it was suggested that the generalized Boccotti distribution (Alkhalidi & Tayfun (2013)) performs best for the shallow water data, particularly for large waves with $H > H_S$.

The fact that the steepness and asymmetries of extreme waves increase with shallower water depths is also found by Chen et al. (2018c), which proposes an empirical parametrization of wave steepness and asymmetries in nearshore environments.

The effect of variations in bottom topography on the distribution of wave heights is investigated in Bolles et al. (2019), suggesting that this may qualitatively influence the wave statistics. They found that abrupt depth changes can lead to random Gaussian seas becoming close to a gamma distribution a short distance downstream. This may give more frequent extreme waves, since the gamma distribution generally has heavier tails than the normal distribution. Statistical transitions from near Gaussian sea to highly skewed statistics in shallow water waves with an

abrupt depth change are also studied in Majda et al. (2019) and Majda & Qi (2019) where statistical dynamical models are proposed to explain and predict such effects.

The study presented in Malliouri et al. (2019) aims at obtaining a more accurate description of the long-term wave climate in shallow waters by combining short- and long-term statistics in deep waters. First, the joint long-term statistics of wave height and period in deep waters are found by combining the conditional short-term joint distribution of these parameters with the long-term joint distribution of the sea state's significant wave height and mean zero-crossing wave period. Then, the joint distribution in shallow waters is estimated by considering the wave transformation of each individual wave as the waves propagate from the open sea towards shallower waters. They find that wave statistics in shallower water differ from those in deeper water, but ends up with the same parametric family for intermediate waters as in deep water for the long-term distribution of sea states, i.e. Weibull or Gamma distributions for the significant wave height and conditional lognormal for mean zero-crossing period. However, the distributional parameters change.

7.2   *Extreme value analysis and extreme wave statistics*

Often in marine engineering applications it is the extremes of the environmental conditions that are of most interest, and extreme value analysis is often needed in order to extrapolate the tail of a statistical distribution to describe events occurring with a frequency that is small compared to the length of observations. Hence, statistical extreme value analysis is a useful tool that, even though it is well established in the industry, still has a number of unsolved challenges and remains an area of active research. In this sub-section, a review of recent developments in extreme value modelling will be presented, with a particular focus on applications to ocean climate variables. A recent review of some approaches to statistical modelling of extreme ocean environments are presented in Vanem et al. (2019a), see also Jonathan & Ewans (2013).

There are obviously large uncertainties in extreme value estimation, both aleatory and epistemic and the reliability of extreme value estimates is of great concern. Hence, in Samayam et al. (2017) a statistical approach for assessing the reliability of return value estimates from a particular extreme value estimation method is proposed, based on a variability criterion. The variations in return value estimates of ocean waves are also addressed in Naseef & Kumar (2017), where estimates from different methods and for both measured buoy data and reanalysis data are compared. They found, inter alia, that the influence of a single storm in the data can give a large difference in the extreme value estimates compared to the differences due to varying lengths of data. The effect of parameter estimation method and the available sample size for extreme value analysis of metocean conditions are also studied in Soukissian & Tsalis (2018). The uncertainty of extreme value estimates of ocean waves from different sources is also discussed Wada & Waseda (2018), and a Bayesian approach to account for these various sources of uncertainty is proposed in Jones et al. (2018) In fact, this paper suggests that Bayesian uncertainty analysis should be the preferred framework for estimation of uncertainty, and they propose a framework consisting of a statistical emulator that should try to predict hindcast simulator output and a statistical discrepancy model to predict the differences between hindcast output and the true wave environment.

Traditionally, there are three main approaches to univariate extreme value analysis, sometimes referred to as the initial distribution approach, where a probability distribution is fitted to all the available data and extreme quantiles are estimated based on this distribution; the peaks over threshold (POT) approach, where a distribution is fitted directly to the tail using only data that are above a certain threshold; and the block maxima (BM) approach, where a distribution is fitted for the tail using only block maxima, see e.g. Vanem (2015b), Orimolade et al. (2016), Takbash et al. (2019). The choice of approach is typically a traditional bias-variance tradeoff,

and extreme value methods such as POT and BM will typically be less biased for the tail behaviour but will have much larger variance due to the reduced sample size. The effect of a difference in sampling between the BM and POT methods is investigated in Shao et al. (2018), suggesting that annual maxima may be too few to yield reasonable extrapolation but that the POT method can be reasonable when the threshold is suitable. However, threshold selection remains a challenging task in POT modelling, where the choice of threshold may significantly influence the results. The differences in extreme wave height estimation in practical engineering practice, by following various guidelines and industry practices, are investigated in Katalinic & Parunov (2020).

From theory, it is known that the peaks over a sufficiently high threshold follow, asymptotically, the generalized Pareto distribution (see e.g Coles (2001)). The exponential distribution is a special case of the generalized Pareto distribution with one less degree of freedom. The appropriateness of the generalized Pareto distribution for modelling significant wave height data above a threshold is addressed in Teixeira et al. (2018), suggesting that it is more appropriate than for example a 2-parameter Weibull distribution or the exponential distribution. However, it is stressed that the results are highly sensitive to the choice of threshold, and a new threshold selection methodology is suggested based on the second order derivatives of the cumulative density function. The idea is that the point of the probability density function with maximum curvature represents a shift from the bulk of the data to the tail. The Weibull-Pareto distribution is proposed for modelling extreme wave heights above a threshold in Chen et al. (2019a).

A new fitting method for estimating the parameters of the generalized Pareto distribution for exceedances over thresholds are presented in (Chen et al. (2019b), based on transformations of order statistics, namely the weighted nonlinear least squares method. Simulation studies and real data analyses indicate that this method compares well with other methods for parameter estimation of the generalized Pareto distribution. Extreme value estimation based on small samples of low quality is addressed in Wada et al. (2016), proposing a practical approach based on Bayesian inference with the group likelihood rather than the standard likelihood and assuming near-uniform priors on the parameters. The group likelihood incorporates data uncertainty due to for example measurement errors. The effect of return value estimates from peaks over threshold analysis according to how parameter uncertainty is handled is discussed in Jonathan et al. (2021), illustrating that there are notable differences.

Threshold selection in peaks-over-threshold modelling remains an active area of research, even though there are several well established approaches to determine a suitable threshold. Some of these require manual interpretation and for example graphical inspection of various plots and leave room for subjectivity. Moreover, manual inspection means that threshold selection cannot be included in automated scripting of extreme value analysis. In order to remedy this, a novel automated threshold selection method is proposed in Liang et al. (2019), based on the characteristics of extrapolated significant wave height. The method investigates the differences in extrapolated return significant wave heights for neighboring thresholds to identify a stable threshold range. The highest threshold within the stable threshold range is then automatically selected as a suitable threshold. A comparison with some established threshold selection methods is presented, indicating reasonable agreement in resulting return value estimates. See also Shao et al. (2020) for a proposed automated method for extracting IID (independent and identically distributed) samples from time series for subsequent extreme value analysis.

One obvious drawback of the peaks-over-threshold approach is that it is wasteful. All data below the selected threshold is disregarded, even though they may contain useful information. In order to alleviate this problem, an approach applying multiple thresholds in parameter esti-

mation is proposed in Sun & Samorodnitsky (2019). These multiple levels are introduced as a means to incorporate more observations to reduce the variance of parameter estimates. In Northrop et al. (2017) a Bayesian cross-validation scheme is proposed to address the bias-variance trade-off in threshold selection by comparing thresholds based on extreme level predictive ability. They use Bayesian model averaging to combine inferences from many thresholds in order to reduce the sensitivity of the choice of a single threshold and to incorporate the uncertainty in the threshold choice. The approach is applied to data of significant wave height.

A new four-parameter extreme value distribution is proposed in Yousof et al. (2018), which is a generalization of the Frechet distribution for block maxima. There also exist other approaches to extreme value analysis, and some methods that have been applied to ocean waves include the equivalent storm approach (Laface et al. (2018)) and the average conditional exceedance rate (ACER) approach. A k-th order Markov model for extremes is proposed in Winter & Tawn (2017), which can account for temporal dependencies.

7.3   *Multivariate analysis and joint distributions*

Ships and other marine structures are typically affected by several environmental variables, and the joint effect of these on the environmental loads needs to be concidered. Failure to accurately account for the dependence between the variables may lead to overly conservative or non-conservative assessment of the structural reliability. Hence, multivariate statistical models for the joint behaviour of selected variables will give more accurate descriptions of environmental loads and responses and are important for improved design and operation of ships and other marine structures. Typically, assuming either independent or fully dependent variables may give wrong results even if the marginal, univariate models are appropriate Ross et al. (2020). However, it is increasingly challenging to find good distribution models with increasing number of variables, and even in the bivariate case, joint statistical modelling remains challenging. Thus, there has recently been considerable attention and research on multivariate analysis and joint statistical models for sea-state variables relevant for ship design and a brief review will be presented in this sub-section of the report. The evolution of joint probability methods used for coastal engineering applications is described Hames et al. (2019), including recent developments in multivariate statistical approaches such as joint exceedance curves and response based methods.

Examples of sea state variables that are often modelled jointly are significant wave height, mean wave period and mean wave direction. However, models that also include other variables such as wind speed and direction and sea level are also sometimes needed. More recently, joint distribution of waves and currents has been studied, although the availability of current data is still scarce and makes it difficult to establish good models for these variables (Bruserud & Haver (2017), Bruserud & Haver (2019)).

There are different ways of establishing a multivariate statistical model and three common approaches are to assume a parametric multivariate distribution, the so-called conditional modelling approach and the copula-based approach, see e.g. Vanem (2016). Non-parametric approaches are also sometimes used (Han et al. (2018a)), but these will have difficulties in extrapolation and cannot be expected to model the extremes accurately. With the former approach there exist some multivariate distributions that are often used, such as the multivariate normal or log-normal distributions, and the model parameters can then be fitted to the data. Typically, this involves estimation of the covariance matrix as well as location parameters and variable transformations can be applied to fit a multivariate normal distribution to non-Gaussian data (see e.g. Lucas & Guedes Soares (2015)). However, this approach is somewhat restrictive and not too frequently used in practice. An approach to multivariate modelling based

on multivariate probability distribution class is proposed in Faridafshin & Naess (2017), conditioned on log-concavity of the joint probability density function (Samworth (2018)). Although the numerical example given in Faridafshin & Naess (2017) is not for an environmental variable vector, it is assumed that this approach could also be used to model joint environmental variables, and the method is versatile enough to cover many multivariate probability models and it facilitates fitting a model to data with limited amounts of data.

The joint distribution of several variables can also be modelled by a hierarchical model as a product of marginal and conditional distributions (Bitner-Gregersen (2015)). Hence, a multivariate model for variables $X_1, X_2, \ldots, X_n$ can be modelled in the following form

$$f(X_1, X_2, \ldots, X_n) = f_1(X_1)\, f_{2|1}(X_2|X_1) \cdots f_{n|1,\ldots,n-1}(X_n|X_1, X_2, \ldots, X_{n-1}). \qquad (7.1)$$

Estimation of the model then involves estimating the marginal model for the primary variable and the various conditional models for the remaining variables. Sometimes, conditional independence between some of the variables can simplify the modelling, but it remains challenging to define the conditional models for all relevant variables. A new set of marginal and conditional distribution models for metocean variables is suggested in Horn et al. (2018), including conditional models for wind sea and swell variables as well as wind and water levels. They assume a sparse dependency table, where many of the variables can be modelled as independent from many of the other variables. They report a reasonable fit to the data. A conditional model was also assumed for modelling the joint distribution of significant wave height and current speed in Bruserud et al. (2018). The joint distribution of significant wave height and spectral peak period is modelled by a conditional model in Choi et al. (2019), where a hybrid Lonowe distribution is used for the marginal significant wave height and a conditional lognormal distribution for wave period. A conditional model based on Weibull-lognormal and lognormal distributions are used to model significant wave height and spectral wave steepness in Myrhaug et al. (2020). Different distributions were tried out to model the joint distribution of wave height and period using the conditional modelling approach in Huang et al. (2018a).

Hierarchical conditional models have also been used to model the joint distribution of circular-linear variables such as wind speed and direction, as outlined in Haghayeghi & Ketabdari (2018) and Vanem et al. (2020b). They assume a mixture of von Mises distributions for the marginal model of wind direction (the circular variable) and a conditional Weibull distribution for wind speed conditioned on the direction. Similar models extended to the tri-variate case for a combination of circular and linear variables are proposed in Haghayeghi et al. (2020).

Different bivariate time series models for significant wave height and spectral wave period are investigated in Sandvik et al. (2019), taking the joint behaviour of the variables into account together with temporal dependencies. They assume a conditional model for the joint distribution and transform the data to a standard normal space using the Rosenblatt transform and then apply a seasonal transform before various time-series models are applied to the transformed data. Vector autoregressive (VAR) models, vector ARMA (VARMA) models and Markov models are explored and it is concluded that the VAR and VARMA models perform well.

The use of copula to establish multivariate statistical models is an alternative that has received increasing attention in recent years. Essentially, a joint distribution of variables $X_1, X_2, \ldots, X_n$ can be modelled by way of their marginal distributions and a copula describing their dependence structure in the following way (see e.g. Nelsen (2006)),

$$f(X_1, X_2, \ldots, X_n) = f_1(X_1)\, f_2(X_2) \cdots f_n(X_n) c(F_1(X_1), F_2(X_2); \ldots, F_n(X_n)). \qquad (7.2)$$

The joint model can then be established by estimating the marginal models $f_1(X_1), f_2(X_2), \ldots, f_n(X_n)$, independently, and the copula density $c(\cdot)$. Such methods have been applied to environmental sea states variables (Li et al. (2018a), Chen et al. (2019d)), although it has been shown that straightforward use of standard symmetric copulae may not be appropriate, meaning that asymmetric copula-constructions are needed Vanem (2016), Zhang et al. (2018), Fazeres-Ferradosa et al. (2018). A combination of parametric and non-parametric marginal distributions and c-vine copulas is used to model multivariate wave and wind variables in Li & Zhang (2020), Bai et al. (2020), Bai et al. (2021).

Even though there exist several parametric copulas to choose from, it may not be straightforward to find the best one, even in the bivariate case. The copula approach can also be extended to three or more dimensions, for example by pair-copula constructions (Aas et al. (2009) or vine copulas Czado (2019)), including also circular variables (Lin & Dong (2019), Heredia-Zavoni & Montes-Iturrizaga (2019)), but modelling becomes increasingly challenging as the number of variables increases. A pair-copula based model for the trivariate probability distribution of typhoon-induced wind, wave and the time lag between them was outlined in Wei et al. (2021). More complicated models based on mixtures of copulae have also recently been suggested (Lin et al. (2020), Huang & Dong (2021)), offering an interesting approach to construct more complex multivariate models using copulas. Copulas are also used in a double entropy approach for establishing the joint distribution function for wave height and period in Liu et al. (2019a), and for modelling significant wave height in different locations in Jane et al. (2016).

Different copula-based models for modelling the joint distribution of circular-linear wind variables are explored in Soukissian & Karathanasi (2017), and compared to the so-called Johnson-Wehrly model (Johnson & Wehrly (1978)). It concluded that the Johnson-Wehrly model performs best and that this is a useful model for joint bivariate models of wind speed and direction. This model has also previously been applied to wave height and direction data in Soukissian (2014).

7.3.1 Multivariate extreme value analysis and environmental contours

The analysis and description of extreme values is especially challenging in the multivariate case, and it is even ambiguous what a multivariate return value is (Serinaldi (2015), see also e.g. Vanem (2018), Ross et al. (2020)). There are various statistical modelling approaches for multivariate extremes, and e.g. the conditional extremes model has recently been promoted as a good approach (Heffernan & Tawn (2004), Jonathan & Ewans (2013)). A critical review of this approach along with a comparison to classical multivariate extreme value models is given in Drees & JanBen (2017). Several applications of the conditional extremes model to metocean data are reported, including non-stationary models, in e.g. Ross et al. (2017b), Ross et al. (2018), Hansen et al. (2020) and Gouldby et al. (2017).

An event-based approach for the modelling of joint extremes of waves and sea levels is presented in Mazas & Hamm (2017), focusing on an event-based sampling from the bivariate time series and then joint modelling of the extreme samples by way of extreme value copulas. Various sampling methods are explored, and it is demonstrated that this has great influence on the results. The bivariate approach is also extended to higher-dimensional cases.

The environmental contour method is one approach for describing joint extremes which, given a joint statistical model, is often used for structural reliability assessment of ships and other marine structures. Traditionally, contours based on iso-density or IFORM have been used (Haver (1985), Haver & Winterstein (2009)), but recently a number of other approaches to environmental contours have been proposed, see e.g. Manuel et al. (2018), Haselsteiner et al.

(2017), Ross et al. (2020), Wrang et al. (2021), Eckert et al. (2021), and also the direct sampling method Huseby et al. (2015) is now recommended in DNV's recommended practice on environmental conditions DNV GL (2019). The effect of sampling variability on the uncertainties of environmental contours is studied in a simulation experiment reported in Vanem et al. (2019b), suggesting that this is an important aspect to consider when constructing environmental contours based on finite datasets. Other uncertainties in environmental contours are assessed in Montes-Iturrizaga & Heredia-Zavoni (2017).

Recent applications of the environmental contour method for different problems are discussed also in e.g. Horn & Winterstein (2018), Velarde et al. (2019), Raed et al. (2020), Li & Zhang (2020), Chen et al. (2020a) and Zhao et al. (2020b). Environmental contours based on non-parametric bivariate kernel density estimation is also proposed in Wang (2020), but it is advised to use such methods with great care when the interest is in the tails of the distributions, as is the case when constructing environmental contours. Recently, free software has been released allowing for easy computation of environmental contours (Haselsteiner et al. (2019b)), but it is noted that this software has serious limitations with regards to the choice of parametric distribution functions and fitting methods that can be used. Different contour methods are compared with response-based methods for extreme ship response analysis in Vanem et al. (2020a), suggesting that results are in general agreement.

There have been several proposed developments of contour methods for describing joint extreme conditions recently. Buffered environmental contours are presented in Dahl & Huseby (2018), based on buffered failure probabilities. Similar adjustments corresponding to a number of unwanted events are presented in Vanem (2020a). Environmental contours based on a particular version of inverse SORM is proposed in Chai & Leira (2018), to give more conservative contours than the IFORM method, and contours based on inverse directional simulation are presented in Dimitrov (2020). A variance reduction technique is proposed in Clarindo et al. (2021). A novel approach to construct environmental contours without the need for fitting a joint distribution is developed in Derbanne & de Hauteclocque (2019), based on fitting a number of univariate distributions to data projected in various search directions.

Most applications of environmental contours focus on bivariate problems but are in principle extendable to arbitrary dimensions. An extension of the direct sampling approach to higher dimensions, with examples of 3-dimensional problems is presented in Vanem (2019). A similar approach is also taken in Raillard et al. (2019). In some cases, one of the variables in a multivariate problem may be circular (e.g. direction or period/season), and environmental contours for such situations are proposed in Haghayeghi & Ketabdari (2017), Vanem et al. (2020b). Environmental contours for a three-dimensional problem where one of the variables are circular are presented in Heredia-Zavoni & Montes-Iturrizaga (2019), based on three-dimensional vine copulas.

Given the fact that environmental contours have been an active area of research in recent years, a benchmarking exercise was announced at OMAE 2019 (Haselsteiner et al. (2019b)), where researchers and practitioners were invited to construct contours for datasets that were made available. Several responses to this call were presented at OMAE 2020 and summarized in Haselsteiner et al. (2021). This summary revealed that there is significant variability in contour results from different practitioners, due to differences in data handling, statistical modelling and contour methods. One particular issue that was highlighted as important in this benchmark study was how to account for serial dependence in the statistical modelling, something that is further investigated in Mackay et al. (2021). A forthcoming special issue of Ocean Engineering will present the summary as well as individual contributions to this benchmark.

7.4   *Non-stationary analysis and covariate effects*

The statistics of environmental variables will typically be dependent on many factors such as season of the year, location, long-term trends (e.g. due to climate change) and prevailing wind or wave directions. That is, the IID assumption will generally not be met and data describing the environment will typically not be stationary. These non-stationarities could be important and should be incorporated in the statistical models (Serinaldi & Kilsby (2015)). One way of doing this is by including covariate effects in the statistical models. Another is to perform pre-processing of the data to remove the non-stationary effects and to assume stationary models on the residuals or pre-processed data. Yet another approach could be to use time-series to account for autocorrelations and dependencies in space and time. The effect of non-stationarity would be important for both univariate and joint models, and for extreme value models and distribution models for all the data.

Stationary and non-stationary extreme value models for significant wave height are compared in Calderon-Vega et al. (2019). The non-stationary models account for the seasonal variations and results suggest that non-stationary models perform better. A number of simulation studies are presented in Mackay & Jonathan (2020), where stationary extreme value models are fitted to non-stationary data, non-stationary models are fitted to stationary data and non-stationary models are fitted to non-stationary data, to assess the performance of stationary and non-stationary extreme value models. They conclude that non-stationary extreme value models can give improved estimates of return values, provided that the models are consistent with the data-generating model. However, in general, the relative performance of stationary and non-stationary extreme value models will be problem specific, and in some cases stationary models may be sufficient to obtain omnicovariate return values.

A number of recent publications address the problem of accounting for non-stationarity in extreme value modelling of sea state variables. A review of methods for non-stationary extreme events is presented in Salas et al. (2018), and some approaches to model and make inference of the effect of covariates for extreme ocean environments are critically compared in Jones et al. (2016). A simple approach to account for non-stationarity due to seasonal effects is presented in Vanem (2018), where data are pre-processed by seasonal normalization in order to make the IID assumption more reasonable, and then fitting stationary statistical models to the pre-processed data. The effect of seasonality can then be put back in for estimation of return values for particular seasons, or for omni-seasonal estimates. Spatiotemporal trends in significant wave height are based on non- parametric methods such as the Theil-Sen estimator and the line of best fit in Wang et al. (2021a), see also De Leo et al. (2020).

Extreme value models for ocean environments with covariates are addressed in several papers. The directional time evolution of extreme significant sea states is modelled assuming a nonstationary Markov extremal model in Tendijck et al. (2019). Directional-seasonal extreme value analysis of storm peak significant wave height is presented in Ross et al. (2017b), where a piecewise gamma-generalized Pareto distribution is assumed, for body and tail, respectively, where the effect of covariates is based on discrete bins in the covariate space but smoothed by way of splines across bins. Bayesian inference is used with conjugate priors. The effect of long-term climatic trends may also be incorporated in extreme value models by using time as a covariate (see e.g. Vanem (2015a) for a block maximum approach and Montoya et al. (2018) for a peaks-over-threshold approach). A non-stationary generalized extreme value model with a cyclic time-covariate with a period of around 30 years was used to model extremes in Jagtap et al. (2019). The need for non-stationary extreme value analysis for significant wave height in the Mediterranean Sea was explored in De Leo et al. (2021).

Non-stationary extreme value models for multivariate extremes are also being promoted. Non-stationary conditional extremes models composed from piecewise stationary models in covariate bins are presented in Ross et al. (2018), and non-stationary marginal models with stationary conditional extremes models are suggested in Hansen et al. (2020). The effects of several covariates such as direction, season, surge and tide on the joint distribution of extreme significant wave height, individual wave and crest heights and total water level are modelled in Feld et al. (2019). A joint model for several storm wave climate variables based on combining marginal models with copulas for describing the dependencies on time and ENSO variations, and using a vine copula to model different storm summary statistics is presented in Davies et al. (2017). A multivariate non-stationary model for marine storms using time and climate indices as covariates and assuming copulas for the dependence modelling is presented in Lin-Ye et al. (2017).

Non-stationary joint time-series of significant wave height and mean zero-crossing wave periods that captures seasonal and inter-annual patterns are modelled in Jager et al. (2019), assuming a model with several components including renewal processes, Fourier series with random coefficients, ARMA processes and copulas. A regime switching approach is applied to account for switches in main wave direction.

7.5   *Spatial and temporal statistics*

The oceans, by their nature, cover a large area and one is often interested in the spatial and temporal variability of sea states and other environmental variables and to model the spatial and temporal dependencies of relevant parameters, as well as their extremes. Hence techniques from spatial statistics and time series modelling are relevant and useful for statistical modelling of the ocean environment, and several applications of spatial modelling have been applied to ocean environment data. Spatio-temporal modelling considers dependencies in both space and time and combines spatial models and temporal models. In the following, a brief review of relevant literature will be presented.

7.5.1   *Spatial statistics*

A review of some methods for spatial analysis of extremes is given in Hiles et al. (2019), including regressing distributional parameters on spatially varying covariates and regional frequency analysis. They develop an approach for modelling the spatial variability of extreme significant wave height utilizing both long-term measurements and high resolution hindcast. A spatial model for extremes is proposed in Reich & Shaby (2019), where the extremes are modelled by a generalized extreme value model and where the parameters vary in space according to a clustering of the locations and a spatial Markov model for the clusters. The GEV model is also combined with a spatial model in Sartini et al. (2017).

The regional frequency analysis is a method to utilize spatial data by pooling data from locations that can be regarded as homogeneous in order to effectively increase the sample size in estimating the probability distribution (or equivalently, the quantile function) within the region. The location-specific probability distributions can then be found from this common regional distribution function (growth curve) by applying a site-specific scaling factor (the index flood). Regional frequency analysis has traditionally been applied in hydrology, and a few recent applications of this method have been reported for ocean wave data (Vanem (2017), Sartini et al. (2018), Campos et al. (2019b), Lucas et al. (2020), Lucas et al. (2017)) and wind data (Campos et al. (2018a)). These studies indicate that regional frequency analysis is a useful tool for spatial modelling of ocean environment data and that improved estimates of extreme return values can be obtained, if the underlying assumptions of homogeneous regions are reasonable. Confidence bounds for extreme quantile estimates obtained by regional frequency analysis

were constructed in Lucas et al. (2019a), suggesting that uncertainties are small. An application of bivariate regional frequency analysis for significant wave height and wave period is presented in Vanem (2020b), demonstrating that the regional frequency analysis approach can be extended and is useful for multivariate extreme value analyses.

Spatial extreme statistics can be modelled as so-called max-stable processes in order to characterize the spatial dependence, and spatial models based on such processes are applied for modelling storm peak significant wave height in Ross et al. (2017a). However, as pointed out in Drees et al. (2018) space-time processes are typically only observed at discrete points, and the influence of interpolation to fill such gaps in the marginal distributions is discussed. Spatial extreme events have also been modelled by the conditional extremes model, where the distribution of extreme events over a spatial region can be conditioned on the spatial process being extreme at observed locations within the region (Tawn et al. (2018)). Such conditional extremes spatial models are applied to ocean storm severity data, i.e. significant wave height, in Shooter et al. (2019), see also Shooter et al. (2021) where the conditional dependence of a spatial process measured at one or more locations are conditioned on extreme values of the process at other locations.

A spatial model for extreme significant wave height in cyclone-dominated regions is proposed in Wada et al. (2018b), which combines models for the space-time maximum with models for the exposure. The space-time maximum is defined as the largest significant wave height observed anywhere in the spatial region during the time period of a cyclone, and such space-time maxima above a threshold are modelled by a generalized Pareto distribution. Since space-time maxima are used, data from all cyclone events are used and not only data from a single location. This is then combined with the exposure for a particular location, which is defined as the storm severity at those locations as a fraction of the space-time maximum. A marginal distribution is then estimated for the exposure at all locations, providing a spatial model over the domain. The joint STM-E model is then found by assuming that exposure is independent of the space-time maximum. The model is applied to data from Gulf of Mexico in Wada et al. (2019).

A non-stationary spatial model for significant wave height using stochastic partial differential equations (SPDE) is proposed in Hildeman et al. (2019b). They combine a SPDE representation of a Gaussian Matern field with a deformation approach to capture both non-stationarities and anisotropies. It is shown that this model agrees well with significant wave height data from the North Atlantic Ocean. This model is extended to jointly model significant wave height and wave period over space in Hildeman et al. (2019a). Other multivariate stochastic differential equation random fields for multivariate spatial modelling are discussed in Bolin & Wallin (2020).

Graphical models have recently been proposed as alternatives to spatial models, see e.g. Engelke & Hitz (2019), Nerantzaki & Papalexiou (2019), and a model for spatial extremes based on ensemble of trees of pairwise copulas are presented in Yu et al. (2017b). High-dimensional dependence modelling using vine copulas and graphical methods are suggested in Muller & Czado (2019). Spatial and temporal clustering of extreme wave events are outlined in Santos et al. (2017), where main spatial footprints were identified around the coast of UK.

7.5.2   Time series analysis

In time-series analysis, one wants to model the temporal evolution of stochastic variables, and several techniques are available for such temporal dependencies or correlations. For multivariate time-series, one needs to model both the cross-correlations, or dependencies between variables, and the temporal dependencies, or autocorrelations, in the time series.

A generic approach to modelling and simulating time series with specified marginal distribution and correlation structures are proposed in Papalexiou (2018). This is based on establishing proper transformations and finding a parent Gaussian autoregressive model that yields a time series with the desired properties after transformation. Such methods could be applied to time-series of metocean data in order to obtain statistical models that not only describe the marginal distribution, but also the serial correlation, see also Papalexiou et al. (2018).

Fuzzy time-series have been proposed for modelling non-stationary time series of wave and wind data in Stefanakos (2016), and extensions and applications at various time scales of such modelling have been presented in Stefanakos & Vanem (2018) and Wu et al. (2019). Whereas a conventional time series is considered as a realization of a random process, a fuzzy time series is considered a realization of a fuzzy random process, i.e. a sequence of fuzzy random variables. A fuzzy time series is then modelling the temporal relationship between such fuzzy variables. Typically, fuzzy time series modelling involves fuzzification of the input variables (data; crisp values), inference and defuzzification to transfer fuzzy output to crisp values.

A shapelet transform was applied to time-series of ocean wave data to classify and identify breaking waves in Arul & Kareem (2021).

Bivariate time-series of significant wave height and wave period using vine-copulas and assuming the Markov property for the temporal evolution are presented in Jager et al. (2017). Joint time series modelling of wave height, period and directional data are also presented in Jager et al. (2019).

In a comprehensive study, Klahn et al. (2021) presents a detailed investigation of the role played by the wave steepness in connection with the statistical properties of the surface elevation and fluid kinematics in irregular, directionally spread, deep-water wave fields initially given by a JONSWAP spectrum. Using ensembles of large wave fields obtained from fully nonlinear simulations, they consider the statistical properties of the surface elevations, velocities and accelerations. Furthermore, they investigate the joint PDF of the surface elevation and each of the velocities and accelerations at the surface, and use it to determine the surface elevations for which the velocities and accelerations at the surface are large. Finally, they consider the PDFs of the location at which the largest velocities and accelerations occur relative to the crest.

7.6   *Machine learning applications*

Advanced statistical models and algorithms for describing or predicting random behaviour based on sampled data are often referred to as machine learning. Typically, machine learning is used for regression and classification tasks, relating various responses or outputs to input data, in what is commonly referred to as supervised learning, or in pattern recognition and clustering of unlabelled data in what is referred to as unsupervised learning. As alternatives to more traditional statistical models for regression and classification, machine learning has recently been used in a number of applications related to the description and prediction of the ocean environment. A brief review of some recent applications will be given herein. A recent survey on machine learning methods for various sea wave parameters can be found in Umair et al. (2019)

Artificial neural networks are powerful algorithms that can be used to model highly nonlinear relationships between inputs and outputs, and several recent applications of such models to predict wave parameters reported. Significant wave height predictions based on neural networks using wind speed and previous observations of significant wave height is presented in Mudronja et al. (2017), see also Fan et al. (2020), Demetriou et al. (2021) and Wang et al. (2021b). Neural networks, as well as support vector machines are applied in Berbic et al. (2017)

to predict near-future significant wave height based on previous measurements of significant wave height and wind measurements. Sequential neural networks, with the capability of updating the network as it learns, are applied to predict wave heights based on several input variables including previous wave heights and wind speed in Kumar et al. (2017). Hybrid models combining neural networks with the mind evolutionary algorithm and the genetic algorithm, respectively, are explored in Wang et al. (2018b). Machine learning models are trained by numerical wave model output to forecast wave conditions in James et al. (2018), where a neural network is used to model significant wave height and a support vector machine is used to model wave period. Neural networks are applied for wave ensemble averaging based on 20 ensemble members of a wave forecast model in Campos et al. (2019a), reporting a benefit corresponding to gaining five forecast days compared to using the arithmetic ensemble mean averaging. Convolutional neural networks have also been used to predict wave conditions from acceleration data Liu et al. (2019c), deep neural networks have been used to estimate significant wave height in real time from raw ocean images Choi et al. (2020), and recurrent and sequence-to-sequence networks have been used to forecast significant wave height Pirhooshyaran & Snyder (2020).

Although different variants of neural networks are perhaps the most commonly used machine learning technique, there are several other approaches that have been used to predict ocean wave conditions or other related variables, see e.g. Sinha et al. (2018), Wei (2018). These include fuzzy k-nearest neighbour models (Nikoo et al. (2018)), Group Method of Data Handling (GMDH) models (Shahabi et al. (2016)), deep learning models (Zhang & Dai (2019), Kumar et al. (2018a)), hybrid models (Oh & Suh (2018)), support vector machines (Chen (2019)), random forests (Hengl et al. (2018)), sequential sampling and Gaussian processes regression (Mohamad & Sapsis (2018)) and ensembles of neural networks (Kumar et al. (2018b), Ali & Prasad (2019)). A genetic algorithm is proposed to estimate JONSWAP spectral wave parameters from measured data in Rueda-Bayona et al. (2020). Ensembles of computationally lightweight surrogate models for forecasting ocean waves were combined with aggregation techniques in O'Donncha et al. (2019).

8. WAVE-COUPLED PHENOMENA

Wave-induced effects in the lower atmosphere and the upper ocean have been a major research topic over the last decade (see e.g. Babanin et al. (2012) for introduction to this topic). It is rapidly becoming clear that many large-scale geophysical processes are essentially coupled with the surface waves, and those include weather, tropical cyclones, storm surges, climate and other phenomena in the atmosphere, at air/sea and sea/land interface, including coupled interactions of waves with sea ice and fast ice, and many issues of the upper-ocean mixing and ocean currents below the surface. Besides, the wind-wave climate itself experiences large-scale trends and fluctuations (Young et al. (2011), Young & Ribal (2019)).

Until now, coupling of the wave-related air-sea interactions into weather and climate research has been conducted in ad hoc manner or not conducted at all, due to two main reasons. In terms of geophysics, the reason is the traditional perception that processes of such distant scales can be studied and modelled separately, and exchange between the scales can be parameterized as some larger-scale average (mean fluxes of energy and momentum in this case). In technical terms, the computational costs of such coupling have been prohibitive until recently. Things, however, are changing now.

8.1 Wave breaking

Wave breaking, if it did not exist, would have to be invented. Its role in the coupled air-wave-ocean systems is hard to overestimate. On the surface, it limits the wave growth and hence

prevents occurrence of very high waves, and serves as a major dissipation mechanism which controls wave evolution. Above the surface, it facilitates the fluxes of momentum and energy (through the sea drag), heat and moisture (through spray). Spray and spume, furthermore, link waves to aerosol production and thus all the way to inland corrosion, cloud physics, and climate. Below the surface, wave breaking is a major source of turbulence and the main source of bubbles (hence a major contributor to the ambient noise). The former is relevant for ocean mixing, sediment and nutrient suspension and transport, the latter to gas exchange, aeration, and underwater acoustics, and both offer links to biology (biomass production). Wave momentum, lost due to breaking, goes to surface currents and contributes to scattering of surface debris and pollutants.

In normal conditions, one or two waves out of 100 breaks, and therefore every wave record contains breaking waves. Liberzon et al. (2019) suggested an original method to distinguish such breaking waves from those that are non-breaking. This new method enables the detection of breakers by using only surface elevation fluctuation measurements from a single wave gauge. The detection is based on the use of the phase-time method to identify breaking-associated patterns in the instantaneous frequency variations of surface elevation fluctuations. A wavelet-based pattern recognition algorithm is devised to find such patterns and provide accurate detection of breakers in the examined records. Validation and performance tests, conducted using both laboratory and open-sea data, including mechanically generated and wind-forced waves, are reported in this paper. The method is shown to be capable to achieve a positive detection rate exceeding 90%.

As the trigger of the main dissipation mechanism (often called whitecapping dissipation), wave breaking is parameterized and included in all modern models for wave forecast and wave evolution. Still, descriptions of this mechanism contain very large uncertainties, and field measurements of wave-breaking dissipations are very few. In this regard, a recent study of Viana et al. (2020) attempted such measurement by means of satellite remote sensing. They used polarimetric Synthetic Aperture Radar (SAR) data to estimate wave energy dissipation under different wind and sea conditions. The methodology considered decomposing the backscatter SAR return in terms of two contributions: a polarized contribution, associated with the fast response of the local wind (Bragg backscattering), and a non-polarized (NP) contribution, associated with wave breaking (Non-Bragg backscattering). Wind and wave parameters were estimated from the NP contribution and used to calculate the dissipation from a parametric model dependent of these parameters. The results were analysed using outputs of wave model WAVEWATCH III. For wind-sea conditions, the estimates obtained from pol-SAR data showed good agreement with whitecapping dissipation obtained in numerical simulations. Under prevailing swell conditions, the total energy dissipation rate was higher than expected.

Wave breaking is closely related to the problem of rogue waves. Those are waves of maximal possible height, usually induced either by the modulational instability or by superposition of waves, but the growth of this height is limited by breaking. Effects of breaking on formation and probability of rogue waves in 1D and 2D wave fields with JONSWAP spectrum were considered by Kirezci et al. (2021a, b, respectively). Detailed laboratory modelling of the well-known Draupner rogue wave, and of the role of wave breaking in crossing seas was conducted by McAllister et al. (2019).

The effect of wind on the wave breaking induced by the modulational instability was investigated numerically by Iafrati et al. (2019). The two-phase flow was modelled by the two-dimensional Navier-Stokes equations for a single incompressible fluid and a Volume of Fluid technique was employed to capture the air–water interface. Simulations covered the initial

development of the wind profile, the growth of the modulation instability, the breaking and post breaking phases. The latter is particularly interesting as investigations of this phase of wave breaking are very rare. It was shown that an initial growth of the energy content in water was observed, followed by a dissipation stage which is not related to the breaking process. The dissipation rate for the wind case was noticeably higher and was found to be related to the larger amount of air entrained by the breaking process, which links this problem to the topic of air-sea gas exchange.

This link was explored in detail by Li et al. (2021b) and resulted in parameterization of the CO_2 exchange in terms of both wind and waves. The CO_2 gas transfer velocity (KCO2) at air–sea interface is usually parameterized with the wind speed, but to a great extent it is defined by waves and wave breaking. To investigate the direct relationship between KCO2 and waves, laboratory experiments were conducted in a wind-wave flume. Three types of waves were forced in the flume: modulated wave trains generated by a wavemaker, wind waves with 10-m wind speed ranging from 4.5 to 15.5m/s, and (mechanically generated) modulated wave trains coupled with superimposed wind force. The wave height and wave orbital velocity were found to be well correlated with KCO2 whereas wind speed alone cannot adequately describe KCO2. To reconcile various measurements, non-dimensional equations were established in which gas transfer velocity is expressed of wave parameters (including wave-breaking rate) and an additional secondary factor to account for influence of the wind.

8.2   *Wave-current interactions*

Surface waves are wind-generated, but the respective fluid motion is mostly a part of the water side of the interface and is strongly linked to the upper-ocean dynamics including the ocean currents. Wave-current interactions are common conditions both in the open ocean and in coastal areas. Major currents such as the Gulfstream, Kuroshio, or Agulhas are well known for harsh seas and high likelihood of abnormal (rogue) waves. Tidal inlets with waves on strong and variable currents are a typical feature of shipping routes in coastal areas. While linear effects of currents on waves, such as refraction, Doppler shift, or relative speed with respect to the wind are assumed to be implicitly or explicitly accommodated in wave-forecast models (often unverified and not validated), nonlinear effects are usually left out or, at this stage, even unknown. These include changes to wave-wave nonlinear interactions in presence of currents with horizontal or vertical velocity gradients, wave–current energy and momentum exchanges, and nonlinear modifications of the wave spectrum.

A review paper by Babanin et al. (2017) outlines principles of phase-resolving and phase-averaged wave models, with emphasis on the state of the art of wave-current interaction physics. They argue that these interactions are the least well-developed part of such models. Linear and nonlinear dynamics of waves on currents are discussed, depth-integrated and depth-varying approaches are described, examples of numerical model performance for waves on currents in realistic oceanic scenarios are presented.

Waves, in turn, can substantially influence the surface currents through their Stokes drift, and even more so through radiation stress due to momentum lost in wave breaking (even in deep water). These influences are largely missing in modelling the ocean circulation of open oceans, hence an understanding of this gap brings the old topic of wave-current interactions into the active research focus again. Most essential is the role of waves in influencing and even producing currents in finite depths where wave breaking is extensive. Fully coupled wave-current models are difficult, both scientifically and numerically (computationally), and can be a subject of an entire thesis such as Tran (2020). This author investigated, experimentally and numerically, hydrodynamics in Port Phillip Bay (PPB), a large tidal inlet in Australia, both due to natural causes and in response to channel deepening. The coupled hydrodynamic modelling

system included SCHISM (ocean model) and WWMIII (wave model). Typical for an inlet, the current velocity is strong (e.g. an excess of 3m/s) at the entrance of PPB, and it is weak in other parts of PPB, which fact finds its reflection on the wave climate and trends. The navigation channel deepening (on the way to the Port of Melbourne at the North top of PPB) could increase the current speed by up to 10% at both-ends of the channel system. Consequently, this would modify the wave field in the south of the Bay. For example, the wave height at the entrance was flattened due to a strong current during the ebb tide, while an increase of 10% of significant wave height was found in the area of coastlines nearby the south channel system.

Surface currents in the open seas usually involve a substantial proportion of the upper ocean, but the vertical profile of such currents remain hidden from observations. Lund et al. (2018) offered a very innovative paper to estimate such profiles experimentally. A HZG marine X-band radar (MR) onboard research vessel m/v "F.G. Walton Smith" was used to yield near-surface current maps at ~500 m resolution up to a maximum range of ~3 km. This study employed the drifter measurements to perform the first comprehensive validation of near-surface current maps. For a total of 4130 MR–drifter pairs the root-mean-square error for the current speed was 4 cms and for the current direction 12°. Underpinned by the in-situ measurements, the MR samples currents at a greater effective depth than the drifters (1-5 m vs. ~0.4 m). The mean MR–drifter differences are consistent with a wave- and wind-driven vertical current profile that weakens with increasing depth and rotates clockwise from the wind direction (by 0.7% of the wind speed and 15°). The technique presented has great potential in observational oceanography, as it allows research vessels with X-band radars to map the horizontal flow structure, complementing the vertical profiles measured by ADCP.

8.3   *Wave-ice interactions*

Wave-ice interactions have long been a marginal field of research, but with the Arctic opening from ice in summer months, and with some major infrastructure projects in Antarctica, wave-ice modelling acquires important practical meaning. Among the various theories to explain wave-ice interactions, some differ qualitatively, i.e. wave scattering (without dissipation) and dissipation (with or without scattering); others differ quantitatively. In the field, all the mechanisms are acting together, depending on their relative magnitude, and practical guidance of the existing theoretical knowledge in forecasting waves in Marginal Ice Zones (MIZ) is limited. Additional complications in this regard are due to waves being able to break the ice and thus facilitate its melt - this makes wave-ice interaction an essentially coupled problem.

The wave-ice problem can be roughly subdivided into three large groups of interactions. First is the interaction of waves with solid or uniform ice. Second, once the ice is broken, which is the definition of the Marginal Ice Zone (MIZ), the dissipation mechanism is different: it is due to various interactions of ice floes with each other, such as collisions, rafting etc., all of which take energy from the mean wave motion. Therefore, third, for wave models to predict waves in ice, they should be able to identify the moment of ice breakup by waves.

Starting from the third problem, Voermans et al. (2020) proposed a universal nondimensional threshold for the wave-ice breakup. Based on field observations, they produced a breakup parameterization for an observational threshold which separates breaking and non-breaking cases. The data cover a wide range of scales, from laboratory-grown ice to polar field observations. Both field and laboratory observations tend to converge to a single quantitative threshold at which the wave-induced sea-ice breakup takes place, which opens a promising avenue for robust parametrization in operational forecasting models.

This threshold separates interactions of group one and group two types, but a traditional method of modelling waves in ice (i.e. when the threshold is not known or cannot be identified based

on available initial conditions), is to merge the different mechanisms into a single parameterization where 'effective' ice properties (mostly viscosity) are meant to roughly describe wave attenuation in any sea-ice circumstances. Liu et al (2020) implemented three dissipative (two viscoelastic and one viscous) ice models in the spectral wave model WAVEWATCH-III to estimate the ice-induced wave attenuation rate. These models are then explored and intercompared through hindcasts of two field cases: one in the autumn Beaufort Sea in 2015 and the other in the Antarctic MIZ in 2012. The capability of these dissipative models, along with their limitations and applicability to operational forecasts, were analysed and discussed. The sensitivity of the simulated wave height to different source terms – the ice-induced wave decay and other physical processes (e.g., wind input, nonlinear four-wave interactions) was also investigated. For the Antarctic MIZ experiment, the ''other'' terms were found to be remarkably less than the ice term and thus contributed little to the simulated significant wave height. Nonetheless, these other physical mechanisms should not be disregarded within a more general modelling perspective, as the simulations suggest that they could be comparable to the ice influence in the Beaufort Sea case where wave and ice conditions are remarkably different.

Visco-elastic properties of solid ice, thus described, cause dissipation and change of rate of propagation of wave energy. Below such ice, Voermans et al. (2019a) presented observations indicating that turbulence generated by the differential velocity between the sea-ice cover and the orbital wave motion may also be an important dissipative mechanism of wave energy. Through field measurements of under-ice turbulence dissipation rates in pancake and frazil ice, it was shown that turbulence-induced wave attenuation coefficients were in agreement with observed wave attenuation in MIZ, hence the wave-ice-turbulence mechanism of dissipation is as effective as the visco-elastic process. The paper suggested a parameterization based on the characteristic wave properties and a coefficient determined by the ice layer properties.

Thus, the rich and complex nature of wave-ice interactions caused a surge of dedicated research in recent years. This combined the relative novelty of the topic with the sudden demand on the practical outcomes for wave forecast in the freezing seas and specifically in MIZ.

8.4 Atmospheric wave boundary layer

Connection of the surface waves with the wind is most intimate and makes the Wave Boundary Layer (WBL), which is the part of the Atmospheric BL near the surface, different to any other boundary layer in fluid mechanics or geophysics. The wind generates the waves, but the waves then change the very wind which produced them. The waves do not provide a constant roughness because they grow, they move and they break. In the classical wall-layer sense, the waves are not roughness at all, as the roughness scale of the logarithmic profiles in the constant-flux layer is orders of magnitude smaller than the wave height. The logarithmic profile is characteristic of the constant turbulent flux, and in WBL this is not the case. The total flux in WBL is indeed constant, but apart from the turbulent flux, it is also supported by form drag which goes into wave growth and tangential drag which passes momentum to the surface currents. As a result, the actual turbulent flux in the constant-flux layer is reduced towards the surface and the wind profile in WBL deviates from the logarithmic profile (see Babanin & McConochie (2013)). We refer to the book of Chalikov (2016) which has chapters on wind-wave interactions and Wave Boundary Layer written by one of the leading experts in this field.

Most noticeable effects of waves in the AWBL are the case of large waves and strong winds, and Voermans et al. (2019b) investigated them in a Tropical Cyclone. A common method to approximate the wind stress is by measuring the turbulent momentum flux directly. However, during high wind speeds, wave heights are typically of the same order of magnitude as instrument heights, and thus, turbulent momentum flux observations alone are insufficient to

estimate wind stresses in tropical cyclones, as wave-induced stresses contribute to the wind stress at the height of measurements. In Voermans et al. (2019b), wind stress observations during the near passage of Tropical Cyclone Olwyn were presented through measurements of the mean wind speed and turbulent momentum flux at 8.8 and 14.8 m above the ocean surface. The high sampling frequency of the water surface displacement (up to 2.5 Hz) allowed for estimations of the wave-induced stresses by parameterizing the wave input source function. During high wind speeds, their results show that the discrepancy between the wind stress and the turbulent stress can be attributed to the wave-induced stress. It is observed that for u* >1m/s, the wave-induced stress contributes to 63% and 47% of the wind stress at 8.8 and 14.8m above the ocean surface, respectively. Thus, measurements of wind stresses based on turbulent stresses alone underestimate wind stresses during high wind speed conditions. The paper showed that this discrepancy can be solved through a simple predictive model of the wave-induced stress using only observations of the turbulent stress and significant wave height.

Wind-wave energy exchange is the most traditional application in the wave-coupled science, since such wind input is a necessary term for any wave model. This exchange, however, remains an active area of research as the theory and the observations of the wind input are still far apart. Such uncertainty can be overcome by direct implementation of the WBL model in air-sea interaction models, instead of using sea-drag parameterizations. Chalikov and Babanin (2019) used a WBL numerical model for parameterization of the ocean-atmosphere interactions in coupled air-sea models and wave-prediction models. Their equations explicitly take into account the vertical flux of momentum generated by the wave-produced fluctuations of pressure, velocity and stresses. The surface values are calculated with the use of the spectral beta-functions whose expression was obtained by means of the 2-D simulations of WBL. Hence, the model directly connects the properties of WBL with an arbitrary wave spectrum.

Researching this old problem of wind input, Janssen and Bidlot (2021) investigated novel effects by using the critical layer theory, the oldest analytical theory of wind-wave exchange (Miles (1957)). For extreme winds, they assumed that nonlinearity is so large that the slope of the wind waves has reached a limiting steepness. This limitation was implemented in the WAM model version at ECMWF and resulted in a reduced increase of the drag coefficient with wind speed in the range of large wind speeds. The slowing down of the wind is a nonlinear process because it depends on the wave spectrum itself. Therefore, the growth rate of the waves by wind depends on the wave spectrum, and following work by Miles (1965) it is straightforward to obtain the sea state dependence of the growth rate. For strong winds it is found that   since the waves are typically steep, this nonlinear effect gives a further reduction of the wind input (see also experimental paper by Donelan et al. (2006)). As a consequence, in these extreme circumstances the drag coefficient may decrease with increasing wind.

8.5   *Wave influences in the upper ocean*

Dynamic wave influences in the upper ocean can be subdivided into two parts: momentum which the waves pass to the surface currents, and the energy which is passed to the upper layer of the ocean. The latter, apart from the currents, goes to the turbulence and mixes the ocean. If the mixing is limited to the ocean's mixed layer, then it does not change the sea surface temperature and basically just affects sediment suspension and transport of other admixtures (e.g. nutrient transport for the biomass production). If, however, the mixing through the pycnocline occurs because it is close enough to the surface (which is usually the case in spring-summer period), then such mixing can impact thermohaline circulation, cool the surface – with important consequences for large-scale processes discussed in Section 8.6 below. Note that we do not include wave breaking influences here, which were the topic of Section 8.1 – they are

powerful bursts of momentum and energy transfer, but are different: random, sporadic and concentrated very near the surface, at the scale of wave height.

In terms of the wave-induced turbulence, unrelated to the breaking, there are three different mechanisms proposed to describe the generation of such turbulence over the years. None of them cancels the other two; all are feasible, so the upper-ocean dynamics is a matter of their relative significance. Historically the first one was due to viscous effects (solutions) of wave dynamics (equations) being able to produce vorticity which, stretched by random waves, becomes turbulence.

The second mechanism is the turbulence generated by potential (non-viscous) waves; hence the turbulence must be pre-existing, which is always the case in the ocean. Babanin (2017) proposed a similarity theory of isotropic turbulence induced by waves on the water with free surface due to such mechanism. Scaling is obtained from experimental and numerical observations of dissipation rates for surface waves, and then used to estimate the turbulent viscosity of the locally-isotropic turbulence.

Langmuir turbulence which requires the Stokes drift and therefore nonlinear waves is a yet different mechanism, three-dimensional as opposed to the first two. This is a phase-average theory where the Stokes drift shear plays a role of mean flow shear. Kukulka & Veron (2019) conducted investigation of this mechanism in the ocean surface boundary layer (OSBL) by means of the Lagrangian approach. This was based on a large-eddy simulation (LES) model coupled to a Lagrangian stochastic model (LSM). Langmuir turbulence (LT) was captured by the Craik–Leibovich wave forcing that generates LT through the Craik-Leibovich type 2 (CL2) mechanism. Breaking wave (BW) effects were modelled by a surface turbulent kinetic energy flux that is constrained by wind energy input to surface waves. With LT, Lagrangian autocorrelations of velocities reveal three distinct turbulent time scales: an integral, a dispersive mixing, and a coherent structure time. With and without waves, the high frequency spectral tail is consistent with expectations for the inertial subrange, but BWs substantially increase spectral levels at high frequencies. These results indicated that the Lagrangian analysis framework is effective and physically intuitive to characterize OSBL turbulence. Further numerical investigations of this mechanism were carried out by Fujimara et al. (2018), Yoshikawa et al. (2018).

Experimental research of such multi-scale phenomena is always difficult, and Wei et al. (2018) conducted a laboratory experiment in a wind wave tank to investigate the wave induced turbulence. In this experiment, the wave surface elevation and velocity beneath the water surface were measured simultaneously to estimate the relation between the waves and turbulence. The profile of the turbulent dissipation rate and Reynolds stress were calculated using experimental data. It was found that the turbulence decreased with increasing depth from the water surface and that the turbulence induced by a wave with larger wavelength and wave height was much stronger. Finally, it was shown that the wind-forced waves are more effective in activating the wave induced turbulence.

Therefore, with wave-induced turbulence and mixing being a relatively new topic, research in this field concentrates on clarifying and validating physical concepts responsible for such turbulence. While qualitatively three different mechanisms possible, and all of them appear to be relevant, their quantitative significance remains a subject of active research and may differ in different circumstances.

8.6   *Waves in the large-scale air-sea-system*

The wave-coupled effects in large-scale air-sea systems were singled out in the previous Section because they bring the wave modelling into poorly charted waters of large-scale and

long-term simulations of weather, climate and general oceanic circulation. Here, 'large-scale' means large by comparison with the scale of wind-generated waves. Weather and climate are phenomena of very different scales (days and years or even longer in time, hundreds of kilometers and global in space). Both scales, however, are much larger with respect to the scale of ocean surface waves (seconds in time and hundreds of meters in space).

Substantial amount of excellent work was published in this space over the 2018-2021 period. Shi et al. (2018) investigated data assimilation of a global high-resolution wave-tide-circulation coupled model using the tropical Pacific TAO buoy observations. Couverlard et al. (2019) described development and assessment of a 2-way coupled ocean-wave model based on a global NEMO(v3.6)-WW3(v6.02) coupled configuration. Lucas et al. (2019b) studied influence of autumn storms on the processes that control the evolution of the ocean surface boundary layer (OSBL). Observations of the rate of dissipation of turbulent kinetic energy (TKE), temperature, salinity, current structure, and wave field over a period of 9.5 days in the northeast Atlantic during the Ocean Surface Mixing were presented. The focus of this study is a storm that passed over the observational area during this period. The profiles of TKE in the OSBL were consistent with profiles from large-eddy simulation (LES) of Langmuir turbulence (see also Section 8.5).

Most difficult are fully coupled modelling efforts in the polar seas, where the sea-ice model has to be added to the suite of air-sea-wave coupled systems. Li et al. (2021a) investigated the role of sea-ice wave breakup in the Arctic. They introduced two independent parameterizations in a high-resolution coupled ice-ocean model to investigate the effects of wave-induced sea ice breakup (through albedo change) and mixing on the Arctic sea ice simulation (as described in Section 8.5). The results showed that wave-induced sea ice break-up leads to increase in the sea ice concentration and thickness in the Bering Sea, the Baffin Sea and the Barents Sea during the ice growth season, but accelerated the sea ice melt in the Chukchi Sea and the East Siberian Sea in summer. Furthermore, wave-induced mixing can decelerate the sea ice formation in winter and the sea ice melt in summer by exchanging the heat fluxes between the surface and subsurface layer. Therefore, since the baseline models underestimate sea ice cover in winter and produce more sea ice in summer, wave-induced sea ice breakup plays a positive role in improving the sea ice simulation. This study provides two independent parameterizations to directly include the wave effects into the sea ice models, with important implications for the future sea ice model development.

In Summary, Section 8 outlines multiple effects and feedbacks which surface ocean waves have in the lower atmosphere and upper ocean. These include wave breaking, wave-current and wave-ice interactions, Wave Boundary Layer in the wind flow, wave-induced currents and mixing in the upper ocean. Taken beyond the problem of wave dynamics and wave forecast, these effects can have impact on large-scale processes such as weather, including tropical cyclones, ocean circulation and climate.

9.   EXTREME EVENTS AND CONDITIONS

9.1   *Rogue waves*

In an integrable system, the mechanism of rogue wave generation is different and the probability of rogue wave formation depends significantly on the relative number of breathers and solitons in the initial conditions.

Taking advantage of the fission of a sinusoidal wave in a shallow water regime to continuously inject solitons that propagate along the tank in both directions, Redor et al. (2019) reported an experimental realization of a bidirectional soliton gas in a wave flume. Despite the unavoidable

damping, solitons can retain their profile while decaying. The two-soliton interaction is compared favourably with the analytical solutions of the Kaup-Boussinesq integrable equation.

Solitons and breathers are nonlinear models that exist in a wide range of physical systems and are fundamental solutions of a number of nonlinear wave evolution equations. Chabchoub et al. (2019) experimentally observe their propagation obliquely to the direction of the wave field, which is in an agreement with the numerical prediction of (2D+1) NLSE. The coherent waves with a peculiarity of finite crest length might be a consequence of nonlinear beam dynamics, suggesting that the nonlinearity is also a possible underlying mechanism for the actual finite-length-crested rogue wave events, complementing the linear superposition and interference arguments as has been generally suggested.

The Peregrine breather propagating over an adverse uniform current region is experimentally observed by Liao et al. (2018), showing that the opposite currents tend to shift the focusing point upstream and enhance the amplitude of the Peregrine solution. Moreover, the total energy of the wave train increases exhibited by the broadening of wave spectrum and enlarged horizontal asymmetry around the peak frequency. Zhang et al. (2021a) numerically studied the effect of irregular background wave on the evolution of Peregrine breather solution and concluded whether the abnormal wave induced by breather dynamics can be generated is mainly a localized behaviour, strongly dependent on the initial wave group energy as well as the detailed structure of the group.

Based on a forced-damped MNLS equation, Eeltink et al. (2017) numerically investigated the effect of wind forcing on the spectral dynamics of Akhmediev breathers, a wave-type known to model the modulation instability, showing a good agreement with the corresponding laboratory experiments within the range of the facility's length. Interestingly, the wind forcing can induce a permanent upshift of the spectral mean. However, due to the dissipation effects including wave breaking, the permanent downshift of the spectral mean and of the spectral peak is often observed in wind experiments.

According to the integrable turbulence theory for the NLSE, the coexistence of solitons and extreme events should be expected and in the context of hydrodynamic waves Cazaubiel et al. (2018) experimentally observe these nonlinear coherent structures within the incoherent wave background. The extreme events result from the strong steepening of wave train fronts and their emergence occurs after roughly one nonlinear length scale of propagation. Solitons arise when nonlinearity and dispersion are weak, and of the same order of magnitude. The spectral and statistical properties of this state are compatible with the theoretical prediction although some deviations can be identified.

The partially coherent waves can be seen as a set of independent humps at the early stage of the nonlinear propagation. In the case when nonlinearity significantly dominates dispersion, self-focusing dynamics can lead to the gradient catastrophe which asymptotically tends to the Peregrine soliton. Tikan (2020) numerically demonstrated the effect of the universal local emergence of Peregrine solitons on the evolution of statistical properties of random waves. The position of the most probable emergence of local Peregrine solitons coincides well with the maximum of the fourth-order statistical moment.

The link between soliton interaction and the modulation instability of the plane wave has been explored by Gelash et al. (2019). Based on *N*-soliton solution of the focusing one-dimensional nonlinear Schrödinger equation, a theoretical model is proposed for the asymptotic stage of the noise-induced modulation instability. A remarkable agreement has been revealed between spectral (Fourier) and statistical properties of the long-term evolution of the modulation instability and those of the constructed multisoliton, random-phase bound states.

Most studies of rogue wave concentrate on the occurrence rate and/or wave height while little is known about its shape and relative position within a wave group. Based on the statistical analysis of surface elevation records from two locations in the northeast Pacific, around 2×10^6 wave groups, Gemmrich & Thomson (2017) concluded there is tendency for steep waves to occur at the front of wave group, but these are not the largest waves of the group and do not meet the rogue wave criterion. Actually, rogue waves are not necessarily steep and tend to occur in the middle of the wave group. Besides, the estimation of group dynamics in terms of spectral width also suggests that random superposition of higher order Stokes waves seems to be sufficient to explain the observations of individual rogue waves.

Groupiness is one of the most obvious properties of ocean waves and the number of waves within a group is strictly related to the relative width of the spectrum. Based on the deep water laboratory experiments with monochromatic waves, Babanin et al. (2019a) showed that due to BF-like instability mechanism, there seems to be a natural modulation bandwidth, determined by the initial wave steepness, for all wave trains. This is also consistently observed in wind-forced regular waves, in the presence of three-dimensional instabilities and even in wind-generated wave fields characterized by continuous frequency-directional spectrum.

With the help of a fully nonlinear numerical simulation, Slunyaev (2018) showed a drastically different scenario of coherent nonlinear wave groups induced by self-modulation of water wave trains. It is mainly demonstrated by the deviation from the dispersive relation in Fourier space, which results in the excitation of new waves due to the Cherenkov-type resonance. Consequently, the groups may emit waves with similar or different lengths, which propagate in the same or opposite direction. Slunyaev & Dosaev (2019) also numerically revealed that due to the same physical mechanism the recurrence of modulation unstable water wave trains is incomplete, i.e. quasi-periodic breathing. Note that the incomplete process is observed in the simulation governed by integrable NLS equation as well whereas it is due to the hardly controllable effects of noise.

9.1.1 Unimodal Sea State

Extreme wave statistics of long-crested irregular water surface waves over a shoal are experimentally investigated by Trulsen et al. (2020), who find that for a sufficiently shallow shoal the surface elevation can have a local maximum of skewness and kurtosis above the shallower part of shoal close to the edge on the incoming side, and a local minimum of skewness over the downward slope on the lee side of the shoal. Meanwhile, the horizontal velocity is also considered therein, which can have a local maximum and minimum of skewness at the same locations as those for the surface elevation while its local maximum of kurtosis is quite different, i.e. located over the lee side of the shoal.

For practical and computational reasons, the bandwidth and amplitude limited model such as the modified nonlinear Schrodinger equation is often used to investigate the properties of deepwater ocean waves. Simanesew et al. (2017) reported that for long-crested irregular waves with moderate steepness, reliable prediction can be performed up to about 40 characteristic wavelengths while for short-crested waves the accuracy of prediction is strongly reduced with increasing directional spread.

To estimate the accuracy of various deterministic wave prediction models, i.e. the linear wave solution, NLS, MNLS and HOSM, a comparative study on the evolutions of nine different irregular sea states characterized by JONSWAP wave spectra is made by Klein et al. (2020). The incoming surface elevation snapshot, which is normally taken by a ship's X-band radar in reality, is used as the initial input condition. As indicated by the surface similarity parameter (SSP), with the increased nonlinearity the more complex wave model has a better performance

but at the cost of computational effort which is in principle in agreement with the former conclusions presented in the review of Zhang et al. (2019c).

However, the linear dispersion focusing is still likely the generation mechanism of freak wave and the influence of water depth can change the wave mechanism completely. With the aim of unifying the two apparently incompatible mechanism of formation of rogue waves, i.e., the nonlinear focusing and the linear superposition, Dematteis et al. (2019) proposed that the hydrodynamic instanton can be used to describe rogue waves. It not only reconciles these two theories but also smoothly interpolates between them. The hydrodynamic instanton is a complex spatiotemporal wave field configuration that can be defined using the mathematical framework of large deviation theory and calculated via tailored numerical methods.

Moreover, the vorticity can also influence the property of solitary wave that can be considered as the prototype of rogue waves in realistic sea state. Within the framework of 1D and 2D NLS equations, Abid et al. (2019) found that for gravity-capillary solitary wave the negative constant vorticity is capable of reducing the wave height and amplifying the rate of growth and bandwidth of transverse instability, and vice versa.

To date, two main approaches have been proposed to study the nonlinear stage of modulation instability (MI). One is related to the spontaneous oscillations (auto-modulation) and the other is super-regular breathers in term of particular pairs of breathers with opposite velocities. Conforti et al. (2018) reconcile the two approaches and show that, more generally, auto-modulations and breather pair formation coexist, strongly dependent on the shape and the parameters of the initial perturbation.

For the deep-water surface waves with the initial envelope in the form of large-scale near-rectangular barriers, Bonnefoy et al. (2020) experimentally reveal that for a range of initial parameters the nonlinear wave packet is not disintegrated by the Benjamin-Feir instability but exhibits a specific, strongly nonlinear modulation which propagates from the edges of the wave packet towards the center with finite speed. The observed counter-propagating dispersive dam break flows can be described within the framework of the semi-classical 1D NLSE and can be viewed as an example of dispersive shock wave (DSW) dynamics persisting in focusing nonlinear media.

In the past, it is believed that if the wave propagates with opposite or oblique direction to a surface current field, large-amplitude wave can be formed simply due to the linear focusing mechanism (caustic theory), i.e. coalescence of wave energy in certain areas. Although the currents can locally increase steepness, trigger rogue waves and rapidly lead to non-Gaussian statistics, Toffoli et al. (2019) experimentally confirmed that the modulation instability, demonstrated by the nonlinear energy transfer in the frequency domain, can also be triggered in the case with a certain strength of current. It becomes more complex in a wider wave basin as directional properties can develop even for initial unidirectional wave fields. The refracted waves by surface current are reflected from the side walls and consequently facilitate the non-negligible effects of linear directional focusing, further enhancing the occurrence of rogue waves.

Unlike many experiments on rogue waves where waves are mechanically generated, Toffoli et al. (2017) conducted a laboratory wind-sea experiment in an annular flume, over which a constant and quasi-homogeneous wind blows. The peculiar facility allows the full evolution of the wave field (so-called duration-limited condition), from its generation to the fully developed stage. For the first time in the laboratory, rogue waves are detected during the development of a wind-forced wave field, just before reaching a stationary state.

Motivated by the two deep water freak waves registered by the JKEO GPS buoy in the same storm, Fujimoto et al. (2018) used the third-generation wave model WAVEWATCH III to hindcast their initial wave spectra, which are used to conduct the detailed regional numerical simulation, performed with HOS method, to further investigate their geometry and possible generation mechanisms in statistical sense. The spatio-temporal pattern analysis reveals that the four-wave resonant interaction can prolong the lifetime of freak waves and give rise to the front-rear asymmetry in the case with narrow spectral width and directional distribution. This is further confirmed in the later numerical research Kokorina & Slunyaev (2019), where the maximum rogue wave lifetime in long-crested sea state is found up to be about 90 wave periods and various intricate 3D rogue wave patterns are detected.

More specifically, the four-wave interaction can be separated into the direct interaction of four free waves and the virtual-state interaction of two second-order bound waves induced by them. As indicated by the coefficient of kurtosis Fujimoto et al. (2018), for directional waves the latter interaction is dominant with a positive effect in the evolutionary process in comparison with the former interaction (negative).

In contrast, by virtue of the direct numerical simulation performed with the same method (HOS), Slunyaev (2019) pointed out the irregular nonlinear directional sea waves may violate essentially the Gaussian statistics due to the coherent dynamics of free waves. Moreover, it is reported that under the condition of relatively narrow angle spectrum the dynamic kurtosis may be comparable with the value of the bound wave kurtosis (coherent). This can be verified by the spread of wave number and wave frequency in the spatio-temporal Fourier domain, clearly indicating that the coherent 3D wave patterns persist in the irregular sea field and do not follow the classic dispersion relationship.

With the modified HOS method suitable for varying bathymetry, Ducrozet & Gouin (2017) numerically investigated the rogue wave activity during the wave field propagating over a sloping bottom within unidirectional and directional sea states, demonstrating that the enhancement of the extreme wave occurrence observed close to the shallower side of the slope is reduced when considering the directional spreading effect.

9.1.2 *Bimodal Sea State*

In shallow water, the counterpart of the nonlinear Schrödinger equation is Korteweg-de Vries equation, within the framework of which, Didenkulova et al. (2019) performed direct numerical simulation for irregular unidirectional nonlinear wave with bimodal wave spectrum. Due to the existence of an additional wave system, the evolution of wave statistical characteristics and spectral shape are quite different. Particularly, the inclusion of an extra system with longer waves effectively increases the degree of nonlinearity of the entire wave system which consequently speeds up the evolutionary process and intensifies the extreme wave characteristics.

In agreement with the prediction of 2D+1 NLSE, Steer et al. (2019a) experimentally demonstrated the existence of non-dispersive sing-crossed(?) wave groups and long-lived nonlinear hydrodynamic X wave packets when a carrier wave is modulated by a wave group crossing it at an angle of approximately ±35.26°. The experimental observation of crossed groups propagating unchanged over many wavelengths confirms the lifetime extension of wave groups that contain the potential for extreme events.

The physical mechanisms that give rise to freak waves in intermediate water depths such as the Draupner wave are still contentious. Under unidirectional condition the Draupner wave has been roughly reproduced many times in the rectilinear wave basin. McAllister et al. (2018) reproduced the same Draupner wave, the form of which shows more good agreement with

measurement, in a circular wave tank under conditions where two wave systems cross at a large angle. The presence of a set-up in the second-order difference waves, observed only in crossing wave experiment and field measurement, further supports the hypothesis that crossing conditions created the Draupner wave. Meanwhile, breaking mechanism is fundamentally altered for sufficiently large crossing angles, indicated by less crest-amplitude limiting and the formation of near-vertical jets.

However, for counter-propagating, irregular unidirectional sea states characterized by a JONSWAP frequency spectrum, Støle-Hentschel et al. (2018) experimentally and numerically confirm that both local kurtosis of surface elevation and local exceedance probability of crest height are larger in unidirectional seas than in counter-propagating seas. Even a small amount of waves propagating against an essentially unidirectional wave field can notably suppress the formation of large surface elevation. Consider that one of the wave fields is sufficiently wide-banded, the observed behaviour maybe attribute to nonlinear interactions different from the modulation instability. In the following seas composed by wind wave and swell, Støle-Hentschel et al. (2020) experimentally and numerically exhibited that the extreme wave statistics of combined two wave systems can be quite different from that of the corresponding single one. More concisely, to a certain degree the following swell seems to suppress the formation of large-amplitude wind wave depending on the sea-swell energy ratio.

The statistical properties of extreme and rogue wave activity in crossing directional seas are examined in the ocean wave basin by Luxmoore et al. (2019), showing that the directional spreading of the individual components has more effect on the kurtosis and the exceedance probability than the crossing angle between the components. The kurtosis rarely exceeds the second-order theoretical value, and the wave height distribution is generally grouped around the Rayleigh distribution while the wave crest heights generally slightly exceed the second-order Tayfun distribution. In fact, a set of systematic numerical simulations has been performed by Gramstad et al. (2018) for crossing sea states with respect to spectral shape, crossing angle and separation in peak frequency. It is shown that for a linear sea state the expected maximum crest elevation is largest when two wave systems propagate with a crossing angle close to 90°. However, if the nonlinearity is also considered, a peak in kurtosis will appear at large and small crossing angles while maximal crest height seems independent of crossing angle. Accompanied by analysing the modulation instability of two crossing Stokes waves (the same initial parameters as crossing seas each characterized by JONSWAP spectrum) with the coupled Zakharov equations, it is shown that there is a positive correlation between the value of kurtosis and the maximum unstable growth rate of two crossing Stokes waves.

In a circular wave basin, Steer et al. (2019b) experimentally investigated the effects of crossing angle on the modulation stability of two crossing nonlinear surface gravity wave trains seeded with sideband perturbations, which is also compared with the numerical simulation governed by the coupled nonlinear Schrödinger equation (CNLSE). The results demonstrate that for the cases considered herein, the growth rate reduces with the increasing crossing angle and becomes negligible at and beyond a crossing angle of approximately 30°.

Although various wave models can be used to predict the generation and evolution of ocean waves by wind, their predictive capabilities must be validated by a comprehensive and systematic field in-situ measurement as suggested by Babanin et al. (2019b). The observational network could include distributed system of buoys (drifting and stationary) and autonomous surface vehicles. Moreover, it would help to resolve the issues of limiting fetches, extreme Extra-Tropical cyclones, swell propagation and attenuation, wave-current interactions, and address the topics of wave-induced dispersal of floating objects, wave-ice interactions in the Marginal Ice Zone, Metocean climatology and its connection with the global climate.

Cattrell et al. (2018) collated, quality controlled and analysed the largest dataset of single-point field measurements from surface following wave buoys, but a discernible link between rogue wave occurrence and the short-term wave statistics is not observed. In contrast, there is a potential predictability for rogue wave occurrence from long-term wave statistics. It seems that the generation mechanisms of rogue waves are region specific and rarely due to modulation instabilities considering the wave spectral width is large in most rogue seas.

9.2 Polar Seas

9.2.1 Extreme Ice loads on Ships

The analysis of ice load data collected aboard XueLong in the Arctic showed that the Weibull distribution appears being a well suited distribution Wu et al. (2021). In order to estimate extreme ice loads Chai et al. (2018b) introduced a novel approach named ACER (average conditional exceedance rate). This method is applied by Chai et al. (2018a) for assessing the fatigue damage due to ice loads, while also the Weibull distribution is used to represent the ice induced stress ranges. A numerical analysis of bergy bits and growlers is performed by Yu et al. (2021) which is deemed as such ice features, are difficult to be detected by marine radars. On the basis of numerical simulations it is shown that a critical local sharpness of ice contours exists leading to maximum structural damage for a given impact energy. The investigated conditions led to impact energies being 50% of the maximum sustainable energy of the modelled structure. However, Yu et al. (2021) indicated that the energy can easily increase for larger ice pieces. The energy may also be increased when nomadic ice pieces float on waves von Bock Und Polach et al. (2019) as assessed in Zaman & Akinturk (2020). This interaction is considered to impose great risk in stormy event with large waves. The exercise concluded a good agreement between results of commercial tools.

9.2.2 Extreme Events and Climate Change

Li et al. (2019b) verified numerical WAVEWATCH III hindcast simulation on wave heights in the Arctic Ocean with buoy and altimeter measurements. It is found that the significant wave height is governed by surface winds when the ice extent is beyond $9.4 \times 10^6 \, \text{km}^2$. Below this threshold, the increase is affected by both increasing fetch length and wind speed. The study shows a transition from wind to swell dominated waves with retreating ice cover and implies an increasing wave height (m $(\text{km}^2)^{-1}$) with decreasing ice extent. The reanalysis of ERA-Interim data indicates that more than half of the extreme events are caused by cyclones originating in the Arctic Ocean and mid-latitudes (Waseda et al. (2021). When the ice extent is least (September) this percentage increased from 50% to 80% in the past four decades.

Polar lows (PL) are intense mesocyclones developing over the ice free Arctic Ocean. If those stay stationary they can cause high wind waves (Golubkin et al. (2018). A presented model by Golubkin et al. (2018) shows a significant exceeding level of 6m and 8m of the significant wave height spectrum with the presence of polar lows. An analysis (Radovan et al. (2019) of 33 January PL occurrences over 12 years (2000-2011) showed that, for the cases with lower thermal instability during formation stage, lapse rates throughout the boundary layer were stronger and steeper; therefore, these PLs were fostering convective development. The latter refers to 90% of the PL occurrences. In addition to increased wave heights Polar cyclones are considered causative to Antarctic ice calving (Francis et al. (2021). The study from Francis et al. (2021) showed that the unexpected calving event from the Amery Ice Shelf (September 2019, the largest since 1963) is due to a series of anomalously deep and stationary explosive twin polar cyclones. The generated tides and wind-driven ocean slope lead enforced existing rifts and finally the calving. According to Francis et al. (2021) such extreme events are predicted to occur more frequently under warmer climate.

9.3 Tropical cyclones

Tropical Cyclones (TC, also called hurricanes in the Americas and typhoons in Asia) are small and rare, but have an unproportionally large impact on design and operation of offshore industry and shipping in tropical areas. While prediction of their tracks has advanced significantly, forecast of intensity of TCs has not been improving over decades in spite of rapid progress of numerical methods and computing capabilities. Apparently, some understanding of their physics is missing.

Part of the missing physics is Metocean, i.e. wave-coupled interactions in the air-sea dynamics and thermodynamics of TCs (see also Section 8). TCs are a strongly coupled air-sea phenomenon: i.e. it occurs and develops in the lower atmosphere, but it depends and intensifies by gaining energy from the warm ocean (hence its tropical nature, except specific conditions when the atmospheric forcing directs it to higher latitutes along a warm current like Gulfstream). All the relevant cross-interface fluxes (energy, momentum, heat, mass) are facilitated or moderated by waves, which are not small in hurricanes, but waves are usually not included into the TC models and the fluxes are routinely parameterized in terms of wind speed.

This includes parameterization of spray, which is most obviously not produced by the wind, but does affect the wind because it impacts the sea drag (hence the momentum flux) and heat fluxes (both latent and sensible). Currently, uncertainties in magnitude of the sea spray production estimates reach 3-5 orders of magnitude, hence their use in validation of TC models is problematic. In Ma et al. (2020), the sea spray volume flux (SSVF) was measured by laser altimeters under Tropical Cyclone Olwyn in the Indian Ocean. Their results showed that the SSVF increases gradually with the wind speed and is approximately 2 orders of magnitude larger than the results of two laboratory experiments and existing sea spray generation functions. The SSVF is also influenced by the sea state. When the nondimensional significant wave height is factored in as a new parameter, the correlation coefficients are improved. A new parameterization for SSVF generation function is proposed in terms of the nondimensional wave height and windsea Reynolds number.

Xu et al. (2021) used the same Olwyn data, and made a correction for a missing proportion of the spray located in the troughs of the big waves in TCs. Furthermore, their observations of sea spray cover a broad range of wind and wave properties and offer a universal parameterization, from light winds to hurricane force. Improved performance of the model is observed when wave properties are included, in contrast to a parameterization based on wind properties alone. The novel *in-situ* sea spray observations and the predictive model derived are consistent with the spray model of Andreas (1992) in both trend and magnitude. Such novel parameterizations based on observations provide opportunities to improve the prediction of air-sea fluxes in operational weather forecasting models.

10. WIND-WAVE CLIMATE

10.1 Historic trends

The accurate representation of long-term temporal variation of wind waves is crucial for many applications of design and ship routing, coastal infrastructures, harbour management, offshore wind farms, wave energy converters. Intensive research has been placed into global and regional wave climate over the past years, with the main focus on trends and variability of mean values and high percentiles. Present day climate is usually studied using reanalysis data, satellite or in-situ data, not only in global studies but also regional ones, that focus on coastal impacts.

Stopa (2019) used observations from a multi-platform calibrated altimeter dataset from 1985-2016 to study wind speed and wave height global seasonal patterns and concluded that some

regions of the ocean have distinct seasonal shapes different from sinusoids. He also identified several regions of the ocean that have strong seasonal inter-annual variability while other regions have small year-to-year variability which might be important areas to monitor for long-term changes related to variability in solar radiation or climate change.

Young & Ribal (2019) developed and analysed a global satellite database to determine trends in oceanic wind speed and significant wave height over the 33-year period from 1985 to 2018 using data obtained from 31 satellite missions comprising three types of instruments-altimeters, radiometers, and scatterometers. The analysis showed small increases in mean wind speed and significant wave height over this period, with larger increases in extreme conditions (90th percentiles). The largest increases occur in the Southern Ocean.

The analysis presented by Takbash & Young (2020) using the global ERA5 showed that there has been a statistically significant increase in the value of 100-year significant wave height (H100) over large regions of the Southern Hemisphere, but a smaller decrease in H100 in the Northern Hemisphere was also observed, although the related trends were generally not statistically significant. The increases in the Southern Hemisphere are a result of an increase in either the frequency or intensity of winter storms, particularly in the Southern Ocean.

Timmermans et al. (2020) examined long-term global seasonal significant wave height trends from the CCI Level 4 dataset Dodet et al. (2020) and compared those with other high-quality sea state records over the period of continuous satellite coverage. Results showed variability across datasets, although in all cases intra-dataset variability showed a high degree of spatial coherence. The maximum range of trends across all datasets is approximately the same, but trends from the CCI L4 appear to be substantially more positive than those from the Ribal & Young (2019) and in better agreement with the ERA5 reanalysis of Takbash & Young (2020).

Bitner-Gregersen (2018), investigated how realistic the adverse weather conditions proposed by the IMO in 2013 are, using data from selected ocean locations. It compared open sea and coastal water wind and wave climate applying hindcast data in the analysis. The study was focussed on the open sea metocean conditions of the North Atlantic while European waters were used as representative for coastal regions. Challenges in providing metocean description for assessment of ship manoeuvrability were discussed and three approaches for doing it were proposed, giving attention to associated uncertainties. Correlations between wind speed and significant wave height as well as significant wave height and spectral peak period were compared with the ones suggested by the 2013 Interim Guidelines and other existing standards.

Caloiero et al. (2019) performed an analysis of present wave climate in the coast of the Cantabria region (Mediterranean Sea), using ERA-Interim reanalysis data. Trends in significant wave height and energy period were studied at annual and seasonal time scales. Also using the same reanalysis data set, Ding et al. (2019) analysed the present wave climate on the coast of Guangdong in China. Variability of main wave parameters was studied and its impacts on beach morphology as well as the relation between wave conditions and weather systems.

Wind wave climate trends have also been investigated in other regions. Some examples are the positive trends in monthly and annual significant wave height of total sea that were found by Kumar et al. (2018c) for the North Indian Ocean using a 15-year wave hindcast and recently confirmed by Sreelakshmi & Bhaskaran (2020) that used the ERA5 reanalysis data to evaluate trends in swell and wind sea in the Indian Ocean, for a longer period. Shamji et al. (2020) studied trends in the extreme values of significant wave height of the total sea, in the Red Sea finding also positive values for the period 1979-2010.

Liu et al. (2021) used the observation-based version ST6 of WAVEWATCH-III (Liu et al. (2019d)) and developed a global Metocean database for the period of 1950-2020. The paper analyses (a) a long-term hindcast (1979-2019) forced by the ERA5 conventional winds U10 and (b) two short-term hindcasts (2011-2019) driven by the NCEP climate forecast system (CFS)v2 U10 and the ERA5 neutral winds U10, respectively. The input field for ice was sourced from the Ocean and Sea Ice Satellite Application Facility (OSI SAF) sea-ice concentration climate data records. These wave simulations, together with the driving wind forcing, are validated against extensive in-situ observations and satellite altimeter records. The performance of the ST6 wave hindcasts shows promising results across multiple wave parameters, including the conventional wave characteristics (e.g., wave height Hs and wave period) and high-order spectral moments (e.g., the surface Stokes drift and mean square slope). The ERA5-based simulations generally present lower random errors, but the CFS-based run represents extreme sea states considerably better. The hindcast included novel features such as dominant wave breaking probability, wave-induced mixed layer depth, freak wave indexes and wave spreading factor, which were briefly analysed. Inter-comparisons of Hs from the long-term (41 years) wave hindcast, buoy measurements and two different calibrated altimeter data sets highlight the inconsistency in these altimeter records arising from different calibration methodology. Significant errors in the low-frequency bins (period T > 15 s) for both wave energy and directionality call for further model development.

10.2 Arctic and Antarctic

The wave climate in the Arctic and Antarctic oceans is undergoing a dramatic change due to the sea ice retreat. These regions are experiencing some of the most rapid changes over the globe, and projected changes are significant. As sea ice coverage shrinks and ice-free period lengthens, new water areas become available for ocean wave generation, growth, and propagation for a longer period. However, these regions are the ones less covered by in-situ observations, and the need to increase these types of observations is clear.

Derkani et al. (2021), presented a data set of simultaneous observations of winds, surface currents, and ocean waves obtained during the Antarctic Circumnavigation Expedition (ACE), which went around the Southern Ocean from December 2016 to March 2017 (Austral summer). The data set is the most extensive and comprehensive collection of observations of surface processes for the Southern Ocean and is intended to underpin improvements of wave prediction models around Antarctica and research of air–sea interaction processes

Liu et al. (2020), used the WW3 model, applying the SMC grid and the viscoelastic wave-ice model to find the relation between the growth of wave height and the retreating ice cover, in the Arctic. Results showed that when the ice extent is smaller than 9.4×10^6 km^2, the mean wave height in the Arctic Ocean will increase by 0.07 m with shrinkage of 10^6 km^2 ice cover and roughly 51% of the increase is contributed by the enlarged effective fetch. For the ice extent larger than 9.4×10^6 km^2, ice extent and mean wave height are positively correlated.

Wojtysiak et al. (2018), characterized wind wave climate of the west coast of Spitsbergen using modelled results from spectral wave models Wave Watch III (WW3) hindcast and the ERA-interim reanalysis WAM, and observed the presence of seasonal cycle with difference of up to 1 m between significant wave heights in summer and winter, extreme events analysis revealed that storms occur mainly in winter, but the most energetic ones occur in spring and autumn. Positive trends in frequency of storms and total duration of storms were also identified.

Waseda et al. (2018) evaluated trends of extreme ocean waves in the emerging ice-free waters of the summer Arctic using ERA-Interim wave reanalysis. Results revealed an increase in the expected largest significant wave height from 2.3 m to 3.1 m in the ice-free water from the

Laptev to the Beaufort Seas during October that is highly correlated with the expected increase in highest wind speed. Also, this increase in the largest significant wave height follows from the enhanced probability of storms in ice-free waters.

Duan et al. (2019), investigated the wave climate in the ice-free waters of Kara Sea using the ERA-Interim dataset. Results showed that the significant wave height and mean wave period are slightly higher in September than in August and that the largest waves predominantly occur in the zone of 77-79°N and 67-80°E.

Casas-Prat et al. (2018), used the WW3 wave model with a customized unstructured Spherical Multi-Cell grid of ~100 km offshore and ~50 km along coastlines, forced with five CMIP5 climate models for the historical (1979-2005) and RCP8.5 scenario future (2081-2100) periods, to produce simulations of the global ocean wave climate. The results showed that all five sets of wave simulations projected lower waves in the North Atlantic, corresponding to decreased surface wind speeds there in the warmer climate but also consistently projected an increase in the surface wind speed in the Southern Hemisphere mid-high latitudes, which translates in an increase in the WW3 simulated significant wave height in this region. The Arctic regional wave climate was studied in more detail, using the same data, by Casas-Prat & Wang (2020a). The obtained results showed that annual maximum significant wave height is projected to increase up to 6 m offshore and up to two to three times greater than the corresponding 1979–2005 value along some coastlines, as waves become more exposed to the fall storms there. Also, the connection between the Atlantic Ocean and the Arctic wave climates is projected to strengthen due to increase of swell influence. In Casas-Prat & Wang (2020b), projected changes and trends in the regional annual and monthly maxima of the significant wave height in the Arctic Ocean were studied. Results showed that the regional annual maximal Hs increases on average up to ~3 cm/year, or >0.5%/year, relative to the 1986–2005 climatological value, in many Arctic areas. It was concluded that changes in wind speed alone cannot explain the increases in the regional maximal Hs and that sea ice retreat also plays an important role by increasing fetch to promote wave growth.

10.3   *Future trends*

To evaluate future wind wave climate, there is a need to rely on climate simulations. Coupled Model Intercomparison Project Phase 5 CMIP5 has provided simulations for the earth system, until the end of the 21st century, for different types of emission scenarios (RCP's), but these simulations do not include ocean waves. So, most wind wave climate studies depend on global scale wave simulations using the WAM or the WW3 model, for global assessment and other models for more regional studies, forced by CMIP5 wind and ice cover information. Future climate is usually divided into different periods: near future, mid-century and end of the 21st century.

In recent years, intensive research has been placed into global and regional wave climate with the main focus in trends and variability of mean values and high percentiles. Under the auspices of the Coordinated Ocean Wave Climate Project (COWCLIP) effort, several global studies have considered how global wave climate may respond to projected future climate scenarios with increase greenhouse gas concentrations using both the dynamical and the statistical approach. Some studies present results from a single wave climate simulation, other analyse an ensemble of climate projections.

One example of these studies is the one presented by Morim et al. (2018) where an analysis of 91 published global and regional scale wind-wave climate projection studies were evaluated to establish consistent patterns of impacts of global warming on the wind-wave climate across the globe. Consensus amongst studies regarding an increase of the mean significant wave height

Hs across the Southern Ocean, tropical eastern Pacific, and Baltic Sea, and conversely, a decrease of Hs over the North Atlantic and Mediterranean Sea was found. The authors observed that the projection uncertainty surrounding wind-wave climate projections has been poorly sampled and identify sets of coordinated experiments within existing studies that can be used as a basis to systematically quantify these uncertainties.

Bricheno & Wolf (2018) analysed historic and future wave conditions around the European Atlantic coast, making projections out to the year 2100 under RCP4.5 and RCP8.5 scenarios and find a decrease in mean significant wave height of the order 0.2 m is projected across most of the European coast. Increases in the annual maximum and 99th percentile wave height as large as 0.5– 1 m are observed in some areas but with a more complex spatial pattern. Bitner-Gregersen et al. (2018) and Aarnes et al. (2017) presented results from the same Norwegian research project ExWaCli. The past (1971-2000) and the future wave (2071-2100) climate was simulated in this project by the Norwegian Meteorological Institute using the WAM model and Bitner-Gregersen et al. (2018) summarizes the results of the entire project (wave data, statistical analysis and impact on design) led by DNV GL with the Norwegian Meteorological Institute and the University of Oslo as partners. Six climate models, including the EC-Earth (with three ensemble members) and two emission scenarios RPC4.5 and RPC8.5 were used in these investigations. Annual statistics of significant wave height are analysed including mean parameters and upper percentiles.

In Lemos et al. (2019), the near future impact of a warmer climate on the global ocean wave climate towards the mid-21st century (2031–2060) was investigated using a 4-member "coherent" ensemble of wave climate projections: single-model, single-forcing and RCP8.5 scenario. Statistically significant increases in the global mean wind speed, wave height, wave period and wave energy flux are to be expected towards the mid-twenty first century, these changes being more striking in the mid-to-high latitudes of the Southern Hemisphere.

Bonaduce et al. (2019), assessed the wave climate change of the North Atlantic by the end of the 21st century, using a regional wave climate projection under the RCP8.5 scenario. The historical run is validated with in-situ, remote sensing and ERA5 reanalysis. Systematic differences were found but in the general features of the present wave climate were captured by the historical run. In the future climate projection, similar wave climate change patterns were observed when considering both the mean and severe wave conditions, which were generally larger during summer. The range of variation in the projected extremes (±10%) was consistent with those observed in previous studies both at the global and regional spatial scales.

Meucci et al. (2020), used an ensemble of global wave model runs of WW3 model, forced with surface winds simulated by different GCMs, to develop a dataset of storm wave conditions. Under the two emission scenarios (RCP4.5 and RCP8.5), found that the magnitude of a 1 in 100-year significant wave height (Hs) event increases by 5 to 15% over the Southern Ocean by the end of the 21st century, compared to the 1979-2005 period. The North Atlantic shows a decrease at low to mid latitude (≈5 to 15%) and an increase at high latitudes (≈10%). The extreme significant wave height in the North Pacific increases at high latitudes by 5 to 10%.

Bernardino et al. (2021), used the WW3 wave model forced with wind and ice-cover data from an RCP8.5 EC-Earth system integration for two 30-year time slices 1980-2009 representing present climate and the second 2070-2099, representing the climate in the end of the 21st century. Changes from present to future climate were evaluated, regarding both mean and extreme events. It was observed a generalized decrease in Hs (mean and 95th percentile) that is in line with results obtained from other authors for the North Atlantic. Changes in Tp and Tm are very small both in mean and in the extremes, but a small increase is observed in very high latitudes.

Lobeto et al. (2021), analysed hourly time series of significant wave heigh of a seven-member ensemble of wave climate simulations and estimated changes for return periods from 5 to 100 years by the end of the century under RCP4.5 and RCP8.5 scenarios. Results obtained conclude that increases cover wider areas and are larger in magnitude than decreases for higher return periods. The Southern Ocean is the region where the most robust increase in extreme Hs is projected, showing local increases of over 2 m regardless the analysed return period under RCP8.5 scenario. On the contrary, the tropical north Pacific shows the most robust decrease in extreme Hs, with local decreases of over 1.5 m. Relevant divergences are found in several ocean regions between the projected behaviour of mean and extreme wave conditions. An example is an increase in Hs return values and a decrease in annual mean Hs found in the SE Indian, NW Atlantic and NE Pacific.

O'Grady et al. (2021) evaluated how global climate change will alter wind sea and swell waves, modifying the severity, frequency, and impact. The authors conclude that extreme wave heights are not projected to increase everywhere, the largest increases will typically be experienced at higher latitudes, and that there is high ensemble model agreement on an increase (doubling of events) for the waters south of Australia, the Arabian Sea and the Gulf of Guinea by the end of the twenty-first century.

So, in general, considering the available ensemble of wave climate projections, it can be said that there is consensus amongst studies regarding an increase of the mean significant wave height across the Southern Ocean, tropical eastern Pacific and Baltic Sea, and a decrease of Hs over the North Atlantic and Mediterranean Sea. However, there are other regions where is a lack of consensus among models. Similarly, future projections of extreme Hs lack consensus everywhere, except for the Southern Ocean and North Atlantic.

11.   CONCLUSIONS

While being a very old research field, Metocean topics remain at the forefront of ocean sciences and ocean engineering. The presented Chapter can effectively be subdivided into two large parts: the first part follows the traditional breakdown of methods for Metocean research, and the second part outlines novel or recently intensified applications.

The mainstream part starts from Analytical Theory (Section 2), the centuries-long way of researching the surface waves and other Metocean interactions, followed by Section 3 on Numerical Modelling which came flourished in the new century with rapid advances of modern computing and supercomputing. Effectively, these are both analytical methods where numerical approaches allow us to solve the analytical equations, even if approximately, when explicit mathematical solutions are not possible. We see that both continue to cover the full spectrum of wave problems, i.e. non-linear waves in deep and shallow waters, plus wave-ice interactions attracting major attention of researchers these days to a point of having a separate subsection in both analytical and numerical Sections.

In engineering and science, any theory and numerical models require experimental verification, calibration and validation. Even if an analytical description of a physical mechanism is undoubtedly correct (e.g. follows from an explicit mathematical derivation), there is a question of a relative significance of this mechanism with respect to other relevant processes which in a complex Metocean environment are always present together and superimposed. Therefore, the experimental Section 4 (Measurements and Observations) is the largest in this review and covers the traditional range of laboratory experiments, where the physical phenomena can be split and scrutinised, and in situ observations where they interact in their full complexity. The last four decades have also seen an enormous surge of Remote Sensing of the ocean, and the Chapter has a separate Section 5 dedicated to this growing field of observations, with its own

methods and technologies ranging from ship, coastal and airborne radars to the satellite probing of the ocean.

Section 5 in some way is a divider of the traditional and new applications in Metocean topics. With enormous serge of computing capabilities, data science and Data Analysis become a discipline of its own, and Section 6 is dedicated to this topic. Among other issues, it has a subsection on Machine Learning which is a rapidly growing application across most engineering fields. One of the most essential applications of the data analysis in ocean engineering is the traditional topic of Statistics, Theory and Analysis, which is the subject of Section 7.

Sections 8-10 are the most recent themes in Metocean research, to a great extent a product of the last decade or two. Although concepts of the Wave-Coupled Phenomena (Section 8) on the ocean interface, in the Atmospheric Boundary Layer and in the upper ocean are not new, extensive research in these areas was marginal until recently. Rapid breakthrough in this field happened and is continuing due to both better understanding (and better measurements) of such coupled phenomena and, importantly, due to advances in computing and data science that allow us to implement outputs of such research into practical outcomes such as coupling small-scale and large-scale air-sea models. This is particularly essential for Extreme Events and Conditions (Section 9), which are often (if not always) a result of wave-coupled interactions in complex Metocean systems, and for studies on Wind-Wave Climate (Section 10) which in such coupled systems becomes another proxy for the large-scale climate.

Thus, the reported 2018-2021 period demonstrates ongoing advances across the full spectrum of Metocean studies, from most traditional topics of analytical wave theories to the new methods and approaches such as remote sensing of the ocean and investigations and modelling of wave-coupled phenomena and effects. It would be fair to expect that this advance will continue as the new understanding of Metocean environment and new experimental/computing capabilities develop at accelerating rate.

REFERENCES

Aarnes, O. J., Reistad, M., Breivik, Ø., Bitner-Gregersen, E., Ingolf Eide, L., Gramstad, O., Magnusson, A. K., Natvig, B., Vanem, E. (2017). Projected changes in significant wave height toward the end of the 21st century: Northeast Atlantic. Journal of Geophysical Research: Oceans, 122(4), pp. 3394-3403.

Aas, K., Czado, C., Frigessi, A., Bakken, H. (2009). Pair-copula constructions of multiple dependence. Insurance: Mathematics and Economics, 44(2), pp. 182-198.

Abdalla, S., Dinardo, S., Benveniste, J., Janssen, P. A. E. M. (2018). Assessment of CryoSat-2 SAR mode wind and wave data. Advances in Space Research, 62(6), pp. 1421–1433. doi: 10.1016/j.asr.2018.01.044.

Abdolali, A., van der Westhuysen, A., Ma, Z., Mehra, A., Roland, A., Moghimi, S. (2021). Evaluating the accuracy and uncertainty of atmospheric and wave model hindcasts during severe events using model ensembles. Ocean Dynamics, 71, pp. 217–235, doi: 10.1007/s10236-020-01426-9.

Abid, M., Kharif, C., Hsu, H. C., Chen, Y. Y. (2019). Transverse instability of gravity-capillary solitary waves on deep water in the presence of constant vorticity. Journal of Fluid Mechanics. Vol. 871, pp. 1028-1043. doi: 10.1017/jfm.2019.350.

Alberello, A., Chabchoub, A., Gramstad, O., Babanin, A. V., Toffoli, A. (2016). Non-Gaussian properties of second-order wave orbital velocity. Coastal Engineering, 110, pp. 42-459. doi: 10.1016/j.coastaleng.2016.01.001.

Alberello, A., Iafrati, A. (2019). The Velocity Field Underneath a Breaking Rogue Wave: Laboratory Experiments Versus Numerical Simulations. Fluids, 4(2). doi: 10.3390/fluids4020068.

Alford, L. K., Beck, R. F., Johnson, J. T., Lyzenga, D., Nwogu, O., Zundel, A. (2015). A Real-Time System for Forecasting Extreme Waves and Vessel Motions. Proc. of ASME 34th Int. Conf. on Ocean, Offshore and Arctic Eng. (OMAE), 42420. doi: 10.1115/OMAE2015-42420.

Ali, K., K., Nuruddeen, I., I. (2017). Analytical treatment for the conformable space-time fractional Benney-Luke equation via two reliable methods. International Journal of Physical Research, 5(2), pp. 109-114. doi: 10.14419/ijpr.v5i2.8403.

Ali, M., Prasad, R. (2019). Significant wave height forecasting via an extreme learning machine model integrated with improved complete ensemble empirical mode decomposition. Renewable and Sustainable Energy Reviews, 104, pp. 281-295.

Alkhalidi, M. A., Tayfun, M. A. (2013). Generalized Boccotti distribution for nonlinear wave heights. Ocean Engineering, 74, pp. 101-106.

Alqushaibi, A., Abdulkadir, S. J., Rais, H. M. D., Al-Tashi, Q., Ragab, M.G., Alhussian, H. (2021). Enhanced Weight-Optimized Recurrent Neural Networks Based on Sine Cosine Algorithm for Wave Height Prediction. J. Mar. Sci. Eng., 9(5), 524. doi: 10.3390/jmse9050524.

Alvise, B., Francesco, B., Filippo, B., Sandro, C. (2017). Space-time extreme wind waves: Analysis and prediction of shape and height. Ocean Modelling, 113, pp. 201-216.

Amarouche, K., Akpınar, A., Bachari, N.E.I., Çakmak, R.E., Houma, F. (2019). Evaluation of a high-resolution wave hindcast model SWAN for the West Mediterranean basin. Applied Ocean Research 84, pp. 225-241. doi: 10.1016/j.apor.2019.01.014.

Amrutha, M. M., Kumar, S. V. (2017). Observation of dominance of swells over wind seas in the coastal waters of the Gulf of Mannar, India. Ocean Science 13 (5), pp. 703-717.

Andreas, E. L. (1992). Sea Spray and the Turbulent Air-Sea Heat Fluxes. Journal of Geophysical Research, 97, pp. 11429-11441, 476. doi:10.1029/92jc00876.

Aoki, K., Kataoka, T. (2018). High-frequency ocean radar derived characteristics of sea surface currents in the Ariake Sea, Japan. Journal of Oceanography, 74(4), pp. 431–437. doi: 10.1007/s10872-018-0464-2.

Ardhuin, F., Brandt, P., Gaultier, L., Donlon, C., Battaglia, A., Boy, F., Casal, T., Chapron, B., Collard, F., Cravatte, S., Delouis, J.-M., de Witte, E., Dibarboure, G., Engen, G., Johnsen, H., Lique, C., Lopez-Dekker, P., Maes, C., Martin, A., Marié, L., Menemenlis, D., Nouguier, F., Peureux, C., Rampal, P., Ressler, G., Rio, M.-H., Rommen, B., Shutler, J. D., Suess, M., Tsamados, M., Ubelmann, C., van Sebille, E., van den Oever, M., Stammer, D. (2019a). SKIM, a Candidate Satellite Mission Exploring Global Ocean Currents and Waves. Frontiers in Marine Science, 6. doi: 10.3389/fmars.2019.00209.

Ardhuin, F., Stopa, J. E., Chapron, B., Collard, F., Husson, R., Jensen, R. E., Johannessen, J., Mouche, A., Passaro, M., Quartly, G. D., Swail, V., Young, I. (2019b). Observing Sea States. Frontiers in Marine Science, 6. doi: 10.3389/fmars.2019.00124.

Arul, M., Kareem, A. (2021). Applications of shapelet transform to time series classification of earthquake, wind and wave data. Engineering Structures, 228, 111564.

Austefjord, H. (2019). IACS Evaluation of Recommendation No. 34. the 1st International Symposium on Extreme Maritime Weather: Towards Safety of Life at Sea and a Sustainable Blue Economy.

Babanin, A. V. (2017). Similarity theory for turbulence, induced by orbital motion of surface water waves. Procedia IUTAM, 20, pp. 99-102. doi: 10.1016/j.piutam.2017.03.014.

Babanin, A. V., McConochie, J. (2013). Wind measurements near the surface of waves. Proc. of the ASME 2013 32nd International Conference on Ocean, Offshore and Arctic Engineering OMAE2013, 6 p. doi:10.1115/OMAE2013-10146.

Babanin, A. V., Onorato, M., Cavaleri, L. (2019a). On natural modulational bandwidth of deep-water surface waves. Fluids, 4(2), 67. doi: 10.3390/fluids4020067.

Babanin, A. V., Onorato, M., Qiao, F. (2012). Surface waves and wave-coupled effects in lower atmosphere and upper ocean. Journal of Geophysical Research, 117(C11), 10 p. doi:10.1029/2012JC007932.

Babanin, A. V., Rogers, W. E., de Camargo, R., Doble, M., Durrant, T., Filchuk, K., Ewans, K., Hemer, M., Janssen, T., Kelly-Gerreyn, B., Machutchon, K., McComb, P., Qiao, F., Schulz, E., Skvortsov, A., Thomson, J., Vichi, M., Violante-Carvalho, N., Wang, D., Waseda, T., Williams, G., Young, I. R. (2019b). Waves and swells in high wind and extreme fetches, measurements in the Southern Ocean. Front. Mar. Sci. Vol. 6, Issue JUL. doi: 10.3389/fmars.2019.00361.

Babanin, A. V., van der Westhuysen, A., Chalikov, D., Rogers, W. E. (2017). Advanced wave modelling including wave-current interaction, Journal of Marine Research, 75(3), pp. 239-262. doi: 10.1357/002224017821836798.

Babanin, A., Palenque, E. (2021). High-Altitude Experimental Test of the Wind-Wave Interaction Models. EGU General Assembly Conference Abstracts. https://ui.adsabs.harvard.edu/abs/2021EGUGA..2310544B.

Bai, X., Jiang, H., Huang, X., Song, G., Ma, X. (2021). 3-Dimensional direct sampling-based environmental contours using a semi-parametric joint probability model. Applied Ocean Research, 112, 102710.

Bai, X., Jiang, H., Li, C., Huang, L. (2020). Joint probability distribution of coastal wind and waves using a log-transformed kernel density estimation and mixed copula approach. Ocean Engineering, 216, 107937.

Bakker, W., Hofland, B., de Almeida, E., Oldenziel, G., Overmars, E. F. J. (2021). Pulsed LED line light for large-scale PIV-development and use in wave load measurements. Meas. Sci. Technol, 32, 115205. doi: 10.1088/1361-6501/ac17ce.

Bandringa, H., Helder, J. A. (2018). On the Validity and Sensitivity of CFD Simulations for a Deterministic Breaking Wave Impact on a Semi Submersible. Proc. of ASME 2018 37th International Conference on Ocean, Offshore and Arctic Engineering (OMAE), 78089, V001T01A004, 15 p. doi: 10.1115/OMAE2018-78089.

Bandringa, H., Helder, J. A., van Essen, S. M. (2020). On the Validity of CFD for Simulating Extreme Green Water Loads on Ocean-Going Vessels. Proc. of ASME 2020 39th International Conference on Ocean, Offshore and Arctic Engineering (OMAE), 18290, V001T01A063; 12 pages. doi: 10.1115/OMAE2020-18290.

Baquet, A., Jang, H., Lim, H.-J., Kyoung, J., Tcherniguin, N., Lefebvre, T., Kim, J. (2019). CFD-Based Numerical Wave Basin for FPSO in Irregular Waves. Proc. of ASME 2019 38th International Conference on Ocean, Offshore and Arctic Engineering (OMAE), 96838, V001T01A009; 9 pages. doi: 10.1115/OMAE2019-96838.

Baquet, A., Kim, J., Huang, Z. (2017). Numerical Modelling Using CFD and Potential Wave Theory for Three-Hour Nonlinear Irregular Wave Simulations. Proc. of ASME 2017 36th International Conference on Ocean, Offshore and Arctic Engineering (OMAE). 61090, V001T01A002; 14 p. doi: 10.1115/OMAE2017-61090.

Barbariol, F., Benetazzo, A., Bertotti, L., Cavaleri, L., Durrant, T., McComb, P., Sclavo, M. (2019). Large waves and drifting buoys in the Southern Ocean. Ocean Engineering, 172. doi: 10.1016/j.oceaneng.2018.12.011

Barbat, M. M., Rackow, T., Wesche, C., Hellmer, H. H., Mata, M. M. (2021). Automated iceberg tracking with a machine learning approach applied to SAR imagery: A Weddell sea case study. ISPRS Journal of Photogrammetry and Remote Sensing, 172(January), pp. 189-206. doi: 10.1016/j.isprsjprs.2020.12.006.

Begam, K. M. and Deepa, S. N. (2019). Optimized nonlinear neural network architectural models for multistep wind speed forecasting. Computers and Electrical Engineering. Elsevier Ltd, 78, pp. 32–49. doi: 10.1016/j.compeleceng.2019.06.018.

Berbić, J., Ocvirkb, E., Carević, D., Lončar, G. (2017). Application of neural networks and support vector machine for significant wave height prediction. Oceanologia. Polish Academy of Sciences 59(3), pp. 331–349. doi: 10.1016/j.oceano.2017.03.007.

Bernardino, M., Goncalves, M., Guedes Soares, C. (2021). Marine climate projections towards the end of the 21st century in the North Atlantic. ASME. J. Offshore Mech. Arct. Eng. doi: 10.1115/1.4050698.

Beyramzade, M., Siadatmousavi, S.M. (2017). Implementation of viscoelastic mud-induced energy attenuation in the third-generation wave model, SWAN. Ocean Dynamics 68 (1), pp. 47-63. doi: 10.1007/s10236-017-1118-4.

Bian, G.-F., Nie, G.-Z., Qiu, X. (2021). How well is outer tropical cyclone size represented in the ERA5 reanalysis dataset? Atmospheric Research 249, 105339, doi: 10.1016/j.atmosres.2020.105339.

Bitner-Gregersen, E. M. (2015). Joint met-ocean description for design and operations of marine structures. Applied Ocean Research, 51, pp. 279-292.

Bitner-Gregersen, E. M. (2018). Comparison of wind and wave climate in open sea and coastal waters. Ocean Engineering. doi: 10.1016/j.oceaneng.2018.10.016.

Bitner-Gregersen, E. M., Gramstad, O. (2019). Proc. of ASME 2019 38th International Conference on Ocean, Offshore and Arctic Engineering (OMAE), 95357, V003T02A001, 10 p. doi: 10.1115/OMAE2019-95357.

Bitner-Gregersen, E. M., Vanem, E., Gramstad, O., Hørte, T., Aarnes, O. J., Reistad, M., Breivik, Ø., Magnusson, A.K., Natvig, B. (2018). Climate change and safe design of ship structures. Ocean Eng. 149, 226–237. doi: 10.1016/j.oceaneng.2017.12.023.

Blockley, E., Vancoppenolle, M., Hunke, E., Bitz, C., Feltham, D., Lemieux, J.-F., Losch, M., Maisonnave, E., Notz, D., Rampal, P., Tietsche, S., Tremblay, B., Turner, A., Massonnet,

F., Ólason, E., Roberts, A., Aksenov, Ye., Fichefet, T., Garric, G., Iovino, D., Madec, G., Rousset, C., y Melia, D. S., Schroeder, D. (2020). The Future of Sea Ice Modelling: Where Do We Go from Here? Bulletin of the American Meteorological Society, 101(8), pp. E1304–E1311. doi: 10.1175/BAMS-D-20-0073.1.

Bogaert, H. (2018). An experimental investigation of sloshing impact physics in membrane LNG tanks on floating structures. Doctoral thesis. doi: 10.4233/uuid:96870b88-e07b-4ec2-8bd4-ef2cd3713568.

Bolin, D., Wallin, J. (2020). Multivariate type G Matern stochastic differential equation random fields. Journal of the Royal Statistical Society Series B, 82(1), pp. 215-239.

Bolles, T. C., Speer, K., Moore, M. (2019). Anomalous wave statistics induced by abrupt depth change. Physical Review Fluids, 4, 011801:1-8.

Bonaduce, A., Staneva, J., Beherens, A., Bidlot, J., Anna, R, Wilcke, I. (2019). Wave Climate Change in the North Sea and Baltic Sea. Journal of Marine Science and Engineering, 7(6). doi: 10.3390/jmse7060166.

Bonnefoy, F., Tikan, A., Copie, F., Suret, P., Ducrozet, G., Prabhudesai, G., Michel, G., Cazaubiel, A., Falcon, E., El, G., Randoux, S. (2020). From modulational instability to focusing dam breaks in water waves. Physical Review Fluids 5, 034802. doi: 10.1103/physrevfluids.5.034802.

Borderies, M., Caumont, O., Delanoë, J., Ducrocq, V., Fourrié, N. (2019). Assimilation of wind data from airborne Doppler cloud-profiling radar in a kilometre-scale NWP system. Natural Hazards and Earth System Sciences, 19(4), pp. 821–835. doi: 10.5194/nhess-19-821-2019.

Bouscasse, B., Ducrozet, G., Kim, J., Lim, H., Choi, Y., Bockman, A., Pâkozdi, C., Croonenborghs, E., Bihs, H. (2020). Development of a Protocol to Couple Wave and CFD Solvers Towards Reproducible CFD Modelling Practices for Offshore Applications. Proc. of ASME 39th International Conference on Ocean, Offshore and Arctic Engineering (OMAE), 19188, V001T01A014; 8 p. doi: 10.1115/OMAE2020-19188.

Brennan, J., Dudley, J. M., Dias, F. (2018). Extreme waves in crossing sea states. International Journal of Ocean and Coastal Engineering, 1(1), 1850001.

Bricheno, L. M., Wolf, J. (2018). Future Wave Conditions of Europe, in Response to High-End Climate Change Scenarios. Journal of Geophysical Research: Oceans, 123(12), pp. 8762-8791.

Bridges, R., Riska, K., Hopkins, M., Wei, Y. (2019). Ice interaction processes during ice encroachment. Marine Structures, 67, 102629. doi: 10.1016/j.marstruc.2019.05.007.

Bruno, M. F., Molfetta, M. G., Totaro, V., Mossa, M. (2020). Performance Assessment of ERA5 Wave Data in a Swell Dominated Region. Journal of Marine Science and Engineering, 8, 214. doi:10.3390/jmse8030214.

Bruserud, K., Haver, S. (2017). Uncertainties in Current Measurements in the Northern North Sea. Journal of Atmospheric and Oceanic Technology, 34, pp. 855-876.

Bruserud, K., Haver, S. (2019). Waves and associated currents - experiences from 5 years metocean measurements in the northern North Sea. Marine Structures, 63, pp. 429-443.

Bruserud, K., Haver, S., Myrhaug, D. (2018). joint description of waves and currents applied in a simplified load case. Marine Structures, 58, pp. 416-433.

Bryant, M.A., Jensen, R.E. (2017). Application of the Nearshore Wave Model STWAVE to the North Atlantic Coast Comprehensive Study. Journal of Waterway, Port, Coastal, and Ocean Engineering 143 (5). doi: 10.1061/(ASCE)WW.1943-5460.0000412.

Bulgakov, K., Kuzmin, V., Shilov, D. (2018). Evaluation of extreme wave probability on the basis of long-term data analysis. Ocean Science, 14, pp. 1321-1327.

Bunnik, T., de Ridder, E.-J. (2018). Using Nonlinear Wave Kinematics to Estimate the Loads on Offshore Wind Turbines in 3-Hour Sea States. Proc. of ASME 2018 37th International

Conference on Ocean, Offshore and Arctic Engineering (OMAE), 77807, V010T09A079; 8 p. doi: 10.1115/OMAE2018-77807.

Bunnik, T., Scharnke, J., de Ridder, E.-J. (2019). Efficient Indicators for Screening of Random Waves for Wave Impacts on a Jacket Platform and a Fixed Offshore Wind Turbine. Proc. of ASME 2019 38th International Conference on Ocean, Offshore and Arctic Engineering (OMAE), 95481, V001T01A061; 8 p. doi: 10.1115/OMAE2019-95481.

Bunnik, T., Stansberg, C. T., Pakozdi, C., Fouques, S., Somers, L. (2018). Useful Indicators for Screening of Sea States for Wave Impacts on Fixed and Floating Platforms. Proc. of ASME 2018 37th International Conference on Ocean, Offshore and Arctic Engineering (OMAE), 78544, V001T01A076; 8 p. American. doi: 10.1115/OMAE2018-78544.

Cai, Z. W., Chen, W. W., Liu, X. L., Sun, Z. (2020). Observations of Typhoon Waves in a Reef Lagoon of the South China Sea. Journal of Physical Oceanography, 50(1), pp. 161–173. doi: 10.1175/jpo-d-19-0146.1.

Caires, S., Kim, J., Groeneweg, J. (2018). Korean East Coast wave predictions by means of ensemble Kalman filter data assimilation. Ocean Dynamics 68 (11), pp. 1571-1592. doi: 10.1007/s10236-018-1214-0.

Calderon-Vega, F., Mosso, C., Garda-Soto, A., Delgadillo-Ruiz, D. (2019). Singe Site Extreme Wave Analysis in the Pacific Ocean Comparing Stationary and Non-stationary GEV Models. Current Journal of Applied Science and Technology, 32(6), pp. 1-12.

Caloiero, T., Aristodemo, F., Algieri Ferraro, D. (2019). Trend analysis of significant wave height and energy period in southern Italy. Theoretical and Applied Climatology. Theoretical and Applied Climatology. doi: 10.1007/s00704-019-02879-9.

Calvert, R., Whittaker, C., Raby, A., Taylor, P. H., Borthwick, A. G. L., van den Bremer, T. S. (2019). Laboratory study of the wave-induced mean flow and set-down in unidirectional surface gravity wave packets on finite water depth. Physical Review Fluids, 4(11). doi: 10.1103/PhysRevFluids.4.114801.

Campos, R. M., Alves, J.-H., Penny, S. G., Krasnopolsky, V. (2018c). Assessments of Surface Winds and Waves from the NCEP Ensemble Forecast System. Weather & Forecasting 33, pp. 1533-1546. doi: 10.1175/WAF-D-18-0086.1.

Campos, R. M., Costa, M. O., Almeida, F., Guedes Soares, C. (2021). Operational Wave Forecast Selection in the Atlantic Ocean Using Random Forests. J. Mar. Sci. Eng. 9(3), 298. doi: 10.3390/jmse9030298.

Campos, R. M., Krasnopolsky, V., Alves, J.-H. G.M., Penny, S.G. (2019a). Nonlinear wave ensemble averaging in the Gulf of Mexico using neural networks. Journal of Atmospheric and Oceanic Technology. American Meteorological Society, 36(1), pp. 113–127. doi: 10.1175/JTECH-D-18-0099.1.

Campos, R. M., Krasnopolsky, V., Alves, J.-H., Penny, S.G. (2020a). Improving NCEP's global-scale wave ensemble averages using neural networks. Ocean Modelling. Elsevier Ltd, Vol. 149, id. 101617. doi: 10.1016/j.ocemod.2020.101617.

Campos, R., Guedes Soares, C. (2018a). Spatial distribution of offshore wind statistics on the coast of Portugal using Regional Frequency Analysis. Renewable Energy, 123, pp. 806-816.

Campos, R., Guedes Soares, C., Alves, J., Parente, C., Guimaraes, L. (2019). Regional long-term extreme wave analysis using hindcast data from the South Atlantic Ocean. Ocean Engineering, 179, pp. 202-212.

Campos, R., Krasnopolsky, V., Alves, J.-H., Penny, S. (2017). Improving NCEP's Probabilistic Wave Height Forecasts Using Neural Networks: A Pilot Study Using Buoy Data. NCEP/NOAA Office Note. doi: https://doi.org/10.7289/V5/ON-NCEP-490.

Campos, R.M., Alves, J.-H., Penny, S. G., Krasnopolsky, V. (2020b). Global assessments of the NCEP Ensemble Forecast System using altimeter data. Ocean Dynamics, 70, pp. 405–419. doi: 10.1007/s10236-019-01329-4.

Campos, R.M., Alves, J.H.G.M., Guedes Soares, C., Guimaraes, L.G., Parente, C. E. (2018b). Extreme wind-wave modelling and analysis in the south Atlantic ocean. Ocean Modelling 124, pp. 75-93. doi: 10.1016/j.ocemod.2018.02.002.

Capodici, F., Cosoli, S., Ciraolo, G., Nasello, C., Maltese, A., Poulain, P.-M., Drago, A., Azzopardi, J., Gauci, A. (2019). Validation of HF radar sea surface currents in the Malta-Sicily Channel. Remote Sensing of Environment, 225, pp. 65–76. doi: 10.1016/j.rse.2019.02.026.

Casas-Prat, M., Wang, X. L. (2020a). Projections of extreme ocean waves in the Arctic and potential implications for coastal inundation and erosion. Journal of Geophysical Research: Oceans, 125(8), e2019JC015745. doi: 10.1029/2019JC015745.

Casas-Prat, M., Wang, X. L. (2020b). Sea ice retreat contributes to projected increases in extreme Arctic ocean surface waves. Geophysical Research Letters, 47, 2020GL088100. doi: 10.1029/2020GL088100.

Casas-Prat, M., Wang, X. L., Swart, N. (2018). CMIP5-based global wave climate projections including the entire Arctic Ocean. Ocean Modelling, 123, pp. 66-85. doi: 10.1016/j.ocemod.2017.12.003.

Cattrell, A. D., Srokosz, M., Moat, B. I., Marsh, R. (2018). Can Rogue Waves Be Predicted Using Characteristic Wave Parameters? Journal of Geophysical Research: Oceans. Vol. 123(8), pp. 5624-5636. doi: 10.1029/2018JC013958.

Cavaleri, L., Abdalla, S., Benetazzo, A., Bertotti, L., Bidlot, J.R., Breivik, Ø., Carniel, S., Jensen, R.E., Portilla-Yandun, J., Rogers, W.E., Roland, A., Sanchez-Arcilla, A., Smith, J.M., Staneva, J., Toledo, Y., van Vledder, G.P., van der Westhuysen, A.J. (2018). Wave modelling in coastal and inner seas. Progress in Oceanography 167, pp. 164-233. doi: 10.1016/j.pocean.2018.03.010.

Cazaubiel, A., Michel, G., Lepot, S., Semin, B., Aumaître, S., Berhanu, M., Bonnefoy, F., Falcon, E. (2018). Coexistence of solitons and extreme events in deep water surface waves. Physical Review Fluids 3, 114802. doi: 10.1103/PhysRevFluids.3.114802.

Cerlini, P. B., Silvestri, L., Saraceni, M. (2020). Quality control and gap-filling methods applied to hourly temperature observations over central Italy. RMets, Meteorol., 27, 1913. doi: org/10.1002/met.1913.

Chabchoub, A., Mozumi, K., Hoffmann, N., Babanin, A. V., Toffoli, A., Steer, J. N., van den Bremer, T. S., Akhmediev, N., Onorato, M., Waseda, T. (2019). Directional soliton and breather beams. Proceedings of the National Academy of Sciences of the United States of America, 116 (20) pp. 9759-9763. doi: 10.1073/pnas.1821970116.

Chai, W., Leira, B. J. (2018). Environmental contours based on inverse SORM. Marine Structures, 60, pp. 34-51.

Chai, W., Leira, B. J., Naess, A. (2018a). Short-term extreme ice loads prediction and fatigue damage evaluation for an icebreaker. Ships and Offshore Structures, 13(sup1), pp. 127-137. doi: 10.1080/17445302.2018.1427316.

Chai, W., Leira, B. J., Naess, A. (2018b). Probabilistic methods for estimation of the extreme value statistics of ship ice loads. Cold Regions Science and Technology, 146, pp. 87-97. doi: 10.1016/J.COLDREGIONS.2017.11.012.

Chalikov, D. V. (2016). Numerical Modelling of Sea Waves. Springer, 330 p.

Chalikov, D. V., Babanin, A. V. (2019). Parameterization of Wave Boundary Layer. Atmosphere, 10, 686, 30 p., doi: 10.3390/atmos10110686.

Chen, B.-y., Zhang, K.-y., Wang, L.-p., Jiang, S., Liu, G.-l. (2019a). Generalized Extreme Value-Pareto Distribution Function and Its Applications in Ocean Engineering. China Ocean Engineering, 33(2), pp. 127-136.

Chen, H., Cheng, W., Rong, Y., Zhao, X. (2019b). Fitting the generalized Pareto distribution to data based on transformations of order statistics. Journal of Applied Statistics, 46(3), pp. 432-448.

Chen, H., Tang, X., Gao, J., Fan, G. (2018c). Parametrization of geometric characteristics for extreme waves in shallow water. Ocean Engineering, 156, pp. 61-71.

Chen, M., Zhu, Z.-N., Zhang, C., Zhu, X.-H., Zhang, Z., Wang, M., Zheng, H., Zhang, X., Chen, J., He, Z., Dai, L., Kaneko, A. (2021). Mapping of tidal current and associated nonlinear currents in the Xiangshan Bay by coastal acoustic tomography. Ocean Dynamics, 71(8), pp. 811–821. doi: 10.1007/s10236-021-01470-z.

Chen, S.-T. (2019). Probabilistic forecasting of coastal wave height during typhoon warning period using machine learning methods. Journal of Hydroinformatics, 21(2), pp. 343-358.

Chen, T., Zhang, Q., Wu, Y., Ji, C., Yang, J., Liu, G. (2018a). Development of a wave-current model through coupling of FVCOM and SWAN. Ocean Engineering 164, pp. 443-454. doi: 10.1016/j.oceaneng.2018.06.062.

Chen, X., Ginis, I., Hara, T. (2018b). Sensitivity of Offshore Tropical Cyclone Wave Simulations to Spatial Resolution in Wave Models. Journal of Marine Science and Engineering 6 (4), 116. doi: 10.3390/jmse6040116.

Chen, X., Jiang, Z., Li, Q., Li, Y., Ren, N. (2020a). Extended Environmental contour Methods for Long-Term Extreme Response Analysis of Offshore Wind Turbines. Journal of Offshore Mechanics and Arctic Engineering, 142(5), 052003.

Chen, X., Okada, T., Kawamura, Y., Mitsuyuki, T. (2020b). Estimation of on-site directional wave spectra using measured hull stresses on 14,000 TEU large container ships. Journal of Marine Science and Technology, 25(3). doi: 10.1007/s00773-019-00673-w.

Chen, Y., Li, J., Pan, S., Gan, M., Pan, T., Xie, D., Clee, S. (2019d). Joint probability analysis of extreme wave heights and surges along China's coasts. Ocean engineering, 177, 97107.

Chen, Y., Zhang, S., Zhang, W., Peng, J., Cai, Y. (2019e). Multifactor spatio-temporal correlation model based on a combination of convolutional neural network and long short-term memory neural network for wind speed forecasting. Energy Conversion and Management. Elsevier Ltd, 185, pp. 783–799. doi: 10.1016/j.enconman.2019.02.018.

Chen, Z., Chen, X., Zhao, C., Li, J., Huang, W., Gill, E. W. (2019c). Observation and intercomparison of wave motion and wave measurement using shore-based coherent microwave radar and HF radar. IEEE Transactions on Geoscience and Remote Sensing, 57(10), pp. 7594-7605. doi: 10.1109/TGRS.2019.2914437.

Cheng, S., Tsarau, A., Evers, K., Shen, H. (2019). Floe Size Effect on Gravity Wave Propagation Through Ice Covers. Journal of Geophysical Research. Oceans, 124(1), pp. 320–334. doi: 10.1029/2018jc014094.

Choi, H., Park, M., Son, G., Jeong, J., Park, J., Mo, K., Kang, P. (2020). Real-time significant wave height estimation from raw ocean images based on 2D and 3D deep neural networks. Ocean Engineerin, 201, 107129.

Choi, J., Jang, B.-S., Park, J.-H., Kim, H.-j., Park, S. C. (2019). Improved environmental contour method based on an optimization of hybrid models. Applied Ocean Research, 91, 101901.

Clarindo, G., Teixeira, A., Guedes Soares, C. (2021). Environmental wave contours by inverse FORM and Monte Carlo Simulation with variance reduction techniques. Ocean Engineering, 228, 108916.

Coles, S. (2001). An Introduction to Statistical Modelling of Extreme Values. London: Springer-Verlag, 223 p.

Collins, K. M., Stripling, S., Simmonds, D. J., Greaves, D. M. (2018). Quantitative metrics for evaluation of wave fields in basins. Ocean Engineering, 169, pp. 300–314. doi: 10.1016/j.oceaneng.2018.09.010.

Collins, M. J., Ma, M., Dabboor, M. (2019). On the Effect of Polarization and Incidence Angle on the Estimation of Significant Wave Height from SAR Data. IEEE Transactions on Geoscience and Remote Sensing, 57(7), pp. 4529-4543. doi: 10.1109/TGRS.2019.2891426.

Conforti, M., Li, S., Biondini, G., Trillo, S. (2018). Auto-modulation versus breathers in the nonlinear stage of modulational instability. Optics Letters, 43, pp. 5291-5294. doi: 10.1364/ol.43.005291.

Connell, B. S. H., Rudzinsky, J. P., Brundick, C. S., Milewski, W. M., Kusters, J. G., Farquharson, G. (2015). Development of an Environmental and Ship Motion Forecasting System. Proc. of ASME 34th Int. Conf. on Ocean, Offshore and Arctic Eng. (OMAE), 42422. doi: 10.1115/OMAE2015-42422.

Cosoli, S., Grcic, B., Vos, S., Hetzel, Y. (2018). Improving data quality for the australian high frequency ocean radar network through real-time and delayed-mode quality-control procedures. Remote Sensing, 10(9), pp. 1–15. doi: 10.3390/rs10091476.

Cotton, J., Francis, P., Heming, J., Forsythe, M., Reul, N., Donlon, C. (2018). Assimilation of SMOS L-band wind speeds: impact on Met Office global NWP and tropical cyclone predictions. Quarterly Journal of the Royal Meteorological Society, 144(711), pp. 614–629. doi: 10.1002/qj.3237.

Couvelard, X., Lemarié, F., Samson, G., Redelsperger, J.-L., Ardhuin, F., Benshila, R., Madec, G. (2019). Development of a 2-way coupled ocean-wave model: assessment on a global NEMO (v3.6) - WW3 (v6.02) coupled configuration. Geoscientific Model Development Discussions, Copernicus Publ., pp. 1-36. doi: 10.5194/gmd-2019-189.

Craciunescu, C. C., Christou, M. (2020). Wave breaking energy dissipation in long-crested focused wave groups based on JONSWAP spectra. Applied Ocean Research, 99. doi: 10.1016/j.apor.2020.102144.

Cui, C., Fearn, T. (2018). Modern practical convolutional neural networks for multivariate regression: Applications to NIR calibration. Chemometrics and Intelligent Laboratory Systems. Elsevier B.V., 182, pp. 9–20. doi: 10.1016/j.chemolab.2018.07.008.

Curcic, M., Haus, B. K. (2020). Revised Estimates of Ocean Surface Drag in Strong Winds. Geophysical Research Letters, 47(10). doi: 10.1029/2020gl087647.

Czado, C. (2019). Analyzing Dependent Data with Vine Copulas. Cham: Springer, 273 p.

Dahl, K. R., Huseby, A. B. (2018). Buffered environmental contours. Safety and Reliability – Safe Societies in a Changing World. Proceedings of ESREL 2018, June 17-21, 2018, Trondheim, Norway: CRC Press, pp. 2285-2292.

Dansereau, V., Weiss, J., Saramito, P. (2021). A Continuum Viscous-Elastic-Brittle, Finite Element DG Model for the Fracture and Drift of Sea Ice. Proc. of International Conference IACMAG 2021: Challenges and Innovations in Geomechanics, pp. 125-139. (Lecture Notes in Civil Engineering, vol. 125. Springer, Cham.) doi: 10.1007/978-3-030-64514-4_8.

Dao, D. T., Chien, H., Lai, J. W., Huang, Y. H., Flament, P. (2019). Evaluation of HF radar in mapping surface wave field in Taiwan Strait under winter monsoon. Proc. of OCEANS 2019 MTS/IEEE, pp. 0-6. doi: 10.1109/OCEANSE.2019.8867519.

Davidson, F., Alvera-Azcárate, A., Barth, A., Brassington, G. B., Chassignet, E. P., Clementi, E., de Mey-Frémaux, P., Divakaran, P., Harris, C., Hernandez, F., Hogan, P., Hole, L. R., Holt, J., Liu, G., Lu, Y., Lorente, P., Maksymczuk, J., Martin, M., Mehra, A., Melsom, A., Mo, H., Moore, A., Oddo, P. Pascual, A., Pequignet, A-.C., Kourafalou, V., Ryan, A., Siddorn, J., Smith, G., Spindler, D., Spindler, T., Stanev, E. V., Staneva, J., Storto, A., Tanajura, C., Vinayachandran, P. N., Wan. L., Wang, H., Zhang, Y., Zhu, X., Zu, Z.

(2019). Synergies in Operational Oceanography: The Intrinsic Need for Sustained Ocean Observations. Frontiers in Marine Science, 6. doi: 10.3389/fmars.2019.00450.

Davies, G., Callaghen, D. P., Uriah, G., Jiang, W., Hanslow, D., Nichol, S., Baldock, T. (2017). Improved treatment of non-stationary conditions and uncertainties in probabilistic models of storm wave climate. Coastal Engineering, 127, pp. 1-19.

de Hauteclocque, G., Zhu, T., Johnson, M., Austefjord, H., Bitner-Gregersen, E. (2020). Assessment of Global Wave Datasets for Long Term Response of Ships. Proc. of ASME 39th Int. Conf. on Ocean, Offshore and Arctic Eng. (OMAE), 18874. doi: 10.1115/OMAE2020-18874.

De Leo, F., Besio, G., Briganti, R., Vanem, E. (2021). Non-stationary extreme value analysis of sea states based on linear trends. Analysis of annual maxima series of significant wave height and peak period in the Mediterranean Sea. Coastal Engineering, 167, 103896.

De Leo, F., De Leo, A., Besio, G., Briganti, R. (2020). Detection and quantification of trends in time series of Significant wave heights: An Application in the Mediterranean Sea. Ocean Engineering, 202, 107155.

Dematteis, G., Grafke, T., Onorato, M., Vanden-Eijnden, E. (2019). Experimental Evidence of Hydrodynamic Instantons: The Universal Route to Rogue Waves. Physical Review X, 9(4), 041057, pp. 1-12. doi: 10.1103/PhysRevX.9.041057.

Dematteis, G., Grafkea, T., Vanden-Eijndena, E. (2018). Rogue waves and large deviations in deep sea. PNAS 115(5), pp. 155-160. www.pnas.org/cgi/doi/10.1073/pnas.1710670115.

Demetriou, D., Michailides, C., Papanastasiou, G., Onoufriou, T. (2021). Coastal zone significant wave height prediction by supervised machine learning classification algorithms. Ocean Engineering, 108592, 108592.

Demiray, S. T., Bulut, H. (2017). New exact solutions for generalized Gardner equation. Kuwait Journal of Science, 44(1), pp. 1-8.

Dentale, F., Furcolo, P., Carratelli, E. P., Reale, F., Contestabile, P., Tomasicchio, G. R. (2018). Extreme Wave Analysis by Integrating Model and Wave Buoy Data. Water, 10, 373: pp. 1-15.

Derbanne, Q., de Hauteclocque, G. (2019). A new approach for environmental contour and multivariate de-clustering. Proc. OMAE 2019. Glasgow: ASME.

Derkani, M. H., Alberello, A., Nelli, F., Bennetts, L. G., Hessner, K. G., MacHutchon, K., Reichert, K., Aouf, L., Khan, S., Toffoli, A. (2021). Wind, waves, and surface currents in the Southern Ocean: observations from the Antarctic Circumnavigation Expedition. Earth System Science Data, 13(3), pp. 1189-1209. doi: 10.5194/essd-13-1189-2021.

Dicopoulos, J., Roarty, H., Daugharty, M., Glenn, S. (2018). Improving CODAR SeaSonde wave measurements. Proc. of OCEANS 2018 MTS/IEEE, pp. 16–19. doi: 10.1109/OCEANSKOBE.2018.8559077.

Didenkulova, E., Slunyaev, A., Pelinovsky, E. N. (2019). Fluids Numerical simulation of random bimodal wave systems in the KdV framework. European Journal of Mechanics – B/Fluids, 78, pp. 21–31. doi: 10.1016/j.euromechflu.2019.05.015.

Dimitrov, N. (2020). Inverse Directional Simulation: an environmental contour method providing an exact return period. Journal of Physics: Conference Series, 1618, 062048.

Dinardo, S., Fenoglio-Marc, L., Becker, M., Scharroo, R., Fernandes, M. J., Staneva, J., Grayek, S., Benveniste, J. (2021). A RIP-based SAR retracker and its application in North East Atlantic with Sentinel-3. Advances in Space Research, 68(2), pp. 892-929. doi: 10.1016/j.asr.2020.06.004.

Ding, F., Shen, H., Perrie, W., He, Y. (2020). Is radar phase information useful for sea ice detection in the marginal ice zone? Remote Sensing, 12(11), pp. 1-15. doi: 10.3390/rs12111847.

Ding, Y., Yu, J., Cheng, H. (2019). Long-term wave climate characteristics and potential impacts on embayed beaches along the west Guangdong coastline. Regional Studies in Marine Science. Elsevier B.V., 30: 100741. doi: 10.1016/j.rsma.2019.100741.

DNV GL. (2019). Environmental conditions and environmental loads. Recommended practice. DNVGL-RP-C205. DNV GL, p. 252.

Dodet, G., Piolle, J.-F., Quilfen, Y., Abdalla, S., Accensi, M., Ardhuin, F., Ash, E., Bidlot, J.-R., Gommenginger, C., Marechal, G., Passaro, M., Quartly, G., Stopa, J., Timmermans, B., Young, I., Cipollini, P., Donlon, C. (2020). The Sea State CCI dataset v1: towards a sea state climate data record based on satellite observations. Earth System Science Data, 12(3), pp. 1929-1951.
doi:10.1115/OMAE2019-95993.

Donelan, M. A., Babanin, A. V., Young, I. R., Banner, M. L. (2006). Wave follower measurements of the wind input spectral function. Part 2. Parameterization of the wind input. Journal of Physical Oceanography, 36(8), pp. 1672-1688.

Dong, G., Liu, D., Ma, Y., Perlin, M. (2019). Experimental investigation of weakly three-dimensional nonlinear wave interactions. European J. of Mechanics B/Fluids, 77, pp. 239-251. doi: 10.1016/j.euromechflu.2019.05.003.

Doong, D. J., Peng, J. P., Chen, Y. C. (2018). Development of a warning model for coastal freak wave occurrences using an artificial neural network. Ocean Engineering. Elsevier Ltd, 169, pp. 270–280. doi: 10.1016/j.oceaneng.2018.09.029.

Dora, G.U., Kumar, V.S. (2018). Hindcast of breaking waves and its impact at an island sheltered coast, Karwar. Ocean Dynamics 68 (1), pp. 1-16. doi: 10.1007/s10236-017-1112-x.

Douglas, S., Cornett, A., Nistor, I. (2020). Image-Based Measurement of Wave Interactions with Rubble Mound Breakwaters. Journal of Marine Science and Engineering, 8(6). doi: 10.3390/jmse8060472.

Drees, H., de Haan, L., Turkman, F. (2018). Extreme value estimation for discretely sampled continuous processes. Extremes, 21, pp. 533-550.

Drees, H., JanBen, A. (2017). Conditional extreme value models: fallacies and pitfalls. Extremes, 20, pp. 777-805.

Du, Y., Dong, X., Jiang, X., Zhang, Y., Zhu, D., Sun, Q., Wang, Z., Niu, X., Chen, W., Zhu, C., Jing, Z., Tang, S., Li, Y., Chen, J., Chu, X., Xu, C., Wang, T., He, Y., Han, B., Zhang, Y., Wang, M., Wu, W., Xia, Y., Chen, K., Qian, Y.-K., Shi, P., Zhan, H., Peng, S. (2021). Ocean surface current multiscale observation mission (OSCOM): Simultaneous measurement of ocean surface current, vector wind, and temperature. Progress in Oceanography, 193. doi: 10.1016/j.pocean.2021.102531.

Duan, C., Dong, S., Wang, Z. (2019). Wave climate analysis in the ice-free waters of Kara Sea. Regional studies in marine science, 30, 100719. doi: 10.1016/j.rsma.2019.100719.

Ducrozet, G., Bonnefoy, F., Mori, N., Fink, M., & Chabchoub, A. (2020). Experimental reconstruction of extreme sea waves by time reversal principle. Journal of Fluid Mechanics, 884. doi: 10.1017/jfm.2019.939.

Ducrozet, G., Bonnefoy, F., Mori, N., Fink, M., Chabchoub, A. (2020). Experimental Reconstruction of Extreme Sea Waves by Time Reversal Principle. J. of Fluid Mechanics, 884, A20. doi: 10.1017/ jfm.2019.939.

Ducrozet, G., Gouin, M. (2017). Influence of varying bathymetry in rogue wave occurrence within unidirectional and directional sea-states. Journal of Ocean Engineering and Marine Energy, 3, pp. 309–324. doi: 10.1007/s40722-017-0086-6.

Düz, B., Lindeboom, R., Scharnke, J., Helder, J., Bandringa, H. (2017). Comparison of Breaking Wave Kinematics From Numerical Simulations With PIV Measurements. Proc. of ASME 2017 36th International Conference on Ocean, Offshore and Arctic Engineering (OMAE), 61698. 11 p. doi: 10.1115/OMAE2017-61698.

Düz, B., Mak, B., Hageman, R., Grasso, N. (2021). Real time estimation of local wave characteristics from ship motions using artificial neural networks. Proc. of 14th Symp. on Practical Design of Ships and Other Floating Structures (PRADS). Lecture Notes on Civil Eng. (LNCE) 65. doi: 10.1007/978-981-15-4680-8_45.

Düz, B., Scharnke, J., Hallmann, R., Tukker, J., Khurana, S., Blanchard, K. (2020). Comparison of the CFD Results to PIV Measurements in Kinematics of Spilling and Plunging Breakers. Proc. of ASME 2020 39th International Conference on Ocean, Offshore and Arctic Engineering (OMAE), 19268, V06BT06A065. 17 p. doi: 10.1115/OMAE2020-19268.

Dyachenko, A., Kachulin, D., Zakharov, V. (2017). Super compact equation for water waves. Journal of Fluid Mechanics, 828, pp. 661-679. doi:10.10 17/jfm.2017.529

Dzvonkovskaya, A., Petersen, L., Helzel, T., Kniephoff, M. (2018). High-frequency ocean radar support for Tsunami Early Warning Systems. Geoscience Letters, 5(1). doi: 10.1186/s40562-018-0128-5.

Eckert, A., Martin, N., Coe, R. G., Seng, B., Stuart, Z., Morrell, Z. (2021). Development of a Comparison Framework for Evaluating Environmental Contours for Extreme Sea States. Journal of Marine Science and Engineering, 9, 16: pp. 1-24.

Eeltink, D., Lemoine, A., Branger, H., Kimmoun, O., Kharif, C., Carter, J. D., Chabchoub, A., Brunetti, M., Kasparian, J. (2017). Spectral up- and downshifting of Akhmediev breathers under wind forcing. Physics of Fluids, Vol. 29(10). doi: 10.1063/1.4993972.

Ellenson, A., Pei, Y., Wilson, G., Ozkan-Haller, H. T., Fern, X. (2020). An application of a machine learning algorithm to determine and describe error patterns within wave model output. Coastal Engineering, 157, 103595. doi:10.1016/j.coastaleng.2019.103595.

Engelke, S., Hitz, A. S. (2019). Graphical Models for Extremes. arxiv:1812.01734v2, pp. 1-37.

Ermoshkin, A. V., Kapustin, I., Molkov, A., Bogatov, N., Bakhanov, V. (2019). On the features of Doppler velocities estimation with coherent radar of high spatial resolution. October 2019, 52. doi: 10.1117/12.2533072.

Fan, S., Xiao, N., Dong, S. (2020). A novel model to predict significant wave height based on long short-term memory network. Ocean Engineering, 205, 107298. doi: 10.1016/j.oceaneng.2020.107298.

Fan, S., Zhang, B., Mouche, A. (2018). Tropical Cyclone Wind Direction Retrieval from C-Band Dual-Polarization Synthetic Aperture Radar. Progress in Electromagnetics Research Symposium, 2018-Augus, 1423–1427. doi: 10.23919/PIERS.2018.8597711.

Faridafshin, F., Naess, A. (2017). Multivariate log-concave probability density class for structural reliability applications. Structural Safety, 69, pp. 57-67.

Fazeres-Ferradosa, T., Taveira-Pinto, F., Vanem, E., Reis, M. T., das Neves, L. (2018). Asymmetric copula-based distribution models for met-ocean data in offshore wind engineering applications. Wind Engineering, 42(4), pp. 304-334.

Feld, G., Randell, D., Ross, E., Jonathan, P. (2019). Design conditions for waves and water levels using extreme value analysis with covariates. Ocean Engineering, 173, pp. 851-866.

Francis, D., Mattingly, K. S., Lhermitte, S., Temimi, M., Heil, P. (2021). Atmospheric extremes caused high oceanward sea surface slope triggering the biggest calving event in more than 50 years at the Amery Ice Shelf. The Cryosphere, 15(5), pp. 2147–2165. doi: 10.5194/tc-15-2147-2021.

Francius, M., Kharif, C. (2017). Two-dimensional stability of finite-amplitude gravity waves on water of finite depth with constant vorticity. Journal of Fluid Mechanics, 830, pp. 631-659. doi:10.1017/jfm.2017.603.

Fujimoto, W., Waseda, T., Webb, A. (2019). Impact of the four-wave quasi-resonance on freak wave shapes in the ocean. Ocean Dynamics, 69(1). doi: 10.1007/s10236-018-1234-9.

Fujiwara, Y., Yoshikawa, Y., Matsumura, Y. (2018). A Wave-Resolving Simulation of Langmuir Circulations with a Nonhydrostatic Free-Surface Model: Comparison with

Craik–Leibovich Theory and an Alternative Eulerian View of the Driving Mechanism. Journal of Physical Oceanography, 48, pp. 1691-1708.

Gangeskar, R. (2018). Verifying High-Accuracy Ocean Surface Current Measurements by X-Band Radar for Fixed and Moving Installations. IEEE Transactions on Geoscience and Remote Sensing, 56(8), pp. 4845-4855. doi: 10.1109/TGRS.2018.2840133.

Gao, Y., Guan, C., Sun, J., Xie, L. (2020). Tropical cyclone wind speed retrieval from dual-polarization sentinel-1 ew mode products. Journal of Atmospheric and Oceanic Technology, 37(9), pp. 1713-1724. doi: 10.1175/JTECH-D-19-0148.1.

Ge, Z., Shen, Z., Yan, D., Chien, H. (2018). CFD-predicted slamming loads on a ship in head and oblique seas. Proc. of 32nd Symposium on Naval Hydrodynamics.

Geerts, S., Delefortrie, G., Lataire, E., Troch, P. (2018). Flanders maritime laboratory, new large scale facilities for towing tank and wave basin research. Proc. of the 2nd International Symposium on Hydraulic Modelling and Measuring Technology (ISHMMT 2018), pp. 1-7.

Gelash, A., Agafontsev, D., Zakharov, V., El, G., Randoux, S., Suret, P. (2019). Bound State Soliton Gas Dynamics Underlying the Spontaneous Modulational Instability. Physical Review Letters, 123(23), pp. 1-7. doi: 10.1103/PhysRevLett.123.234102.

Gemmrich, J., Thomson, J. (2017). Observations of the shape and group dynamics of rogue waves. Geophysical Research Letters, 44(4). doi: 10.1002/2016GL072398.

Genthon, C., Veron, D. E., Vignon, E., Six, D., Dufresne, J.-L., Madeleine, J.-B., Sultan, E., Forget, F. (2021). Ten years of temperature and wind observation on a 45-m tower at Dome C, East Antarctic plateau. doi: 10.5194/essd-2021-204.

Gharamti, I. E., Dempsey, J. P., Polojärvi, A., Tuhkuri, J. (2021a). Fracture of warm S2 columnar freshwater ice: size and rate effects. Acta Materialia, 202. doi: 10.1016/j.actamat.2020.10.031.

Gharamti, I. E., Dempsey, J. P., Polojärvi, A., Tuhkuri, J. (2021b). Creep and fracture of warm columnar freshwater ice. The Cryosphere, 15(5). doi: 10.5194/tc-15-2401-2021.

Gill, E. W., Ma, Y., Huang, W. (2018). Motion compensation for high-frequency surface wave radar on a floating platform. IET Radar, Sonar and Navigation, 12(1), pp. 37-45. doi: 10.1049/iet-rsn.2017.0220.

Golubkin, P., Kudryavtsev, V., Smirnova, J., Chapron, B. (2018). Abnormal Waves Generated by Polar Lows: Evaluation of Expectancy. Proc. of 2018 IEEE International Geoscience and Remote Sensing Symposium, pp. 3286–3289. doi: 10.1109/IGARSS.2018.8517460.

Gommenginger, C., Chapron, B., Hogg, A., Buckingham, C., Fox-Kemper, B., Eriksson, L., Soulat, F., Ubelmann, C., Ocampo-Torres, F., Nardelli, B. B., Griffin, D., Lopez-Dekker, P., Knudsen, P., Andersen, O., Stenseng, L., Stapleton, N., Perrie, W., Violante-Carvalho, N., Schulz-Stellenfleth, J., Woolf, D., Isern-Fontanet, J., Ardhuin, F., Klein, P., Mouche, A., Pascual, A., Capet, X., Hauser, D., Stoffelen, A., Morrow, R., Aouf, L., Breivik, Ø., Fu, L.-L., Johannessen, J. A., Aksenov, Ye., Bricheno, L., Hirschi, J., Martin, A. C. H., Martin, A. P., Nurser, G., Polton, J., Wolf, J. H, Johnsen, H., Soloviev, A., Jacobs, G. A., Collard, F., Groom, S., Kudryavtsev, V., Wilkin, J., Navarro, V., Babanin, A., Martin, M., Siddorn, J., Saulter, A., Rippeth, T., Emery, B., Maximenko, N., Romeiser, R., Graber, H., Azcarate, A. A., Hughes, C. W., Vandemark, D., da Silva, J., Leeuwen, P. J. V., Naveira-Garabato. A., Gemmrich, J., Mahadevan, A., M. J., Munro, Y., Doody, S., Burbidge, G. (2019). SEASTAR: A Mission to Study Ocean Submesoscale Dynamics and Small-Scale Atmosphere-Ocean Processes in Coastal, Shelf and Polar Seas. Frontiers in Marine Science, 6. doi: 10.3389/fmars.2019.00457.

Gong, H., Polojärvi, A., Tuhkuri, J. (2019a). Discrete element simulation of the resistance of a ship in unconsolidated ridges. Cold Regions Science and Technology, 167, 102855. doi: 10.1016/j.coldregions.2019.102855.

Gong, H., Polojärvi, A., Tuhkuri, J. (2019b). The effect of ship bow shape on ridge resistance in a narrow ridge. Proc. of 25th International Conference on Port and Ocean Engineering under Arctic Conditions (POAC 2019). https://www.poac.com/Papers/2019/pdf/POAC19-070.pdf

Goulart, A. J. H., Camargo, R. (2021). On data selection for training wind forecasting neural networks. Computers & Geosciences, 155, 104825. doi: 10.1016/j.cageo.2021.104825.

Gouldby, B., Wyncoll, D., Panzeri, M., Franklin, M., Hunt, T., Hames, D., Tozer, N., Hawkes, P., Dornbusch, U., Pullen, T. (2017) Multivariate extreme value modelling of sea conditions around the coast of England. Proceedings of the Institution of Civil Engineers, Maritime Engineering, 170(1), pp. 3-20.

Gramcianinov, C. B., Campos, R., De Camargo, R., Hodges, K., Guedes Soares, C., Silva D. P. (2020). Analysis of Atlantic extratropical storm tracks characteristics in 41 years of ERA5 and CFSR/CFSv2 databases. Ocean Engineering 216, 108111, doi: 10.1016/j.oceaneng.2020.108111.

Gramstad, O., Agrell, C., Bitner-Gregersen, E., Guo, B., Ruth, E., Vanem, E. (2020). Sequential sampling method using Gaussian process regression for estimating extreme structural response. Marine Structures, 72, 102780.

Gramstad, O., Bitner-Gregersen, E., Breivik, O., Magnusson, A. K., Reistad, M., Aarnes, O. J. (2018a). Analysis of rogue waves in North-Sea in-situ surface wave data. Proc. OMAE 2017. Madrid: ASME. doi:10.1115/OMAE2018-77858.

Gramstad, O., Bitner-Gregersen, E., Trulsen, K., Nieto Borge, J. C. (2018b). Modulational instability and rogue waves in crossing sea states. Journal of Physical Oceanography, 48(6), pp. 1317-1331. doi: 10.1175/JPO-D-18-0006.1.

Gribanov, I., Taylor, R., Sarracino, R. (2018a). Cohesive zone micromechanical model for compressive and tensile failure of polycrystalline ice. Engineering Fracture Mechanics, 196, pp. 142-156. doi: 10.1016/j.engfracmech.2018.04.023.

Gribanov, I., Taylor, R., Sarracino, R. (2018b). Parallel implementation of implicit finite element model with cohesive zones and collision response using CUDA. International Journal for Numerical Methods in Engineering, 115(7), pp. 771-790. doi: 10.1002/nme.5825.

Guo, J., Liu, B., Gong, W., Shi, L., Zhang, Y., Ma, Y., Zhang, J., Chen, T., Bai, K., Stoffelen, A., de Leeuw, G., Xu, X. (2021a). Technical note: First comparison of wind observations from ESA's satellite mission Aeolus and ground-based radar wind profiler network of China. Atmospheric Chemistry and Physics, 21(4), 2945–2958. doi: 10.5194/acp-21-2945-2021.

Guo, W., Du, H., Cheong, J. W., Southwell, B. J., Dempster, A. G. (2021b). GNSS-R Wind Speed Retrieval of Sea Surface Based on Particle Swarm Optimization Algorithm. IEEE Transactions on Geoscience and Remote Sensing, Ddm, pp. 1-14. doi: 10.1109/TGRS.2021.3082916.

Häfner, D., Gemmrich, J., Jochum, M. (2021a). FOWD: A Free Ocean Wave Dataset for Data Mining and Machine Learning. Journal of Atmospheric and Oceanic Technology. doi: 10.1175/JTECH-D-20-0185.1

Häfner, D., Gemmrich, J., Jochum, M. (2021b). Real-world rogue wave probabilities. Nature Scientific Reports, 11(1). doi: 10.1038/s41598-021-89359-1.

Haghayeghi, Z. S., Imani, H., Karimirad, Madjid. (2020). Directional dependence of extreme metocean conditions for analysis and design of marine structures. Applied Ocean Research, 100, 102181.

Haghayeghi, Z. S., Ketabdari, M. J. (2017). Development of Environmental Contours for Circular and Linear Metocean Variables. International Journal of Renewable Energy Research, 7(2), pp. 682-693.

Haghayeghi, Z. S., Ketabdari, M. J. (2018). A long-term joint probability model for metocean circular and linear characteristics. Applied Ocean Research, 75, pp. 143-152.

Hames, D. P., Gouldby, B. P., Hawkes, P. J. (2019). Evolution of joint probability methods in coastal engineering practice in the UK. Proceedings of the Institution of Civil Engineers, Maritime Engineering, 172(2), pp. 45-54.

Han, B. W., Seo, J., Lee, S. J., Seol, D. M., Rhee, S. H. (2018b). Uncertainty assessment for a towed underwater stereo PIV system by uniform flow measurement. Int. J. of Naval Arch. and Ocean Eng. 10(5), pp. 596-608. doi: 10.1016/j.ijnaoe.2017.11.005.

Han, Q., Hao, Z., Hu, T., Chu, F. (2018a). Non-parametric models for joint probabilistic distributions of wind speed and direction data. Renewable Energy, 126, pp. 1032-1042.

Hansen, H. F., Randell, D., Zeeberg, A. R., Jonathan, P. (2020). Directional-seasonal extreme value analysis of North Sea storm conditions. Ocean Engineering, 195, 106665.

Hartmann, M. C. N., von Bock und Polach, R. U. F., Klein, M. (2020). Damping of Regular Waves in Model Ice. Proc. of ASME 39th Int. Conf. on Ocean, Offshore and Arctic Eng. (OMAE), 18152. doi: 10.1115/OMAE2020-18152.

Hasegawa, K., Uto, S., Shimoda, H., Wako, D., Matsuzawa, T. (2019). Non-smooth DEM Simulation for Interaction of Conical Structure and Managed Ice Floes using Breakable Ice Element. Proc. of 25th International Conference on Port and Ocean Engineering under Arctic Conditions (POAC 2019), 12 p. https://www.poac.com/Papers/2019/pdf/POAC19-079.pdf

Haselsteiner, A. F., Coe, R. G., Manuel, L., Nguyen, P. T., Martin, N., Eckert-Gallup, A. (2019a). A benchmarking exercise on estimating extreme environmental conditions: Methodology baseline results. Proc. OMAE 2019 (pp. OMAE2019-96523). Glasgow: ASME.

Haselsteiner, A. F., Coe, R., G., Manuel, L., Chai, W., Leira, B., Clarindo, C., Guedes Soares, C., Hannesdóttir, Á., Dimitrov, N., Sander, A., Ohlendorf, J.-H.., Thoben, K.-D., Hauteclocque, G., Mackay, E., Jonathan, Ph., Qiao, Ch., Myers, A., Rode, A., Hildebrandt, A., Schmidt, B., Vanem, E., Huseby, A. B. (2021). A benchmarking exercise for environmental contours. Ocean Engineering, 236, 109504.

Haselsteiner, A. F., Lehmkuhl, J., Pape, T., Windmeier, K.-L., Thoben, K.-D. (2019b). ViroCon: A software to compute multivariate extremes using the environmental contour method. SoftwareX, 9, pp. 95-101.

Haselsteiner, A. F., Ohlendorf, J.-H., Wosniok, W., Thoben, K.-D. (2017). Deriving environmental contours from highest density regions. Coastal Engineering, 123, pp. 42-51.

Haselsteiner, A. F., Thoben, K.-D. (2020). Predicting wave heights for marine design by prioritizing extreme events in a global model. Renewable Energy, 156, pp. 1146--1157.

Hauser, D., Tourain, C., Hermozo, L., Alraddawi, D., Aouf, L., Chapron, B., Dalphinet, A., Delaye, L., Dalila, M., Dormy, E., Gouillon, F., Gressani, V., Grouazel, A., Guitton, G., Husson, R., Mironov, A., Mouche, A., Ollivier, A., Oruba, L., Piras, F., Suquet, R. R., Schippers, P., Tison, C., Tran, N. (2021). New Observations from the SWIM Radar On-Board CFOSAT: Instrument Validation and Ocean Wave Measurement Assessment. IEEE Transactions on Geoscience and Remote Sensing, 59(1), pp. 5-26. doi: 10.1109/TGRS.2020.2994372.

Haver, S. (1985). Wave climate off northern Norway. Applied Ocean Research, 7(2), pp. 85-92.

Haver, S., Winterstein, S. (2009). Environmental contour lines: A method for Estimating Long Term Extremes by a Short Term Analysis. Transactions of the Society of Naval Architects and Marine Engineers, 116, pp. 116-127.

Heffernan, J. E., Tawn, J. A. (2004). A conditional approach for multivariate extreme values. Journal of the Royal Statistical Society: Series B, 66(3), pp. 497-546.

Heidarzadeh, M., Šepić, J., Rabinovich, A., Allahyar, M., Soltanpour, A., Tavakoli, F. (2019). Meteorological Tsunami of 19 March 2017 in the Persian Gulf: Observations and

Analyses. Pure and Applied Geophysics, 177(3), 1231–1259. doi: 10.1007/s00024-019-02263-8.

Hengl, T., Nussbaum, M., Wright, M. N., Heuvelink, G. B., Graler, B. (2018). Random forest as a generic framework for predictive modelling of spatial and spatio-temporal variables. PeerJ, 6, e5518.

Henry, D., Thomas G.P. (2017). Prediction of the free-surface elevation for rotational water waves using the recovery of pressure at the bed. Phil. Trans. R. Soc. A 376. dx.doi.org/10.1098/rsta.2017.0102.

Heredia-Zavoni, E., Montes-Iturrizaga, R. (2019). Modelling directional environmental contours using three-dimensional vine copulas. Ocean Engineering, 187, 106102.

Herman, A., Cheng, S., Shen, H. H. (2019). Wave energy attenuation in fields of colliding ice floes − Part 2: A laboratory case study. The Cryosphere, 13(11), 2901–2914. doi: 10.5194/tc-13-2901-2019.

Hersbach, H. Bell, B., Berrisford, P., Hirahara, S., Horányi, A., Muñoz-Sabater, J., Nicolas, J., Peubey, C., Radu, R., Schepers, D., Simmons, A., Soci, C., Abdalla, S., Abellan, X., Balsamo, G., Bechtold, P., Biavati, G., Bidlot, J., Bonavita, M., De Chiara, G., Dahlgren, P., Dee, D., Diamantakis, M., Dragani, R., Flemming, J., Forbes, R., Fuentes, M., Geer, A., Haimberger, L., Healy, S., Hogan, R. J., Hólm, E., Janisková, M., Keeley, S., Laloyaux, P., Lopez, P., Lupu,C., Radnoti,G., de Rosnay, P., Iryna Rozum, Vamborg, F., Villaume, S., Thépaut, J.-N. (2020).The ERA5 global reanalysis. RMetS, vol. 146, iss. 730, Part A, pp. 1999-2049. doi: 10.1002/qj.3803.

Hildeman, A., Bolin, D., Rychlik, I. (2019a). Joint spatial modelling of significant wave height and wave period using the SPDE approach. arXiv:1906-00286v1, pp. 1-26.

Hildeman, A., Bolin, D., Rychlik, I. (2019b). Spatial modelling of significant wave height using stochastic partial differential equations. arXiv:1903.06296v1, pp. 1-22.

Hiles, C. E., Robertson, B., Buckham, B. J. (2019). Extreme value statistical methods and implications for coastal analyses. Estuarine, Coastal and Shelf Science, 223, pp. 50-60.

Holt, J., Hyder, P., Ashworth, M., Harle, J., Hewitt, H. T., Liu, H., New, A. L., Pickles, S., Porter, A., Popova, E., Allen, J. I., Siddorn, J., Wood R. (2017). Prospects for improving the representation of coastal and shelf seas in global ocean models. Geoscientific Model Development, 10(1), pp. 499–523. doi: 10.5194/gmd-10-499-2017.

Horn, J.-T., Bitner-Gregersen, E., Krokstad, J. R., Leira, B. J., Amdahl, J. (2018). A new combination of conditional environmental distributions. Applied Ocean research, 73, 17-26.

Horn, J.-T., Winterstein, S. R. (2018). Extreme response estimation of offshore wind turbines with an extended contour-line method. Journal of Physics: Conference Series, 1104, 012031.

Hsu, T.W., Lan, Y.J., Lin, Y.S. (2018). Extended wind wave model (WWM) incorporating the effect of submerged porous media with high permeability. Coastal Engineering 140, pp. 87-99. doi: 10.1016/j.coastaleng.2018.06.003.

Hu, H., van der Westhuysen, A. J., Chu, P., Fujisaki-Manome, A. (2021). Predicting Lake Erie wave heights and periods using XGBoost and LSTM. J. Ocean Modelling, 164, 101832. doi: 10.1016/j.ocemod.2021.101832.

Hu, J., Wang, J., Xiao, L. (2017). A hybrid approach based on the Gaussian process with t-observation model for short-term wind speed forecasts. Renewable Energy. Elsevier Ltd, 114, pp. 670–685. doi: 10.1016/j.renene.2017.05.093.

Huang, L., Ren, K., Li, M., Tuković, Ž., Cardiff, P., Thomas, G. (2019). Fluid-structure interaction of a large ice sheet in waves, Ocean Engineering, Volume 182, 102-111, ISSN 0029-8018. doi: 10.1016/j.oceaneng.2019.04.015.

Huang, L., Tuhkuri, J., Igrec, B., Li, M., Stagonas, D., Toffoli, A., Cardiff, P., Thomas, G. (2020). Ship resistance when operating in floating ice floes: A combined CFD&DEM approach. Marine Structures, 74, 102817. doi: 10.1016/j.marstruc.2020.102817.

Huang, W., Dong, S. (2019). Probability distribution of wave periods in combined sea states with finite mixture models. Applied Ocean Research, 92, 101938.

Huang, W., Dong, S. (2021). Joint distribution of significant wave height and zero-up- crossing wave period using mixture copula method. Ocean Engineering, 219, 108305.

Huang, W., Tao, S., Bai, Q., Dong, S. (2018a). Bivariate distribution modelling for wave height and period in Jiaozhou bay. Proc. OMAE 2018, 77395. Madrid: ASME. doi:10.1115/OMAE2018-77395.

Huang, Z. C., Yeh, C. Y., Tseng, K. H., Hsu, W. Y. (2018b). A UAV-RTK lidar system for wave and tide measurements in coastal zones. Journal of Atmospheric and Oceanic Technology, 35(8), pp. 1557-1570. doi: 10.1175/JTECH-D-17-0199.1.

Huang, Z., Zhang, Y. (2018). Semi-empirical single realization and ensemble crest distributions of long-crest nonlinear waves. Proc. of ASME 37th Int. Conf. on Ocean, Offshore and Arctic Eng. (OMAE), 78192. doi: 10.1115/OMAE2018-78192.

Hunke, E., Allard, R., Blain, P., Blockley, E., Feltham, D., Fichefet, T., Garric, G., Grumbine, R., Lemieux, J.-F., Rasmussen, T., Ribergaard, M., Roberts, A., Schweiger, A., Tietsche, S., Tremblay, B., Vancoppenolle, M., Zhang, J. (2020). Should Sea-Ice Modelling Tools Designed for Climate Research Be Used for Short-Term Forecasting? Current Climate Change Reports, 6(4), pp. 121–136. doi: 10.1007/s40641-020-00162-y.

Huseby, A. B., Vanem, E., Natvig, B. (2015). Alternative environmental contours for structural reliability analysis. Structural Safety, 54, pp. 32-45.

Hutchings, N., Long, D. G. (2019). Improved Ultrahigh-Resolution Wind Retrieval for RapidScat. IEEE Transactions on Geoscience and Remote Sensing, 57(6), pp. 3370-3379. doi: 10.1109/TGRS.2018.2884128.

Hutter, N., Losch, M., Menemenlis, D. (2018). Scaling Properties of Arctic Sea Ice Deformation in a High-Resolution Viscous-Plastic Sea Ice Model and in Satellite Observations. Journal of Geophysical Research: Oceans, 123(1), pp. 672-687. doi: 10.1002/2017JC013119.

Hutter, N., Zampieri, L., Losch, M. (2019). Leads and ridges in Arctic sea ice from RGPS data and a new tracking algorithm. The Cryosphere, 13(2). doi: 10.5194/tc-13-627-2019.

IACS (2001). Recommendations No.34, Standard Wave Data. Int. Ass. Classification Societies.

Iafrati, A., De Vita, F., Verzicco, R. (201). Effects of the wind on the breaking of modulated wave trains. European Journal of Mechanics - B/Fluids, v.73, pp. 6-23.

Iliescu, D., Murdza, A., Schulson, E. M., Renshaw, C. E. (2017). Strengthening ice through cyclic loading. Journal of Glaciology, 63(240). doi: 10.1017/jog.2017.32.

Integrated Ocean Observing System. (2019). Manual for Real-Time Quality Control of In-Situ Surface Wave Data: A Guide to Quality Control and Quality Assurance of In-Situ Surface Wave Observations. V. 2.1, National Oceanic and Atmospheric Administration. https://ioos.noaa.gov/ioos-in-action/wave-data/.

Iqbal, K., Zhang, M., Piao, S., He, G. (2019). Gradual but Persistent Quest for the Ocean Observation by Employing Multifarious Sensing Gadgets: A Preview. Proc. of OCEANS 2019 Conference. doi: 10.1109/OCEANSE.2019.8867397.

ITTC (2017). Final report and recommendations of the seakeeping committee. 28th Int. Towing Tank Conf., Volume I.

Jacobi, G. (2020). The application of particle image velocimetry for the analysis of high-speed craft hydrodynamics. PhD thesis Delft University of Technology, Delft, The Netherlands. doi: 10.4233/uuid:12a7e93e-34f1-41b5-864f-156ac0f60d30.

Jager, W., Morales Napoles, O. (2017). A vine-copula Model for Time Series of Significant Wave Heights and Mean Zero-Crossing Periods in the North Sea. ASCE-ASME Journal of Risk and Uncertainty in Engineering Systems - A, 3(4), pp. 1-25.

Jager, W., Nagler, T., Czado, C., McCall, R. (2019). A statistical simulation method for joint time-series of non-stationary hourly wave parameters. Coastal Engineering, 146, pp. 14-31.

Jagtap, R., Gedam, V., Kale, M. M. (2019). Generalized extreme value model with cyclic covariate structure for analysis of non-stationary hydrometeorological extremes. Journal of Earth System Science, 0014.

James, S. C., Zhang, Y., O'Donncha, F. (2018). A machine learning framework to forecast wave conditions. Coastal Engineering. Elsevier B.V., 137, pp. 1–10. doi: 10.1016/j.coastaleng.2018.03.004.

Jane, R., Dalla Valle, L., Simmonds, D., Raby, A. (2016). A copula-based approach for the estimation of wave height records through spatial correlation. Coastal Engineering, 117, pp. 1-18.

Jansen, R. W., Raj, R. G., Rosenberg, L., Sletten, M. A. (2018). Practical Multichannel SAR Imaging in the Maritime Environment. IEEE Transactions on Geoscience and Remote Sensing, 56(7), pp. 4025-4036. doi: 10.1109/TGRS.2018.2820911.

Janssen, P. A. E. M, Bidlot, J.-R. (2021). On the consequences of nonlinearity and gravity-capillary waves on wind-wave interaction. Technical Memorandum No. 882, European Centre for Medium range Weather Forecast, 42 p.

Jiang, H., Wu, Y., Lyu, K., Wang, H. (2019). Ocean Data Anomaly Detection Algorithm Based on Improved k-medoids. 2019 Eleventh International Conference on Advanced Computational Intelligence (ICACI). IEEE, pp. 196–201. doi: 10.1109/icaci.2019.8778515.

Jiang, M., Xu, K., Liu, Y. (2018). Calibration and validation of reprocessed HY-2A altimeter wave height measurements using data from Buoys, Jason-2, Cryosat-2, and SARAL/AltiKa. Journal of Atmospheric and Oceanic Technology, 35(6), pp. 1331-1352. doi: 10.1175/JTECH-D-17-0151.1.

Jin, R., Guo, Q., Chen, S., Geng, B. (2021). Experimental study on a new riser in large flume under the influence of wave and current. IOP Conference Series: Earth and Environmental Science, 621. doi: 10.1088/1755-1315/621/1/012153.

Jing, C., Niu, X., Duan, C., Lu, F., Di, G., Yang, X. (2019). Sea Surface Wind Speed Retrieval from the First Chinese GNSS-R Mission: Technique and Preliminary Results. Remote Sensing, 11(24). doi: 10.3390/rs11243013.

Johannessen, T. B. (2020). Estimating Wave Induced Kinematics Underneath Measured Time Histories of Surface Elevation. Proc. of ASME 2020 39th International Conference on Ocean, Offshore and Arctic Engineering (OMAE), 18727, V06BT06A061, 7 p. doi: 10.1115/OMAE2020-18727.

Johannessen, T. B., Lande, Ø. (2018). Long Term Analysis of Steep and Breaking Wave Properties by Event Matching. Proc. of ASME 37th International Conference on Ocean, Offshore and Arctic Engineering (OMAE), 78283, V003T02A040, 8 pages. doi: 10.1115/OMAE2018-78283.

Johnson, R. A., Wehrly, T. E. (1978). Some Angular-Linear Distributions and Related Regression Models. Journal of the American Statistical Association, 73(363), pp. 602-606.

Jolliff, J. K., Kindle, J. C., Shulman, I., Penta, B., Friedrichs, M. A. M., Helber, R., Arnone, R. A. (2009) 'Summary diagrams for coupled hydrodynamic-ecosystem model skill assessment. J Mar Syst, 76, pp. 64-82, doi: 10.1016/j.jmarsys.2008.05.014/

Jonathan, P., Ewans, K. (2013). Statistical modelling of extreme ocean environments for marine design: a review. Ocean Engineering, 62, pp. 91-109.

Jonathan, P., Randell, D., Wadsworth, J., Tawn, J. (2021). Uncertainties in return values from extreme value analysis of peaks over threshold using the generalised Pareto distribution. Ocean Engineering, 220, 107725.

Jones, M., Hansen, H. F., Zeeberg, A. R., Randell, D., Jonathan, P. (2018). Uncertainty quantification in estimation of extreme environments. Coastal Engineering, 141, pp. 36-51.

Jones, M., Randell, D., Ewans, K., Jonathan, P. (2016). Statistics of extreme ocean environments: Non-stationary inference for directionality and other covariate effects. Ocean Engineering, 119, pp. 40-56.

Jourdier, B. (2020). Evaluation of ERA5, MERRA-2, COSMO-REA6, NEWA and AROME to simulate wind power production over France. Adv. Sci. Res., 17, pp. 63-77. doi: 10.5194/asr-17-63-2020.

Karmpadakis, I., Swan, C., Christou, M. (2019). Laboratory investigation of crest height statistics in intermediate water depths. Proceedings of the Royal Society A, 475(2229), 20190183: pp. 1-24.

Katalinic, M., Parunov, J. (2020). Uncertainties of Estimating Extreme Significant Wave Height for Engineering Applications Depending on the Approach and Fitting Technique - Adriatic Sea Case Study. Journal of Marine Science and Engineering, 8, 259: pp. 1-18.

Kawamura, K., Hashimoto, H., Matsuda, A., Terada, D. (2016). SPH simulation of ship behaviour in severe water-shipping situations. Ocean Engineering, 120, pp.220-229. doi: 10.1016/j.oceaneng.2016.04.026.

Kellner, L., Stender, M., Von Bock Und Polach, R. U. F., Herrnring, H., Ehlers, S., Hoffmann, N., Høyland, K. V. (2019). Establishing a common database of ice experiments and using machine learning to understand and predict ice behaviour. Cold Regions Science and Technology. Elsevier. doi: 10.1016/J.COLDREGIONS.2019.02.007.

Khait, A., Shemer, L. (2019). Nonlinear Wave Generation by a Wavemaker in Deep to Intermediate Water Depth. Ocean Engineering, 182, pp. 222-234.
doi: 10.1016/j.oceaneng.2019.04.065.

Kirezci, C., Babanin, A. V., Chalikov, D. V. (2021a). Probabilistic assessment of rogue wave occurrence in directional wave fields. Ocean Dynamics, accepted on September 17, 2021

Kirezci, C., Babanin, A. V., Chalikov, D. V. (2021b). Modelling rogue waves in 1D wave trains with the JONSWAP spectrum, by means of the High Order Spectral Method and a fully nonlinear numerical model. Ocean Engineering, 231, 21 p.,
doi: 10.1016/j.oceaneng.2021.108717.

Klahn, M., Madsen, P., Fuhrman, D.R. (2021). On the statistical properties of surface elevation, velocities and accelerations in multi-directional irregular water waves. Journal of Fluid Mechanics, vol. 910, A23. doi:10.1017/jfm.2020.968.

Klein, M., Dudek, M., Clauss, G. F., Ehlers, S., Behrendt, J., Hoffmann, N., Onorato, M. (2020). On the deterministic prediction of water waves. Fluids, 5(1), 9. 19 p. doi: 10.3390/fluids5010009.

Kokorina, A., Slunyaev, A. (2019). Lifetimes of rogue wave events in direct numerical simulations of deep-water irregular sea waves. Fluids, 4(2), 70. 16 p. doi: 10.3390/fluids4020070.

Kolari, K. (2017). A complete three-dimensional continuum model of wing-crack growth in granular brittle solids. International Journal of Solids and Structures, vol. 115-116, pp. 27-42. doi: 10.1016/j.ijsolstr.2017.02.012.

Kolari, K. (2019). Modelling Splitting and Spalling of Columnar Ice Compressed Biaxially: The Role of Crack Nucleation. Journal of Geophysical Research: Solid Earth, 124(4), pp. 3271-3287. doi: 10.1029/2018JB017032.

Komarov, A. S., Buehner, M. (2018). Adaptive Probability Thresholding in Automated Ice and Open Water Detection from RADARSAT-2 Images. IEEE Geoscience and Remote Sensing Letters, 15(4), pp. 552-556. doi: 10.1109/LGRS.2018.2806189.

Kozlov, I., Zubkova, E. (2019). Spaceborne SAR observations of internal solitary waves in the Chukchi and Beaufort Seas. Conference: Remote Sensing of the Ocean, Sea Ice, Coastal Waters, and Large Water Regions 2019, 13. doi: 10.1117/12.2532604.

Krumpen, T., Birrien, F., Kauker, F., Rackow, T., von Albedyll, L., Angelopoulos, M., Belter, H. J., Bessonov, V., Damm, E., Dethloff, K., Haapala, J., Haas, C., Harris, C., Hendricks, S., Hoelemann, J., Hoppmann, M., Kaleschke, L., Karcher, M., Kolabutin, N., Lei, R., Lenz, J., Morgenstern, A., Nicolaus, M., Nixdorf, U., Petrovsky, T., Rabe, B., Rabenstein, L., Rex, M., Ricker, R., Rohde, J., Shimanchuk, E., Singha, S., Smolyanitsky, S., Sokolov, V., Stanton, T., Timofeeva, A., Tsamados, M., Watkins, D. (2020). The MOSAiC ice floe: sediment-laden survivor from the Siberian shelf. The Cryosphere, 14(7). doi: 10.5194/tc-14-2173-2020.

Kukulka, T., Veron, F. (2019). Lagrangian Investigation of Wave-Driven Turbulence in the Ocean Surface Boundary Layer. Journal of Physical Oceanography, 49, pp. 409-429, doi: 10.1175/JPO-D-18-0081.1.

Kumar, A. Sridevi, Ch., Durai, V.R., Singh, K. K., Mukhopadhyay, P., Chattopadhyay, N. (2019). MOS guidance using a neural network for the rainfall forecast over India. J. Earth Syst. Sci, 128, p. 130. doi: 10.1007/s12040-019-1149-y.

Kumar, N. K., Savitha, R., Al Mamun, A. (2017). Regional ocean wave height prediction using sequential learning neural networks. Ocean Engineering. Elsevier Ltd, 129, pp. 605–612. doi: 10.1016/j.oceaneng.2016.10.033.

Kumar, N. K., Savitha, R., Al Mamun, A. (2018a). Ocean wave characteristics prediction and its load estimation on marine structures: A transfer learning approach. Marine Structures, 61, pp. 202-219.

Kumar, N. K., Savitha, R., Al Mamun, A. (2018b). Ocean wave height prediction using ensemble of Extreme Learning Machine. Neurocomputing, 277, pp. 12-20. doi: 10.1016/j.neucom.2017.03.092

Kumar, N. K., Savitha, R., Al Mamun, A. (2018d). Ocean wave height prediction using ensemble of Extreme Learning Machine. Neurocomputing. Elsevier B.V., 277, pp. 12–20. doi: 10.1016/j.neucom.2017.03.092.

Kumar, V. S., Joseph, J., Amrutha, M. M., Jena, B. K., Sivakholundu, K. M., Dubhashi, K. K. (2018c). Seasonal and interannual changes of significant wave height in shelf seas around India during 1998–2012 based on wave hindcast. Ocean Engineering, 151, pp. 127-140.

Kurt, A., Rezazadeh, H., Senol. M., Neirameh, A., Tasbozan, O., Eslami, M., Mirzazadeh, M. (2019). Two effective approaches for solving fractional generalized Hirota-Satsuma coupled KdV system arising in interaction of long waves. Journal of Ocean Engineering and Science, 4, pp. 24–32.

Kutupoğlu, V., Çakmak, R.E., Akpınar, A., van Vledder, G.P. (2018). Setup and evaluation of a SWAN wind wave model for the Sea of Marmara. Ocean Engineering 165, pp. 450-464. doi: 10.1016/j.oceaneng.2018.07.053.

Kvingedal, B., Bruserud, K., Nygaard, E. (2018). Individual wave height and wave crest distributions based on field measurements from the northern North Sea. Ocean Dynamics, 68, pp. 1727-1738.

Laface, V., Magnusson, A. K., Bitner-Gregersen, E. M., Reistad, M., Romolo, A., Arena, F. (2018). Equivalent Storm Model for Long-Term Statistics of Sea Storms Off Norway. Proc. OMAE 2018, 78747. Madrid: ASME. doi:10.1115/OMAE2018-78747.

Lande, Ø. and Johannessen, T. B. (2018). Propagation of Steep and Breaking Short-Crested Waves: A Comparison of CFD Codes. Proc. of ASME 2018 37th International Conference on Ocean, Offshore and Arctic Engineering (OMAE). doi: 10.1115/OMAE2018-78288.

Lavidas, G., Venugopal, V. (2018). Application of numerical wave models at European coastlines: A review. Renewable and Sustainable Energy Reviews 92, pp. 489-500. doi: 10.1016/j.rser.2018.04.112.

Law, Y. Z., Santo, H., Lim, K.Y., Chan, E. S. (2020). Deterministic wave prediction for unidirectional sea-states in real-time using Artificial Neural Network. Ocean Engineering. Elsevier Ltd, 195, p. 106722. doi: 10.1016/j.oceaneng.2019.106722.

Law-Chune, S. Aouf, L., Dalphinet, A., Levier, B., Drillet Y., Drevillon M. (2021). WAVERYS: a CMEMS global wave reanalysis during the altimetry period. Ocean Dynamics, vol. 71, pp. 357-378. doi: 10.1007/s10236-020-01433-w.

Lemos, G., Semedo, A., Dobrynin, M, Behrens, A., Staneva, J., Bidlot, J. R., Miranda, P. M. A. (2019). Mid-twenty-first century global wave climate projections: Results from a dynamic CMIP5 based ensemble. Global and Planetary Change.
doi: 10.1016/j.gloplacha.2018.09.011.

Lemström, I., Polojärvi, A., Tuhkuri, J. (2020). Numerical experiments on ice-structure interaction in shallow water. Cold Regions Science and Technology, 176, 103088. doi: 10.1016/j.coldregions.2020.103088.

Li, F., Ren, G., Lee, J. (2019a). Multi-step wind speed prediction based on turbulence intensity and hybrid deep neural networks. Energy Conversion and Management. Elsevier Ltd, 186, pp. 306–322. doi: 10.1016/j.enconman.2019.02.045.

Li, F., Zhou, J., Liu, C. (2018a). Statistical modelling of extreme storms using copulas: A comparison study. Coastal Engineering, 142, pp. 52-61.

Li, J., Babanin, A. V., Liu, Q., Voermans, J., Heil, P., Tang, Y. (2021a). Effects of wave-induced sea ice break-up and mixing in a high-resolution coupled ice-ocean model. Journal of Marine Science and Engineering, 9, 365, 23 p, doi: 10.3390/jmse9040365.

Li, J., Ma, Y., Liu, Q., Zhang, W., Guan, C. (2019b). Growth of wave height with retreating ice cover in the Arctic. Cold Regions Science and Technology, 164, 102790. doi: 10.1016/j.coldregions.2019.102790.

Li, L., Xiao, Y., Zhou, H., Xing, F., Song, L. (2018b). Turbulent wind characteristics in typhoon Hagupit based on field measurements. International Journal of Distributed Sensor Networks, 14(10). doi: 10.1177/1550147718805934.

Li, M., Zhang, L., Wu, X., Yue, X., Emery, W. J., Yi, X., Liu, J., Yang, G. (2018c). Ocean surface current extraction scheme with high-frequency distributed hybrid sky-surface wave radar system. IEEE Transactions on Geoscience and Remote Sensing, 56(8), pp. 4678-4690. doi: 10.1109/TGRS.2018.2834938.

Li, S., Babanin, A. V., Qiao, F., Dai, D., Jiang, S., Guan, C. (2021b). Laboratory experiments on CO_2 gas exchange with wave breaking. Journal of Physical Oceanography, 51, pp. 3105-3116, doi:10.1175/JPO-D-20-0272.1.

Li, S., Guan, S., Hou, Y., Liu, Y., Bi, F. (2018d). Evaluation and adjustment of altimeter measurement and numerical hindcast in wave height trend estimation in China's coastal seas. International Journal of Applied Earth Observation and Geoinformation 67, pp. 161-172. doi: 10.1016/j.jag.2018.01.007.

Li, X., Zhang, W. (2020). Long-term assessment of a floating offshore wind turbine under environmental conditions with multivariate dependence structures. Renewable Energy, 147, pp. 764-775.

Li, Y., Chong, J., Sun, K., Zhao, Y., Yang, X. (2021d). Measuring Ocean Surface Current in the Kuroshio Region Using Gaofen-3 SAR Data. Applied Sciences, 11(16), 7656. doi: 10.3390/app11167656.

Li, Z., Bouscasse, B., Ducrozet, G., Gentaz, L., Le Touzé, D., Ferrant, P. (2021c). Spectral Wave Explicit Navier-Stokes Equations for wave-structure interactions using two-phase Computational Fluid Dynamics solvers. Ocean Engineering, 221, 108513, 50 p. doi: 10.1016/j.oceaneng.2020.108513.

Liang, B., Shao, Z., Li, H., Shao, M., Lee, D. (2019). An automated threshold selection method based on the characteristics of extrapolated significant wave heights. Coastal Engineering, 144, pp. 22-32.

Liang, S., Sun, Z., Chang, Y., Shi, Y. (2020). Evolution characteristics and quantization of wave period variation for breaking waves. Journal of Hydrodynamics, 32(2), 361–374. doi: 10.1007/s42241-020-0017-1.

Liao, B., Ma, Y., Ma, X., Dong, G. (2018). Experimental study on the evolution of Peregrine breather with uniform-depth adverse currents. Physical Review E, 97(053102). doi: 10.1103/ PhysRevE.97.053102.

Liberzon, D., Vreme, A., Knobler, S., Bentwich, I. (2019). Detection of Breaking Waves in Single Wave Gauge Records of Surface Elevation Fluctuations. Journal of Oceanic and Atmospheric Technology, 36, pp. 1863-1879.

Lilja, V. P., Polojärvi, A., Tuhkuri, J., Paavilainen, J. (2019a). A free, square, point-loaded ice sheet: A finite element-discrete element approach. Marine Structures, 68, 102644. doi: 10.1016/j.marstruc.2019.102644.

Lilja, V. P., Polojärvi, A., Tuhkuri, J., Paavilainen, J. (2019b). Effective material properties of a finite element-discrete element model of an ice sheet. Computers and Structures, 224, 106107. doi: 10.1016/j.compstruc.2019.106107.

Lilja, V. P., Polojärvi, A., Tuhkuri, J., Paavilainen, J. (2021). Finite-discrete element modelling of sea ice sheet fracture. International Journal of Solids and Structures, vol. 217–218, pp. 228-258. doi: 10.1016/j.ijsolstr.2020.11.028.

Lima, V. V., Avilez-Valente, P., Baptista, M. A. V., Miranda, J. M. (2019). Generation of N-waves in laboratory. Coastal Engineering, 148, pp. 1-18. doi: 10.1016/j.coastaleng.2019.02.012.

Lin, S. Y., Chiang, C. C., Li, J. B., Hung, Z. S., Chao, K.-M. (2018). Dynamic fine-tuning stacked auto-encoder neural network for weather forecast. Future Generation Computer Systems. Elsevier B.V., 89, pp. 446–454. doi: 10.1016/j.future.2018.06.052.

Lin, S., Sheng, J. (2017). Assessing the performance of wave breaking parameterizations in shallow waters in spectral wave models. Ocean Modelling 120, pp. 41-59. doi: 10.1016/j.ocemod.2017.10.009.

Lin, Y., Dong, S. (2019). Wave energy assessment based on trivariate distribution of significant wave height, mean period and direction. Applied Ocean Research, 87, pp. 47-63.

Lin, Y., Dong, S., Tao, S. (2020). Modelling long-term joint distribution of significant wave height and mean zero-crossing wave period using a copula mixture. Ocean Engineering, 197, 106856.

Linow, S., Dierking, W. (2017). Object-Based Detection of Linear Kinematic Features in Sea Ice. Remote Sensing, 9(5). doi: 10.3390/rs9050493.

Lin-Ye, J., Garda-Leon, M., Gracia, V., Ortego, M., Lionello, P., Sanchez-Arcilla, A. (2017). Multivariate statistical modelling of future marine storms. Applied Ocean Research, 65, pp. 192-205.

Lipa, B., Barrick, D., Whelan, C. (2019).A Quality Control Method for Broad-Beam HF Radar Current Velocity Measurements. J. Mar. Sci. Eng. 2019, 7(4), 112; doi: /10.3390/jmse7040112.

Liu, G., Chen, B., Jiang, S., Fu, H., Wang, L., Jiang, Wei. (2019a). Double Entropy Joint Distribution Function and Its Application in Calculation of Design Wave Height. Entropy, 21, 64: pp. 1-13.

Liu, G., Chen, B., Wang, L., Zhang, S., Zhang, K., Lei, X. (2019b). Wave height statistical characteristics analysis. Journal of Oceanology and Limnology, 37(2), pp. 448-460.

Liu, H., Mi, X. W., Li, Y. F. (2018). Wind speed forecasting method based on deep learning strategy using empirical wavelet transform, long short term memory neural network and Elman neural network. Energy Conversion and Management. Elsevier Ltd, 156, pp. 498–514. doi: 10.1016/j.enconman.2017.11.053.

Liu, Q., Babanin, A., Fan, Y., Zieger, S., Guan, C., Moon, I.-J. (2017). Numerical simulations of ocean surface waves under hurricane conditions: Assessment of existing model performance. Ocean Modelling 118(6), pp. 73-93. doi: 10.1016/j.ocemod.2017.08.005.

Liu, Q., Rogers, W.E., Babanin, A.V., Young, I.R., Romero, L., Zieger, S., Qiao, F., Guan, C. (2019d). Observation-Based Source Terms in the Third-Generation Wave Model WAVEWATCH III: Updates and Verification. Journal of Physical Oceanography 49 (2), pp. 489-517. doi: 10.1175/JPO-D-18-0137.1.

Liu, Q., Rogers, W. E., Babanin, A. V., Li, J., Guan, C. (2020). Spectral modelling of ice-induced wave decay. Journal of Physical Oceanography, 50(6), pp. 1583-1604, doi: 10.1175/JPO-D-19-0187.1

Liu, Q., Babanin, A.V., Rogers, W. E., Zieger, S., Young, I. R., Bidlot, J.-R., Durrant, T., Ewans, K., Guan, C., Kirezci, C., Lemos, G., MacHutchon, K., Moon, I.-J., Rapizo, H., Ribal, A., Semedo, A., Wang, J. (2021). Global wave hindcasts using the observation-based source terms: description and validation. Journal of Advances in Modelling Earth Systems (JAMES), vol 13(8), 38 p. doi: 10.1029/2021MS002493.

Liu, T., Zhang, Y., Qi, L., Dong, J., Lv, M., Wen, Q. (2019c). WaveNet: learning to predict wave height and period from accelerometer data using convolutional neural network. IOP Conference series: Earth and Environmental Science, 369, 012001: pp. 1-8.

Lobeto, H., Menendez, M., Losada, I. J. (2021). Future behaviour of wind wave extremes due to climate change. Scientific Reports, 11(1), pp. 1-13. doi: 10.1038/s41598-021-86524-4.

Lorente, P., Lin-Ye, J., García-León, M., Reyes, E., Fernandes, M., Sotillo, M. G., Espino, M., Ruiz, M. I., Gracia, V., Perez, S., Aznar, R., Alonso-Martirena, A., Álvarez-Fanjul, E. (2021). On the Performance of High Frequency Radar in the Western Mediterranean During the Record-Breaking Storm Gloria. Frontiers in Marine Science, 8. doi: 10.3389/fmars.2021.645762.

Lu, Z., Zhou, R., Yuan, Y., Wu, X. (2018). The research on ocean current inversion algorithm based on X-band radar. ICIC Express Letters, 12(2), pp. 135-143. doi: 10.24507/icicel.12.02.135.

Lucas, C., Guedes Soares, C. (2015). Bivariate distributions of significant wave height and mean wave period of combined sea states. Ocean Engineering, 106, pp. 341-353.

Lucas, C., Muraldeedharan, G., Guedes Soares, C. (2020). Assessment of extreme waves in the North Atlantic Ocean by regional frequency analysis. Applied Ocean Research, 100, 102165.

Lucas, C., Muraleedharan, G., Guedes Soares, C. (2017). Regional frequency analysis of extreme waves in a coastal area. Coastal Engineering, 126, pp. 81-95.

Lucas, C., Muraleedharan, G., Guedes Soares, C. (2019a). Assessment of the uncertainty of estimated extreme quantiles by regional frequency analysis. Ocean Engineering, 190, 106347.

Lucas, N.S., Grant, A. L. M., Rippeth, T. P., Polton, J. A., Palmer, M. R., Brannigan, L., Belcher, S. E. (2019b). Evolution of Oceanic Near-Surface Stratification in Response to an Autumn Storm. Journal of Physical Oceanography, 49, pp. 2961-2977.

Lucio-Eceiza, E. E., González-Rouco, J. F., Navarro, J., Beltrami, H. (2018a). Quality control of surface wind observations in Northeastern North America. Part I: Data management issues.

Journal of Atmospheric and Oceanic Technology, 35(1), pp. 163–182. doi: 10.1175/JTECH-D-16-0204.1.

Lucio-Eceiza, E. E., González-Rouco, J. F., Navarro, J., Beltrami, H., Conte, J. (2018b). Quality control of surface wind observations in northeastern North America. Part II: Measurement errors. Journal of Atmospheric and Oceanic Technology, 35(1), pp. 183–205. doi: 10.1175/JTECH-D-16-0205.1.

Lund, B., Graber, H. C., Persson, P. O. G., Smith, M., Doble, M., Thomson, J., Wadhams, P. (2018). Arctic Sea Ice Drift Measured by Shipboard Marine Radar. J. Geophys. Res. C: Oceans, 123(6), pp. 4298-4321.

Luo, Y. P., Fu, J. Y., Li, Q. S., Chan, P. W., He, Y. C. (2020). Observation of Typhoon Hato based on the 356-m high meteorological gradient tower at Shenzhen. Journal of Wind Engineering and Industrial Aerodynamics, 207. doi: 10.1016/j.jweia.2020.104408.

Luo, Y., Wang, D., Gamage, T. P., Zhou, F., Widanage, C. M., Liu, T. (2018). Wind and wave dataset for Matara, Sri Lanka. Earth System Science Data, 10(1), pp. 131-138. doi: 10.5194/essd-10-131-2018.

Lux, O., Lemmerz, C., Weiler, F., Marksteiner, U., Witschas, B., Rahm, S., Schäfler, A., Reitebuch, O. (2018). Airborne wind lidar observations over the North Atlantic in 2016 for the pre-launch validation of the satellite mission Aeolus. Atmospheric Measurement Techniques, 11(6), pp. 3297-3322. doi: 10.5194/amt-11-3297-2018.

Luxmoore, J. F., Ilic, S., Mori, N. (2019). On kurtosis and extreme waves in crossing directional seas: A laboratory experiment. Journal of Fluid Mechanics, 876, pp. 792-817. doi: 10.1017/jfm.2019.575.

Ma, H., Babanin, A. V., Qiao, F. (2020). Field observations of sea spray under Tropical Cyclone Olwyn. Ocean Dynamics, 70, pp. 1439-1448. doi: 10.1007/s10236-020-01408-x.

Ma, T., Wang, C., Wang, J., Cheng, J., Chen, X. (2019). Particle-swarm optimization of ensemble neural networks with negative correlation learning for forecasting short-term wind speed of wind farms in western China. Information Sciences. Elsevier Inc., 505, pp. 157–182. doi: 10.1016/j.ins.2019.07.074.

Mackay, E. B., Johanning, L. (2018a). A simple and robust method for calculating return periods of ocean waves. Proc. OMAE 2018, 78729. Madrid: ASME. doi:10.1115/OMAE2018-78729.

Mackay, E., de Hauteclocque, G., Vanem, E., Jonathan, P. (2021). The Effect of Serial Correlation in Environmental conditions for Estimates of Extreme Events. Ocean Engineering, Submitted.

Mackay, E., Johanning, L. (2018b). A generalised equivalent storm model for long-term statistics of ocean waves. Coastal Engineering, 140, pp. 411-428.

Mackay, E., Johanning, L. (2018c). Long-term distributions of individual wave and crest heights. Ocean Engineering, 165, pp. 164-183.

Mackay, E., Jonathan, P. (2020). Assessment of Return Value Estimates from Stationary and Non-Stationary Extreme Value Models. Ocean Engineering, submitted.

Mahjouri, S., Shabani, R., Badiei, P., Rezazadeh, G. (2020). A bottom mounted wavemaker in water wave flumes. Journal of Hydraulic Research, pp. 1-8. doi: 10.1080/00221686.2020.1818314.

Mahmoodi, K., Ghassemi, H. (2018). Outlier detection in ocean wave measurements by using unsupervised data mining methods. Polish Maritime Research, 25(1), pp. 44–50. doi: 10.2478/pomr-2018-0005.

Mahmoudof, S.M., Badiei, P., Siadatmousavi, S.M., Chegini, V. (2018). Spectral wave modelling in very shallow water at Southern Coast of Caspian Sea. Journal of Marine Science and Application 17 (1o), pp. 140-151. doi: 10.1007/s11804-018-0011-y.

Majda, A. J., Moore, M., Qi, D. (2019). Statistical dynamical model to predict extreme events and anomalous features in shallow water waves with abrupt depth change. Proceedings of the National Academy of Sciences of the United States of America, 116(10), 39823987.

Majda, A. J., Qi, D. (2019). Statistical Phase Transitions and Extreme Events in Shallow Water Waves with an Abrupt Depth Change. Journal of Statistical Physics, pp. 1-24. doi:10.1007/s10955-019-02465-3

Mak, B., Düz, B. (2019a). Ship as a wave buoy: estimating relative wave direction from in-service ship motion measurements using machine learning. Proc. of ASME 38th Int. Conf. on Ocean, Offshore and Arctic Eng. (OMAE), 96201. doi: 10.1115/OMAE2019-96201.

Mak, B., Düz, B. (2019b). Ship as a wave buoy: using simulated data to train neural networks for real time estimation of relative wave direction. Proc. of ASME 38th Int. Conf. on Ocean, Offshore and Arctic Eng. (OMAE), 96225. doi: 10.1115/OMAE2019-96225.

Malliouri, D. I., Memos, C. D., Tampalis, N. D., Soukissian, T. H., Tsoukala, V. K. (2019). Integrating short- and long-term statistics for short-crested waves in deep and intermediate waters. Applied Ocean Research, 82, pp. 346-361.

Mantovani, C., Corgnati, L., Horstmann, J., Rubio, A., Reyes, E., Quentin, C., Cosoli, S., Asensio, J. L., Mader, J., Griffa, A. (2020). Best Practices on High Frequency Radar Deployment and Operation for Ocean Current Measurement. Frontiers in Marine Science, 7, pp. 1-21. doi: 10.3389/fmars.2020.00210.

Manuel, L., Nguyen, P. T., Canning, J., Coe, R. G., Eckert-Gallup, A. C., Martin, N. (2018). Alternative approaches to develop environmental contours from metocean data. Journal of Ocean Engineering and Marine Energy, 4, pp. 293-310.

Mas-Soler, J., Simos, A. N., Tannuri, E. A. (2018). Estimating on-site wave spectra from the motions of a semi-submersible platform: An assessment based on model scale results. Ocean Engineering, 153. doi: 10.1016/j.oceaneng.2018.01.069.

Mazas, F., Hamm, L. (2017). An event-based approach for extreme joint probabilities of waves and sea levels. Coastal Engineering, 122, pp. 44-59.

McAllister, M. L., Draycott, S., Adcock, T. A. A., Taylor, P. H., Van Den Bremer, T. S. (2019). Laboratory recreation of the Draupner wave and the role of breaking in crossing seas. Journal of Fluid Mechanics, 860, pp. 767-786. doi: 10.1017/jfm.2018.886.

McAllister, M. L., van den Bremer, T. S. (2019). Lagrangian Measurement of Steep Directionally Spread Ocean Waves: Second-Order Motion of a Wave-Following Measurement Buoy. Journal of Physical Oceanography, 49(12). doi: 10.1175/JPO-D-19-0170.1.

McAllister, M. L., van den Bremer, T. S. (2020). Experimental Study of the Statistical Properties of Directionally Spread Ocean Waves Measured by Buoys. Journal of Physical Oceanography, 50(2). doi: 10.1175/JPO-D-19-0228.1.

McCann, D. L., Bell, P. S. (2018). A Simple Offset "calibration" Method for the Accurate Geographic Registration of Ship-Borne X-Band Radar Intensity Imagery. IEEE Access, 6, pp. 13939-13948. doi: 10.1109/ACCESS.2018.2814081.

Mendes, S., Scotti, A., Stansell, P. (2021). On the physical constraints for the exceeding probability of deep water waves. Applied Ocean Research, 108, 102402.

Mentaschi, L., Besio, G., Cassola, F., Mazzino, A., (2013). Problems in RMSE-based wave model validations. Ocean Modell., 72, pp. 53-58, doi: 10.1016/j.ocemod.2013.08.003.

Mentaschi, L., Kakoulaki, G., Vousdoukas, M., Voukouvalas, E., Feyen, L., Besio, G. (2018). Parameterizing unresolved obstacles with source terms in wave modeling: A real-world application. Ocean Modelling 126, pp. 77-84. doi: 10.1016/j.ocemod.2018.04.003.

Meucci, A., Young, I. R., Hemer, M., Kirezci, E., Ranasinghe, R. (2020). Projected 21st century changes in extreme wind-wave events. Science Advances, 6(24), pp. 1–10. doi: 10.1126/sciadv.aaz7295.

Meylan, M. H., Bennetts, L. G., Mosig, J. E. M., Rogers, W. E., Doble, M. J., Peter, M. A. (2018). Dispersion Relations, Power Laws, and Energy Loss for Waves in the Marginal Ice Zone. Journal of Geophysical Research: Oceans, 123(5), 3322–3335. doi: doi: 10.1002/2018JC013776.

Migliaccio, M., Huang, L., Buono, A. (2019). SAR Speckle Dependence on Ocean. IEEE Transactions on Geoscience and Remote Sensing, 57(8), pp. 5447-5455. doi: 10.1109/TGRS.2019.2899491.

Miles, J.W. (1957). On the generation of surface waves by shear flows. J. Fluid Mech. 3, pp. 185-204.

Miles, J.W. (1965). A note on the interaction between surface waves and wind profiles. J. Fluid Mech., 22, pp. 823-827.

Minola, L., Zhang, F., Azorin-Molina, C., Safaei Pirooz, A. A., Flay, R. G. J., Hersbach, H., Chen, D. (2020). Near-surface mean and gust wind speeds in ERA5 across Sweden: towards an improved gust parametrization. Climate Dynamics, 55, pp. 887-907. doi: https://doi.org/10.1007/s00382-020-05302-6.

Miratsu, R., Fukui, T., Matsumoto, T., Zhu, T. (2019). Quantitative Evaluation of Ship Operational Effect in Actually Encountered Sea States. 38th Int. Conf. on Ocean, Offshore and Arctic Eng. (OMAE), Glasgow, Scotland, UK. doi: 10.1115/OMAE2019-95121.

Miratsu, R., Fukui, T., Matsumoto, T., Zhu, T. (2020). Study on Ship Operational Effect for Defining Design Values on Ship Motion and Loads in North Atlantic. Proc. of ASME 39th Int. Conf. on Ocean, Offshore and Arctic Eng. (OMAE), 18193. doi: 10.1115/OMAE2020-18193.

Miratsu, R., Sasmal, K., Kodaira, T., Fukui, T., Zhu, T., Waseda T. (2021). Evaluation of ship operational effect based on long-term encountered sea states using wave hindcast combined with storm avoidance. Submitted to Marine Structures Journal.

Mohamad, M. A., Sapsis, T. P. (2018). Sequential sampling strategy for extreme event statistics in nonlinear dynamical systems. Proceedings of the National Academy of Sciences of the United States of America, 115(44), pp. 11138-11143.

Molfetta, M. G., Bruno, M. F., Pratola, L., Rinaldi, A., Morea, A., Preziosa, G., Pasquali, D., di Risio, M., Mossa, M. (2020). A Stereoscopic System to Measure Water Waves in Laboratories. Remote Sensing, 12(14). doi: 10.3390/rs12142288.

Montes-Iturrizaga, R., Heredia-Zavoni, E. (2017). Assessment of uncertainty in environmental contours due to parametric uncertainty in models of the dependence structure between metocean variables. Applied Ocean Research, 64, pp. 86-104.

Montoya, R. D., Menendez, M., Osorio, A. F. (2018). Exploring changes in Caribbean hurricane-induced wave heights. Ocean Engineering, 163, pp. 126-135.

Morim, J., Hemer, M., Cartwright, N., Strauss, D., Andutta, F. (2018). On the concordance of 21st century wind-wave climate projections. Global and planetary change, 167, pp. 160-171.

Mucha, P. (2019). Fully-Coupled CFD-DEM for Simulations of Ships Advancing Through Brash Ice. Proc. of SNAME SMC 2019.

Mudronja, L., Matic, P., Katalinic, M. (2017). Data-Based Modelling of Significant Wave Height in the Adriatic Sea. Transactions on Maritime Sciences, 6(1), pp. 5-13.

Mukhtar, M. I., Mohammed, I., Mudassir, N., Bello, I. M., Yahaya, A. A. (2020). Evaluation of Wind Potential for the Generation of Electricity in Aliero, Kebbi State. Asian Journal of Research and Reviews in Physics, 1–7. doi: 10.9734/ajr2p/2020/v3i130110.

Muller, D., Czado, C. (2019). Dependence modelling in ultra high dimensions with the vine copulas and the Graphical Lasso. computational Statistics Data Analysis, 137, 211232.

Murdza, A., Marchenko, A., Schulson, E. M., Renshaw, C. E. (2021a). Cyclic strengthening of lake ice. Journal of Glaciology, 67(261). doi: 10.1017/jog.2020.86.

Murdza, A., Schulson, E. M., Renshaw, C. E. (2020). Strengthening of columnar-grained freshwater ice through cyclic flexural loading. Journal of Glaciology, 66(258). doi: 10.1017/jog.2020.31

Murdza, A., Schulson, E. M., Renshaw, C. E. (2021b). Behaviour of saline ice under cyclic flexural loading. The Cryosphere, 15(5). doi: 10.5194/tc-15-2415-2021.

Myrhaug, D. (2018). Some probabilistic properties of deep water wave steepness. Oceanologica, 60, pp. 187-192.

Myrhaug, D., Leira, B. J., Chai, W. (2020). Application of a sea surface roughness formula using joint statistics of significant wave height and spectral wave steepness. Journal of Ocean Engineering and Marine Energy, 6 (2020), pp. 91-97.

Naaijen, P. (2018). Deterministic Prediction of Waves and Wave Induced Vessel Motions. Future Telling by Using Nautical Radar as a Remote Wave Sensor. Doctoral thesis. doi: 10.4233/uuid:49bf7c26-e260-448a-b94a-5fcb038fa602.

Naaijen, P., van Oosten, K., Roozen, K., van 't Veer, R. (2018). Validation of a Deterministic Wave and Ship Motion Prediction System. Proc. of ASME 37th Int. Conf. on Ocean, Offshore and Arctic Eng. (OMAE), 78037. doi: 10.1115/OMAE2018-78037.

Nadai, A. (2019). Airborne Sar Observation of Wind Direction Dependence of Ocean Surface Backscattering. International Geoscience and Remote Sensing Symposium (IGARSS), pp. 8094-8097. doi: 10.1109/IGARSS.2019.8898107.

Naseef, T. M., Kumar, V. S. (2017). Variations in return value estimate of ocean surface waves - a study based on measured buoy data and ERA-Interim reanalysis data. Natural Hazards and Earth System Sciences, 17, pp. 1763-1778.

National Data Buoy Center. (2009). Handbook of Automated Data Quality Control Checks and Procedures' NDBC Technical Document 09-02. https://www.ndbc.noaa.gov/ NDBCHandbookofAutomatedDataQualityControl2009.pdf.

Navarro, W., Velez, J. C., Orfila, A., Lonin, S. (2019). A shadowing mitigation approach for sea state parameters estimation using X-band remotely sensing radar data in coastal areas. IEEE Transactions on Geoscience and Remote Sensing, 57(9), pp. 6292-6310. doi: 10.1109/TGRS.2019.2905104.

Nelsen, R. B. (2006). An Introduction to Copulas (2 ed.). New York: Springer-Verlag.

Nerantzaki, S. D., Papalexiou, S. M. (2019). Tails of extremes: Advancing a graphical method and harnessing big data to assess precipitation extremes. Advances in Water Resources, 134, 103448.

Nielsen, U. D. (2017). A concise account of techniques available for shipboard sea state estimation. Ocean Engineering, 129. doi: 10.1016/j.oceaneng.2016.11.035.

Nielsen, U. D., Brodtkorb, A. H., Sørensen, A. J. (2019). Sea state estimation using multiple ships simultaneously as sailing wave buoys. Applied Ocean Research, 83. doi: 10.1016/j.apor.2018.12.004.

Nielsen, U. D., Dietz, J. (2020). Ocean wave spectrum estimation using measured vessel motions from an in-service container ship. Marine Structures, 69. doi: 10.1016/j.marstruc.2019.102682.

Nikoo, M. R., Kerachian, R., Alizadeh, M. R. (2018). A fuzzy KNN-based model for significant wave height prediction in large lakes. Oceanologia, 60, pp. 153-168.

Nilsen, V., Engen, G., Johnsen, H. (2019). A novel approach to SAR ocean wind retrieval. IEEE Transactions on Geoscience and Remote Sensing, 57(9), pp. 6986-6995. doi: 10.1109/TGRS.2019.2909838.

Niroomandi, A., Ma, G., Ye, X., Lou, S., Xue, P. (2018). Extreme value analysis of wave climate in Chesapeake Bay. Ocean Engineering 159, pp. 22-36. doi: 10.1016/j.oceaneng.2018.03.094.

Niu, X., Ma, X., Ma, Y., Dong, G. (2020). Controlled extreme wave generation using an improved focusing method. Applied Ocean Research, 95, 102017. doi: 10.1016/j.apor.2019.102017.

Northrop, P. J., Attalides, N., Jonathan, P. (2017). Cross-validatory extreme value threshold selection and uncertainty with applications to ocean storm severity. Applied Statistics Series C, 66, pp. 93-120.

Novaković, V., Costas, J. J., Schreier, S., Kimmoun, O., Fernandes, A., Ezeta, R., Birvalski, M., Bogaert, H. (2020). Study of global wave repeatability in the new Multiphase Wave Lab (MWL). 30th ISOPE Conference.

O'Connor, D., West, B., Haehnel, R., Asenath-Smith, E., Cole, D. (2020). A viscoelastic integral formulation and numerical implementation of an isotropic constitutive model of saline ice. Cold Regions Science and Technology, 171(2), 102983. doi: 10.1016/j.coldregions.2019.102983.

O'Grady, J. G., Hemer, M. A., McInnes, K. L., Trenham, C. E., Stephenson, A. G. (2021). Projected incremental changes to extreme wind-driven wave heights for the twenty-first century.Scientific Reports, 11(1), pp. 1–9. doi: 10.1038/s41598-021-87358-w.

O'Donncha, F., Zhang, Y., Chen, B., James, S. C. (2019). Ensemble model aggregation using a computationally lightweight machine-learning model to forecast ocean waves. Journal of Marine Systems, 199, 103206.

Oh, J., Suh, K. D. (2018). Real-time forecasting of wave heights using EOF – wavelet – neural network hybrid model. Ocean Engineering. Elsevier Ltd, 150, pp. 48–59. doi: 10.1016/j.oceaneng.2017.12.044.

Oikkonen, A., Haapala, J., Lensu, M., Karvonen, J., Itkin, P. (2017). Small-scale sea ice deformation during N-ICE2015: From compact pack ice to marginal ice zone. Journal of Geophysical Research: Oceans, 122(6). doi: 10.1002/2016JC012387.

Oka, M., Ma, C., Ochi, H. (2019a). Estimation of wave loads acted on ships in service based on AIS Data (2nd report): long-term prediction considering with the conditional probability of ship operations given sea states. Journal of the Japan Society of Naval Architects and Ocean Engineers, 30, pp. 105-113.

Oka, M., Takami, T., Ma, C. (2018). Estimation of wave loads acted on ships in service based on AIS data: evaluation of operational effects on the maximum loads. Journal of the Japan Society of Naval Architects and Ocean Engineers, 28, pp. 89-95.

Oka, M., Takami, T., Ma, C. (2019b). Evaluation Method for the Maximum Wave Load Based on AIS and Hindcast Wave Data. 14th Symp. on Practical Design of Ships and Other Floating Structures (PRADS), Yokohama, Japan. Published in Lecture Notes on Civil Eng (LNCE) 65. doi: 10.1007/978-981-15-4680-8_22.

Olauson, J. (2018). ERA5: The new champion of wind power modelling? Renewable Energy, 126, pp. 322-331. doi: 10.1016/j.renene.2018.03.056.

Optis, M., Perr-Sauer, J. (2019). The importance of atmospheric turbulence and stability in machine-learning models of wind farm power production. Renewable and Sustainable Energy Reviews. Elsevier Ltd, 112, pp. 27–41. doi: 10.1016/j.rser.2019.05.031.

Orimolade, A. P., Haver, S., Gudmestad, O. T. (2016). Estimation of extreme significant wave heights and the associated uncertainties: A case study using NORA10 hindcast data for the Barents Sea. Marine Structures, 49, pp. 1-17.

Ortiz, G. P., Lorenzzetti, J. A. (2018). Observing Multimodal Ocean Wave Systems by a Multiscale Analysis of Polarimetric SAR Imagery. IEEE Geoscience and Remote Sensing Letters, 15(11), pp. 1735–1739. doi: 10.1109/LGRS.2018.2859810.

Osborne, A. R. (2018). Nonlinear Fourier Methods for Ocean Waves. Proceeding of IUTAM Symposium Wind Waves, ELSEVIER, 26, pp. 112-123. 4-8 September 2017, London, UK.

Ozbahceci, B. O. (2020). Extreme value statistics of wind speed and wave height of the Marmara Sea based on combined radar altimeter data. Advances in Space Research, 66(10), pp. 2302–2318. doi: 10.1016/j.asr.2019.08.025.

Pákozdi, C. Wang, W., Bihs, H., Fouques, S. (2019). Validation of a High-Performance Computing Nonlinear Potential Theory Based Numerical Wave Tank for Wave Structure Interaction. Proc. of Coastal Structures Conference 2019, 12 p. doi: 10.18451/978-3-939230-64-9_014.

Pákozdi, C., Östman, A., Bachynski-Polić, E., Stansberg, C. T. (2016). CFD Reproduction of Model Test Generated Extreme Irregular Wave Events and Nonlinear Loads on a Vertical Column. Proc/ of ASME 2016 35th International Conference on Ocean, Offshore and Arctic Engineering (OMAE), 54869, V002T08A024, 9 p. doi: 10.1115/OMAE2016-54869.

Pan, Y., Liu, Y., Yue, D. K. P. (2018). On high-order perturbation expansion for the study of long-short wave interactions. Journal of Fluid Mechanics, 846, pp. 902-915. doi:10.1017/jfm.2018.296.

Papalexiou, S. M. (2018). Unified theory for stochastic modelling of hydroclimatic processes: Preserving marginal distributions, correlation structures, and intermittency. Advances in Water Resources, 115, pp. 234-252.

Papalexiou, S. M., Markonis, Y., Lombardo, F., AghaKouchak, A., Foufoula-Georgiou, E. (2018). Precise Temporal Disaggregation Preserving Marginals and Correlations (DiPMaC) for Stationary and Nonstationary Processes. Water Resources Research, 54 (10), pp. 7435-7458. doi:10.1029/2018WR022726.

Parra, S. M., Sree, D. K. K., Wang, D., Rogers, E., Lee, J. H., Collins, C. O., Law, A. W.-K., Babanin, A. v. (2020). Experimental study on surface wave modifications by different ice covers. Cold Regions Science and Technology, 174. doi: 10.1016/j.coldregions.2020.103042.

Parsons, M. J., Crosby, A. R., Orelup, L., Ferguson, M., Cox, A. T. (2018). Evaluation of ERA5 Reanalysis Wind Forcing for Use in Ocean Response Modeling. Waves In Shallow Environments. Proc. of WISE Conference, pp. 22-26. Tel Aviv University, Israel. https://www.oceanweather.com/about/papers/.

Pascual, D., Clarizia, M. P., Ruf, C. (2021). Spaceborne Demonstration of GNSS-R Scattering Cross Section Sensitivity to Wind Direction. IEEE Geoscience and Remote Sensing Letters, PP(99), pp. 1–5. doi: 10.1109/LGRS.2021.3049526.

Passerotti, G., Alberello, A., Dolatshah, A., Bennetts, L., Puolakka, O., von Bock und Polach, F., Klein, M., Hartmann, M., Monbaliu, J., Toffoli, A. (2020). Wave Propagation in Continuous Sea Ice: An Experimental Perspective. Proc. of ASME 39th International Conference on Ocean, Offshore & Arctic Engineering (OMAE), 18181. doi: 10.1115/OMAE2020-18181.

Peng, S., Zhu, Y., Li, Z., Li, Y., Xie, Q., Liu, S., Luo, Y., Tian, Y., Yu, J. (2019). Improving the Real-time Marine Forecasting of the Northern South China Sea by Assimilation of Glider-observed T/S Profiles. Sci Rep, 9(1), 17845. doi: 10.1038/s41598-019-54241-8.

Pereira, H. P. P., Violante-Carvalho, N., Nogueira, I. C. M., Babanin, A., Liu, Q., de Pinho, U. F., Nascimento, F., Parente, C. E. (2017). Wave observations from an array of directional buoys over the southern Brazilian coast. Ocean Dynamics 67 (12), pp. 1577-1591. doi: 10.1007/s10236-017-1113-9.

Perlin, M., Bustamante, M. D. (2016). A robust quantitative comparison criterion of two signals based on the Sobolev norm of their difference. Journal of Engineering Mathematics, 101(1). doi: 10.1007/s10665-016-9849-7.

Perrie, W., Toulany, B., Roland, A., Dutour-Sikiric, M., Chen, C., Beardsley, R.C., Qi, J., Hu, Y., Casey, M.P., Shen, H. (2018). Modelling North Atlantic Nor'easters With Modern

Wave Forecast Models. Journal of Geophysical Research: Oceans 123 (1), pp. 533-557. doi: 10.1002/2017JC012868.

Pirhooshyaran, M., Snyder, L. V. (2020). Forecasting, hindcasting and feature selection of ocean waves via recurrent and sequence-to-sequence networks. Ocean Engineering, 207, 107424.

Polojärvi, A., Gong, H., Tuhkuri, J. (2021). Comparison of Full-scale and DEM simulation Data on Ice Loads Due to Floe Fields on a Ship Hull. Proc. of the 26th International Conference on Port and Ocean Engineering under Arctic Conditions (POAC'21), 9 p. https://www.poac.com/Papers/2021/pdf/POAC21-063.pdf

Portilla-Yandún, J., Barbariol, F., Benetazzo, A., Cavaleri, L. (2019). On the statistical analysis of ocean wave directional spectra. Ocean Engineering. Elsevier Ltd, 189(November 2018), p. 106361. doi: 10.1016/j.oceaneng.2019.106361.

Prasanna, M. (2020). A laboratory study of the breakage of floating saline ice blocks subjected to in-plane loading. Submitted to The Cryosphere Journal.

Qiu, B., Chen, S., Klein, P., Torres, H., Wang, J., Fu, L.-L., Menemenlis, D. (2020). Reconstructing Upper-Ocean Vertical Velocity Field from Sea Surface Height in the Presence of Unbalanced Motion. Journal of Physical Oceanography, 50(1), 55–79. doi: 10.1175/jpo-d-19-0172.1.

Qiu, J., Zhang, B., Chen, Z., He, Y. (2017). A new modulation transfer function with range and azimuth dependence for ocean wave spectra retrieval from X-band marine radar observations. IEEE Geoscience and Remote Sensing Letters, 14(8), pp. 1373-1377. doi: 10.1109/LGRS.2017.2713438.

Qu, Z., Mao, W., Zhang, K., Zhang, W. (2019). Multi-step wind speed forecasting based on a hybrid decomposition technique and an improved back-propagation neural network. Renewable Energy. Elsevier Ltd, 133, pp. 919–929. doi: 10.1016/j.renene.2018.10.043.

Qu, Z., Zhang, K., Mao, W., Wang, J. (2017). Research and application of ensemble forecasting based on a novel multi-objective optimization algorithm for wind-speed forecasting. Energy Conversion and Management. Elsevier Ltd, 154, pp. 440–454. doi: 10.1016/j.enconman.2017.10.099.

Quach, B., Glaser, Y., Stopa, J. E., Mouche, A. A., Sadowski, P. (2020). Deep Learning for Predicting Significant Wave Height From Synthetic Aperture Radar. 59(3), pp. 1-9. doi: 10.1109/TGRS.2020.3003839.

Rabault, J., Sutherland, G., Jensen, A., Christensen, K. H., Marchenko, A. (2019). Experiments on wave propagation in grease ice: combined wave gauges and particle image velocimetry measurements. Journal of Fluid Mechanics, 864, pp. 876-898. doi: 10.1017/jfm.2019.16.

Radovan, A., Crewell, S., Knudsen, E. M., Rinke, A. (2019). Environmental conditions for polar low formation and development over the Nordic Seas: study of January cases based on the Arctic System Reanalysis. Tellus A: Dynamic Meteorology and Oceanography, 71(1), 1618131. doi: 10.1080/16000870.2019.1618131.

Raed, K., Teixeira, A., Guedes Soares, C. (2020). Uncertainty assessment for the extreme hydrodynamic responses of a wind turbine semi-submersible platform using different environmental contour approaches. Ocean Engineering, 195, 106719.

Raghukumar, K., Chang, G., Spada, F., Jones, C., Janssen, T., Gans, A. (2019). Performance Characteristics of "Spotter," a Newly Developed Real-Time Wave Measurement Buoy. Journal of Atmospheric and Oceanic Technology, 36(6), pp. 1127-1141. doi: 10.1175/jtech-d-18-0151.1.

Raillard, N., Prevesto, M., Pineau, H. (2019). 3-D environmental extreme value models for the tension in a mooring line of a semi-submersible. Ocean Engineering, 184, pp. 23-31.

Raizer, V. (2019). Advanced Optical Observations. Optical Remote Sensing of Ocean Hydrodynamics, pp. 225-262. doi: 10.1201/9781351119184-7.

Rampal, P., Dansereau, V., Olason, E., Bouillon, S., Williams, T., Korosov, A., Samaké, A. (2019). On the multi-fractal scaling properties of sea ice deformation. The Cryosphere, 13(9), pp. 2457-2474. doi: 10.5194/tc-13-2457-2019.

Ranta, J., Polojärvi, A. (2019). Limit mechanisms for ice loads on inclined structures: Local crushing. Marine Structures, 67, 102633. doi: 10.1016/j.marstruc.2019.102633.

Ranta, J., Polojärvi, A., Tuhkuri, J. (2018a). Limit mechanisms for ice loads on inclined structures: Buckling. Cold Regions Science and Technology, 147, pp. 34-44. doi: 10.1016/j.coldregions.2017.12.009.

Ranta, J., Polojärvi, A., Tuhkuri, J. (2018b). Scatter and error estimates in ice loads – Results from virtual experiments. Cold Regions Science and Technology, 148, pp. 1-12. doi: 10.1016/j.coldregions.2018.01.002.

Rapuc, S., Crepier, P., Jaouen, F., Bunnik, T., Regnier, P. (2018). Towards guidelines for consistent wave propagation in CFD simulations. Proc. of 19th International Conference on Ship and Maritime Research (NAV2018), 10 p.

Redor, I., Barthélemy, E., Michallet, H., Onorato, M., Mordant, N. (2019). Experimental Evidence of a Hydrodynamic Soliton Gas. Physical Review Letters, 122(21), 214502. doi: 10.1103/PhysRevLett.122.214502.

Reich, A., Payne, G. S., C.R. Pascal, R., Spinneken, J. (2018). Investigation into wave basin calibration based on a focused wave approach. Ocean Engineering, 152. doi: 10.1016/j.oceaneng.2018.01.044.

Reich, B. J., Shaby, B. A. (2019). A spatial Markov model for climate extremes. Journal of Computational and Graphical Statistics, 28(1), pp. 117-126.

Ren, L., Yang, J., Zheng, G., Wang, J. (2019). Joint Retrieval of Directional Ocean Wave Spectra from SAR and RAR. Advances in SAR Remote Sensing of Oceans, pp. 239–256. doi: 10.1201/9781351235822-14.

Ribal, A., Young, I. R. (2019). 33 years of globally calibrated wave height and wind speed data based on altimeter observations. Scientific data, 6(1), 77, pp. 1-15. doi:10.1038/s41597-019-0083-9.

Ribal, A., Young, I. R. (2020). Calibration and Cross Validation of Global Ocean Wind Speed Based on Scatterometer Observations. Journal of Atmospheric and Oceanic Technology, 37, pp. 279-297. doi: 10.1175/JTECH-D-19-0119.1

Rienecker, M. M., Fenton, J. D. (1981). A Fourier approximation method for steady water waves. J. Fluid Mech., vol. 104, pp. 119-134.

Roberts, A. F., Hunke, E. C., Kamal, S. M., Lipscomb W. H., Horvat, C., Maslowski, W. (2019). A Variational Method for Sea Ice Ridging in Earth System Models. Journal of Advances in Modelling Earth Systems, 11(3), pp. 771–805. doi: 10.1029/2018MS001395.

Rosa, T. L., Piecho-Santos, A. M., Vettor, R., Guedes Soares, C. (2021). Review and Prospects for Autonomous Observing Systems in Vessels of Opportunity. Journal of Marine Science and Engineering, 9(4). doi: 10.3390/jmse9040366.

Ross, E., Astrup, O. C., Bitner-Gregersen, E., Bunn, N., Feld, G., Goudlby, B., Huseby, A., Liu, Y., Randell, D., Vanem, E., Jonathan, P. (2020). On environmental contours for marine and coastal design. Ocean Engineering, 195. doi:10.1016/j.oceaneng.2019.106194.

Ross, E., Kereszturi, M., van Nee, M., Randell, D., Jonathan, P. (2017a). On the spatial dependence of extreme ocean storm seas. Ocean Engineering, 145, pp. 359-372.

Ross, E., Randell, D., Ewans, K., Feld, G., Jonathan, P. (2017b). Efficient estimation of return value distributions from non-stationary marginal extreme value models using Bayesian inference. Ocean Engineering, 142, pp. 315-328.

Ross, E., Sam, S., Randell, D., Feld, G., Jonathan, P. (2018). Estimating surge in extreme North Sea storms. Ocean Engineering, 154, pp. 430-444.

Rueda-Bayona, J. G., Guzman, A., Silva, R. (2020). Genetic algorithms to determine JONSWAP spectra parameters. Ocean Dynamics, 70, pp. 561-571.

Rusu, E. (2018). Numerical Modelling of the Wave Energy Propagation in the Iberian Nearshore. Energies 11 (4). 18 p. doi: 10.3390/en11040980.

Saba, T., Rehman, A., AlGhamdi, J. S. (2017). Weather forecasting based on hybrid neural model. Applied Water Science. Springer Nature, 7(7), pp. 3869–3874. doi: 10.1007/s13201-017-0538-0.

Salas, J., Obeysekera, J., Vogel, R. (2018). Techniques for assessing water infrastructure for nonstationary extreme events: a review. Hydrological Sciences Journal, 63(3), pp. 325-352.

Salat, J., Pascual, J., Flexas, M., Chin, T. M., Vazquez-Cuervo, J. (2019). Forty-five years of oceanographic and meteorological observations at a coastal station in the NW Mediterranean: a ground truth for satellite observations. Ocean Dynamics, 69(9), pp. 1067-1084. doi: 10.1007/s10236-019-01285-z.

Samayam, S., Laface, V., Annamalaisamy, S. S., Arena, F., Vallam, S., Gavrilovich, P. V. (2017). Assessment of reliability of extreme wave height prediction models. Natural Hazards and Earth Systems Sciences, 17, pp. 409-421.

Samet, H., Reisi, M., Marzbani, F. (2019). Evaluation of neural network-based methodologies for wind speed forecasting. Computers and Electrical Engineering. Elsevier Ltd, 78, pp. 356–372. doi: 10.1016/j.compeleceng.2019.07.024.

Samworth, R. J. (2018). Recent Progress in Log-Concave Density Estimation. Statistical Science, 33(4), pp. 493-509.

Sandvik, E., Lønnum, O. J., Asbjørnslett, B. E. (2019). Stochastic bivariate time series models of waves in the North Sea and their application in simulation-based design. Applied Ocean Research, 82, pp. 283-295.

Santos, V. M., Haigh, I. D., Wahl, T. (2017). Spatial and Temporal Clustering Analysis of Extreme Wave Events around the UK Coastline. Journal of Marine Science and Engineering, 5, 28: pp. 1-19.

Sartini, L., Besio, G., Cassola, F. (2017). Spatio-temporal modelling of extreme wave heights in the Mediterranean Sea. Ocean Modelling, 117, pp. 52-69.

Sartini, L., Weiss, J., Prevesto, M., Bulteau, T., Rohmer, J., Maisondieu, C. (2018). Spatial analysis of extreme sea states affecting Atlantic France: a critical assessment of the RFA approach. Ocean Modelling, 130, pp. 48-65.

Sasmal, K., Kodaira, T., Kita, Y., Miratsu, R., Zhu, T., Fukui, T., Waseda, T. (2021a). Modelled and satellite-derived extreme wave height statistics in the North Atlantic Ocean reaching 20 m. Preprint, Earth and Space Science Open Archive. doi:10.1002/essoar.10506278.1.

Sasmal, K., Miratsu, R., Kodaira, T., Fukui, T., Zhu, T., Waseda, T. (2021b). Statistical model representing storm avoidance by merchant ships in the North Atlantic Ocean. Ocean Engineering, 235. doi: 10.1016/j.oceaneng.2021.109163.

Sasmal, K., Miratsu, R., Kodaira, T., Kita, Y., Zhu, T., Fukui, T., Waseda, T. (2019). Wave climate in the North Atlantic Ocean and extreme value analysis. Proc. of 2nd International Workshop on Waves, Storm Surges and Coastal Hazards.

Saviano, S., Kalampokis, A., Zambianchi, E., Uttieri, M. (2019). A year-long assessment of wave measurements retrieved from an HF radar network in the Gulf of Naples (Tyrrhenian Sea, Western Mediterranean Sea). Journal of Operational Oceanography, 12(1), pp. 1-15.

Scharnke, J. (2019). Elementary Loading Processes and Scale Effects Involved in Wave-in-Deck Type of Loading: A Summary of the BreaKin JIP. Proc. of ASME 38th Int. Conf. on Ocean, Offshore and Arctic Eng. (OMAE), 95004. doi: 10.1115/OMAE2019-95004.

Scholcz, T. P., Mak, B. (2020). Ship as a wave buoy: estimating full directional wave spectra from in-service ship motion measurements using deep learning. . Proc. of ASME 39th Int.

Conf. on Ocean, Offshore and Arctic Eng. (OMAE), 18783. doi: 10.1115/OMAE2020-18783.

Serinaldi, F. (2015). Dismissing return periods! Stochastic Environmental Research and Risk Assessment, 29(4), pp. 1179-1189. doi:10.1007/s00477-014-0916-1

Serinaldi, F., Kilsby, C. G. (2015). Stationarity is undead: Uncertainty dominates the distribution of extremes. Advances in Water Resources, 77, pp. 17-36.

Shahabi, S., Khanjani, M.-J., Kermani, M.-r. H. (2016). Significant wave height forecasting using GMDH model. International Journal of Computer Applications, 133(16), pp. 13-16.

Shamji, V. R., Aboobacker, V. M., Vineesh, T. C. (2020). Extreme value analysis of wave climate around Farasan Islands, southern Red Sea. Ocean Engineering, 207, 107395.

Shao, Z., Liang, B., Gao, H. (2020). Extracting independent and identically distributed samples from time series of significant wave heights in the Yellow Sea. Coastal Engineering, 158, 103693.

Shao, Z., Liang, B., Li, H., Lee, D. (2018). Study of sampling methods for assessment of extreme significant wave heights in the South China Sea. Ocean Engineering, 168, 173184.

Sheng, Y., Shao, W., Li, S., Zhang, Y., Yang, H., Zuo, J. (2019). Evaluation of Typhoon Waves Simulated by WaveWatch-III Model in Shallow Waters Around Zhoushan Islands. Journal of Ocean University of China 18 (2), pp. 365 - 375. doi: 10.1007/s11802-019-3829-2.

Shi, H., Cao, X., Li, Q., Li, D., Sun, J., You Z., Sun Q. (2021). Evaluating the Accuracy of ERA5 Wave Reanalysis in the Water Around China. Journal of Ocean University of China, 20, pp. 1-9. doi: 10.1007/s11802-021-4496-7.

Shi, J., Yin, X., Qi, S., Bin, X., Qiao, F. (2018). Evaluation on data assimilation of a global high resolution wave-tide-circulation coupled model using the tropical Pacific TAO buoy observations. Acta Oceanologica Sinica, 37(3), pp.8–20, doi: 10.1007/s13131-018-1196-2.

Shimura, T., Inoue, M., Tsujimoto, H., Sasaki, K., Iguchi, M. (2018). Estimation of Wind Vector Profile Using a Hexarotor Unmanned Aerial Vehicle and Its Application to Meteorological Observation up to 1000 m above Surface. Journal of Atmospheric and Oceanic Technology, 35(8), pp. 1621-1631. doi: 10.1175/jtech-d-17-0186.1.

Shooter, R., Ross, E., Tawn, J., Jonathan, r. (2019). On spatial conditional extremes for ocean storm severity. Environmetrics, 30, e2562:1-18.

Shooter, R., Tawn, J., Ross, E., Jonathan, P. (2021). Basin-wide spatial conditional extremes for severe ocean storms. Extremes, 24, pp. 241-265.

Shu, Z. R., Jesson, M. (2021). Estimation of Weibull parameters for wind energy analysis across the UK. Journal of Renewable and Sustainable Energy, 13(2). doi: 10.1063/5.0038001.

Shu, Z., Li, Q., He, Y., Chan, P. W. (2020). Investigation of Marine Wind Veer Characteristics Using Wind Lidar Measurements. Atmosphere, 11(11). doi: 10.3390/atmos11111178.

Silva, D., Martinho, P., Guedes Soares, C. (2018). Wave energy distribution along the Portuguese continental coast based on a thirty three years hindcast. Renewable Energy 127, pp. 1064-1075. doi: 10.1016/j.renene.2018.05.037.

Silva, M. T., Shahidi, R., Gill, E. W., Huang, W. (2020). Nonlinear Extraction of Directional Ocean Wave Spectrum from Synthetic Bistatic High-Frequency Surface Wave Radar Data. IEEE Journal of Oceanic Engineering, 45(3), pp. 1004-1021. doi: 10.1109/JOE.2019.2909961.

Simanesew, A., Trulsen, K., Krogstad, H. E., Nieto Borge, J. C. (2017). Surface wave predictions in weakly nonlinear directional seas. Applied Ocean Research, 65, pp. 79-89. doi: 10.1016/j.apor.2017.03.009.

Sinha, P., Vincent, S., Kumar, O. P. (2018). A comparative analysis of machine learning models for prediction od wave heights in large waterbodies. International Journal of Engineering Technology, 7, pp. 91-95.

Sletten, M., Menk, S., Toporkov, J. (2021). Comparison of ocean currents derived from UHF ATI-SAR to dispersive shifts observed in sub-aperture image sequences. Proceedings of the 13th European Conference on Synthetic Aperture Radar, EUSAR 2021, pp. 98-102.

Slunyaev, A. (2019). Strongly coherent dynamics of stochastic waves causes abnormal sea states. EGU General Assembly Conference Abstracts, 5348 2–6.

Slunyaev, A. V. (2018). Group-wave resonances in nonlinear dispersive media: The case of gravity water waves. Physical Review E 97, 010202 . doi: 10.1103/PhysRevE.97.010202.

Slunyaev, A., Dosaev, A. (2019). On the incomplete recurrence of modulationally unstable deep-water surface gravity waves. Communications in Nonlinear Science and Numerical Simulation, 66, pp. 167-182. doi: 10.1016/j.cnsns.2018.05.009.

Soukissian, T. H. (2014). Probabilistic modelling of directional and linear characteristics of wind and sea states. Ocean engineering, 91, pp. 91-110.

Soukissian, T. H. (2021). Probabilistic modelling of significant wave height using the extended generalized inverse Gaussian distribution. Ocean Engineering, 230, 109061.

Soukissian, T. H., Karathanasi, F. E. (2017). On the selection of bivariate parametric models for wind data. Applied Energy, 188, pp. 280-304.

Soukissian, T. H., Tsalis, C. (2018). Effects of parameter estimation method and sample size in metocean design conditions. Ocean Engineering, 169, pp. 19-37.

Sree, D. K. K., Law, A. W.-K., Shen, H. H. (2020). An experimental study of gravity waves through segmented floating viscoelastic covers. Applied Ocean Research, 101. doi: 10.1016/j.apor.2020.102233.

Sreelakshmi, S., Bhaskaran, P. K. (2020). Wind-generated wave climate variability in the Indian Ocean using ERA-5 dataset. Ocean Engineering, 209, 107486.

Stansberg, C. T. (2020). Wave Front Steepness and Influence on Horizontal Deck Impact Loads. Journal of Marine Science and Engineering, 8(5), 314, 24 p. doi: 10.3390/jmse8050314.

Steer, J. N., Borthwick, A. G. L., Onorato, M., Chabchoub, A., Van Den Bremer, T. S. (2019a). Hydrodynamic X Waves. Physical Review Letters, 123(18), 184501. doi: 10.1103/PhysRevLett.123.184501.

Steer, J. N., McAllister, M. L., Borthwick, A. G. L., Van Deen Bremer, T. S. (2019b). Experimental observation of modulational instability in crossing surface gravity wavetrains. Fluids, 4(2), 105. doi: 10.3390/fluids4020105.

Stefanakos, C. (2016). Fuzzy time series forecasting of nonstationary wind and wave data. Ocean Engineering, 121, pp. 1-12.

Stefanakos, C., Vanem, E. (2018). Nonstationary fuzzy forecasting of wind and wave climate in very long time-scales. Journal of Ocean Engineering and Science, 3, pp. 144-155.

Støle-Hentschel, S., Trulsen, K., Nieto Borge, J. C., Olluri, S. (2020). Extreme Wave Statistics in Combined and Partitioned Wind Sea and Swell. Water Waves 2, pp. 169-184. doi:10.1007/s42286-020-00026-w.

Støle-Hentschel, S., Trulsen, K., Olluri, S. (2019). Extreme wave statistics in co-propagating windsea and swell. arXiv:1904.07207,

Støle-Hentschel, S., Trulsen, K., Rye, L. B., Raustøl, A. (2018). Extreme wave statistics of counter-propagating, irregular, long-crested sea states. Physics of Fluids, 30(6), 067102. doi:10.1063/1.5034212.

Stopa, J. E. (2019). Seasonality of wind speeds and wave heights from 30 years of satellite altimetry. Advances in Space Research. COSPAR. doi: 10.1016/j.asr.2019.09.057.

Su, Z., Wang, J., Klein, P., Thompson, A. F., Menemenlis, D. (2018). Ocean submesoscales as a key component of the global heat budget. Nat Commun, 9(1), 775. doi: 10.1038/s41467-018-02983-w.

Sun, D., Zhang, Y., Wang, Y., Chen, G., Sun, H., Yang, L., Bai, Y., Yu, F., Zhao, C. (2021). Ocean Wave Inversion Based on Airborne IRA Images. IEEE Transactions on Geoscience and Remote Sensing, pp. 1-13. doi: 10.1109/TGRS.2021.3101223.

Sun, J., Samorodnitsky, G. (2019). Multiple thresholds in extremal parameter estimation. Extremes, 22, pp. 317-341.

Sun, Y., Li, X. (2021). Denoising Sentinel-1 Extra-Wide Mode. IEEE Transactions on Geoscience and Remote Sensing, 59(3), pp. 2116–2131. doi:10.1109/TGRS.2020.3005831.

Suominen, M., Kujala, P., Romanoff, J., Remes, H. (2017a). Influence of load length on short-term ice load statistics in full-scale. Marine Structures, 52. doi: 10.1016/j.marstruc.2016.12.006.

Suominen, M., Kujala, P., Romanoff, J., Remes, H. (2017b). The effect of the extension of the instrumentation on the measured ice-induced load on a ship hull. Ocean Engineering, 144, pp. 327-339. doi: 10.1016/J.OCEANENG.2017.09.056.

Sutherland, P., Brozena, J., Rogers, W. E., Doble, M., Wadhams, P. (2018). Airborne Remote Sensing of Wave Propagation in the Marginal Ice Zone. Journal of Geophysical Research: Oceans, 123(6), pp. 4132–4152. doi: 10.1029/2018JC013785.

Takagaki, N., Suzuki, N., Troitskaya, Y., Tanaka, C., Kandaurov, A., Vdovin, M. (2020). Effects of current on wind waves in strong winds. Ocean Science, 16(5), pp. 1033-1045. doi: 10.5194/os-16-1033-2020.

Takbash, A., Young, I. R. (2020). Long-Term and Seasonal Trends in Global Wave Height Extremes Derived from ERA-5 Reanalysis Data. Journal of Marine Science and Engineering, 8(12), 1015.

Takbash, A., Young, I. R., Breivik, 0. (2019). Global WindSpeed and Wave Height Extremes Derived from Long-Duration Satellite Records. Journal of Climate, 32, 109126.

Takeyama, Y., Ohsawa, T., Tanemoto, J., Shimada, S., Kozai, K., Kogaki, T. (2020). A comparison between Advanced Scatterometer and Weather Research and Forecasting wind speeds for the Japanese offshore wind resource map. Wind Energy, 23(7), pp. 1596-1609. doi: 10.1002/we.2503.

Tapoglou, E., Forster, R. M., Dorrell, R. M., Parsons, D. (2021). Machine learning for satellite-based sea-state prediction in an offshore windfarm. Ocean Engineering, 235(December 2020), 109280. doi: 10.1016/j.oceaneng.2021.109280.

Tawn, J., Shooter, R., Towe, R., Lamb, R. (2018). Modelling spatial extreme events with environmental applications. Spatial Statistics, 28, pp. 39-58.

Teich, T., Groll, N., Weisse, R. (2018). Long-term statistics of potentially hazardous sea states in the North Sea 1958-2014. Ocean Dynamics, 68, pp. 1559-1570.

Teixeira, R., Nogal, M., O'Connor, A. (2018). On the suitability of the generalized Pareto to model extreme waves. Journal of Hydraulic Research, 56(6), pp. 755-770.

Tendijck, S., Ross, E., Randell, D., Jonathan, P. (2019). A model for the directional evolution of severe ocean storms. Environmetrics, 30(1). doi:10.1002/env.2541.

Tetzner, D., Thomas, E., Allen, C. (2019). A Validation of ERA5 Reanalysis Data in the Southern Antarctic Peninsula - Ellsworth Land Region, and Its Implications for Ice Core Studies. Geosciences 2019, 9, 289. doi: 10.3390/geosciences9070289.

Thompson, I., Huiskamp, E., Grasso, N., Drummen, I., Stambaugh, K. (2019). Virtual hull structural monitoring of a USCG cutter. Proc. of ASNE Technology, Systems and Ships 2019 Proceedings.

Thomson, J., Talbert, J., de Klerk, A., Brown, A., Schwendeman, M., Goldsmith, J., Thomas, J., Olfe, C., Cameron, G., Meinig, C. (2015). Biofouling Effects on the Response of a Wave Measurement Buoy in Deep Water. Journal of Atmospheric and Oceanic Technology, 32(6). doi: 10.1175/JTECH-D-15-0029.1.

Tian, Q., Huang, G., Hu, K., Niyogi, D. (2019). Observed and global climate model based changes in wind power potential over the Northern Hemisphere during 1979–2016. Energy, 167, 1224–1235. doi: 10.1016/j.energy.2018.11.027.

Tian, Y., Wen, B., Tian, Z. (2018). Wave height field measurement using a compact dual-frequency HF radar. OCEANS 2018 - MTS/IEEE, pp. 16–19. doi: 10.1109/OCEANSKOBE.2018.8559375.

Tikan, A. (2020). Effect of local Peregrine soliton emergence on statistics of random waves in the one-dimensional focusing nonlinear Schrödinger equation. Physical Review E, 101(1), 12209. doi:10.1103/PhysRevE.101.012209.

Timmermans, B. W., Gommenginger, C. P., Dodet, G., Bidlot, J. R. (2020). Global wave height trends and variability from new multimission satellite altimeter products, reanalyses, and wave buoys. Geophysical Research Letters, 47(9), e2019GL086880.

Toffoli, A., Ducrozet, G., Waseda, T., Onorato, M., Abdolahpour, M., Nelli, F. (2019). Ocean currents trigger rogue waves. Proceedings of the International Offshore and Polar Engineering Conference, (ISOPE), pp. 2453–2459.

Toffoli, A., Proment, D., Salman, H., Monbaliu, J., Frascoli, F., Dafilis, M., Stramignoni, E., Forza, R., Manfrin, M., Onorato, M. (2017). Wind Generated Rogue Waves in an Annular Wave Flume. Physical Review Letters, 118, 144503.doi: 10.1103/PhysRevLett. 118.144503.

Tomaselli, P. D., Christensen, E. D. (2017). A CFD Investigation on the Effect of the Air Entrainment in Breaking Wave Impacts on a Mono-Pile. Proc. of ASME 2017 36th International Conference on Ocean, Offshore and Arctic Engineering (OMAE). American Society of Mechanical Engineers. 62445, V07AT06A072; 10 pages. doi: 10.1115/OMAE2017-62445.

Tran, H. Q. (2020). Hydrodynamic modelling of a wave-dominated tidal inlet system: Port Phillip Bay, Australia. PhD Thesis, University of Melbourne, Australia, 15 p.

Troch, P., Stratigaki, V., Devriese, P., Kortenhaus, A., de Maeyer, J., Monbaliu, J., Toorman, E., Rauwoens, P., Vanneste, D., Suzuki, T., Verwaest, T. (2018). Design features of the upcoming coastal and ocean basin in Ostend, Belgium, for coastal and offshore applications. Proc. of 7th International Conference on the Application of Physical Modelling in Coastal and Port Engineering and Science (Coastlab).

Trulsen, K., Raustol, A., Jorde, S., Rye, L. B. (2020). Extreme wave statistics of long-crested irregular waves over a shoal. Journal of Fluid Mechanics, 882(c), pp. 1–11. doi:10.1017/jfm.2019.861.

Tuhkuri, J., Polojärvi, A. (2018). A review of discrete element simulation of ice-structure interaction. Philosophical Transactions of the Royal Society A: Mathematical, Physical and Engineering Sciences, 376(2129). doi: 10.1098/rsta.2017.0335.

Tukker, J., Bouvy, A., Bloemhof, F. (2019). Measurement quality of electrical resistance wave gauges. Proc. of 6th International Conference on Advanced Model Measurement Technology for Maritime Industry (AMT), section 6B, 15 p.

Uchida, T. (2018). A New Proposal for Vertical Extrapolation of Offshore Wind Speed and an Assessment of Offshore Wind Energy Potential for the Hibikinada Area, Kitakyushu, Japan. Energy and Power Engineering, 10(04), 154–164. doi: 10.4236/epe.2018.104011.

Umair, M., Hashmani, M. A., Hasan, M. H. (2019). Survey of Sea Wave Parameters Classification and Prediction using Machine Learning Models. Proc AiDAS 2019. Ipoh: IEEE.

Umesh, P.A., Bhaskaran, P.K., Sandhya, K.G., Nair, T.M.B. (2017). High Frequency Tail Characteristics in the Coastal Waters off Gopalpur, Northwest Bay of Bengal: A Nearshore Modelling Study. Pure and Applied Geophysics 175 (6), pp. 2351-2379. doi: 10.1007/s00024-017-1761-1.

Umesh, P.A., Swain, J. (2018). Inter-comparisons of SWAN hindcasts using boundary conditions from WAM and WWIII for northwest and northeast coasts of India. Ocean Engineering 156, pp. 523-549. doi: 10.1016/j.oceaneng.2018.03.029.

Umesh, P.A., Swain, J., Balchand, A.N. (2018). Inter-comparison of WAM and WAVEWATCH-III in the North Indian Ocean using ERA-40 and QuikSCAT/NCEP blended winds. Ocean Engineering 164(4), pp. 298-321. doi: 10.1016/j.oceaneng.2018.06.053.

Valipour, R., Rao, Y. R., León, L. F., Depew, D. (2019). Nearshore-offshore exchanges in multi-basin coastal waters: Observations and three-dimensional modelling in Lake Erie. Journal of Great Lakes Research, 45(1), pp. 50-60. doi: 10.1016/j.jglr.2018.10.005.

van den Berg, M., Lubbad, R., Løset, S. (2018). An implicit time-stepping scheme and an improved contact model for ice-structure interaction simulations. Cold Regions Science and Technology, 155(12), pp. 193-213. doi: 10.1016/j.coldregions.2018.07.001

van den Berg, M., Lubbad, R., Løset, S. (2019). The effect of ice floe shape on the load experienced by vertical-sided structures interacting with a broken ice field. Marine Structures, 65, pp. 229–248. doi: 10.1016/j.marstruc.2019.01.011.

van den Berg, M., Lubbad, R., Løset, S. (2020). Repeatability of ice-tank tests with broken ice. Marine Structures, 74, p. 102827. doi: 10.1016/j.marstruc.2020.102827.

van der A, D. A., van der Zanden, J., O'Donoghue, T., Hurther, D., Cáceres, I., McLelland, S. J., Ribberink, J. S. (2017). Large-scale laboratory study of breaking wave hydrodynamics over a fixed bar. Journal of Geophysical Research: Oceans, 122(4). doi: 10.1002/2016JC012072.

van Essen, S. M. (2019). Variability in encountered waves during deterministically repeated seakeeping tests at forward speed. Proc. of ASME 38th Int. Conf. on Ocean, Offshore and Arctic Eng. (OMAE), 95065. doi: 10.1115/OMAE2019-95065.

van Essen, S. M., Ewans, K., McConochie, J. (2018). Wave buoy performance in short and long waves, evaluated using tests on a hexapod. Proc. of ASME 37th Int. Conf. on Ocean, Offshore and Arctic Eng. (OMAE), 77092. doi: 10.1115/OMAE2018-77092.

van Essen, S. M., Lafeber, W. (2017). Wave-induced current in a seakeeping basin. Proc. of ASME 36th Int. Conf. on Ocean, Offshore and Arctic Eng. (OMAE), 62203. doi: 10.1115/OMAE2017-62203.

van Essen, S. M., Monroy, C., Shen, Z., Helder, J., Kim, D.-H., Seng, S., Ge, Zhongfu. (2021). Screening wave conditions for the occurrence of green water events on sailing ships. Ocean Engineering, 234, 27 p. doi: 10.1016/j.oceaneng.2021.109218.

van Essen, S. M., Peters, H. C. (2017). Design wave and wind environment for minimum power requirements of vessels in the Southern North Sea. Proc. of RIMA Influence of EEDI on Ship Design Operation 2019 Conference.

van Essen, S., Scharnke, J., Bunnik, T., Düz, B., Bandringa, H., Hallmann R., Helder J. (2020). Linking Experimental and Numerical Wave Modelling. Journal of Marine Science and Engineering, 8 (3), 198. doi: 10.3390/jmse8030198.

van Meerkerk, M., Poelma, C., Westerweel, J. (2020). Scanning stereo-PLIF method for free surface measurements in large 3D domains. Experiments in Fluids, 61(1). doi: 10.1007/s00348-019-2846-7.

Vanem, E. (2015a). Non-stationary extreme value models to account for trends and shifts in the extreme wave climate due to climate change. Applied Ocean Research, 52, pp. 201-211.

Vanem, E. (2015b). Uncertainties in extreme value modelling of wave data in a climate change perspective. Journal of Ocean Engineering and Marine Energy, 1, pp. 339-359.

Vanem, E. (2016). Joint statistical models for significant wave height and wave period in a changing climate. Marine Structures, 49, pp. 180-205.

Vanem, E. (2017). A regional extreme value analysis of ocean waves in a changing climate. Ocean Engineering, 144, pp. 277-295.

Vanem, E. (2018). A simple approach to account for seasonality in the description of extreme ocean environments. Marine Systems Ocean Technology, 13, pp. 63-73.

Vanem, E. (2019). 3-dimensional environmental contours based on a direct sampling method for structural reliability analysis of ships and offshore structures. Ships and Offshore Structures, 14(1), pp. 74-85.

Vanem, E. (2020a). Adjusting environmental contours for specified expected number of unwanted events. Proc. OMAE 2020, 19293. Fort Lauderdale: ASME. doi:10.1115/OMAE2020-19293.

Vanem, E. (2020b). Bivariate regional extreme value analysis for significant wave height and wave period. Applied Ocean Research, 101, 102266.

Vanem, E., Fazeres-Ferradosa, T., Rosa-Santos, P., Taveira-Pinto, F. (2019a). Statistical description and modelling of extreme ocean wave conditions. Proceedings of the Institution of Civil Engineers - Maritime Engineering, 172(4), pp. 124-132.

Vanem, E., Gramstad, O., Bitner-Gregersen, E. M. (2019b). A simulation study on the uncertainty of environmental contours due to sampling variability for different estimation methods. Applied Ocean Research, 91, 101870.

Vanem, E., Guo, B., Ross, E., Jonathan, P. (2020a). Comparing different contour methods with response-based methods for extreme ship response analysis. Marine Structures, 69, 102680.

Vanem, E., Hafver, A., Nalvarte, G. (2020b). Environmental contours for circular-linear variables based on the direct sampling method. Wind Energy, 23(3), pp. 563-574.

Vargas, D., Jayaratne, R., Mendoza, E., Silva, R. (2020). On the Estimation of the Surface Elevation of Regular and Irregular Waves Using the Velocity Field of Bubbles. Journal of Marine Science and Engineering, 8(2). doi: 10.3390/jmse8020088.

Velarde, J., Vanem, E., Kramhøft, C., Sørensen, J. D. (2019). Probabilistic analysis of offshore wind turbines under extreme resonant response: Application of environmental contour method. Applied Ocean Research, 93, 101947.

Viana, R. D., Lorenzzetti, J. A., Carvalho J. T., Nunziata, F. (2020). Estimating Energy Dissipation Rate from Breaking Waves Using Polarimetric SAR Images. Sensors, 20, 6540; 18 p., doi:10.3390/s20226540.

Villas Bôas, A. B., Ardhuin, F., Ayet, A., Bourassa, M. A., Brandt, P., Chapron, B., Cornuelle, B. D., Farrar, J. T., Fewings, M. R., Fox-Kemper, B., Gille, S. T., Gommenginger, C., Heimbach, P., Hell, M. C., Li, Q., Mazloff, M. R., Merrifield, S. T., Mouche, A., Rio, M. H., Rodriguez, E., Shutler, J. D., Subramanian, A. C., Terrill E, J., Tsamados, M., Ubelmann, C., van Sebille, E. (2019). Integrated Observations of Global Surface Winds, Currents, and Waves: Requirements and Challenges for the Next Decade. Frontiers in Marine Science, 6. doi: 10.3389/fmars.2019.00425.

Voermans, J. J., Babanin, A.V., Thomson, J., Smith, M. M., Shen, H. H., (2019a). Wave attenuation by sea-ice turbulence. Geophysical Research Letters, 8 p, doi: 10.1029/2019GL082945.

Voermans, J. J., H. Rapizo, H. Ma, F. Qiao, A.V. Babanin, (2019b). Air-sea momentum fluxes during Tropical Cyclone Olwyn. Journal of Physical Oceanography, 49, 1369-1379, doi: 10.1175/JPO-D-18-0261.1.

Voermans, J. J., Rabault, J. , Filchuk, K. , Ryzhov, I. , Heil, P., Marchenko, A., Collins, C. , Dabboor, M., Sutherland, G., Babanin, A. V. (2020). Experimental evidence for a universal threshold characterizing wave-induced sea ice break-up. The Cryosphere, 14, pp. 4265–4278. doi: 10.5194/tc-14-4265-2020.

von Bock und Polach, R. U. F., Ettema, R., Gralher, S., Kellner, L., Stender, M. (2019). The non-linear behaviour of aqueous model ice in downward flexure. Cold Regions Science and Technology, 165. doi: 10.1016/j.coldregions.2019.05.001.

Von Bock Und Polach, R. U. F., Klein, M., Kubiczek, J., Kellner, L., Braun, M., Herrnring, H. (2019). State of the art and knowledge gaps on modelling structures in cold regions. Proc. of ASME 38th Int. Conf. on Ocean, Offshore and Arctic Eng. (OMAE), 8, 11 p doi:10.1115/OMAE2019-95085.

von Bock und Polach, R. U. F., Ziemer, G., Klein, M., Hartmann, M. C. N., Toffoli, A., Monty, J. (2020). Case based scaling: Recent developments in ice model testing technology. Proc. of ASME 39th Int. Conf. on Ocean, Offshore and Arctic Eng. (OMAE), 18320. doi: 10.1115/OMAE2020-18320.

Wada, R., Jonathan, P., Waseda, T., Fan, S. (2019). Estimating extreme waves in the Gulf of Mexico using a simple spatial extremes model. Proc. OMAE 2019, 95442. Glasgow: ASME. doi:10.1115/OMAE2019-95442.

Wada, R., Waseda, T. (2018). Benchmark for the Sources of Uncertainty in Extreme Wave Analysis. Proc. OMAE 2018, 78216. Madrid: ASME. doi:10.1115/OMAE2018-78216.

Wada, R., Waseda, T., Jonathan, P. (2016). Extreme value estimation using the likelihood-weighted method. Ocean Engineering, 124, pp. 241-251.

Wada, R., Waseda, T., Jonathan, P. (2018). A simple spatial model for extreme tropical cyclone seas. Ocean Engineering, 169, pp. 315-325.

Wan, Y., Zheng, C., Zhang, J., Dai, Y., Li, L., Qu, X., Zhang, X. (2020). The Study of Ocean Wave and Wave Power Observations by Synthetic Aperture Radar in Nearshore Waters. Journal of Coastal Research, 99(sp1), pp. 9-15. doi: 10.2112/SI99-002.1.

Wang, H., Ruan, J., Wang, G., Zhou, B., Liu, Y., Fu, X., Peng, J. (2017a). Deep learning based ensemble approach for probabilistic wind power forecasting. Applied Energy. Elsevier Ltd, 188, pp. 56–70. doi: 10.1016/j.apenergy.2016.11.111.

Wang, H., Wang, J., Zhang, B., Zhu, J. (2019d). Evaluating ocean wave spectra derived from quad-polarized GF-3 wave mode SAR images against buoys. Proc. of SPIE 11150, Remote Sensing of the Ocean, Sea Ice, Coastal Waters, and Large Water Regions 2019, 14. doi: 10.1117/12.2532683.

Wang, J., Liu, J., Wang, Y., Liao, Z., Sun, P. (2021a). Spatiotemporal variation and extreme value analysis of significant wave height in the South China Sea based on 71-year long ERA5 wave reanalysis. Applied Ocean Research, 113, 102750.

Wang, J., Wang, Y., Yang, J. (2021b). Forecasting of Significant Wave Height Based on Gated Recurrent Unit Network in the Taiwan Strait and Its Adjacent Waters. Water, 13(1), 86. doi:10.3390/w13010086.

Wang, J., Zhang, N., Lu, H. (2019a). A novel system based on neural networks with linear combination framework for wind speed forecasting. Energy Conversion and Management. Elsevier Ltd, 181, pp. 425–442. doi: 10.1016/j.enconman.2018.12.020.

Wang, L., Han, B., Yuan, X., Lei, B., Ding, C. (2018c). A preliminary analysis of wind retrieval, based on GF-3 wave mode data. Sensors (Switzerland), 18(5). doi: 10.3390/s18051604.

Wang, L., Li, J., Liu, S., Ducrozet, G. (2021c). Statistics of long-crested extreme waves in single and mixed sea states. Ocean Dynamics, 71, pp. 21-42.

Wang, L., Perrie, W., Long, Z., Blokhina, M., Zhang, G., Toulany, B., Zhang, M. (2018e). The impact of climate change on the wave climate in the Gulf of St. Lawrence. Ocean Modelling 128, pp. 87-101. doi: 10.1016/j.ocemod.2018.06.003.

Wang, L., Wanga, Z., Qub, H., Liuc, S. (2018a). Optimal Forecast Combination Based on Neural Networks for Time Series Forecasting. Applied Soft Computing Journal. Elsevier Ltd, 66, pp. 1–17. doi: 10.1016/j.asoc.2018.02.004.

Wang, L., Xu, X., Liu, G., Chen, B., Chen, Z. (2017b). A new method to estimate wave height of specified return period. Chinese Journal of Oceanology and Limnology, 35(5), 1002-1009.

Wang, Q., Zong, Z., Lu, P., Zhang, G., Li, Z. (2021d). Probabilistic estimation of level ice resistance on ships based on sea ice properties measured along summer Arctic cruise paths. Cold Regions Science and Technology,189. doi: 10.1016/j.coldregions.2021.103336.

Wang, W., Tang, R., Li, C., Liu, P., Luo, L. (2018b). A BP neural network model optimized by Mind Evolutionary algorithm for predicting the ocean wave heights. Ocean Engineering, 162, pp. 98-107.

Wang, X., Shao, Y., She, L., Tian, W., Li, K., Liu, L. (2018d). Ocean wave information retrieval using simulated compact polarized SAR from radarsat-2. Journal of Sensors, 2018. doi: 10.1155/2018/1738014.

Wang, X., Zhu, C., Liu. H. (2019c). Wave-Induced Seafloor Instability in the Yellow River Delta: Flume Experiments. Journal of Marine Science and Engineering, 7(10). doi: 10.3390/jmse7100356.

Wang, Y. (2018a). Transformed Rayleigh distribution of trough depths for stochastic ocean waves. Coastal Engineering, 133, pp. 106-112.

Wang, Y. (2018b). Asymptotic Calculation of the Wave Through Exceedance Probabilities in A Nonlinear Sea. China Ocean engineering, 32(2), pp. 189-195.

Wang, Y. (2020). A robust methodology for displaying two-dimensional environmental contours at two offshore sites. Journal of Marine Science and Technology, Online first.

Wang, Y., Han, L., Liu, W., Yang, S. (2019b). Study on wavelet neural network based anomaly detection in ocean observing data series. Ocean Engineering. Elsevier Ltd, 186(February), p. 106129. doi: 10.1016/j.oceaneng.2019.106129.

Wang, Y., Wu, L., (2016). On practical challenges of decomposition-based hybrid forecasting algorithms for wind speed and solar irradiation. Energy, 112(12), pp. 208-220. doi: 10.1016/j.energy.2016.06.075.

Waseda, T., Nose, T., Kodaira, T., Sasmal, K., Webb, A. (2021). Climatic trends of extreme wave events caused by Arctic Cyclones in the western Arctic Ocean. Polar Science, 27, 100625. doi: doi:10.1016/j.polar.2020.100625.

Waseda, T., Webb, A., Sato, K., Inoue, J., Kohout, A., Penrose, B., Penrose, S. (2018). Correlated increase of high ocean waves and winds in the ice-free waters of the Arctic Ocean. Scientific reports, 8(1), pp. 1-9.

Watanabe, S., Fujimoto, W., Kodaira, T., Davies, G., Lechner, D., Waseda, T. (2019). Data Assimilation of the Stereo Reconstructed Wave Fields to a Nonlinear Phase Resolved Wave Model. Proc. of ASME 38th Int. Conf. on Ocean, Offshore and Arctic Eng. (OMAE), 95949. doi: 10.1115/OMAE2019-95949.

Wei, C.-C. (2018). Nearshore wave predictions using data mining techniques during typhoons: A case study near Taiwan's northeastern coast. Energies, 11(1), 11: pp. 1-23. doi: 10.3390/en11010011.

Wei, G., He, Z., Xie, Y., Shang, S., Dai, H., Wu, J., Liu, K., Lin, R., Wan, Y., Lin, H., Chen, J., Li, Y. (2020b). Assessment of HF radar in mapping surface currents under different sea states. Journal of Atmospheric and Oceanic Technology, 37(8), pp. 1403-1422. doi: 10.1175/JTECH-D-19-0130.1.

Wei, K., Shen, Z., Ti, Z., Qin, S. (2021). Trivariate joint probability model of typhoon- induced wind, wave and their time lag based on the numerical simulation of historical typhoons. Stochastic Environmental Research and Risk Assessment, 35, pp. 325-344.

Wei, L., Guan Changlong, C., Troitskaya, Y. (2018). Laboratory Experiment on Wave Induced Turbulence. J. Ocean Univ. China (Oceanic and Coastal Sea Research), 17 (4): pp. 721-726, doi: 10.1007/s11802-018-3528-4.

Wei, M., Polojärvi, A., Cole, D.M., Prasanna, M. (2020a). Strain response and energy dissipation of floating saline ice under cyclic compressive stress. Cryosphere, 14(9). doi: 10.5194/tc-14-2849-2020.

Weiss, J., Dansereau, V. (2017). Linking scales in sea ice mechanics. Philosophical Transactions of the Royal Society A: Mathematical, Physical and Engineering Sciences, 375(2086), p. 20150352. doi: 10.1098/rsta.2015.0352.

Weller, R. A., Baker, D. J., Glackin, M. M., Roberts, S. J., Schmitt, R. W., Twigg, E. S., Vimont, D. J. (2019). The Challenge of Sustaining Ocean Observations. Frontiers in Marine Science, 6, 105. doi: 10.3389/fmars.2019.00105.

Williams, H. E., Briganti, R., Romano, A., Dodd, N. (2019). Experimental Analysis of Wave Overtopping: A New Small Scale Laboratory Dataset for the Assessment of Uncertainty for Smooth Sloped and Vertical Coastal Structures. Journal of Marine Science and Engineering, 7(7). doi: 10.3390/jmse7070217.

Willmott, C., Matsuura, K. (2005). Advantages of the mean absolute error (MAE) over the root mean square error (RMSE) in assessing average model performance. Clim Res 30, pp, 79-82. doi: 10.3354/cr030079.

Windt, C., Untrau, A., Davidson, J., Ransley, E. J., Greaves, D. M., Ringwood, J. V. (2021). Assessing the validity of regular wave theory in a short physical wave flume using particle image velocimetry. Experimental Thermal and Fluid Science, 121. doi: 10.1016/j.expthermflusci.2020.110276.

Winter, H. C., Tawn, J. A. (2017). kth-order Markov extremal models assessing heatwave risks. Extremes, 20, pp. 393-415.

Wojtysiak, K., Herman, A., Moskalik, M. (2018). Wind wave climate of west Spitsbergen: seasonal variability and extreme events. Oceanologia, 60(3), pp. 331-343. doi: 10.1016/j.oceano.2018.01.002.

World Meteorological Organization. (2018).Guide to Instruments and Methods of Observation: Volume V – Quality Assurance and Management of Observing Systems. WMO-No. 8. https://library.wmo.int/doc_num.php?explnum_id=9869.

Wrang, L., Katsidoniotaki, E., Nilsson, E., Rutgersson, A., Ryden, J., Goteman, M. (2021). Comparative Analysis of Environmental Contour Approaches to Estimating Extreme Waves for Offshore Installations for the Baltic Sea and the North Sea. Journal of Marine Science and Engineering, 9, 96: pp. 1-24.

Wu, G., Kong, S., Tang, W., Lei, R., Ji, S. (2021). Statistical analysis of ice loads on ship hull measured during Arctic navigations. Ocean Engineering, 223, 108642. doi:10.1016/j.oceaneng.2021.108642.

Wu, M., Stefanakos, C., Gao, Z., Haver, S. (2019). Prediction of short-term wind and wave conditions for marine operations using a multi-step-ahead decomposition-ANFIS model and quantification of its uncertainty. Ocean Engineering, 188, 106300.

Wu, T., Wu, Z., Wu, J., Jeon, G., Ma, L. (2018). Features of X-band radar backscattering simulation based on the ocean environmental parameters in China offshore seas. Sensors (Switzerland), 18(8). doi: 10.3390/s18082450.

Wyatt, L. R. (2018). Wave and tidal power measurement using HF radar. International Marine Energy Journal, 1(2), pp. 123-127. doi: 10.36688/imej.1.123-127.

Wyatt, L. R., Mantovanelli, A., Heron, M. L., Roughan, M., Steinberg, C. R. (2018). Assessment of Surface Currents Measured with High-Frequency Phased-Array Radars in Two Regions of Complex Circulation. IEEE Journal of Oceanic Engineering, 43(2), pp. 484-505. doi: 10.1109/JOE.2017.2704165.

Xiao, L., Qian, F., Shao, W. (2017). Multi-step wind speed forecasting based on a hybrid forecasting architecture and an improved bat algorithm. Energy Conversion and Management. Elsevier Ltd, 143, pp. 410–430. doi: 10.1016/j.enconman.2017.04.012.

Xie, B., Ren, X., Li, J., Duan, W., Wang, J., Zhao, B. (2019). Study on Gust Parameters and Wind Spectrum of South China Sea. Proc. of ASME 38th Int. Conf. on Ocean, Offshore and Arctic Eng. (OMAE), 95779. doi: 10.1115/OMAE2019-95779.

Xie, J., Li, M., Yao, G., Xi, K. (2019). The Effect of Ship-borne X-band Radar Vertical Motion on Significant Wave Height Estimation. Proc. of 2019 IEEE 2nd International Conference on Electronic Information and Communication Technology, ICEICT 2019, pp. 274-277. doi: 10.1109/ICEICT.2019.8846419.

Xie, J., Yao, G., Sun, M., Ji, Z. (2018). Measuring Ocean Surface Wind Field Using Shipborne High-Frequency Surface Wave Radar. IEEE Transactions on Geoscience and Remote Sensing, 56(6), pp. 3383-3397. doi: 10.1109/TGRS.2018.2799002.

Xie, J., Yao, G., Sun, M., Ji, Z., Li, G., Geng, J. (2017). Ocean surface wind direction inversion using shipborne high-frequency surface wave radar. IEEE Geoscience and Remote Sensing Letters, 14(8), pp. 1283-1287. doi: 10.1109/LGRS.2017.2706742.

Xu, G., Hao, H., Ma, Q., Gui, Q. (2019). An Experimental Study of Focusing Wave Generation with Improved Wave Amplitude Spectra. Water, 11(12). doi: 10.3390/w11122521.

Xu, W., Ning, L., Luo, Y. (2020a). Applying Satellite Data Assimilation to Wind Simulation of Coastal Wind Farms in Guangdong, China. Remote Sensing, 12(6). doi: 10.3390/rs12060973.

Xu, X., Voermans, J. J., Ma, H., Guan, C., Babanin, A. V. (2021). A wind-wave-dependent sea spray volume flux model based on field experiments. Journal of Marine Science and Engineering, 2021, 9(11), 1168. doi: 10.3390/jmse9111168.

Xu, Y., Liang, S., Sun, Z., Xue, Q., Bi, X. (2020b). An experimental comparison of the velocities and energies of focused spilling waves in deep water. Ocean Dynamics, 70(7), pp. 863-877. doi: 10.1007/s10236-020-01369-1.

Yan, Z., Liang, B., Wu, G., Wang, S., Li, P. (2020). Ultra-long return level estimation of extreme wind speed based on the deductive method. Ocean Engineering, 197. doi: 10.1016/j.oceaneng.2019.106900.

Yang, B., Sun, Z., Zhang, G., Wang, Q., Zong, Z., Li, Z. (2021a). Numerical estimation of ship resistance in broken ice and investigation on the effect of floe geometry. Marine Structures, 75, 102867. doi: 10.1016/j.marstruc.2020.102867.

Yang, B., Zhang, G., Huang, Z., Sun, Z., Zong, Z. (2020). Numerical Simulation of the Ice Resistance in Pack Ice Conditions. International Journal of Computational Methods, 17(01), 1844005. doi: 10.1142/S021987621844005X.

Yang, J., Yuan, X., Han, B., Zhao, L., Sun, J., Shang, M., Wang, X., Ding, C. (2021b). Phase Imbalance Analysis of GF-3 Along-Track InSAR Data for Ocean Current Measurement. Remote Sensing, 13(2). doi: 10.3390/rs13020269.

Yang, X., Li, X., Nunziata, F., Mouche, A. (2018). Ocean Remote Sensing with Synthetic Aperture Radar. In Ocean Remote Sensing with Synthetic Aperture Radar. doi: 10.3390/books978-3-03842-719-3.

Yao, G., Xie, J., Huang, W. (2018). First-order ocean surface cross-section for shipborne HFSWR incorporating a horizontal oscillation motion model. IET Radar, Sonar and Navigation, 12(9), pp. 973-978. doi: 10.1049/iet-rsn.2018.0099.

Yao, Y., Chen, S., Zheng, J., Zhang, Q., Chen, S. (2020). Laboratory study on wave transformation and run-up in a 2DH reef-lagoon-channel system. Ocean Engineering, 215. doi: 10.1016/j.oceaneng.2020.107907.

Yao, Y., He, T., Deng, Z., Chen, L., Guo, H. (2019). Large eddy simulation modelling of tsunami-like solitary wave processes over fringing reefs. Natural Hazards and Earth System Sciences, 19(6), 1281–1295. doi: 10.5194/nhess-19-1281-2019.

Yevnin, Y., Toledo, Y. (2018). Reflection source term for the wave action equation. Ocean Modelling 127, pp. 40-45. doi: 10.1016/j.ocemod.2018.05.001.

Yi, X., Wu, X., Yue, X., Zhang, L., Chen, Z., Wan, B. (2021b). Ocean Surface Current Inversion with Anchored Floating High-Frequency Radar: Yaw Compensation. IEEE Journal of Oceanic Engineering, 46(3), pp. 927-939. doi: 10.1109/JOE.2020.3028126.

Yi, Y., Johnson, J. T., Wang, X. (2021a). Diurnal Variations in Ocean Wind Speeds Measured by CYGNSS and Other Satellites. IEEE Geoscience and Remote Sensing Letters, pp. 1-5. doi: 10.1109/LGRS.2021.3074087.

Yiew, L. J., Parra, S. M., Wang, D., Sree, D. K. K., Babanin, A. v, Law, A. W. K. (2019). Wave attenuation and dispersion due to floating ice covers. Applied Ocean Research, 87, pp. 256-263. doi: 10.1016/j.apor.2019.04.006.

Yoshikawa, Y., Baba, Y., Mizutani, H., Kubo, T., Shimoda, C. (2018). Observed Features of Langmuir Turbulence Forced by Misaligned Wind and Waves under Destabilizing Buoyancy Flux. Journal of Physical Oceanography, 48, pp. 2737-2759.

Young I.R., Ribal A. (2019). Multiplatform evaluation of global trends in wind speed and wave height. Science, 364(6440): pp. 548–552. doi: 10.1126/science.aav9527.

Young, I. R. (2019). The Wave Climate of the Southern Ocean. Proc. of ASME 38th Int. Conf. on Ocean, Offshore and Arctic Eng. (OMAE), 95168. doi: 10.1115/OMAE2019-95168.

Young, I. R., Donelan, M. A. (2018). On the determination of global ocean wind and wave climate from satellite observations. Remote Sensing of Environment, 215(June), pp. 228-241. doi: 10.1016/j.rse.2018.06.006.

Young, I. R., Zieger, S., Babanin, A. V. (2011). Global trends in wind speed and wave height. Science, 332, pp. 451-455.

Yousof, H., Jahanshahi, S., Ramires, T., Aryal, G., Hamedani, G. (2018). A new distribution for extreme values: Regression model, characterizations and applications. Journal of Data Science, 16(4), pp. 677-706.

Yu, C., Li, Y., Xiang, H., Zhang, M. (2018a). Data mining-assisted short-term wind speed forecasting by wavelet packet decomposition and Elman neural network. Journal of Wind Engineering and Industrial Aerodynamics. Elsevier B.V., 175, pp. 136–143. doi: 10.1016/j.jweia.2018.01.020.

Yu, C., Li, Y., Zhang, M. (2017a). An improved Wavelet Transform using Singular Spectrum Analysis for wind speed forecasting based on Elman Neural Network. Energy Conversion and Management. Elsevier Ltd, 148, pp. 895–904. doi: 10.1016/j.enconman.2017.05.063.

Yu, H., Li, J., Wu, K., Wang, Z., Yu, H., Zhang, S., Hou, Y., Kelly, R.M. (2018b). A global high-resolution ocean wave model improved by assimilating the satellite altimeter significant wave height. International Journal of Applied Earth Observation and Geoinformation 70, pp. 43-50.

Yu, H., Uy, W. I., Dauwels, J. (2017b). Modelling Spatial Extremes via Ensemble-of-Trees of Pairwise Copulas. IEEE Transactions on Signal Processing, 65(3), pp. 571-586.

Yu, J., Rogers, W. E., Wang, D. W. (2019). A Scaling for Wave Dispersion Relationships in Ice-Covered Waters. Journal of Geophysical Research: Oceans, 124(11), pp. 8429-8438. doi: 10.1029/2018JC014870.

Yu, Z., Lu, W., van den Berg, M., Amdahl, J., Løset, S. (2021). Glacial ice impacts: Part II: Damage assessment and ice-structure interactions in accidental limit states (ALS). Marine Structures, 75, 102889. doi: doi:10.1016/j.marstruc.2020.102889.

Yurovsky, Y., Kudryavtsev, V., Grodsky, S., Chapron, B. (2019). Sea Surface Ka-Band Doppler Measurements: Analysis and Model Development. Remote Sensing, 11(7). doi: 10.3390/rs11070839.

Zaman, H., Akinturk, A. (2020). Semisubmersible Offshore Structure in an Extreme Wave Domain with Itinerant Ice Pieces. Proc. of Global Oceans 2020: Singapore – U.S. Gulf Coast, pp. 1–8. doi:10.1109/IEEECONF38699.2020.9389215.

Zeng, Y., Zhou, H., Huang, W., Lai, Y., Wen, B. (2019). Effect of Current on the First-Order Spectral Power of High-Frequency Radar. IEEE Transactions on Geoscience and Remote Sensing, 57(8), pp. 5686–5700. doi: 10.1109/TGRS.2019.2901581.

Zhang, H. D., Shi, H. D., Guedes Soares, C. (2019c). Evolutionary properties of mechanically generated deepwater extreme waves induced by nonlinear wave focusing. In Ocean Engineering, 186, 106077. doi:10.1016/j.oceaneng.2019.05.059.

Zhang, H. D., Wang, X. J., Shi, H. D., Guedes Soares, C. (2021a). Investigation on abnormal wave dynamics in regular and irregular sea states. Ocean Engineering, 222, 108602. doi:10.1016/j.oceaneng.2021.108602.

Zhang, H., Meng, J., Sun, L., Zhang, X., Shu, S. (2020). Performance analysis of internal solitary wave detection and identification based on compact polarimetric SAR. IEEE Access, 8, pp. 172839-172847. doi: 10.1109/ACCESS.2020.3025946.

Zhang, J., Benoit, M., Kimmoun, O., Chabchoub, A., Hsu, H.-C. (2019a). Statistics of Extreme Waves in Coastal Waters: Large Scale Experiments and Advanced Numerical Simulations. Fluids, 4(2), 99. doi:10.3390/fluids4020099.

Zhang, J., Zhang, X., Deng, W., Ye, L., Yang, Q. (2021b). Information Geometric Means-Based STAP for Nonhomogeneous Clutter Suppression in High Frequency Hybrid Sky-Surface Wave Radar. IEEE Sensors Journal, 21(2), pp. 1787-1798. doi: 10.1109/JSEN.2020.3016673.

Zhang, X., Dai, H. (2019). Significant wave height prediction with the CRBM-DBN model. Journal of Atmospheric and oceanic Technology, 36, pp. 333-351.

Zhang, X., Li, Y., Gao, S., Ren, P. (2021c). Ocean Wave Height Series Prediction with Numerical Long Short-Term Memory. J. Mar. Sci. Eng., 9(5), 514; doi: 10.3390/jmse9050514.

Zhang, Y., Chen, B., Pan, G., Zhao Y. (2019b). A novel hybrid model based on VMD-WT and PCA-BP-RBF neural network for short-term wind speed forecasting. Energy Conversion and Management. Elsevier Ltd, 195, pp. 180–197. doi: 10.1016/j.enconman.2019.05.005.

Zhang, Y., Kim, C.-W., Beer, M., Dai, H., Guedes Soares, C. (2018). Modelling multivariate ocean data using asymmetric copulas. Coastal Engineering, 135, pp. 91-111.

Zhao, C., Chen, Z., Li, J., Zhang, L., Huang, W., Gill, E. W. (2020b). Wind Direction Estimation Using Small-Aperture HF Radar Based on a Circular Array. IEEE Transactions on Geoscience and Remote Sensing, 58(4), pp. 2745–2754. doi: 10.1109/TGRS.2019.2955077.

Zhao, J., Tian, Y., Wen, B., Tian, Z. (2020a). Unambiguous Wind Direction Field Extraction Using a Compact Shipborne High-Frequency Radar. IEEE Transactions on Geoscience and Remote Sensing, 58(10), pp. 7448-7458. doi: 10.1109/TGRS.2020.2982938.

Zhao, J., Wen, B., Tian, Y., Tian, Z., Wang, S. (2019). Sea Clutter Suppression for Shipborne HF Radar Using Cross-Loop/Monopole Array. IEEE Geoscience and Remote Sensing Letters, 16(6), pp. 879-883. doi: 10.1109/LGRS.2018.2884507.

Zhao, X., Jiang, N., Liu, J., Yu, D., Chang J. (2020a). Short-term average wind speed and turbulent standard deviation forecasts based on one-dimensional convolutional neural network and the integrate method for probabilistic framework. Energy Conversion and Management. Elsevier Ltd, 203, p. 112239. doi: 10.1016/j.enconman.2019.112239.

Zhao, Y., Chong, J., Li, Y., Sun, K., Yang, X. (2021). Sea spike suppression method based on optimum polarization ratio in airborne SAR images. Sensors, 21(9), pp. 1-24. doi: 10.3390/s21093269.

Zhao, Y., Liu, D., Dong, S. (2020b). Estimating Design Loads with Environmental contour Approach Using Copulas for an Offshore Jacket Platform. Journal of Ocean University of China, 19, pp. 1029-1041.

Zheng, K., Osinowo, A.A., Sun, J., Hu, W. (2018). Long-Term Characterization of Sea Conditions in the East China Sea Using Significant Wave Height and Wind Speed. Journal of Ocean University of China 17 (4), pp. 733 - 743. foi: 10.1007/s11802-018-3484-z.

Zhou, L., Zheng, G., Yang, J., Li, X., Zhang, B., Wang, H., Chen, P., Wang, Y. (2021). Sea Surface Wind Speed Retrieval From Textures in Synthetic Aperture Radar Imagery. IEEE Transactions on Geoscience and Remote Sensing, pp. 1-11. doi: 10.1109/TGRS.2021.3062401.

Zinchenko, V., Vasilyev, L., Halstensen, S. O., Liu, Y. (2021). An improved algorithm for phase-resolved sea surface reconstruction from X-band marine radar images. Journal of Ocean Engineering and Marine Energy, 7(1), pp. 97-114. doi: 10.1007/s40722-021-00189-9.